Development of A Novel Hand-held Haptic Device Integrating Upper Limb Movement Assessment and Directional Guidance

Shuhao Dong

Submitted in accordance with the requirements for the degree of
PhD in Mechanical Engineering

The University of Leeds
Institute of Design, Robotics and Optimisation
School of Mechanical Engineering

October 2023

The candidate confirms that the work submitted is his own, except where work which has formed part of jointly authored publications has been included. The contribution of the candidate and the other authors to this work has been explicitly indicated below. The candidate confirms that appropriate credit has been given within the thesis where reference has been made to the work of others.

iDRO represents the Institute of Design, Robotics and Optimisation

MEEC 21-003: A machine learning based performance classification for post-stroke rehabilitation using kinematic features.

The following people formed the research team on the MEEC 21-003 study:

- Professor Martin Levesley (IDRO). Main PhD supervisor. Martin was in charge of recruiting experiment participants.
- Dr Justin Gallagher (IDRO). PhD supervisor. Justin was in charge of recruiting experiment participants.
- Dr Andrew Jackson (IDRO). PhD supervisor.

The following publication was produced as a result of the work contained in this thesis.

- Dong, S., Jackson, A., Gallagher, J. and Levesley, M. The Use of Kinematic Features in Evaluating Upper Limb Motor Function Learning Progress Based on Machine Learning. In: *2023 International Conference on Rehabilitation Robotics (ICORR), 24-28 Sept 2023, Singapore.* IEEE, 2023, pp. 1-6.

MEEC 22-006: The ideal characteristics of the input signal for providing the strongest haptic directional cue in a hand-held device for a rehabilitation purpose.

The following people formed the research team on the MEEC 22-006 study:

- Professor Martin Levesley (IDRO). Main PhD supervisor. Martin was in charge of recruiting experiment participants.
- Dr Justin Gallagher (IDRO). PhD supervisor. Justin was in charge of recruiting experiment participants.
- Dr Andrew Jackson (IDRO). PhD supervisor.

The following publications were produced as a result of the work contained in this thesis.

- Dong, S., Jackson, A., Gallagher, J. and Levesley, M. Modelling and Design of Asymmetric Vibrations to Induce Bidirectional Force

Sensation for Portable Rehabilitation Devices. In: *2022 International Conference on Rehabilitation Robotics (ICORR), 25-29 July 2022, Rotterdam.* IEEE, 2022, pp. 1-6.

- Dong, S., Jackson, A., Gallagher, J. and Levesley, M. A Hand-Held Device Presenting Haptic Directional Cues for the Visually Impaired. *Sensors*. 2023, **23** (20), no. 8415.

This research has been carried out by a team which has included Professor Martin Levesley, Dr Justin Gallagher and Dr Andrew Jackson. My own contributions, fully and explicitly indicated in the thesis, have been the development of a hand-held device that integrates movement quality assessment and haptic directional guidance, and a series of experiment to verify the validity and functionality of the proposed device. Some attempts on computer vision and serious game development were also included. The other members of the group and their contributions have been supervision, recruitment of participants for both experiments.

Acknowledgements

I would like to firstly thank the University of Leeds and the China Scholarship Council for supporting my research and life in the UK.

I also would like to thank all my supervisors, Professor Martin Levesley, Doctor Justin Gallagher and Doctor Andrew Jackson for providing patient and professional supervision of the research during the three years. Not only did they help me in research skills, but also provide necessary training in the teaching ability and sufficient assistance in living abroad.

Special thanks to Professor Zhongmin Jin, Professor Martin Levesley, Mrs Li Liao, Mrs Yaoqian Liu and Miss Jiaqi Qu from the Southwest Jiaotong University for providing me the opportunity to pursue a PhD degree with a full scholarship during the application process.

I would like to express my sincere gratitude to every participant involved in the experiments. It is your time and cooperation that make this project meaningful.

Special thanks also given to Ryan Smith for providing professional manufacturing advice for the haptic device and sensors. Many thanks to Sibo Wang, Songlin Dai and Su Zhang for their online accompany with me during the three years, especially during the COVID.

Finally, I would like to thank my family for trusting me and supporting my personal career development and life in the UK. Without your support, I couldn’t make it so far.

Abstract

Visual impairment is one of the most common symptoms after several diseases including cataracts, diabetes, and stroke. It can cause severe impact on the quality of life such as a decrease in workforce participation and productivity and an increase in the chance of depression among all ages. This effect is even worse on patients after stroke because it prevents the use of advanced robotic devices. Most of the current upper limb robotic devices rely on visual cues to guide the movement throughout the rehabilitation process. Therefore, it is beneficial to design a local navigation device based on haptic cues for visually impaired patients after stroke. With the development of sensing techniques, it is also possible to integrate movement assessment function based on kinematic sensor data, which can be more objective, sensitive, and continuous than traditional assessments.

This research aims to design and develop a novel hand-held haptic device for movement guidance and movement assessment for robot-assisted rehabilitation outside clinical environments, especially for visually impaired people after stroke.

The movement assessment was conducted on kinematic data collected from a position sensor or an accelerometer. Two novel position sensing methods were proposed, and several kinematic features were extracted from the measurements to objectively quantify movement smoothness with the help of machine learning. An observational experiment was finally conducted to verify the effectiveness of kinematic assessment. The results showed that kinematic features could reflect subtle progress in motor function learning progress and could contribute to the machine learning models development for a better classification result on both movement type and movement smoothness.

The design of the haptic implementation was firstly explored with three different haptic motors, among which a voice coil actuator was selected to generate asymmetric vibrations for haptic delivery. The input control signal was then parameterised as the main contribution, and five output parameters were discussed. A psychophysical experiment was finally conducted to find the ideal characteristics of input signal that could produce clearer haptic directional cues. The results showed that input signals after optimisation could improve the delivery of haptic directional cues in terms of accuracy, applicability, and user’s confidence.

Table of Contents

Acknowledgements ..... **iv**
Abstract ..... **v**
Table of Contents ..... **vi**
List of Tables ..... **x**
List of Figures ..... **xi**
Preface ..... **xv**
Chapter 1 Introduction **1**
1.1 Background 1
1.2 Aim of the Research 4
1.3 Objectives 4
1.4 Research Timelines 4
1.5 Contribution of the Research 5
1.6 Outlines of the Thesis 6
1.7 Summary 6
Chapter 2 Literature Review **8**
2.1 Aim of the Literature Review 8
2.2 Review Strategy 8
2.2.1 Review Strategy for Kinematic Assessments 8
2.2.2 Review Strategy for Haptic Feedback 10
2.3 Literature Search Results 11
2.3.1 Overview 11
2.3.2 Kinematic Feature Extraction 14
2.3.3 Application of Machine Learning 15
2.3.4 Other Applications 17
2.3.5 Haptic Directional Cues 17
2.4 Literature Discussion 19
2.5 Summary 21
Chapter 3 Methods and Experimental Designs – Movement Smoothness **23**
3.1 Mouse Position Tracking 24
3.1.1 Experiment Procedures 24
3.1.2 Data Processing 25
3.2 Single-Camera Position Tracking 27

3.2.1 Computer Vision Algorithm 27
3.2.2 Experiment Procedures 28
3.2.3 Data Processing 29
3.3 Movement Type Classification 30
3.3.1 Experiment Procedures 31
3.3.2 Data Processing 32
3.3.3 Model Training and Evaluation 32
3.4 Movement Smoothness Assessment 33
3.4.1 Experiment Procedures 34
3.4.2 Data Processing and Feature Extraction 35
3.4.3 Machine Learning Model Preparation 38
3.4.4 Statistical Analysis 40
3.5 Summary 40
Chapter 4 Results on Movement Assessment 43
4.1 Mouse Position Tracking Experiment 43
4.1.1 Results 43
4.1.2 Statistical Analysis 45
4.2 Computer Vision Tracking Experiment 48
4.2.1 Results 48
4.2.2 Statistical Analysis 50
4.3 Movement Type Classification Experiment 52
4.4 Movement Smoothness Assessment Experiment 56
4.4.1 Observation of Learning Progress 56
4.4.2 Movement Pattern Classification 62
4.4.3 Movement Smoothness Classification 64
4.5 Discussion and Summary 67
4.5.1 Position Tracking 67
4.5.2 Movement Type Classification 69
4.5.3 Observation of Learning Progress 72
4.5.4 Movement Smoothness Assessment 74
Chapter 5 Experiment Designs and Hardware Development – Haptic Cue 77
5.1 Eccentric Rotating Mass 78
5.2 Solenoid Test Platform 80
5.2.1 Dynamic Model of Asymmetric Vibrations 80
5.2.2 Dynamic Model Verification 84

5.2.3 Effect of Input Signal Shape and Spring Stiffness 85
5.3 Hand-held Haptic Device 86
5.3.1 Device Design and Manufacturing 87
5.3.2 Source of Vibrations 90
5.3.3 VCA Haptic Test Platform 94
5.4 Results 97
5.4.1 Solenoid Test Platform Results 97
5.4.1.1 Determination of the Solenoid Drive Constant 97
5.4.1.2 Verification of the Dynamic Model 97
5.4.1.3 Effect of the Input Signal Shape 101
5.4.1.4 Effect of Spring Stiffness 104
5.4.2 Voice Coil Actuator Test Results 108
5.4.2.1 Displacement from VCA Test Platform 108
5.4.2.2 Delay Time 108
5.4.2.3 Ramp Down Step Length 110
5.4.2.4 Cut-off Voltage 112
5.4.3 Output Parameter Comparison 115
5.5 Summary 116
5.5.1 Overall 116
5.5.2 Selection of Haptic Motors 119
5.5.3 Solenoid Dynamic Model 119
5.5.4 Effect of Signal Shape and Spring Stiffness 120
5.5.5 Displacement Measurements 121
Chapter 6 Human Experiment Design and Results 123
6.1 Human Experiment Design 123
6.2 Human Experiment Results 126
6.2.1 Left or Right 127
6.2.2 Static Test and Dynamic Test 133
6.2.3 Normal Force and Shear Force 135
6.2.4 Special Concerns 137
6.3 Discussion and Summary 138
Chapter 7 Conclusions and Future Work 142
7.1 Conclusions 142
7.1.1 Overall Research Findings 142
7.1.2 Movement Smoothness Assessment Findings 143

7.1.2.1 Position Tracking 143
7.1.2.2 Kinematic Features and Machine Learning 144
7.1.3 Haptic Directional Guidance Findings 146
7.1.4 Evaluation of Research Aim and Objectives 148
7.1.5 Research Summary 150
7.2 Future Work 151
7.2.1 Extraction of Kinematic Features and Their Applications 152
7.2.2 Haptic Perception Experiment 153
List of References 155
List of Abbreviations 163
Appendix A 165
A.1 Output Features for Delay Time 165
A.2 Output Features for Ramp Down Step Length 165
A.3 Output Features for Cut-off Voltage 165
Appendix B 167
B.1 MEEC 21-003 Experiment Guidance for Participants 167
B.2 MEEC 21-003 Participant Consent Form 169
B.3 MEEC 21-003 Participant Information Sheet 170
B.4 MEEC 21-003 Risk Assessment for Participants 173
Appendix C 175
C.1 MEEC 22-006 Experiment Guidance for Participants 175
C.2 MEEC 22-006 Participant Consent Form 178
C.3 MEEC 22-006 Participant Information Sheet 180
C.4 MEEC 22-006 Risk Assessment for Participants 183
C.5 MEEC 22-006 Data Management Plan 185

List of Tables

Table 2.1 Summary of the kinematic features. 13
Table 3.1 Description on the segmentation algorithm. 26
Table 3.2 Kinematic features extracted from different profiles. 37
Table 4.1 Two-sample t-test results on kinematic features extracted from both measurement systems. 47
Table 4.2 Evaluation on movement type classification models. 53
Table 4.3 Model performance after feature selection process using MRMR. 54
Table 4.4 Average kinematic features over 10 attempts for each movement pattern. 60
Table 4.5 Evaluations on ML models classifying movement patterns using training and test accuracy, F1 score and Cohen's Kappa. 62
Table 4.6 Initial classification results using 7 machine learning models and 2 labelling methods. 65
Table 4.7 Evaluations on ML models classifying movement quality using training and test accuracy, F1 score and Cohen's Kappa. 66
Table 4.8 Summary of the measurement systems. 69
Table 4.9 Main findings on the kinematic assessment of upper limb movements. 75
Table 5.1 Haptic device design specifications. 87
Table 5.2 Parameters of the PWM signals used in the simulation. 98
Table 5.3 Average values of positive and negative acceleration peaks. 99
Table 5.4 Dynamic time warping distance between each acceleration pair. 100
Table 5.5 Average value of positive and negative acceleration peaks in different input signals. 102
Table 5.6 Effect of output parameters on stroke ratio, vibration frequency and simplified speed. 116
Table 5.7 Summary of the inputs and outputs of two haptic systems. 117
Table 5.8 Summary of two haptic implementations. 118
Table 6.1 Input parameters of all haptic configurations. 127
Table 6.2 Output parameters for all configurations used in the experiment. 129
Table 6.3 Statistics of angle difference in static test and dynamic test. 134
Table 6.4 Statistics of angle difference in different zones and tests. 136
Table 7.1 Key findings of the research. 150

List of Figures

Figure 1.1: Timeline overview of the research. 5

Figure 1.2: Thesis structure overview. 6

Figure 2.1: Literature search results for (a) kinematic assessment and (b) haptic feedback. 12

Figure 2.2: Overview of the literature search results on kinematic assessments. 13

Figure 2.3: Overview of the literature search results on haptic feedback. 14

Figure 3.1 Seven-segment point-to-point triangle movement pattern. 25

Figure 3.2 Back projection colour segmentation algorithm. (a) RGB image. (b) HSV image. (c) Colour histogram. (d) Segmented image with contour and centre. 28

Figure 3.3 Single-camera based position tracking using a single pendulum. 29

Figure 3.4 Four movement types including (a) reaching out, (b) turning a key, (c) drawing a full circle and (d) drinking. 31

Figure 3.5 Experiment set up for movement quality classification using two Optotrak systems for a better coverage of detection. 34

Figure 3.6 Experiment procedure for movement quality classification. 35

Figure 3.7 Data preparation pipeline for a single movement pattern. 38

Figure 3.8 Workflow of selecting machine learning models and proper labelling method. 39

Figure 3.9 Summary of experiment designs including inputs, outputs, and verifications. 42

Figure 4.1 Normalised position along X and Y axis in the first attempt. 44

Figure 4.2 Representation of mouse and Optotrak position between two continuous measurements. 45

Figure 4.3 Test-retest reliability for 10 mouse sensor position measurements. 46

Figure 4.4 Average RMSE values over 10 attempts for each kinematics along each axis. 46

Figure 4.5 Normalised position measurements from computer vision system and Optotrak 49

Figure 4.6 Normalised RMSE for all measurements at all distances. 50

Figure 4.7 Two-sample t-test on average NRMSE at all distances. 51

Figure 4.8 Test-retest reliability for 15 measurements. 51

Figure 4.9 Scatter plot with maximum acceleration on X and Y axis. 54
Figure 4.10 Change in kinematic features in DA + 0-degree rotation movement pattern. 58
Figure 4.11 Change in kinematic features in DA + 180-degree rotation movement pattern. 58
Figure 4.12 Change in kinematic features in NDA + 0-degree rotation movement pattern. 59
Figure 4.13 Change in kinematic features in NDA + 180-degree rotation movement pattern. 59
Figure 4.14 Pearson's correlation coefficients for all selected kinematic features in (a) DA + 0-degree rotation, (b) DA + 180-degree rotation, (c) NDA + 0-degree rotation and (d) NDA + 180-degree rotation. 60
Figure 4.15 Inter-feature reliability verified by intraclass correlation coefficient. 61
Figure 4.16 Number of selections for each kinematic feature in the movement pattern classification task. 63
Figure 4.17 Skewness varied from different movement patterns and number of attempts. 71
Figure 4.18 Variance in some kinematic features in the last three attempts (DA+180-degree rotation). 73
Figure 5.1 Two ERMs attached to a frame and controlled by a motor driver. 78
Figure 5.2 A total of 9 ERMs are needed for directional guidance along 8 directions. 79
Figure 5.3 Solenoid haptic test platform. 81
Figure 5.4 Sectional view of the solenoid haptic test platform. 81
Figure 5.5 Input current (unit) signals with different frequencies and duty ratios. 82
Figure 5.6 Dynamic model of the solenoid haptic test platform. Inner and outer springs are considered as parallel connection. 83
Figure 5.7 Simulink model of the solenoid dynamic model with PWM as the input signal. 84
Figure 5.8 Sawtooth and step-ramp input signal with an actuation time of 20 ms. 86
Figure 5.9 The assembly of the hand-held haptic device. 90
Figure 5.10 Modelling of components inside the hand-held haptic device. 91
Figure 5.11 Block diagram of the haptic device. 91
Figure 5.12 Step-ramp input signal that generates asymmetric vibrations. 92

Figure 5.13 Schematic diagram of the custom control circuit for the VCA. 93

Figure 5.14 Simulated RC circuit response with $R = 2000\ \Omega$ and $C = 100\ \mu F$. 94

Figure 5.15 VCA haptic test platform on a slider. 95

Figure 5.16 Illustration of a typical normalised displacement measurement from asymmetric vibrations. 96

Figure 5.17 Determination of the solenoid drive constant using a linear regression method. 97

Figure 5.18 Comparison of simulated and measured accelerations for different PWM frequencies and duty ratios. 98

Figure 5.19 The change in acceleration peak value difference with respect to duty ratio. 100

Figure 5.20 Tukey test results on (a) the effect of duty ratio and (b) the effect of PWM frequency. 101

Figure 5.21 Input signals with corresponding simulated acceleration. 102

Figure 5.22 Acceleration peak difference for difference input shapes and actuation time. 103

Figure 5.23 Change of momentum of haptic output for three input signal shapes (a) throughout the movement and (b) at the input instant. 104

Figure 5.24 Simulated acceleration output with a spring stiffness of (a) $k = 70\ N/m$, (b) $k = 90\ N/m$, (c) $k = 130\ N/m$ and (d) $k = 150\ N/m$ with a small duty ratio. 105

Figure 5.25 Average of upper and lower peaks and the peak difference for different stiffness with a small duty ratio. 105

Figure 5.26 Simulated acceleration output with a spring stiffness of (a) $k = 70\ N/m$, (b) $k = 90\ N/m$, (c) $k = 130\ N/m$ and (d) $k = 150\ N/m$ with a large duty ratio. 106

Figure 5.27 Average of upper and lower peaks and the peak difference for different stiffness with a large duty ratio. 106

Figure 5.28 Change in peak difference with a variation in stiffness. 107

Figure 5.29 Displacement measurements for different delay time settings. 109

Figure 5.30 Change in vibration frequency, simplified speed, and stroke ratio for different delay time settings. 109

Figure 5.31 (a) Displacement measurements for different ramp down step length settings and (b) a secondary platform in the haptic output. 111

Figure 5.32 Change in vibration frequency, simplified speed, and stroke ratio for different ramp down step length settings. 112

Figure 5.33 (a) Displacement measurements for different cut-off voltage settings and (b) damping effect during the delay platform. ... 113

Figure 5.34 Change in vibration frequency, simplified speed, and stroke ratio for different cut-off voltage settings. 114

Figure 5.35 Negative stroke and positive stroke do not show strong linear correlation..... 115

Figure 5.36 Two nonlinear ramp-down curves. 121

Figure 6.1 Summary of the four stages of the human perception experiment. 125

Figure 6.2 A participants was holding the hand-held haptic device during the experiment. 125

Figure 6.3 (a) Experiment results for 9 configurations and comparisons related to cut-off voltage in terms of (b) NOM, (c) NOU and (d) SOC. 128

Figure 6.4 Scatter plot of each haptic configuration. 129

Figure 6.5 Gaussian and quadratic relationship between stroke ratio and NOM..... 131

Figure 6.6 The relationship between NOM and (a) simplified speed, (b) vibration frequency, (c) positive stroke and (d) negative stroke. 132

Figure 6.7 Pearson's correlation coefficients for both quadratic intervals separated by $rs = 0.345$..... 133

Figure 6.8 Angle difference in static test and dynamic test. 134

Figure 6.9 (a) RMSE for dynamic test and static test and (b) the two-sample t-test result on RMSE between two tests. 135

Figure 6.10 Different zones determined by dominant force with local coordinate in the haptic experiment. 136

Figure 6.11 Two-sample t-test on zone difference in (a) static test and (b) dynamic test..... 137

Figure 6.12 Preference on the contact area by participants. 138

Figure 6.13 Constant direction guidance and zig-zag direction guidance. 140

Preface

At the beginning, I hate writing. Not because I couldn't write properly and logically in English, but because I pay too much attention on my own logics. Every time I think this sentence does not make any sense to me or to my reader, I will re-write everything until I am satisfied with the logic and the quality of the writing. Finally, this PhD thesis has been written, following my own logic, to fulfil the graduation requirement for my PhD degree at the University of Leeds. I started my research activities in October 2020 when COVID-19 prevented everything from daily life activities to research. I was writing this thesis from December 2022 to October 2023.

I am very lucky to have this PhD opportunity in the University of Leeds. I graduated from the Southwest Jiaotong University – University of Leeds Joint School in 2020. Professor Jin, the dean of the joint school, asked me if I am interested in pursuing a PhD with a scholarship. I hesitated for a long time because I am not sure if my proven ability in research is strong enough for me to find a supervisor and jump through a master's degree. Professor Levesley and Dr Gallagher seemed to be very satisfied with my experience during the interview. Probably because just one year before, I gave an interview with Professor Levesley at the joint school about his teaching experience here in China. But, still, I was not confident.

So, what motivated me during my three-year journey if I am not confident? It is the pleasant feeling when every time I solved a question from scratch and learn new things. I especially love the fusion of how I conduct research and how my supervision was conducted. I explored the topic myself, they supported me with everything they could. As a consequence, after this journey, when I looked back, I noticed that I have more experience in not only programming, electrical design, mechanical design and experimental design, but also in teaching activities, scientific reach-out activities and so many other abilities that will certainly help me in my future professional development.

I feel relieved now after I have finished this thesis. But I know this is not an end but a fresh start for myself. I will face more challenges and puzzles. However, the only difference is that I am confident now.

Shuhao Dong

Leeds, August 14, 2023

Chapter 1 Introduction

1.1 Background

Upper limb movements play integral roles in people's activities of daily living, ranging from interacting with the environment, such as reaching and touching to fine manipulations like fine finger movements and gasping. A prevalent application scenario of an upper limb movement is to reach for and gasp an object. During this process, precise control of finger forces for gasping and coordination of distal and proximal joints are indispensable. However, various neurological conditions, both in adults and children, would impact the function of upper limb movements, such as stroke or cerebral palsy. Thus, the assessment of upper limb movements would be beneficial during the rehabilitation process.

Additionally, repetitive upper limb movements are often employed to enhance muscle strength or endurance. For example, weight-lifting athletes may be trained over time repeatedly on the single lift-up movement. Both application scenarios will require an objective measurement of upper limb movements so that subtle differences could be observed to guide either the rehabilitation interventions or the training methods.

As one example that can influence upper limb movement, stroke can cause serious sensorimotor function deficits including muscle weakness and changes in muscle sensations and orientations. Despite the availability of acute medical treatment and rehabilitation, upper limb impairment persists in about 60% [1] of post stroke patients, which significantly reduces their ability to perform activities of daily living. It can be beneficial to understand the upper limb sensorimotor function recovery for developing and optimising rehabilitation interventions. One constraint impeding this understanding is the lack of standardised, responsive, and objective approaches to measure the recovery of upper limb deficits.

The recovery of stroke also requires persistent and repetitive training sessions. Traditionally, rehabilitation interventions are provided by experienced physiotherapists who will also be responsible for clinical assessments such as the upper extremity subscale of the Fugl-Meyer Assessment (FMA-UE) and the Action Research Arm Test (ARAT). Even though these clinical assessments have been proved to be repetitive and reliable by numerous research studies [2, 3], they lack the objectiveness and

sensitivity among each repetition in reflecting subtle differences due to the use of ordinal scales. This insufficient sensitivity in different repetition prevents the ability to distinguish between behavioural restitution from movement compensation, which is of vital importance to understand the sensorimotor function recovery from the side of neurological mechanisms. Behavioural restitution is commonly defined as the return toward the normal motor control function with impaired effectors [4] whereas movement compensation requires new behavioural approaches using unimpaired muscles. Repetitive tasks are major components of rehabilitation after stroke. For the upper limb movements, this includes reaching and manipulating of an object [5]. Such interventions have been proved by several systematic reviews [6-8] to be effective for reducing activity limitations. Other research also shows improved muscle strength by repetitive trainings [5]. However, the effect of such repetitive training on movement smoothness is less studied in the literature.

Apart from post-stroke rehabilitation, modern sports training also utilise high-repetition training sessions on endurance performance [9] and muscle strength [10]. Therefore, it would be beneficial to quantify the difference objectively and sensitively between each repetition in order to track the progress of the training.

Kinematic assessments can address these problems to formulate an objective and sensitive evaluation metric, which have the potential to reflect subtle improvements, such as in movement smoothness, and monitor movement compensations at the same time. Furthermore, the effect of COVID-19 has increased the focus on telerehabilitation and digital health [11]. Kinematic assessments also have the potential to enhance rehabilitation in home environment due to its objectiveness and ease of use, which can also provide improved motivations for patients after stroke.

Furthermore, these kinematic assessments are highly valuable in the application of machine learning feature selection process in terms of quantifying motor learning or recovery progress and classifying different movement types.

Apart from the upper limb deficits, it is reported that up to 52% of stroke survivors also suffer from visual field loss, up to 70% of them have central visual problems, 68% of them have eye movement disorders and 80% of them have visual perceptual disorders [12]. Since most of the current rehabilitation systems assisted by robots are vision based (either required during or before the training sessions) [13], it is rather difficult for visual-

impaired patients to receive the same robot-assisted interventions independently in home environment. It is therefore beneficial to study the application of haptics in the field of poststroke rehabilitation, specifically in how to create directional information for visual-impaired people. Since directional guidance based on haptic cues requires users to retain a certain level of hand vibration sensation, it may not be suitable for stroke patients with a decreased vibration discrimination threshold.

Haptics is the sense of touch, which enables humans to perform manipulations and sensations in the real world. Unlike the other four senses (sight, hearing, taste and smell), the sense of touch is not controlled by a specific region of the body but distributed across the entire body through the skin. This characteristic enables humans to sense multiple information such as location, direction, pressure and force etc [14].

The sense of touch is typically categorised into 2 types: Kinesthetic and tactile. Kinesthetic sensations are sensed by muscles, tendons and joints for forces and torques [15]. Tactile sensations are sensed by mechanoreceptors embedded in the skin for pressure and vibrations. The mechanoreceptors are characterised by their temporal resolution and size of their receptive fields [16]. For example, Pacinian corpuscles [17] are fast-adapting mechanoreceptors that are sensitive to high-frequency vibrations ($>$ 60 Hz) and provide transient contact information. Whereas Meissner corpuscles are fast-adapting mechanoreceptors that are sensitive to low-frequency vibrations ($<$60 Hz) [17] and are capable of sensing skin deformation. Therefore, it is possible to use proper stimuli to trigger the Meissner corpuscles in order to obtain directional information through haptics, which is beneficial for poststroke interventions, specifically for visual-impaired people.

Since the haptic information is the main source for visual-impaired people to accurately get directions through physical interactions [18], it is also important to study the input signal's characteristics in order to generate the most feasible directional cues, which means the haptic cues should be perceived by people accurately and confidently. However, the characteristics of the input signal depends on the form of the haptic device and actuation method. For example, electrical actuations involving the vibrations generated by motors can require asymmetric signals whereas mechanical actuations use mechanical linkages to generate vibrations with a similar effect. This makes the parameterisation and optimisation of the input signal important in delivering the desired vibration patterns.

1.2 Aim of the Research

The aim of this research is to design, implement and evaluate the performance of a low-cost hand-held haptic device integrating directional guidance and movement smoothness assessment using machine learning models, potentially for post-stroke patients and people with visual impairment.

1.3 Objectives

The following objectives are set in order to achieve the aim of the research:

a) To review existing applications of kinematic assessments and their use in machine learning models to understand the current status of research in the field.
b) To review existing systems that can present haptic directional cues to understand the control of the vibration and the development of the device.
c) To extract kinematic features from low-cost sensors that will be adopted to assess the movement quality, specifically the change of smoothness in each repetition.
d) To develop and train a machine learning model that can predict the motor learning progress and classify the above movement quality for optimised upper limb movement assessment in smoothness.
e) To design and build a portable haptic device integrating movement assessment and directional guidance in a 2D plane.
f) To optimise control signals for the haptic source to allow subjects to interact with improved resolution, accuracy and confidence.
g) To test and evaluate the integrated portable haptic device across a range of subjects with the ability to reflect their movement quality.
h) To draw conclusions and suggest future improvements.

1.4 Research Timelines

The research presented in this thesis has been done over the last 3 years full time. This has allowed development and refinement of a portable haptic device with the ability to assess movement smoothness. This has also allowed two human-based experiment with respect to movement quality assessment and haptic directional cues. An overview of the research timeline is shown in Figure 1.1.

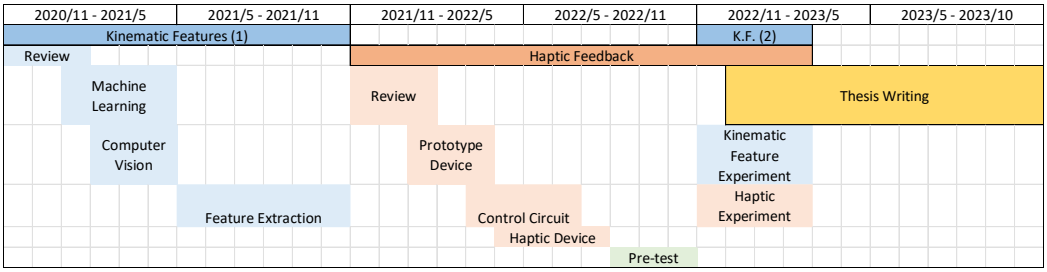

Figure 1.1: Timeline overview of the research.

1.5 Contribution of the Research

This research contributes to the field of upper limb movement assessment in smoothness, which could potentially be applied in the area of post-stroke rehabilitation. This research also contributes to the human-machine interaction through haptic feedback, specifically the parameterisation and optimisation of the haptic input. The following items are of note in the contribution of this research:

- A low-cost portable haptic device that integrates directional guidance and movement smoothness assessment, potentially for post stroke patients, especially for the visually impaired.
- A novel human-machine interaction through haptic feedback with the existing rehabilitation robots for people with visual impairment.
- Kinematic features extracted from low-cost sensors for sensitive, objective, and continuous upper limb movement smoothness assessment, potentially beneficial for post-stroke rehabilitation in home environment and sports training.
- A sensitivity analysis of applied kinematic metrics through repetitive tasks.
- Supervised machine learning models based on kinematic features for movement type classification, movement smoothness classification and prediction throughout a repetitive process for monitoring the muscle learning progress, which can be beneficial for the design of personalised training sessions and rehabilitation interventions.
- The optimisation and parameterisation of the input signal characteristics and the vibration source for generating haptic directional cues based on asymmetric vibrations to improve user's confidence and sensation accuracy.

Despite the above contributions related to the main topic of this research, other work has also been achieved during the initial stage of the PhD, which are highlighted below.

- A computer vision-based gesture recognition and position tracking algorithm specifically built for poststroke serious game development, which enables bilateral training for patients and supports kinematic feature extractions.
- A serious game for poststroke rehabilitation developed by Unity3D using computer vision gesture recognition as a control method for the training of upper limb and hand/finger movements.

1.6 Outlines of the Thesis

The thesis is split into 6 sections, with three sections addressing research questions related to computer vision, kinematic assessment, and haptic feedback, respectively and the others considering the introduction, literature review and conclusions. The structure of the thesis is shown in Figure 1.2.

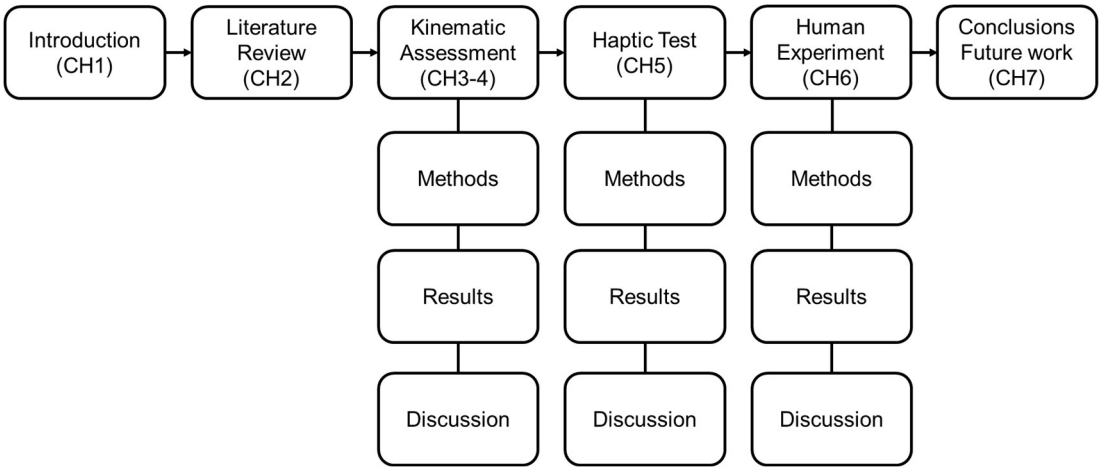

Figure 1.2: Thesis structure overview.

1.7 Summary

Upper limb movements are necessary and essential part of activities of daily living. Various neurological conditions would impact the function of upper limb movements. Repetitive training during the rehabilitation process would help patients re-gain such ability. Additionally, upper limb training sessions also require repetitive movements for improved muscle strength and endurance. Therefore, an objective assessment among each repetition would benefit the design of a rehabilitation intervention and a training method. Specifically, movement smoothness assessment after stroke is important for optimising rehabilitation interventions for patients. Moreover, since most of the current robotic devices are vision-based, it is also

beneficial to study the delivery of haptic directional cues for visual-impaired patients.

The research proposed in this thesis focuses on the design and test of a low-cost hand-held device that integrates upper limb movement smoothness assessment and haptic directional feedback, potentially for visual-impaired patients after stroke. The method proposed in this study could also benefit the monitor of repetitive normal upper limb movements.

In order to achieve this, the existing kinematic assessment method on upper limb smoothness and haptic actuation method need to be explored. This requires a comprehensive knowledge on the extraction of kinematic features and the control and optimisation of the haptic device. Specifically, the design of the device must integrate movement smoothness assessment and haptic feedback.

A supervised machine learning model will also be developed for classifying movement types, identifying subtle smoothness differences among movement repetitions, and potentially monitoring the compensation movement from other muscles.

Two independent experiments can be used to aid the design of the haptic device and the extraction of the kinematic features. The first experiment focuses on the verification of kinematic features in evaluating subtle smoothness differences in a repetitive upper limb movement. The second experiment focuses on the verification of the optimised haptic feedback for delivering a clearer haptic directional cue.

Chapter 2 Literature Review

2.1 Aim of the Literature Review

The purpose of this literature review is to summarise the state of the art regarding upper limb kinematic assessments, with a focus on poststroke with respect to the assessment task, assessment equipment and performance metrics with the potential as the input features for machine learning models. The use of kinematic assessment in other applications would also be reviewed for more comprehensive understanding of the topic. For the haptic feedback, the purpose is to summarise the generation mechanisms and the device design of the haptic directional cues. Subsequently, the potential of haptic applications in upper limb rehabilitation interventions are also studied.

2.2 Review Strategy

2.2.1 Review Strategy for Kinematic Assessments

With the interest of applying kinematic assessment potentially for post-stroke upper limb movement, a wide scoping search was undertaken to find relevant literatures in the area of upper limb rehabilitation assessments. The majority of studies are focused on stroke rehabilitation.

In order to formulate the proper research question, the following key points were considered based on a practical guidance published in [19].

- Research aim: The research is concerned with the subtle movement smoothness assessment on upper limb using kinematic features.
- Variables: The variable is different kinematic features. This includes the applications that use kinematic features as inputs for another system (e.g., machine learning models use kinematic assessments as input features).
- Comparison: Various types of other movement quality assessments (e.g., traditional clinical assessment, surface electromyography etc.).
- Outcome: The application of kinematic assessments is expected to objectively reflect the subtle improvements and distinguish between movement compensation and motor recovery. It is also possible to use the outcomes from kinematic assessments as the input for supervised machine learning data analysis.

The following research questions have been generated, informed by research aims, objectives and the above analysis to focus the literature search:

- Can the application of kinematic features and supervised machine learning models provide more sensitive and continuous smoothness assessment for upper limb movements compared to a traditional clinical assessment?
- What kinematic features have been used for the assessment of upper limb movement smoothness?
- What kinematic features have been applied to a supervised machine learning model for further data analysis and applications?
- Does a specific supervised machine learning model have a superior performance than other models?

In order to answer these research questions, a proper data collection and definition need to be designed. For each search result, information about the kinematic assessment is extracted. If the kinematic assessment is also used in a supervised machine learning model, it will be recorded. Additionally, the assessment task, assessment system will also be recorded to assist the design of the haptic device.

Assessment tasks are categorised into 5 groups based on the movement nature. Two-dimensional (2D) tasks in the horizontal plane includes 2D pointing (discrete movements to predefined targets) and 2D drawing (continuous movements to finish a pattern). Three-dimensional tasks (3D) include 3D pointing and 3D gasping (continuous movements with end effector manipulating objects). Tasks not belonging to any of the above will be categorised as other tasks. This process is also beneficial and inspirational for designing the haptic device since different movement types will require a unique haptic stimulus. For example, pointing movement requires single directional cues whereas drawing movement requires continuous and changing directional cues.

Assessment systems are categorised into 3 groups based on the level of support to the impaired limb. Group A includes the systems with minimum support to the impaired limb. For example, hand-held devices, inertial measurement unit (IMU), etc. Group B includes the systems with medium or partial support, such as systems with arm or shoulder support. Group C includes the system with maximum support, such as exoskeletons. This process can assist the design of the haptic device since it can be alone or to be an additional module added to a current rehabilitation robotic system.

A systematic search was conducted in PubMed, Scopus and IEEE Xplore. The keywords used for search in each database are ‘kinematic assessment’ AND ‘kinematic features’ AND ‘upper limb’ AND ‘rehabilitation’ OR ‘machine learning’. Only peer-reviewed journals and conference papers were included. The results from 2019 to 2023 were included.

2.2.2 Review Strategy for Haptic Feedback

The following key points were considered to formulate the research questions following the same guideline referenced above.

- Research aim: The research is concerned with the design of a haptic device that generates directional cues for movement guidance, potentially to be used in upper limb rehabilitation interventions for the visually impaired.
- Variable: The first variable is the input signal, including signal waveform, frequency, and other characteristics. The second variable is the form of the device, such as hand-held devices, wearable devices like a belt or a backpack etc.
- Comparison: The commonly used input signals and device form in other literatures.
- Outcome: The haptic directional cues are expected to be sensed by participants and the accuracy of the directional cues should be improved by optimising the input signal after signal parameterisation. The form of the device should be designed in such a way that it is suitable for independent use during upper limb rehabilitation interventions in a home environment.

The following research questions have been generated.

- What is the effect of different input signal characteristics on the perception of haptic directional cues in terms of perception accuracy and confidence?
- What combination of the input signal characteristics will generate the most feasible haptic directional cues? Or what is the most important signal characteristic for maximum perception accuracy and confidence?
- What kind of haptic generation mechanism and type of device that can benefit the upper limb rehabilitation in terms of directional guidance in a home environment?

For each search result, information about how to generate the haptic directional cues is extracted. Additionally, the design of the haptic device and the input signal characteristics are also recorded.

Haptic actuation is categorised into 3 groups based on the actuation mechanism. Mechanical actuation refers to the devices that use mechanical mechanism to generate haptic effect, such as linkages, springs and rotational inertia. Electrical actuation refers to the devices that use current to drive the motor to generate the haptic vibration, such as voice coil actuators, solenoids, DC motors and eccentric rotating mass (ERM) motors. Actuation mechanisms that do not belong to the above two types are grouped as others.

Haptic device is categorised into 3 groups based on the interactions between users and the device. Hand-held devices require users to grasp or hold the device that generates the vibrations. Wearable devices are attached on human body to stimulate a certain area such as a belt. Other interaction methods are grouped together as the third category such as a vibrotactile screen.

Input signal characteristics are recorded in terms of signal shape or waveform, signal frequency, duty ratio (if any) etc. If the actuation method is mechanical, signal characteristics are not recorded.

A further systematic search was conducted in PubMed, Scopus and IEEE Xplore. The keywords used for search in each database are ‘haptic’ AND ‘directional cues’ AND ‘feedback’ AND ‘assistive device’ OR ‘asymmetric vibrations’. Results from 2019 to 2023 are included. Notice that this research is focused on generating active haptic directional cues. Thus, any passive haptic sensations, such as roughness sensation and texture rendering, are excluded from the searching results.

2.3 Literature Search Results

2.3.1 Overview

The literature search gave 56 included studies for kinematic assessments and 51 included studies for haptic feedback as shown in Figure 2.1.

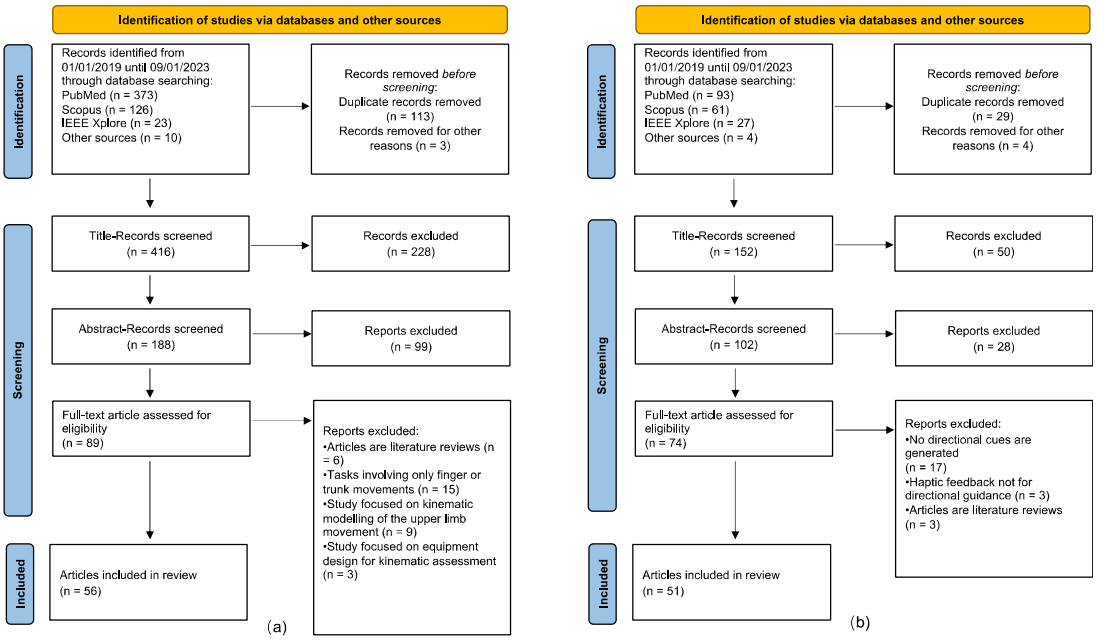

Figure 2.1: Literature search results for (a) kinematic assessment and (b) haptic feedback.

According to the assessment task classification defined in the review strategy, 22 studies used 2D pointing tasks, 8 studies used 2D drawing tasks, 18 studies used 3D pointing tasks, 4 used 3D gasping tasks and 4 used other tasks. Kinematic features were recorded with an assessment system of group A, B and C in 38, 14 and 4 studies, respectively. Kinematic features were mainly extracted from position sensors and inertial measurement units (IMU). Therefore, calculated kinematic features were based on distance and acceleration data. Velocity-based features were mainly extracted from position data (with proper sample rate and filters). However, some studies use acceleration data for integration though this process requires filter design and detrend process. Since some kinematic features were extracted for particular tasks and not being evaluated with clinical properties, Table 2.1 only shows the summary of the extracted kinematic features that were commonly used and evaluated with clinical properties.

Table 2.1 Summary of the kinematic features.

Distance	Velocity	Acceleration
Normalised path length	Peak velocity	Number of zero crossing
Endpoint error	Number of velocity peaks	Normalised jerk
Trajectory error	Mean velocity	Normalised mean acceleration
Distance travelled	Spectral arc length	Peak acceleration

Figure 2.2 shows the overview of the literature search results on kinematic assessment type and assessment equipment.

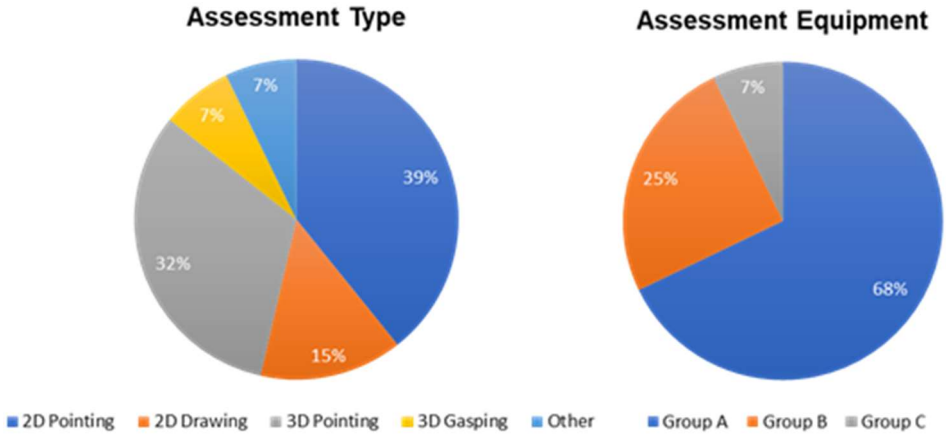

Figure 2.2: Overview of the literature search results on kinematic assessments.

For the haptic directional feedback, according to the haptic actuation method, 42 studies used electrical actuations, 7 studies used mechanical actuations and 2 used other actuation methods. Haptic feedback was delivered by a haptic device of hand-held and wearable in 32 and 12 studies, respectively. 7 studies used a touch screen or similar device for haptic delivery. Figure 2.3 shows the overview of the literature search results on haptic actuation and haptic equipment.

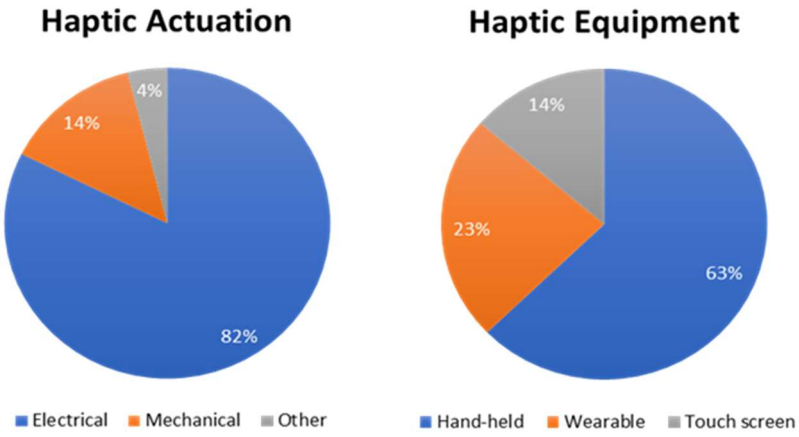

Figure 2.3: Overview of the literature search results on haptic feedback.

The characteristics of input signal depend on different actuation designs and motor types. However, actuation frequency is important for every signal since human skins are only able to sense haptic directional cues by the Meissner corpuscles with movement frequency under 60 Hz [17]. Vibrations with higher frequencies would result to a sensation of normal vibrations.

2.3.2 Kinematic Feature Extraction

This section refers to research objective (c):

To extract kinematic features from low-cost sensors that will be adopted to assess the movement quality, specifically the change of smoothness in each repetition.

Traditional clinical assessments are reliable but not sensitive enough to reflect subtle improvements [20]. Moreover, these assessments are subjective since they are usually conducted by physiotherapists in a certain setup [21]. Finally, the use of ordinal scale [22] is not continuous. Therefore, it lacks the ability to reflect long-term recovery progress. To overcome these drawbacks, kinematic features have been extracted from sensor data to objectively present subtle improvement.

To thoroughly describe a movement quality, features have been grouped and divided into different categories. For example, accuracy measurements describe how accurate poststroke patients can aim. A machine learning model has been trained in [23] using the combination of endpoint error and other features to predict the Fugl-Meyer Assessment (FMA-UE) score. Instead of studying point accuracy, normalised path length [24] calculated the ratio between the shortest point-to-point distance and the actual distance travelled by upper limb to reflect accuracy. The actual distance travelled by the end effector [25] can also be used independently as another accuracy measurement. Other accuracy measurements like axes ratio [26] and

movement end direction [26] have also been applied but without proper clinical evaluations.

Apart from accuracy, smoothness is another essential category to assess movement quality. Movement from poststroke patients can be treated as the sum of various sub-movements. A smoother movement always have a smaller number of sub-movements. Therefore, number of velocity peaks [27-29] have been used widely and evaluated by numerous research for smoothness assessment. It can also be used to train a machine learning model for progress monitor and clinical score prediction [30]. However, velocity profiles require certain computational process before it could be used to extract kinematic features, such as a trend removal process to minimise the effect of a linear trend, a bypass or low-pass filter to reduce the effect of measuring noise and compensatory movements from other muscles and a differentiation process from the position data. The number of acceleration zero crossings [31] can overcome this drawback since acceleration data can be easily captured from a wearable inertial measurement unit (IMU) and only require simple filtering process. From the acceleration profile, the duration and the frequency [32] of the sub-movement can also be derived for smoothness measurement. Other velocity-based smoothness assessment includes normalised mean velocity [33] in time domain and the spectral arc length [27] of the velocity profile in frequency domain. Normalised jerk is also an important measurement for smoothness quantification. It has been verified with clinical assessment scores in [24] although it is only suitable for point-to-point movement [34]. Therefore, it could be used as a gold standard for the validation of other kinematic features from the clinical point of view.

2.3.3 Application of Machine Learning

This section refers to research object (d):

To develop and train a machine learning model that can predict the motor learning progress and classify the above movement quality for optimised upper limb movement assessment in smoothness.

Machine learning can be a powerful tool for analysing kinematic data. There exists a large amount of research using machine learning models to predict the clinical scores for post-stroke patients. However, there are few papers of relevance that study the suitability of a specific machine learning model in the application of rehabilitation movement assessment. This is due to the

diversity of machine learning models. Each model has its own advantages over the others when processing data features.

Support Vector Machine (SVM) is a supervised machine learning model that is particularly suitable for performing classification tasks over small to medium data set. In [35], a SVM model was trained to accurately classify finger movement quality into user-defined groups based on finger peak angle and peak velocity. Instead of using pre-defined classes, Fugl-Meyer Assessment (FMA) score was also successfully predicted by a SVM in [36] using full body key points kinematics. In the above research, SVM were applied on data collected from kinematic sensors (i.e., sensors that collect kinematic information). Kinematic sensors can be low-cost and easy to use independently by patients in a home environment, which is ideal for the research aiming at convenience and performance. SVM had also been applied in poststroke bilateral hand training programme using electromyography for hand gesture recognition [37]. The use of electromyography enables a new interaction between patients and robotic devices. However, the attachment of electromyography sensors requires specialised skills in order to capture the signal from the correct muscle groups. This significantly impedes the suitability of electromyography in a home environment and independent measurement.

Other machine learning models like Random Forest (RF) [38] and deep neural network (DNN) [39] were also applied for upper extremity measurement. Notice that the feature selection process is very important for machine learning models. The same model will generate different training results based on different features. In [38], the flattened feature set (every kinematic feature) outperformed the range of motion (only include features that reflect the range of motion) feature set by 6% on average for the same machine learning model.

Recent research also applied unsupervised machine learning techniques to automatically extract new features from kinematic data for building the evaluation model of patients' progress [40]. Unlike supervised learning models, unsupervised models do not need pre-defined labels for training. This feature makes unsupervised models time efficient. However, in this research, only supervised models will be discussed since unsupervised models require more powerful machine learning techniques that are not included in the main research aim and a much bigger dataset which is difficult to collect during the given time.

2.3.4 Other Applications

The kinematic assessment offers precise and objective insights into motor strategies linked to goal-oriented tasks, and it enables monitoring of therapeutic techniques applied to the upper extremity. In the last two decades, many kinematic assessments have been performed in a laboratory environment to quantify the upper extremity among healthy subjects [41-43], and people with stroke, cerebral palsy [44, 45] and spinal cord injury [46]. For such kinematic assessment in the clinical environment, an important component is the sensitivity of kinematic metrics in describing the rehabilitation outcome. In [47], the responsiveness for kinematic metrics during drinking were analysed, and clinically meaningful improvements and discriminations were identified in movement time, smoothness and trunk displacement.

Apart from applying kinematic assessment for rehabilitation purposes, kinematic assessment has also been developed in other fields. Work-related musculoskeletal disorders and muscle fatigue associated with repetitive work has been identified as a major health problem. Kinematic assessment has the potential to reflect the fatiguing process during such repetitive work. In [48], mean and variability of joint angles were recorded by a motion capture system in a laboratory environment. The study shows that the kinematic measurements differ between fatigued muscles and un-fatigued muscles. In [49], the subtle differences between men and women upper limb muscle fatigue progress were recognised by kinematic assessments. Both research show sufficient sensitivity in describing subtle movement differences. Kinematic assessment has also been applied to several sports analysis such as boxing [50], tennis [51] and cricket bowling [52] to improve athletes' performance and prevent from injuries.

2.3.5 Haptic Directional Cues

This section refers to research object (e) and (f):

To design and build a portable haptic device integrating movement assessment to present haptic directional cues in a 2D plane.

To optimise control signals for the haptic source to allow subjects to interact with improved resolution and accuracy.

Haptic devices have been widely used in our daily life activities such as a mobile phone and a gaming console. In this study, haptic is defined as the touch sensation provided by mass vibrations. The texture and roughness sensation are not of research interest for this thesis.

Most daily haptic feedback does not have the ability to present directional cues since normal vibrations can only present transient alert haptic sensations. However, multiple haptic actuators can solve this problem by sequentially starting each motor in a certain order. In [53], 60 haptic actuators (5×12 array) was developed to present 2 degree-of-freedom (DOF) information on the torso area. The same idea was also applied to the back area in [54]. This multiple actuator solution can achieve a higher accuracy with a greater number of actuators attached. However, this array system requires a large contact area to work. As a consequence, it is difficult to integrate multiple haptic actuators on restricted skin area such as hands locally. Additionally, there exists additional learning cost for the array systems on how to map local directions (i.e., sensed by local muscle groups and tendons) to the world coordinate frame (e.g., the direction of an outdoor walking activity).

To address these problems, a novel method was proposed in [55, 56] where a haptic directional cue was created through asymmetric vibrations of a mass, specifically from a mechanical slider-crank mechanism. They proposed that both amplitude and frequency of the vibration affected the perceptibility of directional cues. They also claimed that this directional cue was due to a virtual force rather than the existence of a physical force. The same asymmetric vibration was also successfully created in [57] by a mass-spring system. Though these systems require less actuators and no coordinate transfer, their mechanical designs are not particularly suitable for portable rehabilitation device due to a relatively heavy weight and the durability of the mechanical connection.

In [58], instead of using mechanical mechanisms, an asymmetric input signal was used to drive a linear resonant actuator. The same idea was implemented in [59] with a voice coil actuator. They both found that driving frequency of the input signal significantly affected the perceptibility of directional cues. Moreover, the ideal frequency depends highly on the dynamic performance of the vibration system. Therefore, it is worthwhile to study the dynamic model of the haptic system and optimise the characteristics of input signals for each unique haptic implementation. In [60], a 2 degree-of-freedom mass-spring-damper system was created to model the force and skin displacement when holding the haptic device. It was confirmed in this study that the perception of haptic cues is achieved by a measurable physical force rather than a virtual force. The results showed that an asymmetric input signal with frequency between 30 Hz and 58.8 Hz

could provide the best pulling sensations for their device. Apart from asymmetric signals, Pulse Width Modulation (PWM) signal was also applied in [61] to drive a linear solenoid to generate measurable asymmetric accelerations. This also proved the idea that the pulling sensation is caused by a physical force rather than a virtual force. In the above designs, asymmetric vibrations can only induce bidirectional cues along a certain axis instead of a plane. Therefore, it is beneficial to design a mechanism that could extend directional cues to another degree of freedom.

2.4 Literature Discussion

The purpose of the literature review was to synthesis current research in the area of kinematic assessment and movement guidance for upper limb movements, specifically through a haptic device, and identify gaps and limitations in the research.

There are an enormous range of kinematic features describing movement quality from multiple dimensions, including accuracy, efficiency and smoothness etc. However, most kinematic features were measured by sophisticated robotic systems that are not suitable for a home setup or independent use. Some features showed excellent correlations with patients' improving performance but lack the validity against clinical scores. Additionally, current research lacks discussions on the sensitivity of kinematic features in the field of upper limb rehabilitation, such as how subtle can kinematic features describe an upper limb movement motor learning progress with or without the help of machine learning techniques. The normalised jerk is one clinically-validated feature to describe movement smoothness, and it has been applied to sufficient research for validations based on the literature review results. Therefore, this feature will be compared with other kinematic features extracted in this work to assess the sensitivity of describing movement smoothness.

Recent research also applied various supervised machine learning models to predict patients' clinical score using kinematic features though the results depended highly on the feature selection process. Unsupervised machine learning models have been deployed to automatically extract potential features for performance monitoring as well. This could be a future research direction. A similar example is the training of intelligent models. For an artificial intelligence (AI) model training and labelling such as ChatGPT, there is a rapid increase in the demand of prompt engineers [62]. However, with the help of unsupervised and supervised machine learning techniques,

the performance of the model was increased and the computational cost of the training process was decreased as reported in [63]. It is therefore hypothesised that similar techniques could be used for automatic kinematic feature extraction for upper limb movement assessment. In the present work, kinematic features will be used as inputs for supervised machine learning models. The output of the model depends on the classification task. For the movement type classification, the outputs are the numbers representing different movements. For the movement smoothness assessment, the outputs are the repetition of a single movement. A higher sensitivity in reflecting subtle smoothness differences would be achieved with a higher number of repetitions.

To provide directional guidance to the visually impaired during a robot-assisted rehabilitation session, haptic directional cues were studied. Haptic directional cues can be generated by different actuation methods. Multi-actuators method only works with large contact area such as back and torso due to the inevitable large area for motor implementations. Mechanical devices with asymmetric vibrations are not beneficial for portable design because of their weights and sizes. Asymmetric input signal can drive a motor to generate asymmetric vibrations. This actuation method allows more control over mechanical actuation and can also be integrated into a smaller device that is suitable for both portability and home-based application. However, the characteristics apart from signal frequency needs to be studied with a large-scale human experiment. Moreover, the input signal that generates asymmetric vibrations lacks proper parameterisation for repeatability test and simulations. Although some work has been done in terms of haptic out parameterisation in [64], their work was limited by the availability of motor dynamic constant such as motor driving factor, linear stiffness and the damping coefficient of the spring inside the motor. Without experimentally determining these values, the simulation and optimisation method proposed in the above reference is difficult to be conducted.

A portable low-cost rehabilitation device with the capability in movement smoothness assessment and directional guidance is possible by combining machine learning based algorithms from the software level with the haptic directional guidance from the hardware level. Though there were various types of wearable haptic guidance implementations that have been proved to be effective as introduced in the above section, they do not target at the sensitive skin receptors located on human fingertips nor have integrated movement smoothness assessment function, potentially for post-stroke

patients. Therefore, it is beneficial to design a hand-held device rather than a wearable device that targets at the fingertip, produces haptic directional cues that are more feasible to users and integrates upper limb movement smoothness assessment. Since the proposed haptic device can only provide 2D directional information, it is recommended to integrate a low-cost 2D position tracking technique for movement smoothness assessment based on position, velocity, acceleration, and jerk features. Though it is possible to differentiate position profiles for velocity, acceleration and jerk performance, extensive pre-processing procedures are mandatory including filtering, smoothing, linear trend removals and outlier removals. Therefore, an alternative for measuring acceleration and jerk during a movement is through the implementation of a low-cost inertial measurement unit (IMU). The complexity of data processing required for only acceleration data is decreased significantly since only filtering process is necessary. This is extremely helpful if the power consumption of the portable device is limited by the battery and the data is processed locally.

2.5 Summary

Review of the literature has shown that there has been a lot of attempts on the extraction of kinematic features and their applications with various machine learning models, both supervised and unsupervised. However, the capture of data requires robotic devices that are not particularly suitable for a home environment and independent use. The most adopted movement assessment method is achieved by 2D pointing tasks and the most adopted movement assessment equipment is with minimum support to the impaired arm. Kinematic features were extracted from displacement, velocity, and acceleration measurements. Specifically, features listed in Table 2.1 have been verified with clinical properties by the existing literatures. Additionally, various features were adopted only for a particular task and lack the ability for generalisation for other upper limb activities. Some supervised machine learning models have been applied to classify movement type and quality. However, the performance of the machine learning models depends highly on the feature selection process. Therefore, unsupervised machine learning models were developed for auto feature selection. It is valuable to study the sensitivity of kinematic feature-machine learning approach on how subtle it can reflect the smoothness difference during an upper limb motor function learning progress.

For haptic devices, studies focused more on the device designs and actuation methods. Though the frequency and amplitude have been raised to enhance the perceptibility of directional cues, other characteristics of the input signals are of low interests and lack parameterisation. Some research works have been conducted to parameterise the input signal based on the simulations on acceleration output. But this parameterisation method lacks the translatability to other haptic implementations due to the uncertainty of the system dynamic constants. The most adopted form of haptic equipment is hand-held device, and the most adopted actuation method is through electrical motors. Recent research focused on asymmetric vibrations for better haptic delivery because of the improved configurability. There are few haptic devices suitable for home rehabilitation integrating movement assessment and directional guidance.

Chapter 3 Methods and Experimental Designs – Movement Smoothness

The extraction of kinematic features is normally conducted on position, velocity, acceleration, and jerk profiles as introduced in the literature review. Therefore, tracking the position of upper limbs during a movement is the basis for kinematic assessment. One of the most common position tracking methods in daily life is to use a mouse to control a curser on a computer screen. Additionally, movement trajectory could also be extracted with the help of modern computer vision algorithm. It is therefore hypothesised that these methods could be extended to track the 2D movements of an upper limb for the extraction of kinematic features.

In this chapter, two experiments were firstly designed to verify the function of movement position tracking. Two novel position tracking methods using a regular mouse sensor and a single-camera vision system were compared with Optotrak Certus position measurement system (hereinafter referred as Optotrak), which underpinned the foundation on an alternative low-cost position tracking method for a portable haptic rehabilitation device in home environments. The Optotrak is developed by Northern Digital© (NDI) for kinetic and kinematic measurement with a reported resolution of 0.01 mm and an accuracy of 0.1 mm [65]. It adopts active optical measurement for positions and orientations of several markers within a large pre-calibrated measurement volume of 20 m^3. It could be used as a gold standard to validate the other two position tracking methods.

Another two experiments were then conducted for movement type classifications and movement smoothness assessments based on the kinematic features extracted from the above-mentioned position measurements. A movement type classification algorithm based on acceleration data was developed, which was verified through four different movements conducted by the author. A single group observational experiment was finally conducted with 14 participants recruited within the University of Leeds to verify the movement smoothness assessment using kinematic features extracted from displacement, velocity, acceleration, and jerk data.

The remainder of this chapter is organised as follows. Section 3.1 introduces the equipment and experimental verification of position tracking using a mouse sensor. Section 3.2 introduces a position tracking method by a single

camera based on computer vision. Section 3.3 presents kinematic features for movement pattern classification. Section 3.4 presents kinematic features for movement smoothness classification. A single group observational experiment is also designed in this section. Section 3.5 presents the summary.

3.1 Mouse Position Tracking

Previous rehabilitation robots adopted rotary encoders or potentiometers for angle measurements and use kinematics to obtain the current position of user's limb [66]. This method is accurate and responsive, which makes it especially suitable for robot control algorithms and movement assessment. However, it always requires a sophisticated robotic device to assist user's movements, which is not particularly suitable for at-home rehabilitation environment due to the volume and price of the device and the operation complexity. Other position tracking techniques also include the application of computer vision such as a dual camera vision system [67] and advanced position sensors [68], which can be very expensive and requires calibration process before use.

Since the movement quality assessment will only be conducted in the 2D plane with the proposed hand-held device, it is beneficial to integrate a low-cost mouse position tracking sensor into the device. A mouse sensor has the following advantages over other position tracking methods. Firstly, it is a low-cost sensor that can be easily found on the market. Secondly, it is small in the volume and easy to operate with very fast learning curve for users. Finally, it does not require any calibration process or expert knowledge for operation. Though it is impossible for a mouse sensor to track rotational information and vertical information perpendicular to the working plane, its accuracy and response time are considered adequate for non-rotational movement assessment. Furthermore, although the position data measured by a mouse sensor is relative rather than absolute to a certain starting point like Optotrak, the same kinematic feature extraction process could be followed since the feature calculations are not influenced by the relative positions.

3.1.1 Experiment Procedures

In order to verify the accuracy and response time of a mouse sensor, a comparison was conducted between Optotrak position sensor and a mouse sensor. A seven-segment point to point triangle movement was chosen for

the verification process as shown in Figure 3.1. The numbers shown in the figure indicates the order for each point to be reached in the experiment. The participant was expected to use a mouse to draw the pattern on the same computer screen for 10 times with a Optotrak position sensor attached to the wrist for further verifications. The mouse was set to have a very low sensitivity (DPI = 200) to prevent compensatory movement from wrist rotations. The position of the Optotrak sensor remained unchanged throughout the experiment, and the compensatory movement from trunk was restricted in order to control the test-retest variability. This experiment was conducted by the author himself at the Rehabilitation Laboratory, University of Leeds, Leeds. No ethical approval was needed for this experiment since the author himself is a part of the research team.

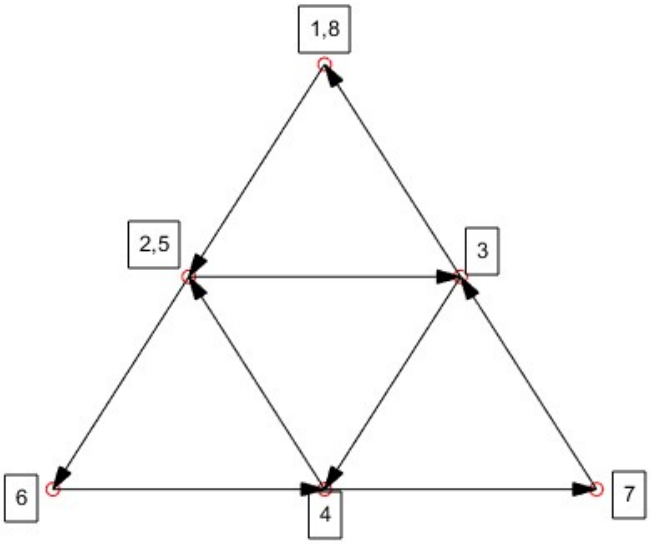

Figure 3.1 Seven-segment point-to-point triangle movement pattern.

This pattern was chosen because it involves multiple point-to-point movements which require muscle coordination and fine motor control. Therefore, this multi-segment triangle movement could better represent the complexity of the activities of daily living (ADL) than a single point-to-point movement such as reaching movement.

The triangle movement pattern was repeated for $N_t = 10$ times in a $T_m = 30$ seconds window length for each attempt. A one-minute rest time was introduced between each attempt to minimise the learning effect. The participant (the author) was aged 24 with no arm impairment at the experiment.

3.1.2 Data Processing

The position of a wireless mouse sensor (Logitech Hero 25k) on a computer screen (resolution of 3800×2400 pixels) was recorded by a self-written

MATLAB (MathWorks, version R2022b) script sampling at $f_{mm} = 100$ Hz. An Optotrak position marker was also attached on the user's wrist about 20 cm distal away from the elbow. The position data of the marker were recorded using the Optotrak system. Data of the marker were captured using the NDI software and stored in CSV files for data processing. The sampling frequency of the system was set to $f_{mo} = 100$ Hz with a reported accuracy of $\pm$ 0.1 mm and a reported resolution of $\pm$ 0.01 mm.

The 2D coordinates of the marker and the 2D coordinates of the mouse sensor were processed in a self-written MATLAB script. Since mouse sensor tracking was achieved in a MATLAB programme, a calibration on the actual sampling frequency f_{mma} was conducted for the same duration as the measurement window length T_m. The movement onset $index_{on}$ and offset $index_{off}$ were determined through a self-written algorithm that repeatedly check the difference between D measurements among a total number of N_p position data against a threshold value $P_{on/off}$ as described in Table 3.1.

Table 3.1 Description on the segmentation algorithm.

$$\boldsymbol{for}\ i = [1, N_t]\ and\ \boldsymbol{for}\ j = \left[1, N_p - D\right]$$

$$\boldsymbol{if}\ |P(i, j + D) - P(i, j)| \geq P_{on/off}$$

$$index(i, j) = j + D$$

$$index_{off}(i) = j + D$$

$$index_{on}(i) = find(index(i, j) \neq 0, 1)$$

$$\boldsymbol{return}\ index_{on}(i), index_{off}(i)$$

A proper threshold value should satisfy the following two conditions:

1) Be robust enough to ignore measurement errors for both systems.
2) Be subtle enough to capture the proper onset and offset points.

The position data segments along each axis were transformed into movement velocity and acceleration using a first order central difference technique. Before each differentiation process, a low-pass filter with a cut-off frequency $f_c = 6$ Hz and a moving average filter with a window length of L_{ma} were applied to remove any high frequency measurement noise. The cut-off frequency for the low-pass filter was determined since the triangle movement shown in Figure 3.1 is a relatively low-frequency movement. The window length L_{ma} for the moving average filter was calculated by Eq. 3.1.

$$L_{ma} = \frac{f_m}{10} \tag{3.1}$$

where: f_m is the measurement frequency for Optotrak and the calibrated frequency of mouse sensor, respectively.

Since Optotrak measurement and mouse sensor measurement have different units and scaling, a z-normalisation method was applied to displacement, velocity, and acceleration profiles to enable direct comparisons and error computing. Root mean square errors (RMSE) were calculated between the normalised Optotrak measurements and mouse sensor measurements. Since the triangle pattern was also used for the later observational study regarding upper limb movement quality assessment, the same set of kinematic features were also extracted from the mouse position data. The method for feature extraction would be discussed in section 3.4.2. A two-sample t-test would be conducted on each kinematic feature from two measurement systems to determine the significance level of difference.

Additionally, the test-retest reliability was verified by intra-class coefficient (ICC A, 1) with two-way random absolute agreement definition among 10 attempts over the kinematic features and RMSEs on displacement, velocity, and acceleration profiles. Since the aim of this verification was to examine how strong the agreement between each attempt but not the potential linear relationship, the absolute agreement definition was chosen. The results of this part of the work are presented in section 4.1.

3.2 Single-Camera Position Tracking

Computer vision has been proved to be an effective tool for position tracking in various industries [69, 70] including upper limb rehabilitation assessment. And it has been applied in the early-stage work to track the key points of a hand. It contributes to the telerehabilitation because it does not require the presence of users in a specific experimental environment. This section presents the application of an open-source vision algorithm for position tracking by a single camera system. The method was verified using a single pendulum system against Optotrak measuring system.

3.2.1 Computer Vision Algorithm

OpenCV (Open Source Computer Vision) is an open-source algorithm for computer vision. For the single camera position tracking in this research, a separation of the green pendulum from background environment was needed. Therefore, a colour-based tracking method was adopted,

specifically using the same Back Projection method as introduced in the early-stage work.

The commonly adopted image format is JPEG that stores the image colour information of pixels in red, green, and blue (RGB). However, a slight change in the lighting condition could result to a huge difference in RGB values. Therefore, a RGB image was firstly converted to HSV (Hue, Saturation, Value) image. Hue is the dominant colour recognised by human eyes such as red, green, and blue. Saturation is the amount of white light assorted with hue. A larger saturation value means more colourfulness. Value is the brightness. After the colour conversion, the region of interest (ROI) was selected. In this experiment, the ROI was the single pendulum. A colour histogram of the ROI was finally calculated to detect the similar colour area from background environment. A colour histogram is a figure to plot the pixel value against the number of pixels that have the corresponding pixel value. The colour segmentation algorithm is illustrated in Figure 3.2 using the green object as the ROI.

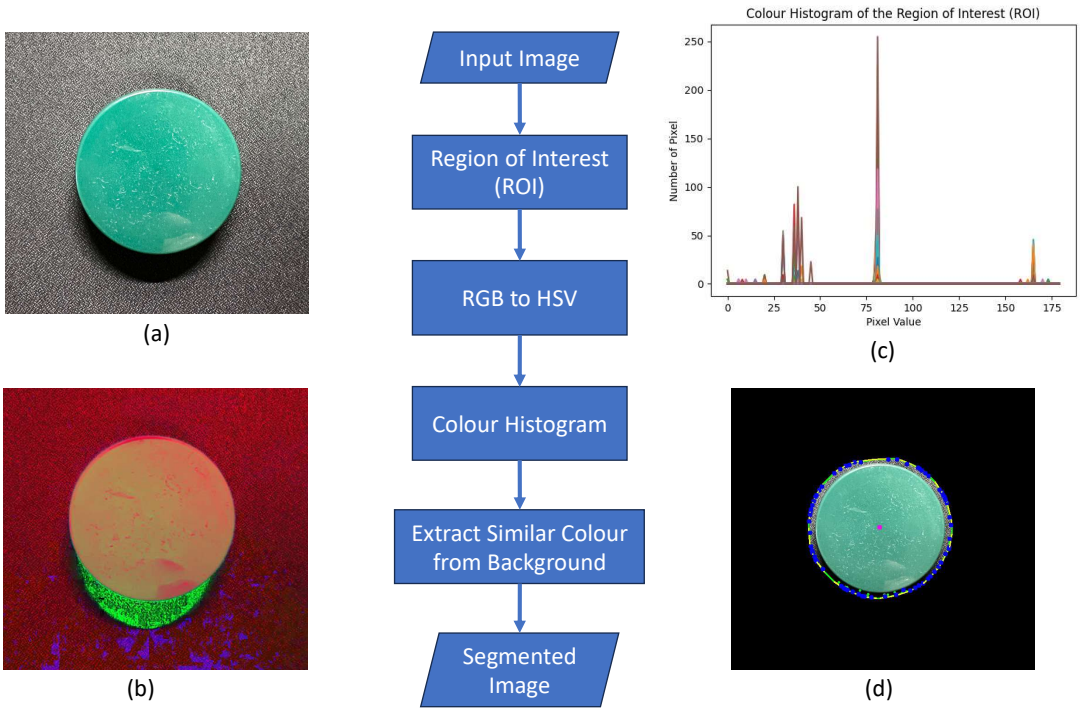

Figure 3.2 Back projection colour segmentation algorithm. (a) RGB image. (b) HSV image. (c) Colour histogram. (d) Segmented image with contour and centre.

3.2.2 Experiment Procedures

A single pendulum was used to verify the position recorded by the single camera vision system and Optotrak as shown in Figure 3.3.

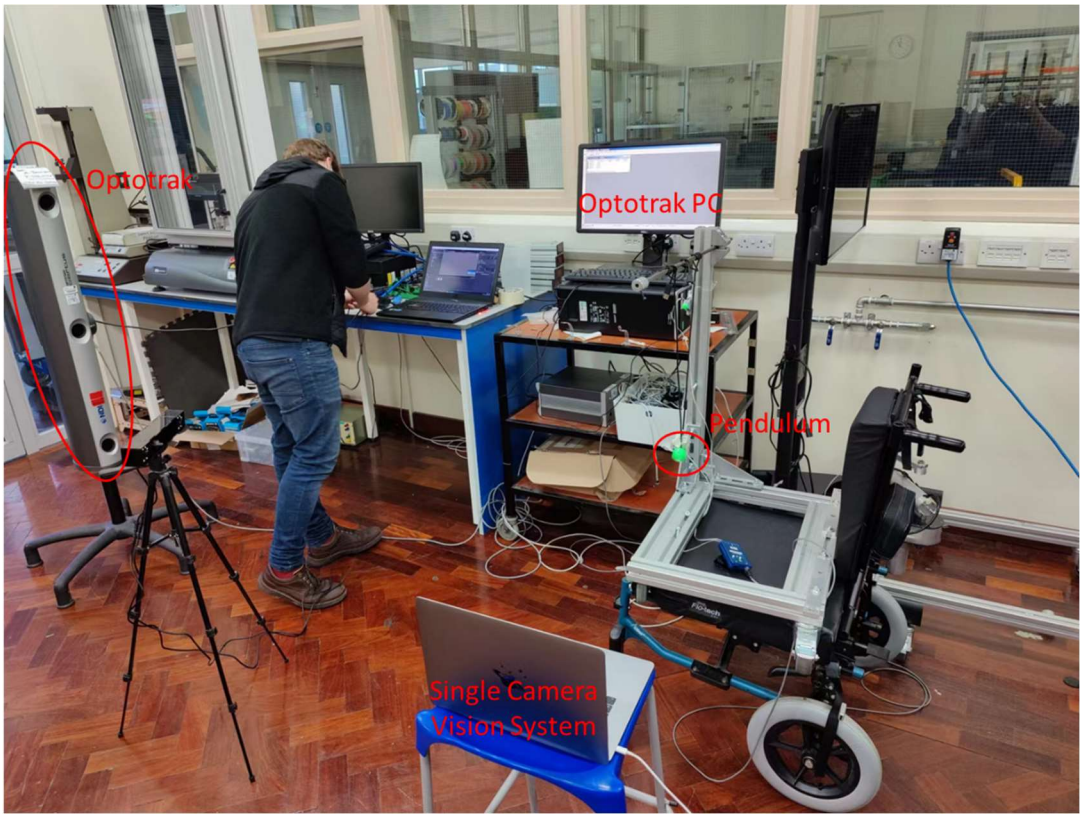

Figure 3.3 Single-camera based position tracking using a single pendulum.

A single camera vision system was placed at l cm away from the pendulum. Since there exists a minimum working distance related to the single camera's focus ability for the vision system, the distance l was set incrementally from 40 cm to 70 cm with an increment of 5 cm. When both systems were ready for recording, the pendulum would be released freely from a certain height manually. Since the aim of the experiment is to compare the position recorded by both system (i.e., system agreement), the height at which the pendulum was released was not recorded and kept random throughout the experiment. Both systems would stop recording the position when the pendulum was in the idle state. A total of 15 pendulum cycles were recorded at each distance.

3.2.3 Data Processing

The camera used in the experiment was a laptop camera (720P FaceTime Camera). An open-source computer vision algorithm (OpenCV) was implemented on the laptop for position tracking. Optotrak position data was captured on the Optotrak PC by the NDI software. The data from both measurement systems was stored in CSV files. Raw data was processed by a self-written MATLAB (MathWorks, version R2021a) script. The sampling frequency of Optotrak was set to $f_{mo} = 100$ Hz. The sampling frequency of

the vision system was set to $f_{mv} = 30$ Hz due to the limitations by the refresh rate of the camera and the screen.

The root mean square error (RMSE) was computed between Optotrak measurements and the vision system measurements. It was normalised by the movement range D_r. The movement onset and offset were determined manually by observations in the Optotrak measurement profiles. The movement onset and offset in the vision system measurements were then determined using the corresponding movement duration extracted from the Optotrak measurements.

Additionally, the test-retest reliability at each distance among 15 measurements were verified using the intraclass corelation coefficient (ICC A, 1) with two-way random absolute agreement definition. The results of this part of the work are presented in section 4.2.

3.3 Movement Type Classification

Movement type classification is conducted for the following two reasons. First of all, identifying current movement could help regulate the sample frequency of the integrated sensors to obtain more battery life in a home environment. For example, when the device is placed still, such as during a charging period, decrease the sample frequency to save power. Whereas when a movement is detected, change to a corresponding sample frequency. Secondly, traditional rehabilitation assessments like Action Research Arm Test (ARAT) and Fugl-Meyer upper extremity assessment (FMA-UE) for stroke, and several recommended exercises for people living with Parkinson involve multiple movement types from 2D drawings to 3D manipulations [71, 72]. Our activities of daily living (ADL) also require multiple different movements to serve different purposes [73]. Since different movements require the cooperation and coordination from different muscle groups, it is beneficial to accurately classify movement types based on sensor data from the rehabilitation device before any movement smoothness assessment is conducted. Therefore, several supervised machine learning models were developed in this section to classify four movement types based on kinematic features extracted from movement accelerations. Notice that only acceleration-based features were discussed here in this section because of the government's restrictions on access to campus during the COVID-19, which prevented further access to Optotrak position tracking system. Although it is mathematically possible to integrate acceleration profiles for velocity and position data, the inevitable cumulative errors

introduced by the integration process also prevented further feature extraction process.

3.3.1 Experiment Procedures

Four movements were selected for the experiment, namely reaching out, turning keys, drawing circles, and drinking as shown in Figure 3.4. Reaching out and drawing circles could be considered as a 2D planar movements if the small vertical displacement is neglected while turning a key and drinking are strictly 3D movements.

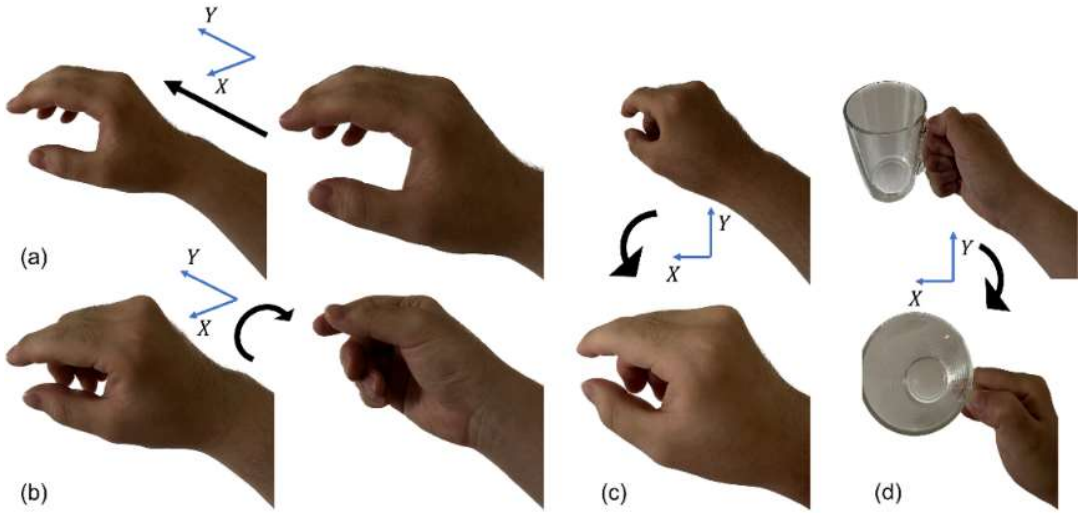

Figure 3.4 Four movement types including (a) reaching out, (b) turning a key, (c) drawing a full circle and (d) drinking.

The four movements require elbow internal/external rotation, shoulder extension and flexion, and wrist rotation, which cover the necessary movement for performing most activities of daily living (ADL). Therefore, they were selected for the verification of the movement classification method. The inter-attempt variability was controlled by a consistent sitting position of the participant, a consistent orientation and position of the sensor, and restriction on the compensatory movement from participant's trunk throughout the experiment. The restriction on the trunk was achieved by attaching the participant's back and the chair with a fastened string. This experiment was conducted by the author with his dominant arm in a home environment with the help of his neighbour due to the government restrictions on access to campus during COVID-19. No ethical approval was needed since the author himself was part of the research group.

During the experiment, each movement was conducted repeatedly for 60 seconds from reaching out to drinking. The first and the last attempt of each movement were excluded to obtain a stable and consistent performance during measurements. The movement onset and offset were determined

using the algorithm as described in Table 3.1. The participant was aged 22 with no arm impairment at the experiment.

3.3.2 Data Processing

An inertial measurement unit (LSM9DS1) was placed on the participant wrist about 20 cm distal away from the elbow by a Velcro fastener. The sensor data were collected by a microcontroller (Arduino Nano 33 BLE) through a USB cable. The sampling frequency of the sensor was set to $f_{sc} = 100$ Hz. Data from the sensor was sent to a PC via Bluetooth Low Energy (BLE) and stored in CSV files for data processing.

The collected data were processed in a self-written MATLAB script. A moving average filter with a window length of $L_c = 10$ calculated by Eq. 3.1 was applied to the raw data. A total of 20 segments were separated during the experiment for each movement type. Six kinematic features were extracted from acceleration profiles on each segment for each movement type, namely the maximum, minimum and average values, the mean square values, the wavelength and the zero crossing of the acceleration profiles as described from Eq. 3.2 to Eq. 3.5. These features were chosen since they have been reported to be efficient in kinematic assessment [74].

$$A_{max}, A_{min}, \bar{A} = \max(A_j), \min(A_j), \frac{\sum_{j=1}^{n} A_j}{n} \tag{3.2}$$

$$A_{ms} = \frac{\sqrt{\sum_{j=1}^{n} A_j^2}}{n} \tag{3.3}$$

$$WL = \sum_{j=1}^{n} |A_{j+1} - A_j| \tag{3.4}$$

$$ZC = \frac{|sgn(A_{j+1}) - sgn(A_j)|}{n} \tag{3.5}$$

where: A_j is the j^{th} value in each segment, and n is the total number of data points in each segment. sgn is a signum function as described in Eq. 3.6.

$$sgn = \begin{cases} 1, x > 0 \\ 0, x = 0 \\ -1, x < 0 \end{cases} \tag{3.6}$$

Six features were extracted from all three axes. Therefore, a total of 18 features were used to train and test the classification models.

3.3.3 Model Training and Evaluation

Four supervised machine learning models were selected for training and validation process, namely Support Vector Machine (SVM), K-Nearest Neighbours (KNN), Decision Trees and Deep Neural Network (DNN). These

four machine learning models were chosen since they are classic models for solving real-world classification problems for a long time in computer science and have been considered as a benchmark test. A 5-fold cross validation was adopted to prevent models from overfitting the training data. 30% of the dataset were separated as the test data set to verify the performance of the trained models.

Though 18 features were prepared prior to model training, a feature selection process using Minimum Redundancy Maximum Relevance (MRMR) algorithm [75] was also conducted for comparisons in terms of computational time and model performance. MRMR is a commonly adopted algorithm for machine learning feature selection process. The computational time on the model training may be effectively reduced after feature selection, which is beneficial for future online model applications. The hyperparameters of each model were optimised by a Bayesian optimiser with a maximum iteration of 30. Model performance was evaluated by F1 score and the area under the receiver operating characteristics (AUC). Results of this part of the work are presented in section 4.3.

3.4 Movement Smoothness Assessment

Traditional movement quality assessment mainly depends on the observations from experienced physicians during a series of assessment tasks, which lacks the sufficient sensitivity to detect subtle motor function improvements and has the potential to introduce examiner bias [76]. The applications of kinematic features have been proved by several studies to facilitate assessing movement quality objectively and sensitively [29, 77]. In the previous sections of this chapter, two novel position tracking methods (a mouse sensor and a computer vision algorithm) and a supervised machine learning approach on movement type classifications were presented to form the basis of movement quality assessment based on kinematic features. In this section, kinematic features were extracted to classify movement quality, specifically movement smoothness, into multiple categories using three supervised machine learning models. The maximum achievable number of categories is the total number of repetitions during the experiment. If a high number of categories is achieved, a high sensitivity in reflecting subtle smoothness differences of this method could be concluded. A single group observational study was conducted to evaluate the proposed method.

3.4.1 Experiment Procedures

This study was designed as an observational, single group study to classify motor learning progress, specifically movement smoothness, using the same multi-segment movement as shown in Figure 3.1. This movement pattern requires directional coordination and fine motor control from several muscle groups on upper limb. Therefore, it is a more realistic representation of activities of daily living (ADL) and was chosen as the movement pattern throughout different experiments reported in this thesis. A single Optotrak position marker was attached to participant's wrist to obtain the position data during the movements. The same marker was placed in the same position of participants throughout the experiment. The distance between Optotrak and its position marker varied slightly from different participants due to the posture difference and different habit in using a mouse. This had no effect on the kinematic feature extraction process since the process was conducted based on the relative positions during a movement rather than the absolute positions of each movement point. The experimental setup was illustrated in Figure 3.5.

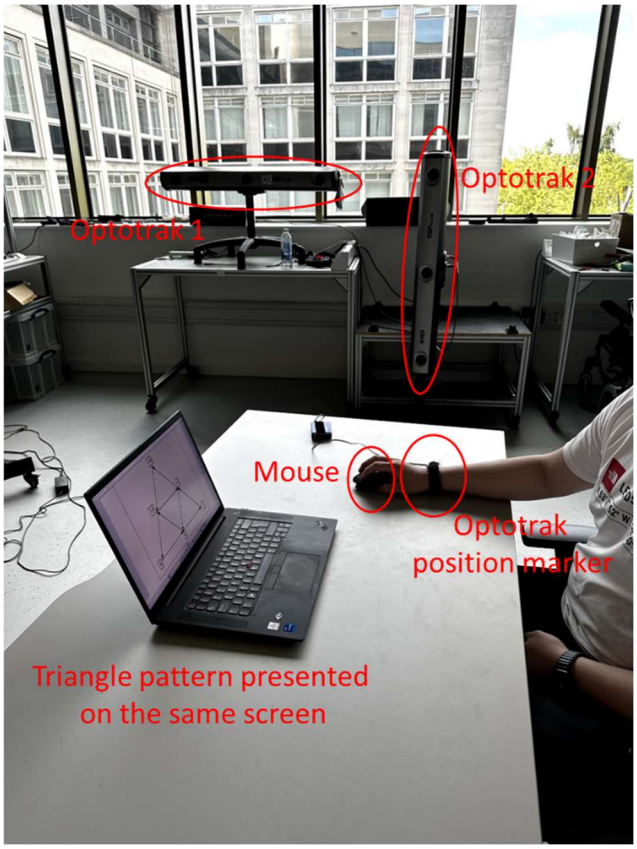

Figure 3.5 Experiment set up for movement quality classification using two Optotrak systems for a better coverage of detection.

During the experiment, participants were asked to use a mouse to draw the triangle pattern with their dominant arm (DA) and nondominant arm (NDA)

respectively. Two mouse orientations (i.e., 0-degree rotation and 180-degree rotation about the vertical axis perpendicular to the workspace) were also considered to increase the difficulty of the task so that a learning progress could be detected. Therefore, a total of 4 movement patterns were designed for each participant. The same mouse settings (i.e., Logitech Hero 25k with DPI = 200) and display settings (i.e., resolution of 3800×2400 pixels) used in the mouse position tracking experiment was also adopted in this experiment. Participants were asked to draw all the patterns with the same order in the experiment (i.e., DA+0-degree rotation, DA+180-degree rotation, NDA+0-degree rotation and NDA+180-degree rotation). Ten attempts were recorded for each movement pattern, and a five-second rest time was provided between each attempt. No feedback about the movement quality was given to any participants until the end of the experiment. A special circumstance was that if a participant did not follow the desired triangle trajectory continuously, the current attempt would not be included in the analysis. A new attempt would be asked in order to have the same number of attempts across different participants. The experiment procedure was shown in Figure 3.6. The study was approved by the Engineering and Physical Science Research Ethics Committee (MEEC 21-003). All participants gave written informed consent. The corresponding ethical review materials were presented in the Appendix.

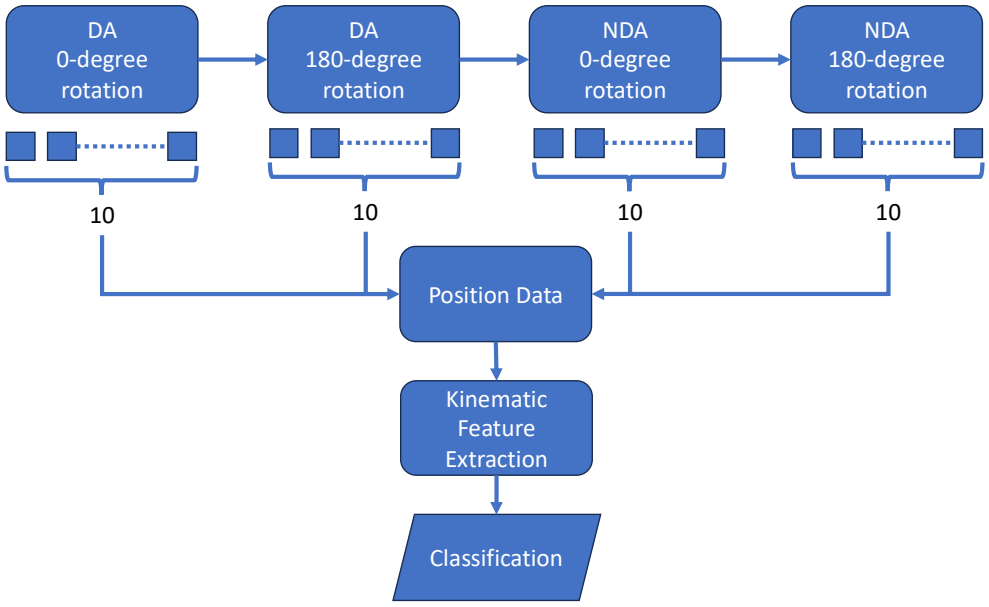

Figure 3.6 Experiment procedure for movement quality classification.

3.4.2 Data Processing and Feature Extraction

Position data were recorded using the two Optotrak systems with a position marker. A single position marker was placed on each participant's wrist on

either DA or NDA depending on the current movement pattern. Position data of the marker was recorded by the NDI software and stored in CSV files. The sampling frequency of the system was set to $f_{mo} = 100$ Hz with a reported accuracy of $\pm$ 0.1 mm and a resolution of $\pm$ 0.01 mm. Prior to the experiment, a 15-second calibration process was conducted for both Optotrak systems in order to validate the consistency between them. A Root Mean Square Error (RMSE) of 0.12 mm was obtained for position measurements between two systems, which is acceptable for kinematic feature extraction based on position profiles and the differentiation process to calculate velocity, acceleration, and jerk. During the experiment, a trained researcher (the author) monitored any data loss or system failure.

The position data of the marker were exported in multiple CSV files for data processing and kinematic features extraction. The velocity and acceleration profiles were calculated from the corresponding vector sum of the position data along each axis. The differentiation process was achieved by a first order central difference method. Before each differentiation process, a moving average filter with a window length of 20 data points was applied to smooth the kinematic profiles. This window length was chosen manually to achieve the ideal filter performance in terms of keeping most of the variability of the original data and removing additional measurement noise introduced by the system. Since the starting point and ending point of the movement in real-world coordinate were not restricted, a mouse position drift (e.g., the ending point was not overlapped with the starting point) was observed from all participants during the experiment. Therefore, a trend removal process was applied using a linear regression model to remove the linear trend in position, velocity, and acceleration profiles.

Since less-smooth movement is always consisted of several high frequency sub-movements, feature extraction process was conducted in both time domain and frequency domain. A total of 12 kinematic features were extracted from position, velocity, and acceleration profiles for each drawing attempt. These features were selected based on the previous literature search results where they have been applied to kinematic assessment for post-stroke and Parkinson's disease movement analysis. The movement onset and offset were determined manually by observations when there was a significant difference in position data. The observations were conducted by the same person for all kinematic profiles. Table 3.2 showed all kinematic features and their related profiles.

Table 3.2 Kinematic features extracted from different profiles.

Position	Velocity	Acceleration	Jerk
Distance Duration	Peak velocity Mean velocity Skewness Kurtosis Variance	Sample entropy Spectral entropy Number of peaks Peak acceleration	Normalised jerk

Kinematic features were defined below.

- Distance D (mm) is defined as the total distance travelled during each drawing attempt.
- Duration T (s) is defined as the time between movement onset and movement offset.
- Peak velocity V_p (mm/s) is defined as the maximum absolute velocity during each drawing.
- Mean velocity $\bar{V}$ (mm/s) is defined as the distance divided by the duration in Eq. 3.7.

$$\bar{V} = \frac{D}{T} \tag{3.7}$$

- Skewness S, kurtosis K and variance Var are defined as the corresponding statistics within the velocity profiles for each drawing attempt.
- Sample entropy $SampEn$ is defined as the measurement of the complexity [78] of the acceleration time series signal.
- Spectral entropy SE is defined as the measurement of signal's spectral power distribution [79].
- Number of peaks NOP is defined as the number of acceleration peaks in each drawing attempt.
- Peak acceleration A_p (mm/s^2) is defined as the maximum absolute acceleration during each drawing attempt.
- Normalised jerk NJ is defined as the measurement of movement smoothness [80] calculated by Eq. 3.8.

$$NJ = \sqrt{\frac{1}{2}\int_{t_{start}}^{t_{end}} J(t)^2 dt \times \frac{T^5}{L^2}} \tag{3.8}$$

where $J(t)$ is the third derivative of position (jerk), T is the movement duration, and L is the difference in position at time t_{start} and t_{end}.

3.4.3 Machine Learning Model Preparation

Extracted features were re-constructed for supervised machine learning model labelling and training. Seven supervised machine learning classifiers were tested for their performance, including the Support Vector Machine (SVM), K-Nearest Neighbours (KNN), Deep Neural Network (DNN), Tree, Ensemble, Naive Bayes, and Discriminant. The data preparation pipeline was shown in Figure 3.7.

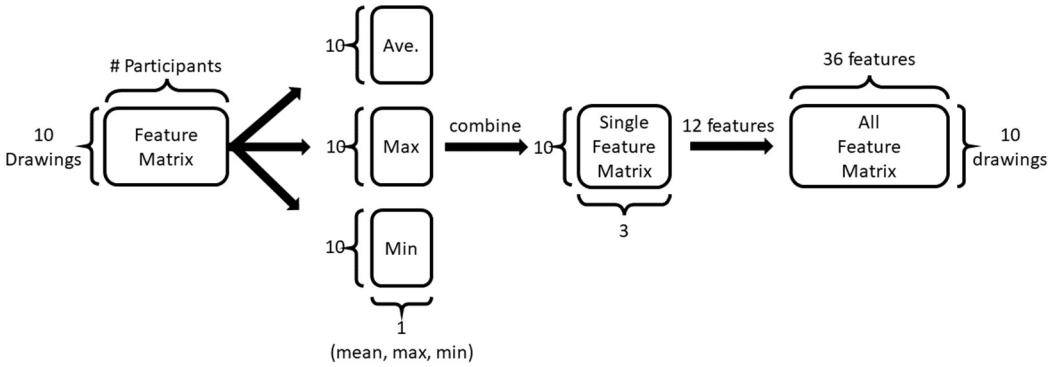

Figure 3.7 Data preparation pipeline for a single movement pattern.

Firstly, each kinematic features listed in Table 3.2 were extracted from all participants and all drawing attempts per movement pattern and were stored in the “Feature Matrix”. The average, maximum and minimum values for each attempt were then calculated and flattened to form the “Single Feature Matrix”. “All Feature Matrix” was finally constructed by combining all 12 features. An additional label column was also constructed at the end of “All Feature Matrix” in a numerical form.

Three labelling methods had been used independently to represent the different movement smoothness categories. The first label column had positive integers from 1 to 10, representing 10 different attempts (observations) into 10 different classes. The second label column had positive integers from 1 to 5, representing 10 attempts into 5 classes. The last label column had positive integers from 1 to 3, representing 10 attempts into 3 classes. For the first labelling method, the Discriminant classifier was not adopted since it requires more observations than the number of classes. Normally, it is more difficult for a machine learning model to classify more numbers of classes for a given dataset. If a specific model could achieve a higher accuracy with more classes being predicted, it means that this model has a superior performance in terms of reflecting subtle smoothness differences. It was also hypothesised that during the consecutive 10 attempts of the experiment, the movement smoothness of each participant should be increased monotonically. Therefore, a larger number of classes

also represent a higher sensitivity in reflecting subtle smoothness differences.

In order to verify the feasibility of the best outcome of a model, an initial training attempt was made on the most difficult movement pattern (NDA + 180-degree rotation) since the change in smoothness was the most obvious. If a best outcome could be achieved with the most difficult pattern, the same procedure would be conducted for the rest of the movement patterns. On the contrary, the number of levels being classified would be decreased (i.e., changed to the next labelling method) until the training accuracy is above 50%. A total of 3 out of 7 machine learning models would be selected after the initial attempt for the final classification task. Figure 3.8 presents the workflow of the above procedure.

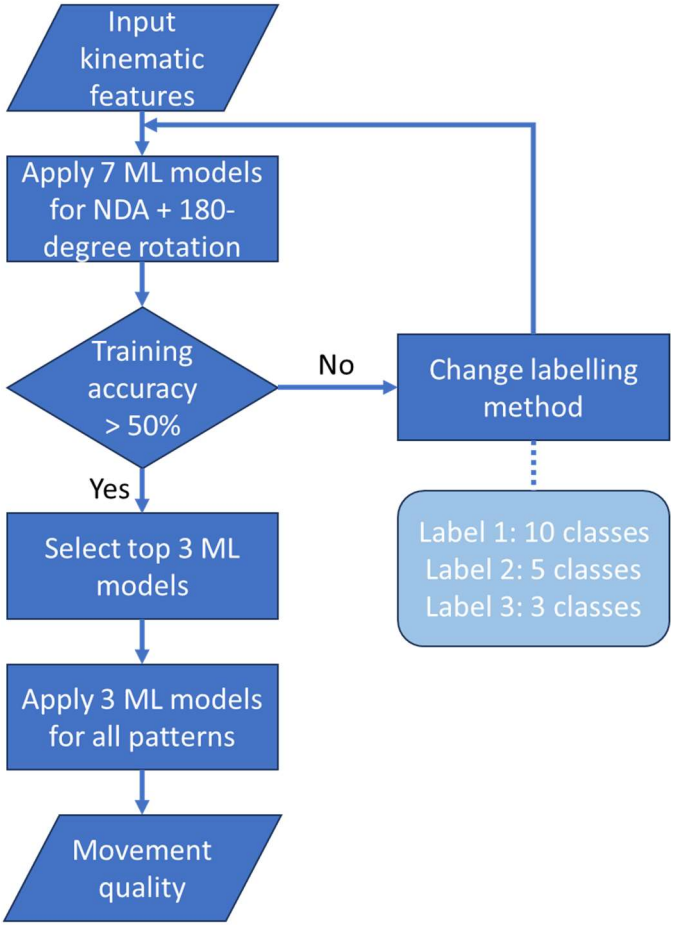

Figure 3.8 Workflow of selecting machine learning models and proper labelling method.

In order to balance the number of classes being predicted and the number of features for classification, a feature selection process was introduced prior to model training. Two commonly-applied feature selection algorithms were adopted for different models, namely ReliefF [81] for distance based models and analysis of variances (ANOVA) for the rest of the models. The resulted

top 50% of the features was selected for model training and tests. A Bayesian optimiser was adopted for hyperparameter optimisation with maximum iterations set to 100.

3.4.4 Statistical Analysis

Firstly, a statistical analysis was conducted on the selected kinematic features to show learning progress among ten drawing attempts in the four movement patterns. This was achieved by computing the coefficients of determination (R^2) for the selected kinematic features using an exponential curve. This analysis was made based on the assumption that the learning curve was monotonic. A larger R^2 value indicate a higher model precision, indicative of more distinguishable learning curves and more reliable prediction results.

Secondly, a statistical analysis was conducted on the selected kinematic features to show inter-feature reliability and inter-feature correlations. Pearson's product moment correlation coefficients (r) were computed to quantify the degree to which the selected features were correlated with each other. The commonly adopted three scales were used to interpret this coefficient, with $0 < r < 0.4$ classified as weak, $0.4 < r < 0.8$ classified as moderate and $0.8 < r < 1$ classified as strong. This analysis was conducted based on the assumption that each kinematic features would have a linear correlation with NJ. Additionally, intraclass correlation coefficients (ICC A,1) were computed to evaluate the inter-feature reliability using the two-way random absolute agreement definition. This definition was chosen because the agreement (i.e., absolute agreement) between the selected features was of the research interest instead of the fitness of linear relationship (i.e., consistency) between them. The ICC coefficients (ICC) were interpreted using the guideline from Koo and Li [82] with $0 < ICC < 0.5$ classified as poor, $0.5 < ICC < 0.75$ classified as moderate, $0.75 < ICC < 0.9$ classified as good and $0.9 < ICC < 1$ classified as excellent.

3.5 Summary

This chapter introduced experimental design and data analysis method for four independent experiments regarding to the upper limb kinematic smoothness assessment. The first two experiments were designed to evaluate and verify the accuracy and performance of novel position tracking methods in 2D workspace using a mouse sensor and computer vision system. This was achieved by comparing the position data from a mouse

sensor and an accurate position measurement system Optotrak during a multi-segment triangle movement pattern. For the computer vision system, the comparison was achieved through a single pendulum verification. Since the movement pattern classification and movement smoothness assessment in the later experiments also require kinematic feature extraction from velocity and acceleration profiles, a first order central difference method was applied to position data from mouse sensor measurements to calculate velocity and acceleration profiles. The evaluation was conducted using the root mean square errors (RMSE). The test-retest reliability was conducted using the intraclass correlation coefficient (ICC A, 1). The kinematic features used for movement type classifications and smoothness assessment were extracted on the normalised and relative position data. Therefore, the unit and the coordinate of position measurement have no influence on feature extraction. This part of the work formed the basis on kinematic feature extraction and movement quality assessment.

The third experiment was designed to classify movement patterns based on statistical kinematic features from acceleration profiles. Different movement patterns were chosen to represent a variety of the activities of daily living (ADL). The classification was achieved by supervised machine learning models using kinematic features extracted from movement acceleration profiles. The performance of each model was evaluated by F_1 scores and the area under the receiver operating characteristics (AUC).

The final experiment was designed to verify the combination of movement pattern classification and movement smoothness assessment based on kinematic features. An observational single group experiment with 14 participants were recruited for the task. Several supervised machine learning models were adopted to classify movement patterns and movement quality into different numbers of categories that were controlled by the labelling methods. Additionally, the learning progress of participants drawing each pattern was verified using both linear and nonlinear models. The inter-feature reliability was also verified using an intraclass correlation coefficient. All experiments and their key functions were presented in Figure 3.9. The experimental results and the results discussion are presented in the next chapter.

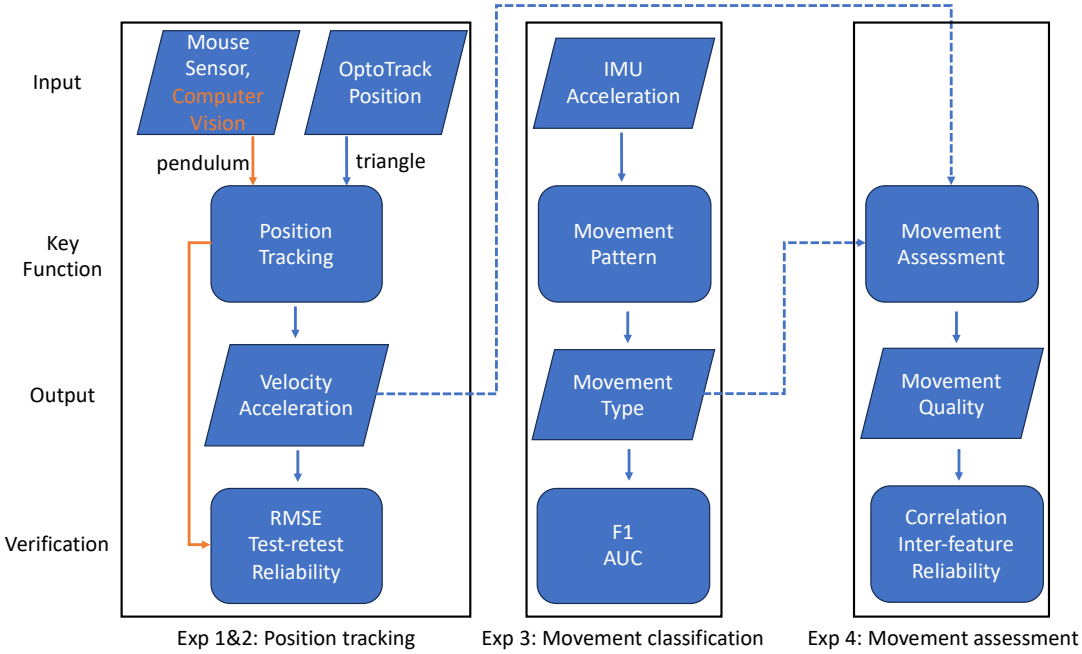

Figure 3.9 Summary of experiment designs including inputs, outputs, and verifications.

Chapter 4 Results on Movement Assessment

4.1 Mouse Position Tracking Experiment

4.1.1 Results

A mouse sensor was firstly used to track the relative position of a 2D triangle movement. The sampling frequency of the mouse sensor on the specific mouse presented in the previous chapter varied slightly due to the uneven execution time of the self-written MATLAB script. Therefore, a frequency calibration process was conducted for mouse sensor measurement prior to the experiment for a duration of the same as experiment window length. The calibration resulted to an actual average sampling frequency of $f_{mma} = 64.5$ Hz. This value would be adopted for all the differentiation process for mouse sensor position data.

A data segmentation was then applied on the normalised position data using the algorithm described in Table 3.1. The position difference was taken between $D = 5$ measurements, and the threshold was set to $P_{on/off} = 0.006$.

The position data along each axis was processed with a low-pass filter before calculation. A first order central difference method was adopted to calculate velocity and acceleration profiles from the recorded position data. A total of 10 measurement were conducted during the experiment. Figure 4.1 showed the normalised position profile, velocity profile and acceleration profile along each axis from the first attempt.

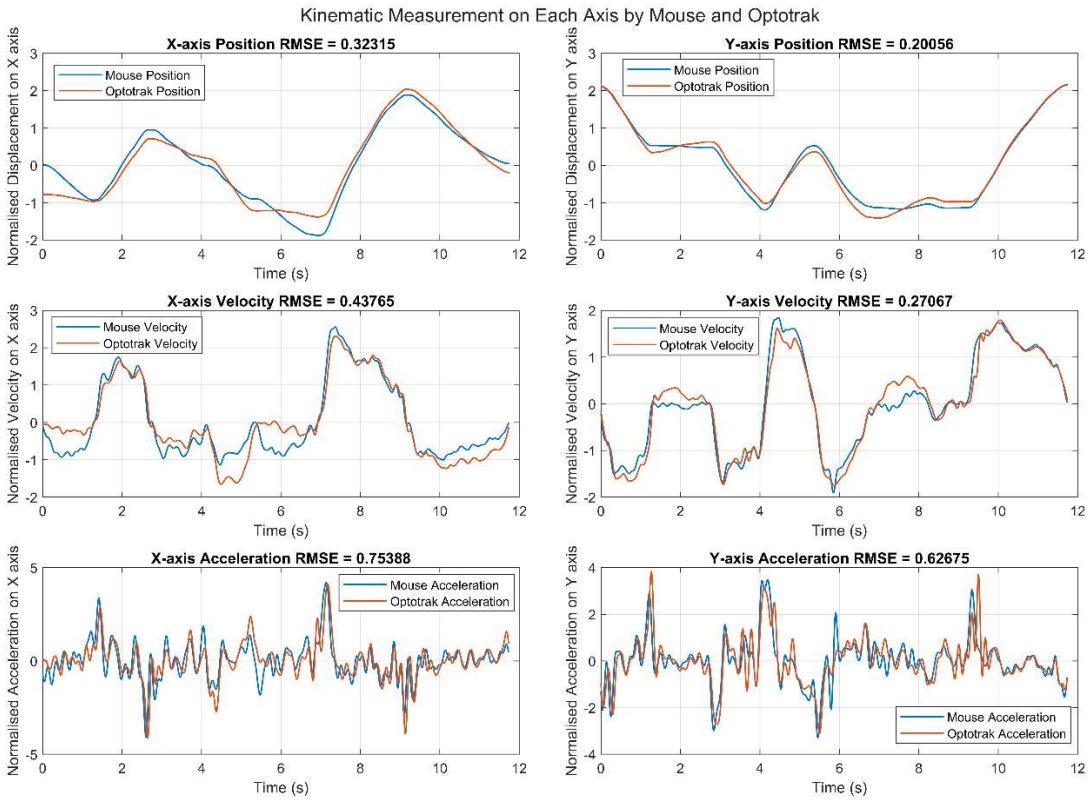

Figure 4.1 Normalised position along X and Y axis in the first attempt.

It was observed that relatively low RMSE values from 0.20056 to 0.75388 were obtained for all kinematic measurements. The RMSE values were increased with more differentiations on both axes. This was as expected mathematically since the differentiation process would magnify the errors. Position errors were found on both axes though a relatively small RMSE was obtained. This could be a result of sensor misalignment as shown in Figure 4.2. The Optotrak position marker was attached to participant's wrist whereas the mouse sensor was at the centre of the participant's palm. P_{m1} and P_{m2} are the two measurements for mouse position. P_{o1} and P_{o2} are the two measurements for Optotrak position. l_1 and l_2 are the distance between mouse sensor and Optotrak marker on Y axis, and d_1 and d_2 are the distances between mouse sensor and Optotrak marker on X axis.

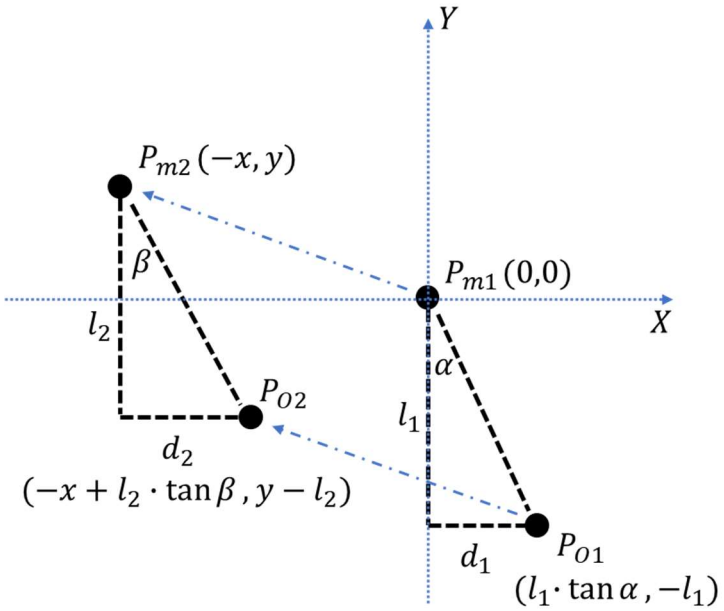

Figure 4.2 Representation of mouse and Optotrak position between two continuous measurements.

Therefore, the distance on each axis between two measurements for both systems can be calculated using Eq. 4.1 to Eq. 4.4.

Along X axis:

$$D_{mx} = |x| \tag{4.1}$$

$$D_{ox} = |-x + l_2 \cdot \tan\beta - l_1 \cdot \tan\alpha| \tag{4.2}$$

Along Y axis:

$$D_{my} = |y| \tag{4.3}$$

$$D_{oy} = |y - l_2 + l_1| \tag{4.4}$$

Since Optotrak marker was not rigidly connected with participant's wrist during the experiment, the distance between the marker and the mouse sensor was not a constant. The rotation angle was also changed because of the slight wrist rotations. Consequently, a larger measurement error between Optotrak and mouse sensor was expected along X axis because the trigonometric functions in Eq. 4.2 introduce nonlinear relationship. This was consistent with the lower RMSE values along X axis presented in Figure 4.1.

4.1.2 Statistical Analysis

In order to verify the measurement reliability, the test-retest reliability was calculated on the RMSE values for both axes and all three kinematics (i.e., 2 axes × 3 kinematics = 6 raters) using intraclass correlation coefficient (ICC A, 1). SPSS Statistics 20 (IBM) was used to compute the coefficient as shown in Figure 4.3.

Intraclass Correlation Coefficient

	Intraclass Correlation[b]	95% Confidence Interval		F Test with True Value 0		
		Lower Bound	Upper Bound	Value	df1	df2
Single Measures	.990[a]	.978	.996	897.345	11	99
Average Measures	.999	.998	1.000	897.345	11	99

Two-way random effects model where both people effects and measures effects are random.

a. The estimator is the same, whether the interaction effect is present or not.

b. Type A intraclass correlation coefficients using an absolute agreement definition.

Figure 4.3 Test-retest reliability for 10 mouse sensor position measurements.

An average value of $ICC = 0.999\,(0.998, 1.000)$ was found between 10 measurements. Using the guideline from Koo and Li [82] to interpret the ICC value, the measurement reliability was considered to be excellent. Additionally, it was found by a Tukey Test that no significant differences were observed between measurements, which was consistent with the ICC coefficient. The average RMSE values from all attempts on each kinematics along each axis were also compared and tested as shown in Figure 4.4, where P denotes the position, V denotes the velocity and A denotes the acceleration.

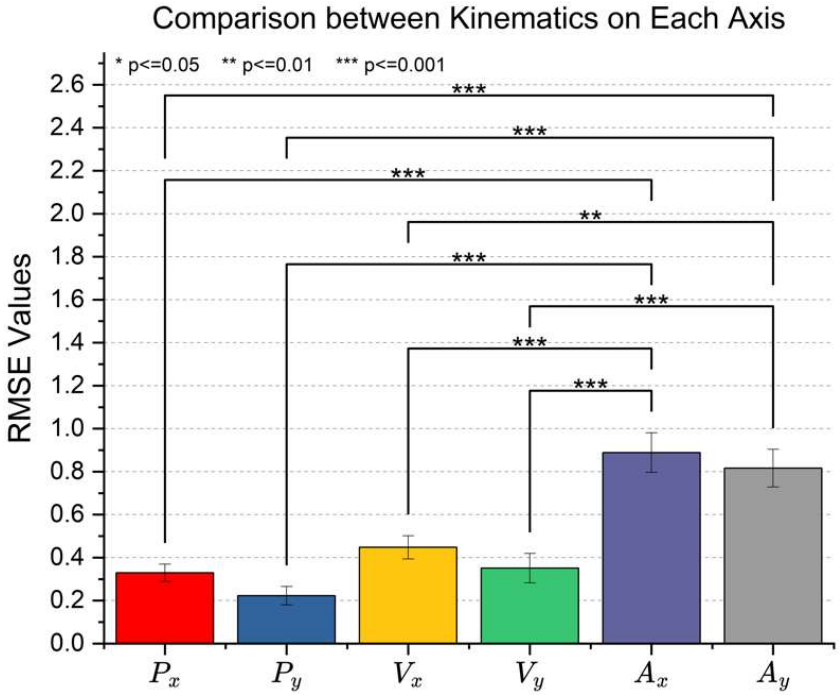

Figure 4.4 Average RMSE values over 10 attempts for each kinematics along each axis.

Significant differences were observed between the acceleration profiles and the rest of the kinematic profiles. This is a result of errors introduced by multiple differentiations when calculating accelerations. Moreover, the average RMSE values on Y axis was lower than those on X axis for all three

kinematic profiles, which was consistent with the mathematical models established by Eq. 4.1 to Eq. 4.4. The misalignment between Optotrak marker and the mouse sensor would likely to result in a relatively larger measurement error on X axis because of the nonlinearity introduced by wrist rotation.

In order to evaluate the influence of the sensor misalignment on the extraction of kinematic features, a two-sample t-test was conducted at 95% confidence level between kinematic features extracted from each measurement system to observe any significant difference between them. The p values of the test are listed in Table 4.1. The extraction method of these kinematic features is reported in Table 3.2.

Table 4.1 Two-sample t-test results on kinematic features extracted from both measurement systems.

D	T	V_p	$\bar{V}$	S	K
1.0000	0.9997	1.0000	1.0000	0.3355	0.0127
Var	$SampEn$	SE	NOP	A_p	NJ
1.0000	0.0654	0.0172	0.0634	1.0000	1.0000

It was shown that except the kurtosis (K) of the velocity profiles and the spectral entropy (SE) of the acceleration profile in frequency domain, no significant difference ($p > 0.05$) was observed among other kinematic features. This suggests two important findings that could be helpful for kinematic assessments in a home environment. Firstly, the mouse sensor could be used as a low-cost alternative for advanced 2D position tracking system in a home environment with a similar accuracy. Secondly, the extraction of most of the kinematic features based on mouse position would not be significantly influenced by the wrist rotation. For kurtosis and spectral entropy, it is therefore recommended to evaluate their effectiveness in upper limb movement assessment to determine whether a mouse-based position tracking method is appropriate.

In summary, mouse position tracking has the potential to replace advanced position sensors in a home environment if 2D planar movement is to be studied. The test-retest reliability was excellent with $ICC = 0.999$, and no significant difference was observed among 10 measurements. Measurement error was accumulated during the differentiation process. Therefore, a significant difference was observed between acceleration profiles and the rest of the kinematic profiles.

Wrist rotations during the movement and the non-rigid connection between sensor and wrist could result in a sensor misalignment, which could cause different measurement errors along each axis. However, the influence of this situation was not significant in terms of the extraction of most of the kinematic features except kurtosis and spectral entropy.

The same sets of kinematic features were extracted from both measurement systems. Except kurtosis of the velocity profiles ($p = 0.0127$) and spectral entropy of the acceleration profiles ($p = 0.0172$), no significant difference was found among other features.

The above findings contribute to the exploration of a low-cost alternative position tracking method in a home environment for 2D movements. This position tracking method has the advantage of accurately recording the relative position during a 2D movement while requiring less learning experience from the users. It could be conveniently integrated with a hand-held device proposed in this research at the hardware level and with a serious game presented in the early-stage work at the software level. One of the major limitations of this tracking method is that no vertical information could be measured. A potential solution to this problem is to add a self-developed Time of Flight (ToF) sensor at the bottom of the mouse or a hand-held device. For example, the VL53L0X ToF sensor has a measuring distance of 30 mm to 1000 mm, which covers sufficient space for a vertical movement.

Except mouse position tracking, computer vision-based position tracking method would be discussed below. It would be beneficial to conduct a comparative analysis between two measuring system to suggest each of their suitable application environment.

4.2 Computer Vision Tracking Experiment

4.2.1 Results

A self-written Python script running an open-source computer vision algorithm was used to track the position of a single pendulum. The tracking was achieved by continuously extract a specific colour from the background noise using the Back Projection method. In order to verify the accuracy of this measuring system, Optotrak was also set up as a gold standard. The measurements from both systems were taken simultaneously with a changing distance between the single camera vision system and the pendulum object. This distance was changed incrementally from 40 cm to 70

cm with an increment of 5 cm. This distance range was determined by the camera specification used during the experiment. A very short or long distance would stop the camera from focusing on the pendulum object. This distance range is also within the recommended distance range (50 cm - 100 cm) between a user and a computer screen. Figure 4.5 shows both measurements at a distance $l = 40$ cm.

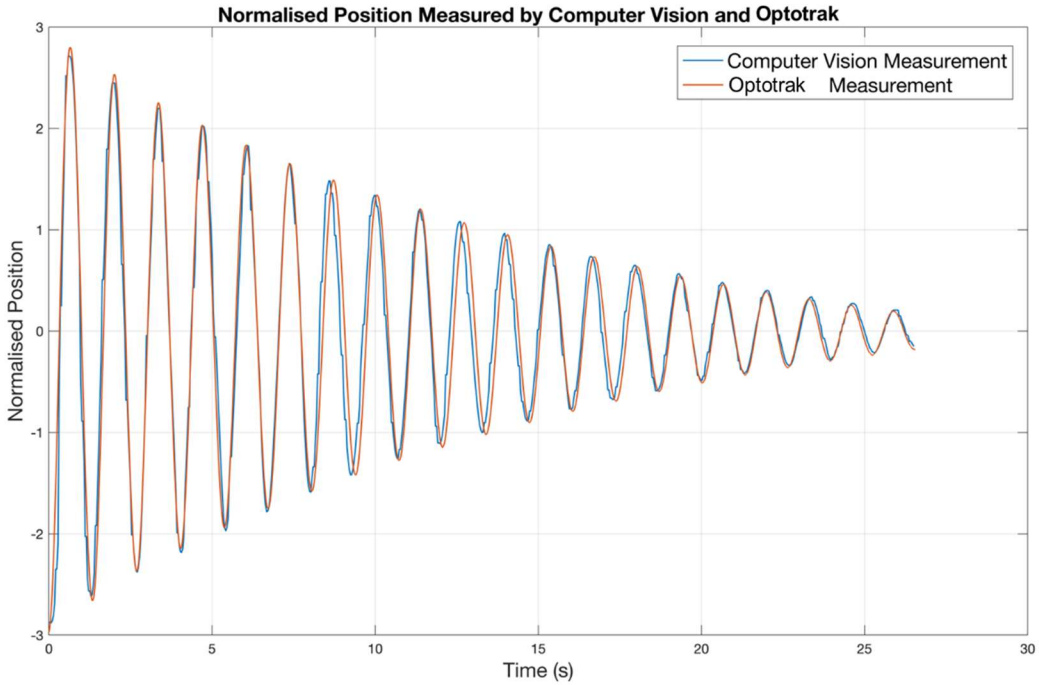

Figure 4.5 Normalised position measurements from computer vision system and Optotrak

It was observed that a relatively small position error existed between two measurement systems. Overall, positions measurement by the computer vision system did not show significant difference from Optotrak measurements. A small amount of time delay (i.e., approximately 0.2 second) was presented in the middle of the measurement by the vision system, which could be the result of the changing frame rate of the camera during the measurement. The frame rate was determined by the speed of the Back Projection algorithm on processing each image frame in a video. The maximum frame rate allowed during the Back Projection is 30 frames per second (FPS).

In order to quantify the measurement error of the vision system, root mean square error (RMSE) of the normalised position measurements between two systems was computed for 15 pendulum cycles at each distance and is shown in Figure 4.6.

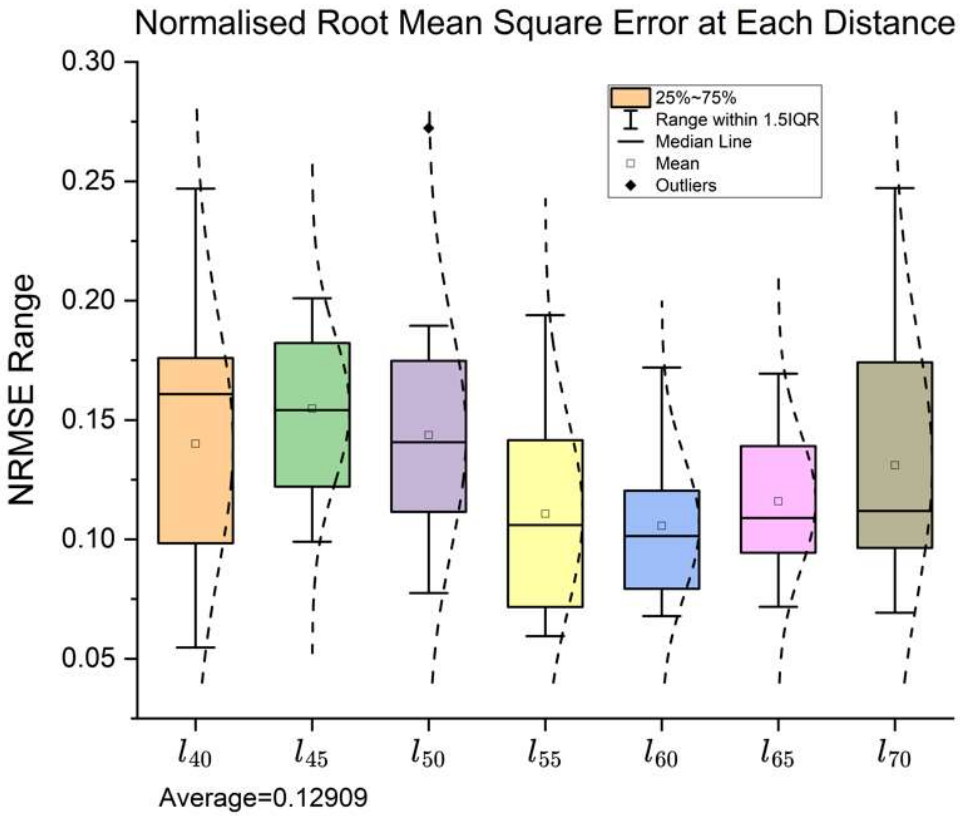

Figure 4.6 Normalised RMSE for all measurements at all distances.

Overall, the average normalised RMSE was 0.12909 for all measurements at all distances between the Optotrak and the computer vision system. The dashed curve near each box also demonstrated a high possibility that data was from a normal distribution. Based on this experiment result, an ideal working distance for the vision system could be recommended in the range of $l = 55$ cm to $l = 65$ cm. The variance of the normalised RMSE value was larger at both ends of the working distances. All these findings suggested that computer vision-based position tracking method is limited by the working distance between the tracked object and the camera. The tracking quality is also restricted by the specification of the camera and the level of background noises.

4.2.2 Statistical Analysis

A two-sample t-test at 95% confidence level was conducted for each distance to detect any significant difference between the two measurement systems as shown in Figure 4.7.

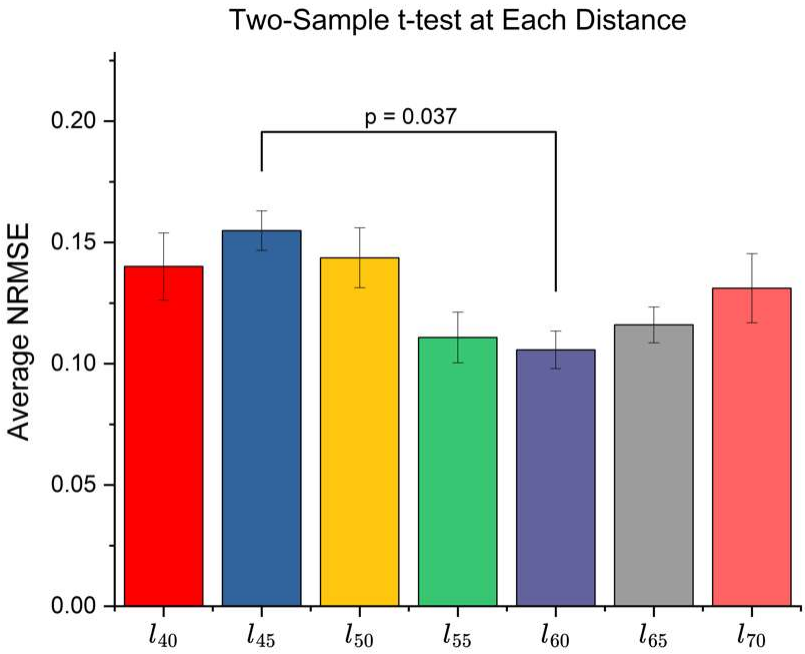

Figure 4.7 Two-sample t-test on average NRMSE at all distances.

It was shown that a significant difference was observed between $l = 45$ cm and $l = 60$ cm. No significant differences were observed for other distances between the two systems. This observation further contributed to the determination of the ideal working distance for this vision system was at $l = 60$ cm.

The test-retest reliability was verified using the intraclass correlation coefficient (ICC A, 1) as shown in Figure 4.8.

Intraclass Correlation Coefficient

	Intraclass Correlation[b]	95% Confidence Interval		F Test with True Value 0		
		Lower Bound	Upper Bound	Value	df1	df2
Single Measures	.199[a]	.042	.654	4.371	5	65
Average Measures	.777	.381	.964	4.371	5	65

Two-way random effects model where both people effects and measures effects are random.

a. The estimator is the same, whether the interaction effect is present or not.

b. Type A intraclass correlation coefficients using an absolute agreement definition.

Figure 4.8 Test-retest reliability for 15 measurements.

Using the same guideline, the test-retest reliability was considered to be good. However, compared to the mouse sensor tracking reliability ($ICC = 0.999$), positions measured by the vision system were less reliable based on a lower ICC score ($ICC = 0.777$).

Overall, the position tracking method based on a computer vision algorithm could record the movement of a single pendulum accurately but with some delay time due to the specification of the camera and the background noise. However, the recorded movement during this experiment was a simple

repetitive pendulum movement that could not represent the complexity of most of the activities of daily living (ADL). Compared to a mouse position tracking method, the decrease in the test-retest reliability also suggests that the computer vision-based tracking method may show weaker performance in the accuracy and response time if multiple measurements are conducted. However, one of the most efficient and commonly applied psychotherapy for post-stroke patients is repetitive exercise. These limitations of the computer vision-based method using a single camera prevent it from being used for kinematic feature extraction. On the other hand, it is more suitable for detecting a simple binary-type problem such as the monitoring on the safe working space of a rehabilitation robot and as the control input for serious games.

The above limitations and suggestions are based on the single camera computer vision algorithm developed in this thesis. Dual camera systems may overcome the existing limitations of the current algorithm. For example, a depth information estimation could be achieved by a dual camera system. However, most of the camera-based systems rely on the colour separation from the background, which will be significantly influenced by surrounding environments and the movement complexity during the application. It is therefore recommended to apply joint localisation measurement for the upper limb movement assessment in the future study. Unlike colour separation, the key joint localisation method uses existing trained machine learning models to detect human joints like wrists, elbows, shoulders and knees, and use a straight line to represent different parts of the limbs. The machine learning approach would have less requirements on the application environments and movement complexity.

A thorough comparison between computer vision-based position tracking algorithm and the mouse sensor-based position tracking method was presented at the end of this chapter in the discussion part.

4.3 Movement Type Classification Experiment

One of the important tasks for kinematic assessment after the measurement of position data is to determine the movement type. Different movement types require different muscle groups to work. Understanding which movement has been done during a rehabilitation intervention helps design a more personalised and specific therapy for different individuals. Additionally, recognising different upper limb movements would help determine the sample frequency of the sensor to save battery life in a home environment.

Therefore, four daily activities including reaching out, turning a key, drawing a circle, and drinking water were selected for the movement classification task based on kinematic features. A total of 6 types of features were extracted from the movement acceleration profiles along the three axes. Therefore, a total of $3\ (dimensions) \times 6\ (features) = 18\ (features)$ were used for model training and evaluation for movement type classification. Prior to feature selection process, all 18 features were adopted for the model training. Table 4.2 presents the model training and evaluation results.

Table 4.2 Evaluation on movement type classification models.

Model	AUC	F_1	Training Accuracy	Test Accuracy	Computational Time
SVM	1	1	100%	100%	22.797
RF	0.9167	[0.63,1,1,1]	94.6%	95.8%	12.729
KNN	1	1	100%	95.8%	15.769
DNN	1	1	100%	95.8%	46.014

It was shown that all classification models could have a training and test accuracy above 90%. However, RF has a lower training and test accuracy though it had the fastest computational time on model training. KNN and DNN both failed a 100% test accuracy, indicative of a model overfitting on the training data set. Specially, DNN consumed the longest computational time among all models. Though the layers of the model were limited to three, the number of neurons in each layer was not limited for the optimiser. Consequently, though the number of training iterations was set to be the same for all models, the computational time for DNN was longer than the others. SVM had an ideal performance on both model accuracy and computational time. A scatter plot for SVM model training result was shown in Figure 4.9.

The computational time is important if online machine learning models will be deployed in the future device. The term online here means that the machine learning model is being trained in real time when new training data is available from sensors. On the contrary, offline models are only trained the first time before the model is being applied to solve a problem. Therefore, the investigation on the computational time here in the thesis contributed to the possibility of applying these machine learning models in real time with existing rehabilitation robotic devices.

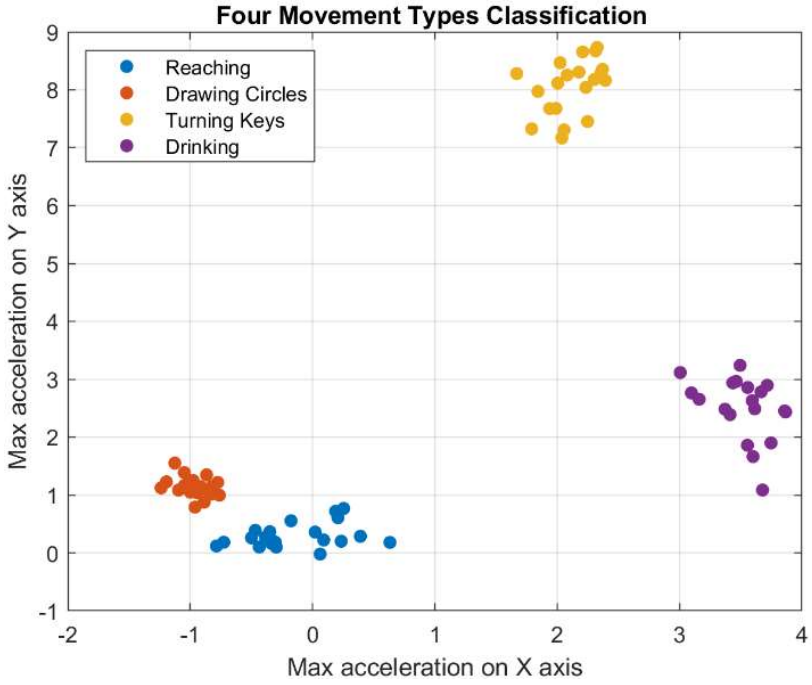

Figure 4.9 Scatter plot with maximum acceleration on X and Y axis.

In order to optimise the computational time and the model performance, a feature selection process using the Minimum Redundancy Maximum Relevance (MRMR) algorithm was adopted prior to model training. The model performance and the computational time after feature selection were compared with the previous base models. Minimum Redundancy Maximum Relevance (MRMR) algorithm minimises the redundancy and maximise the relevance of feature sets to the response value so that the response values could be effectively represented by features with maximum dissimilarity. Table 4.3 presents the training results after selecting the top 66.7% features with decrease in their MRMR scores.

Table 4.3 Model performance after feature selection process using MRMR.

Model	AUC	F_1	Training Accuracy	Test Accuracy	Computational Time
SVM	1	1	100%	100%	30.078
RF	0.9167	[0.63,1,1,1]	94.6%	95.8%	8.577
KNN	1	1	100%	95.8%	11.597
DNN	1	1	100%	100%	142.94

DNN consumed significantly longer time compared to the base model. However, its test accuracy was improved to the same level as SVM after the feature selection process. This suggests that the feature selection process successfully managed to eliminate noisy features from the entire feature set.

No obvious performance changes were observed among SVM, RF and KNN. A further decrease in the number of selected features was also attempted. However, the performances of all models were decreased due to the insufficient number of features in terms of training and test accuracy. Therefore, it was crucial to balance the number of selected features and the number of categories to be classified for classification models in the later movement quality assessment tasks.

Apart from MRMR, other commonly adopted feature selection algorithms, specifically Chi square test [83], ANOVA and Kruskal Wallis test [84], were also applied to the feature sets in order to find the most relevant features for this task. The top 5 selected features by MRMR were: A_{ymax}, $\overline{A_y}$, WL_x, A_{yms} and A_{zmax}. The top 5 selected features by Chi square test were: A_{xmax}, A_{ymax}, A_{yms}, A_{zms} and WL_x. The top 5 selected features by ANOVA were: A_{ymax}, WL_x, A_{xmin}, A_{xmax} and A_{zmin}. The top 5 selected features by Kruskal Wallis test were: WL_x, A_{zms}, A_{yms}, A_{ymax} and A_{xmax}. It was found that the maximum acceleration along Y axis A_{ymax}, the maximum acceleration along X axis A_{xmax} and the wavelength of acceleration along X axis WL_x were mostly selected by all algorithms. This was presented with the four distinct clusters plotted with A_{xmax} and A_{ymax} as shown in Figure 4.9 and the literature search results listed in Table 2.1. However, this classification was achieved only by acceleration profiles. The effectiveness of kinematic features extracted from position and velocity profiles needs to be examined for comparison in a more complex and generalised movement pattern.

In summary, four ML models (i.e., SVM, RF, DNN and KNN) were applied individually to classify four movement patterns using kinematic features extracted only from acceleration profile. The base models without further feature selection could already achieve ideal classification results with SVM having 100% accuracy for both training and test dataset. MRMR algorithm was then applied to the base model for feature selection. The performance of DNN was improved in terms of an increase in test accuracy though its computational time was increased significantly compared to the base model. The performance of other models was not significantly changed after the feature selection. Apart from MRMR, other feature selection algorithms were also adopted to find the most related features for this classification task. Maximum acceleration along X and Y axis was mostly selected. This may be a bias introduced by the particular movement patterns used in the experiment. Therefore, it is worth verifying the effectiveness of these features in a more generalised and complex movement pattern.

So far, kinematic features have been successfully extracted from position, velocity and acceleration profiles measured by both Optotrak measurement system and a mouse position sensor. Kinematic features extracted from the acceleration profiles have demonstrated their ability to classify four different movement types with supervised machine learning models. This proves the feasibility of applying machine learning models to solve more complex problems regarding to the upper limb movement assessment.

4.4 Movement Smoothness Assessment Experiment

Objectively measuring movement smoothness contributes to upper limb movement analysis. Firstly, it could help monitor the recovery process for movement related diseases like a bone fracture. It could also monitor the rehabilitation process in terms of movement progression for neurological, such as stroke and Parkinson. Additionally, it provides an insight into how human progress in a single and repetitive movement, benefiting muscle fatigue monitoring and sports training.

A single group observational study was conducted to verify the application of machine learning models in classifying movement patterns and movement qualities. Overall, 6720 kinematic features were extracted from the experiment using a single position sensor (14 participants $\times$ 4 movement patterns $\times$ 10 drawing attempts $\times$ 12 features). The 4 movement patterns included DA + 0-degree rotation, DA + 180-degree rotation, NDA + 0-degree rotation and NDA + 180-degree rotation. The 12 features are all listed and explained in Table 3.2.

4.4.1 Observation of Learning Progress

In order to present clear learning curves, the first, middle and last three attempts for each movement pattern were grouped together as beginning (1), intermediate (2) and smooth (3) level. Six features were able to reflect a learning progress with more drawing attempts made in all movement patterns as shown from Figure 4.10 to Figure 4.13.

A single-term exponential function (monotonic decrease) was firstly used to fit each kinematic features over 10 drawing attempts. Distance (D) travelled during the experiment failed the curve fitting process except in the NDA + 180-degree rotation pattern. Reasons are listed below.

1) All participants could adapt to this movement pattern quickly during the learning process since the triangle pattern is not complicated to be followed by people with normal upper limb functions.

2) Distance is not sensitive enough to reflect the subtle learning progress throughout the process.

Instead, movement duration (T), normalised jerk (NJ) and number of peaks in acceleration profiles (NOP) could reflect most of the learning progress monotonically and efficiently despite of current movement pattern. Sample entropy ($SampEn$) and spectral entropy (SE) showed limited representations on the learning progress with a poor fitness to the assumed exponential relationship. Other kinematic features listed in Table 3.2 could not reflect the learning progress though they were useful in the later classification tasks.

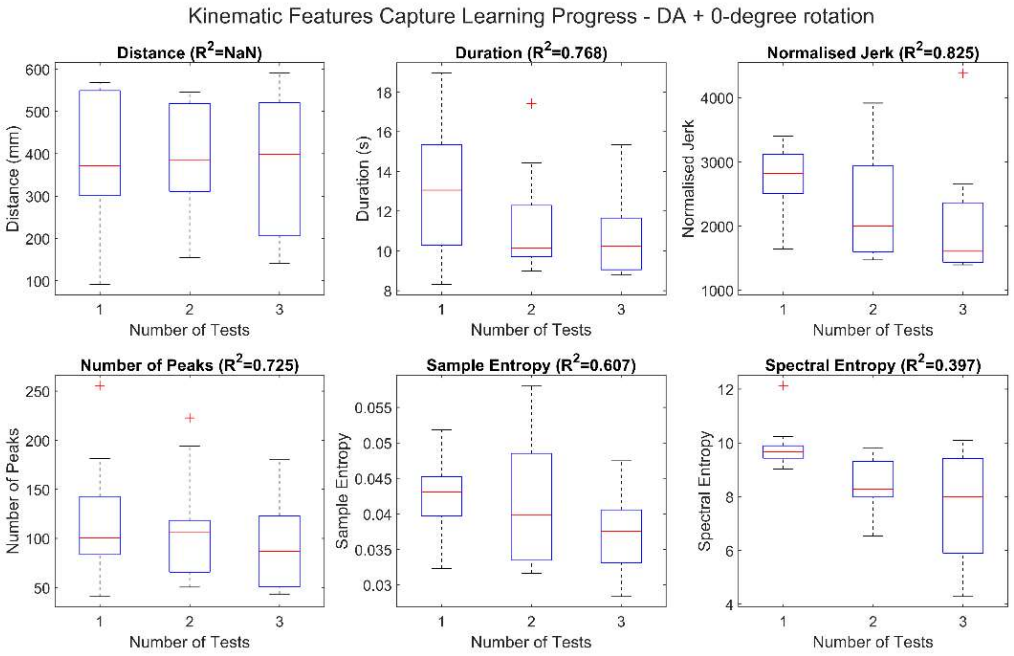

Figure 4.10 Change in kinematic features in DA + 0-degree rotation movement pattern.

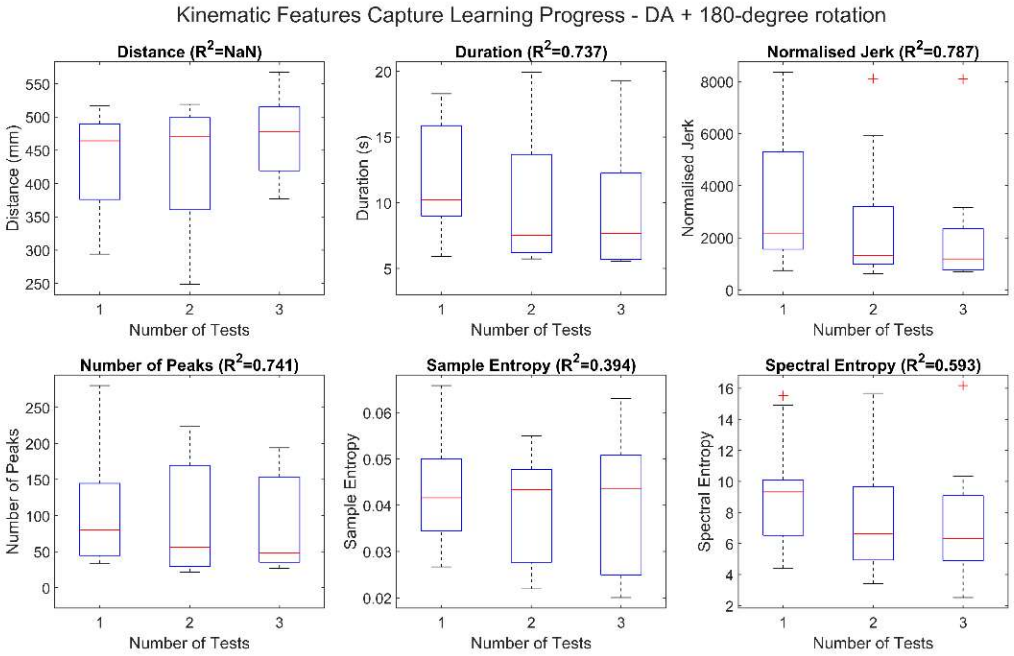

Figure 4.11 Change in kinematic features in DA + 180-degree rotation movement pattern.

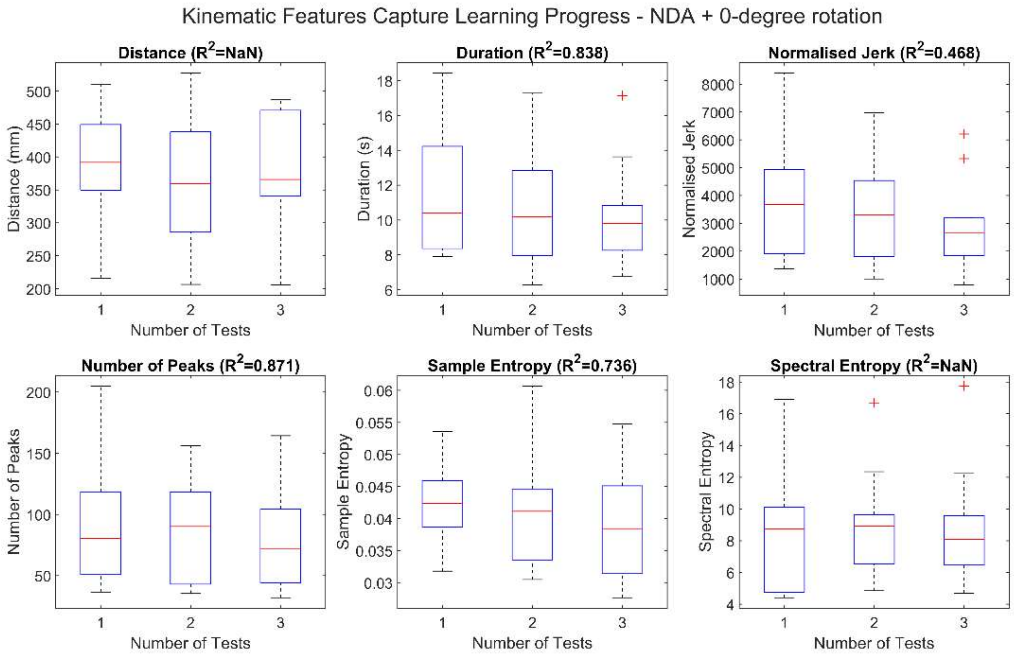

Figure 4.12 Change in kinematic features in NDA + 0-degree rotation movement pattern.

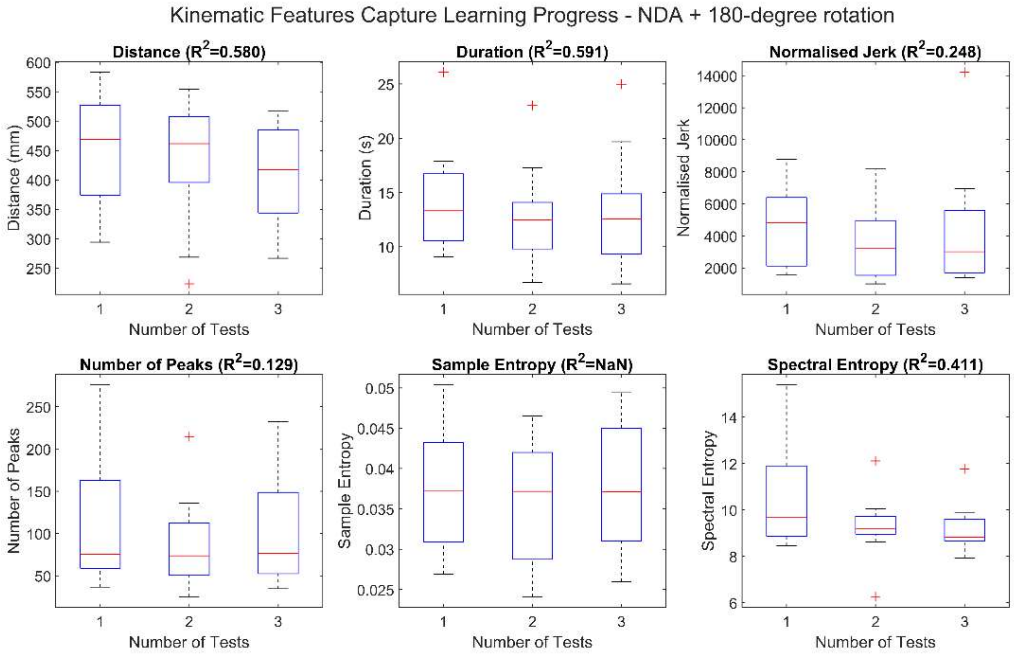

Figure 4.13 Change in kinematic features in NDA + 180-degree rotation movement pattern.

A comparison was then conducted between each movement pattern using the average value over 10 attempts. Table 4.4 presents the average values for each kinematic features.

It was shown that distance (D), duration (T), normalised jerk (NJ) and number of peaks (NOP) increased significantly when a mouse rotation was added. This was expected since additional complexity was intoduced to the

control of muscle groups during the movement. However, no significant changes were observed in sample entropy ($SampEn$) and spectral entropy (SE). This suggests that the two features may not be sensitve enough to reflect movement smoothness difference between each pattern or the two features have a poor test-retest reliability so that a larger variance throughout the ten attempts is presented.

Table 4.4 Average kinematic features over 10 attempts for each movement pattern.

Type	D	T	NJ	NOP	$SampEn$	SE
DA+0	395.0939	13.0147	5402.1	112.5276	0.0402	9.3570
DA+180	465.1987	14.7399	10824	148.8923	0.0407	9.6509
NDA+0	370.1449	12.8656	5685.8	104.476	0.0408	9.3032
NDA+180	436.4009	16.1821	11368	125.4121	0.0368	10.656

To further justify and verify the application of the selected kinematic features, Pearson product moment correlation coefficient (r) and intraclass correlation coefficient (ICC A, 1) were determined to quantify the strength of linear correlation and inter-feature reliability. The correlation coefficients (r) are shown in Figure 4.14.

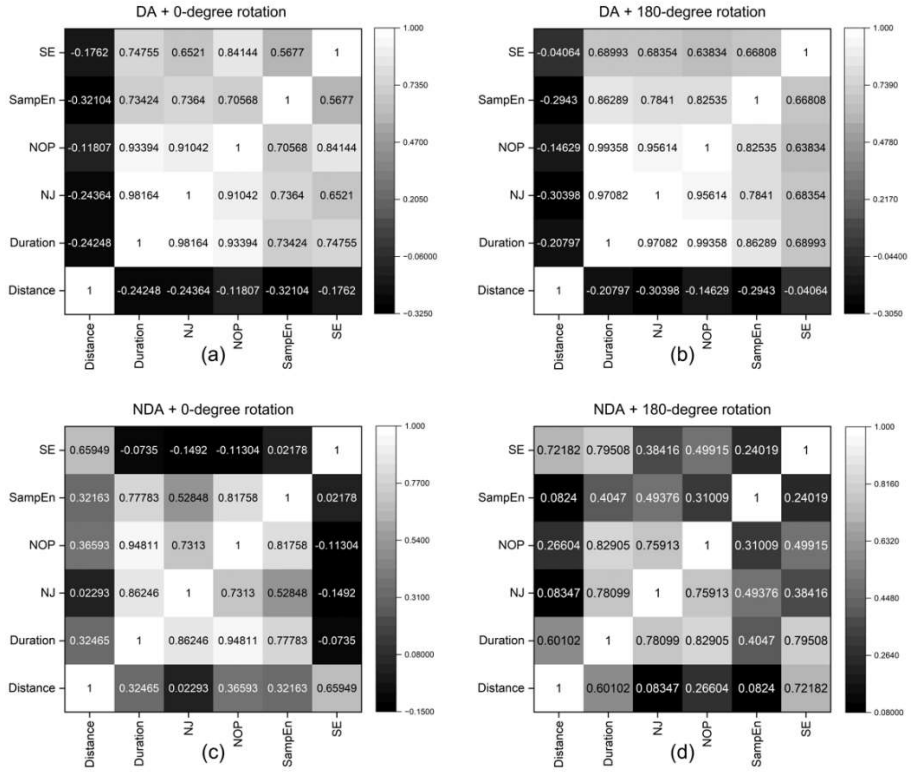

Figure 4.14 Pearson's correlation coefficients for all selected kinematic features in (a) DA + 0-degree rotation, (b) DA + 180-degree rotation, (c) NDA + 0-degree rotation and (d) NDA + 180-degree rotation.

Overall, it was shown that a relatively more consistent correlation was observed in the DA group regardless of mouse rotation whereas changes in correlations existed in the NDA group. The correlation coefficients for each kinematic feature pair decreased from DA to NDA. In the DA group, distance (D) was not well correlated with any other kinematic features. However, it correlated moderately with spectral entropy (SE) in the NDA group. Movement duration (T), normalised jerk (NJ) and number of peaks (NOP) correlated strongly with each other in all movement patterns. Moderate correlations were also observed for sample entropy ($SampEn$) and spectral entropy (SE) with other features in the DA group.

Since normalised jerk (NJ) has been clnically verified by numrous research, its correlation between other kinematic features were of interests. Using the guideline provided in section 3.4.4, moderate to strong correlations were observed with other kinematic features except distance (D) in DA group. However, the correlation between NJ and SE decreased significantly from DA to NDA where only weak to good correlations were found. This suggests that the degree of linearity between the spectral entropy and the normalised jerk may change with respect to the movement complexity.

The inter-feature reliability was verified using the intraclass correlation coefficient (ICC A, 1). The two-way random absolute agreement definition was adopted. ICC for each movement pattern is shown in Figure 4.15.

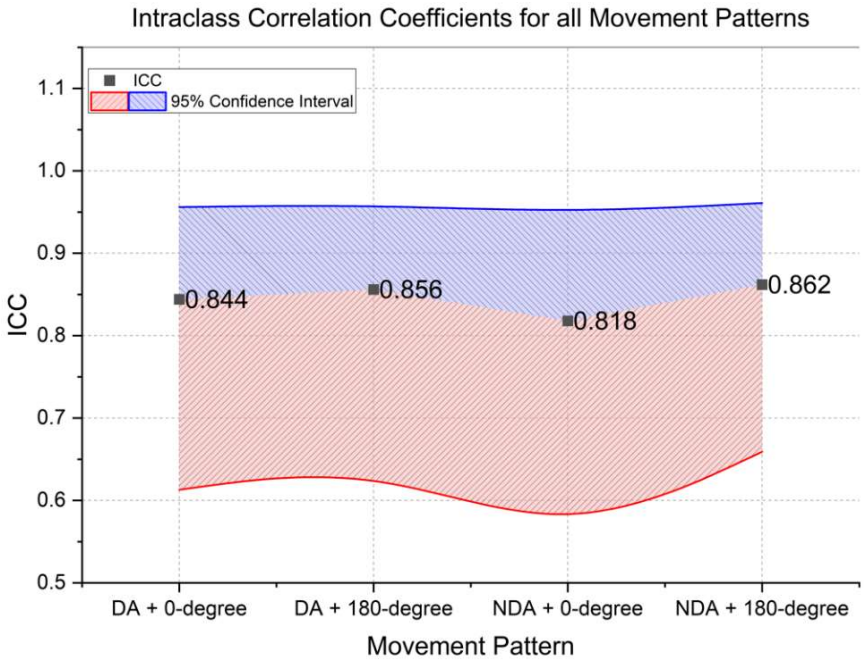

Figure 4.15 Inter-feature reliability verified by intraclass correlation coefficient.

Using the guideline described in section 3.4.4, good inter-feature reliability was observed among all movement patterns. This means that a good

agreement between each kinematic feature pair is observed. This is a positive outcome to show that every kinematic feature presented in this thesis had a good consistency in describing movement smoothness regardless of different movement patterns. Therefore, a machine learning model could be trained next for both movement pattern clasification and movement smoothness assessment.

4.4.2 Movement Pattern Classification

Although previous analysis and results showed good consistency for all kinematic features in describing the motor learning progress, their values varied a lot from the four different movement patterns as shown in Table 4.4. It is therefore important to differentiate between the four movement patterns (dominant/nondominant arm with/without mouse rotation) before a proper movement smoothness analysis could be conducted. The aim of the model is to classify four movement patterns prior to movement smoothness assessment. 12 kinematic features were extracted using the pipeline shown in Figure 3.7. ANOVA was used for feature selection with DNN, and the ReliefF was used with KNN and SVM since the ReliefF is particularly suitable for distance-based models [85]. Random forest (RF) was not adopted for this classification task since it was proved in the previous classification tasks to be less effective in section 4.3 than other ML models in terms of training accuracy. Models without feature selection process were not evaluated either since no significant performance drop was observed in the previous movement pattern classification tasks. 15% of the data was split as the test data set. A 5-fold cross validation was applied to all the models to prevent model overfitting. Training accuracy (A_{train}), test accuracy (A_{test}), F1 score (F_1) and Cohen's Kappa (κ) [86] were used to evaluate the model performance. Table 4.5 shows the classification and evaluation results on movement patterns.

Table 4.5 Evaluations on ML models classifying movement patterns using training and test accuracy, F1 score and Cohen's Kappa.

Evaluation	SVM	KNN	DNN
A_{train}	100%	100%	100%
A_{test}	100%	100%	100%
F_1	1	1	1
κ	1	1	1

All the models could achieve 100% training and test accuracy using the

selected kinematic features. It was shown in section 4.3 that peak accelerations along X and Y directions are the most selected feature by all feature selection algorithms to achieve a good classification result on the previous movement patterns. However, instead of extracting features from all kinematics, only acceleration-based features were used in the previous task. Therefore, it is worthwhile to examine the similarities on the results of the feature selection process, especially peak accelerations by comparing the selection results from both tasks. For each algorithm, the top 50% of the features would be recorded.

The selected kinematic features for DNN are (from the highest ANOVA score to the lowest): S, $\bar{V}$, Var, T, A_p, NJ, V_P and D. The selected features for KNN are (from the highest ReliefF score to the lowest): S, V_p, A_p, T, $SampEn$, $\bar{V}$, D, NJ, Var and K. The selected features for SVM are (from the highest ReliefF score to the lowest): S, V_p, A_p, $SampEn$, T, K, $\bar{V}$, D, NJ and Var. Figure 4.16 presents the number of selections for each kinematic feature in this classification task.

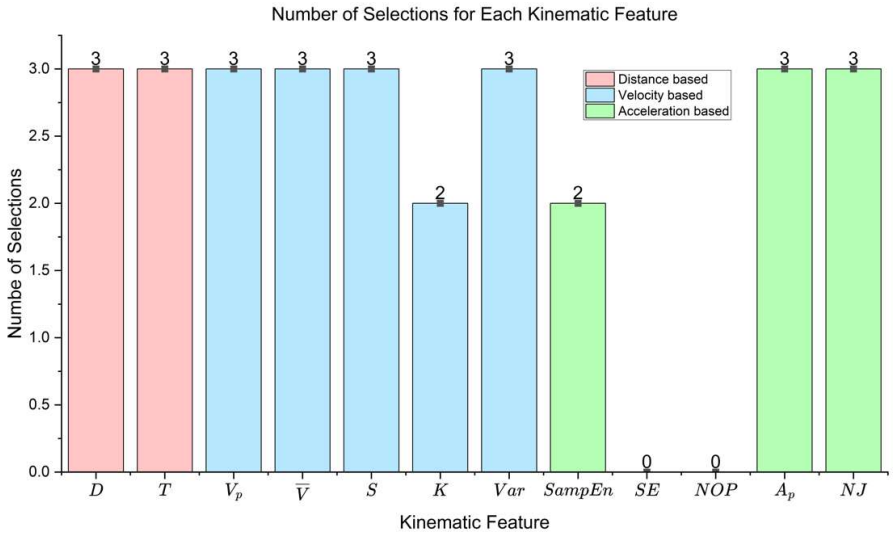

Figure 4.16 Number of selections for each kinematic feature in the movement pattern classification task.

It was shown that distance-based and velocity-based kinematic features also contributed to the classification task. Peak acceleration was also selected by all algorithms, which is consistent with the selection in the previous classification task. The same selection result on the peak acceleration may help reject the hypothesis raised at the end of section 4.3 that movement patterns may introduce bias in the feature selection process. The rejection is made because of the usage of the same triangle pattern throughout the experiment for both DA and NDA.

Though $SampEn$ and NOP were not selected in this task by any algorithm,

they were proved to be beneficial in the observation of learning progress in the previous section. Their usage on the later movement quality classification should be studied. Additionally, based on the score performance listed above, velocity-based features such as skewness (S) were especially suitable for movement pattern classification.

These findings contributed to the classifications of different movements, which is beneficial for telerehabilitation in a home environment since the patients' exercise movement could be checked and monitored automatically.

4.4.3 Movement Smoothness Classification

The goal of applying machine learning models with kinematic features in this thesis is to sensitively classify movement smoothness by predicting as many repetitions as possible. A higher number of repetitions being predicted would illustrate a higher sensitivity in showing subtle smoothness changes throughout the experiment. This contributes to the upper limb rehabilitation process in terms of providing longitudinal monitor of upper limb movement. Additionally, it also helps understand the muscle performance in repetitive movements for sports training, struggle detection, motor learning progress and fatigue detection.

To this end, several machine learning models are trained to classify the movement smoothness into different levels based on the same kinematic features applied in the previous sections. Since the triangle pattern was firstly shown to all participants on site, an increase-steady pattern in movement smoothness was hypothesised to be observed monotonically with more drawing attempts. The most sensitive and the best outcome of a model is to classify different drawing attempts using the first labelling method introduced in the previous chapter, into 10 different levels that is the same as the total number of drawing attempts. This indicates that the proposed machine learning model and kinematic features could reflect very subtle smoothness change in a short time. A total of 7 supervised machine learning models were used for this classification job. The input of the models is the extracted kinematic features, and the output of the models is the number of repetitions (i.e., from 1 to 10). During this process, if the training accuracy does not exceed 50%, another labelling method (labelling method that has 5 and 3 classes) would be adopted. When the training accuracy is above 50% with the current labelling method, the top 3 machine learning models and the current labelling method would be adopted for the rest of the analysis. Table 4.6 presents the training results using all 7

machine learning models and the first two labelling methods.

Table 4.6 Initial classification results using 7 machine learning models and 2 labelling methods.

Model	Training Accuracy	
	Labelling method 1 (10 classes)	Labelling method 2 (5 classes)
SVM	10.0%	44.4%
KNN	0.0%	22.2%
DNN	0.0%	22.2%
Tree	0.0%	0.0%
Ensemble	0.0%	11.1%
Naive Bayes	Failed	Failed
Discriminant	Failed	Failed

It was observed that when the first labelling method was adopted, no machine learning models could achieve a training accuracy above 50%. This suggests that the power and the number of the selected kinematic features does not support the classification into the best outcome. When the second labelling method was used, the performance of SVM, KNN, DNN and Ensemble models increased to a certain level that was still below the expected training accuracy. Based on the results of this initial attempt, three machine learning models including SVM, KNN and DNN were selected for the rest of the classification task. The labelling method were also changed to method 3 that has 3 classes including beginning, intermediate and smooth level.

The same feature extraction and data preparation method was used in the following movement smoothness classification based on the selected machine learning models and labels from the initial attempt. 15% of the data was split as the test set and a 5-fold cross validation was applied to prevent model overfitting. The same metrices were used to evaluate the model performance, specifically training and test accuracy, F1 score and Cohen’s Kappa. Table 4.7 presents the evaluation results on the model.

Table 4.7 Evaluations on ML models classifying movement quality using training and test accuracy, F1 score and Cohen's Kappa.

Movement Pattern	Evaluation Metric	DNN	KNN	SVM
NDA 180-degree rotation	A_{train}	100%	100%	100%
	A_{test}	100%	100%	100%
	F_1	1	1	1
	κ	1	1	1
NDA 0-degree rotation	A_{train}	87.5%	75%	87.5%
	A_{test}	100%	100%	100%
	F_1	[1, 0.86, 0.80]	[0.80, 0.67, 0.80]	[0.67, 0.86, 1]
	κ	0.81	0.63	0.80
DA 180-degree rotation	A_{train}	75%	75%	87.5%
	A_{test}	100%	100%	100%
	F_1	[0.50, 0.67, 1]	[0.80, 0.50, 0.86]	[0.67, 0.86, 1]
	κ	0.62	0.63	0.80
DA 0-degree rotation	A_{train}	62.5%	75%	75.5%
	A_{test}	100%	100%	100%
	F_1	[0.67, 0.57, 0.67]	[0.67, 0.75, 0.80]	[0.67, 0.75, 0.80]
	κ	0.41	0.62	0.62

Overall, the model performance deteriorated from the most difficult pattern (i.e., NDA with 180-degree rotation) to the least difficult pattern (i.e., DA with 0-degree rotation). This is reasonable since a DA inevitably tends to have a faster learning speed than NDA. Therefore, at the end of the experiment with DA, no obvious progress could be monitored. As a consequence, it would be rather difficult for ML models presented in this work to distinguish the movement smoothness towards the end of the experiment session. Therefore, the best classification results were achieved in the NDA with 180-degree pattern, and the worst classification results were achieved in the DA with 0-degree pattern.

Although the training accuracy decreased from the most difficult pattern to

the least difficult pattern, the test accuracy remained at 100% for all the models throughout different patterns. One possible explanation could be the insufficient amount of training data for verification that leads to a model underfitting. Models trained by insufficient amount of training data could not capture all the characteristics of the relationship between input features and output labels. A larger dataset needs to be constructed in order to balance the performance and complexity of the ML models. It is therefore recommended to establish an upper limb movement data repository that contains kinematic data for standardised movements to enable comparison between different algorithms.

Additionally, models tended to misclassify beginning level and intermediate level based on relatively smaller F_1 scores. For all the ML models presented in this section, SVM had overall a better performance over other models.

4.5 Discussion and Summary

In this chapter, the results of the four experiments designed in chapter 3 were presented and verified using a series of experimental results and statistical analysis. The first two experiments explored the application of two position tracking methods using a mouse sensor and a computer vision system, which formed the basis of kinematic movement assessment and provided a potential for alternative low-cost position tracking method in a home environment. The third experiment was designed to classify four different movement types that could represent some of the common human's activities of daily living. The final experiment was conducted among 14 participants in order to verify the application of machine learning models in terms of movement pattern classification and movement smoothness assessment.

4.5.1 Position Tracking

Mouse position tracking was firstly studied. Although this position tracking method does not support the measurement of rotational information and vertical movement, it showed excellent consistency and good accuracy in 2D movement position tracking tasks. This was reflected and verified by a relatively small RMSE in position, velocity, and acceleration profiles (from 0.20056 to 0.75388). The test-retest reliability for this method was excellent with $ICC = 0.999$.

The RMSE was higher in acceleration profiles due to the differentiation process, which makes it rather important in filter design and signal

processing since movement quality assessment relies heavily on acceleration-based features. Another reason for higher RMSE was the misalignment of the two sensors during the experiment. Since mouse sensors cannot measure rotational information, it may still lose some movement characteristics even in 2D planar movements due to the rotation of the wrist. To further examine the effect of this characteristics lost, the same set of kinematic features used in the movement smoothness assessment were extracted from the mouse sensor measurement. It was found that except kurtosis and spectral entropy, no significant difference was observed in other kinematic features. Moreover, it was observed in Figure 4.16 that spectral entropy was not selected by any feature selection algorithm in the later movement smoothness assessment task and kurtosis was not the most relevant feature either. Therefore, the effect of the sensor misalignment was not significant in any of the tasks presented in this research.

Computer vision-based tracking method was then studied and verified with a single pendulum movement. Excellent tracking accuracy was also obtained with an average RMSE $= 0.12909$. An ideal working distance was also confirmed to be around $l = 60$ cm based on a lower-than-average RMSE and its significance level. However, since vision-based tracking method relies heavily on the software environment and camera frame, a small amount of time delay (about 0.2 second) was observed in the pendulum experiment, which could make tests less reliable during long-term monitoring. This is consistent with a smaller test-retest reliability with $ICC = 0.777$.

Both systems could achieve an ideal position tracking result. However, vision-based tracking method is less reliable than a mouse sensor tracking in terms of its test-retest reliability. It is also important to choose the ideal working distance for the vision-based system since the tracking accuracy could change significantly with various distances. Additionally, vision-based systems can only work when the detected object is extracted from the background image. The object detection can be either colour based, or shape based. Therefore, its accuracy is highly dependent on the object detection results, which could be significantly influenced by the surrounding environment such as lighting condition. As a consequence, single camera vision-based position tracking method may be suitable for remote control using different gestures or finger positions. It may also help detect if the moving limb is within the safe working space of the rehabilitation robots.

Table 4.8 presents the characteristics of both tracking methods and the recommended applications.

Table 4.8 Summary of the measurement systems.

	Mouse Sensor	Vision System
Accuracy	Good	Excellent
Delay	None	Slight delay
Cost	Low	Low
Environment Dependency	Low	High
Ease of Use	Easy	Easy
Reliability	Excellent	Good
Limitations	• Unable to measure rotational and vertical information. • Positions are measured in pixel but not real distances.	• Working distance is strictly limited by the camera specifications. • Two cameras are needed to measure depth and rotational information.
Recommended Application	• 2D movement position tracking. • 2D movement quality assessment.	• Remote gesture/position control. • Working space detection.

4.5.2 Movement Type Classification

Movement type classification can be useful for an real-time personalised movement assessment and a longer battery life for the device. When users are assessed by the device, the device has the ability to recognise the user's specific movement in order to change the sensor sample rate to better capture the characteristics of the movement. On the contrary, when no activity is detected, the sensor sample rate would be decreased for battery life. This dynamic re-configuration of the device would only be achieved if movement type classification could be satisfied. The results presented in this section is a proof of such concept due to the following two reasons. Firstly,

the classification results are promising using kinematic data from a single IMU sensor. Secondly, the supervised machine learning models like SVM are proved to be implemented successfully with existing microcontrollers.

In the present work, movement type classification was firstly attempted with four individual upper limb movements including reaching, turning keys, drawing circles and drinking. Four machine learning algorithms (SVM, RF, KNN and DNN) were adopted to classify these movement patterns based on kinematic features extracted from only acceleration measurements. All models could achieve 100% training accuracy except Random Forest (RF). The computational time was hugely influenced by the feature selection process, but it had insignificant influence on model accuracies. The most selected kinematic features for this classification task were the peak accelerations on the 2D plane.

To further verify the machine learning-based movement classification with more complex movement, another movement pattern classification was then conducted as part of a single group observational study with 14 participants. In this study, four movement patterns were consisted of the combinations of different upper limbs (both dominant and non-dominant) and two mouse rotation settings (without rotation and with 180-degree rotation). The same triangle pattern used in the mouse sensor position tracking experiment was adopted. Since Random Forest (RF) had a poorer performance in the previous easier task, only SVM, KNN and DNN were applied to classify four movement patterns based on kinematic features extracted from position, velocity, and acceleration profiles. All models could achieve excellent performances with 100% training and test accuracy. Two feature selection process targeting corresponding ML models was adopted since computational time was not strictly limited in this task. The most selected kinematic features for this classification task were velocity-based features.

Peak acceleration had limited significance in the second task. This is because the four movement patterns in the first classification task have distinctive movement trajectories whereas the same trajectory (triangle pattern) was followed in the second task. Therefore, similar acceleration profiles obtained from the second task would result to similar peak accelerations. As a conclusion, acceleration-based features are mostly suitable for classifications on movements with unique trajectory. On the contrary, velocity-based features are more beneficial for movements with similar trajectories.

Only 6 kinematic features were used to present an exponential monotonic learning curve over 10 attempts. However, all kinematic features contributed to the classification on movement smoothness assessment. For example, skewness of velocity profiles varied so hugely from different participants and number of drawing attempts that neither linear nor exponential relationship could be well fitted as shown in Figure 4.17.

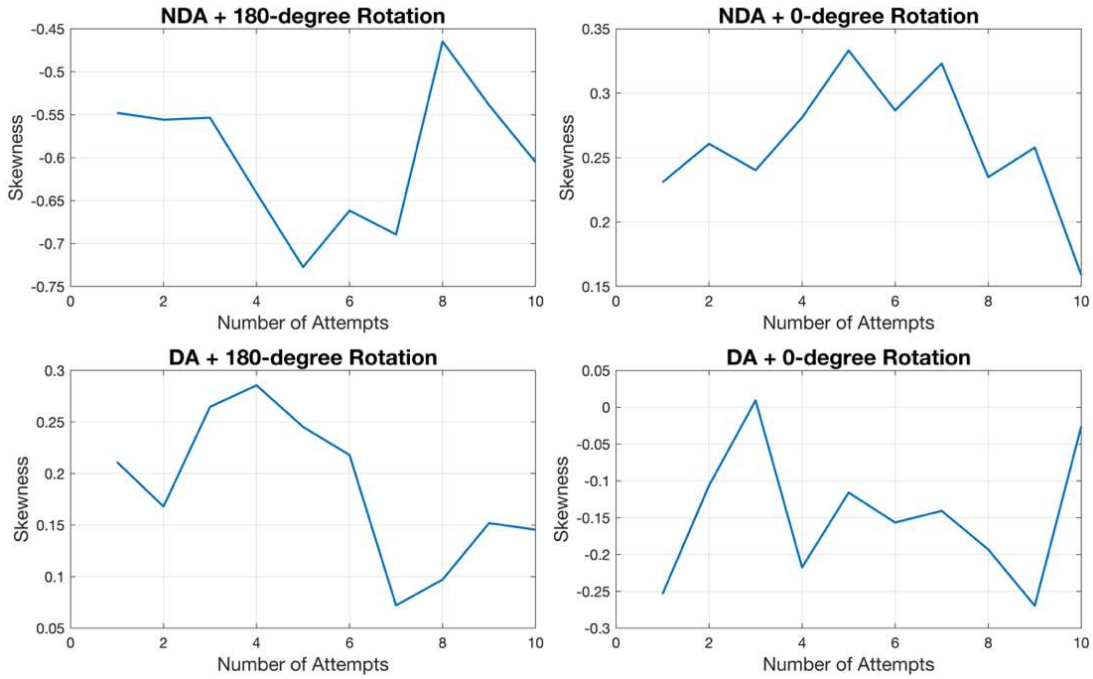

Figure 4.17 Skewness varied from different movement patterns and number of attempts.

However, different movement patterns have very distinguishable skewness as shown in Figure 4.17. It is also considered to be the most related kinematic features by both ANOVA and the ReliefF. Other velocity-based features also had higher ANOVA and the ReliefF scores compared to acceleration-based and distance-based features. This was also reported in [38] where velocity-based features were used to accurately classify different movement trajectories and [40] where upper limb rehabilitation process was sensitively monitored with the aid of robotic devices using velocity-based features.

Support Vector Machine (SVM) had ideal performance on both classification tasks. Though K-Nearest Neighbours (KNN) also achieved excellent classification result on the triangle pattern task, its decreased test accuracy (from 100% to 95.8%) in the first classification task indicated a model overfitting. Deep neural network (DNN) had excellent classification results on both tasks. However, its computational time after feature selection process increased 210.6%. This huge increase computational time may not be

suitable for an online machine learning application that generates real-time feedback. However, if the model is applied offline as a data processing tool, the increase of the computational time would be less essential. A great balance between model performance and training time was achieved only by SVM. This suggests that SVM could be used as a baseline measurement for future machine learning-based movement analysis for both online and offline applications. However, these results were only obtained based on the selected kinematic features described in this thesis. The performance of the same machine learning model may change based on different selections of kinematic features and movements. It is therefore recommended to establish a standard movement repository in the future study that involves inputs from engineers, clinicians, physiotherapists and potentially stroke patients so that comparative analysis could be conducted.

4.5.3 Observation of Learning Progress

A single group observational experiment with 14 participants was conducted in order to assess movement smoothness using kinematic features. An exponential curve was firstly used to fit all kinematic features over 10 attempts for each movement pattern. It was assumed before the experiment that the actual displacement during the movement would help identifying the learning progress since participants were more familiar with the same pattern. However, distance failed the curve fitting process (i.e., extremely small R^2 values) except in the NDA with 180-degree rotation (the most difficult pattern). Two potential reasons are related to the complexity of the pattern and the sensitivity of the feature. Triangle pattern used in the experiment may not be complicated enough or participants got familiar with the pattern so that insufficient diversity was presented by distance. On the contrary, movement duration, normalised jerk and the number of acceleration peaks sensitively reflected a monotonic change over 10 attempts. Sample entropy and spectral entropy both measures the complexity of the acceleration signals in time domain and frequency domain. They have the potential to reflect subtle improvements in quantifying upper limb movement smoothness since they presented moderate correlations over 10 attempts.

During the curve fitting process, it was also found that some features extracted from the last three attempts by participants had larger variances than the previous attempts as shown in Figure 4.18. This may be related to the muscle fatigue and decrease in participants' patience, willingness of cooperation etc toward the end of the experiment. This could also explain

why some kinematic features in a certain movement pattern had only poor to moderate exponential fitting over 10 attempts. From this point of view, sample entropy and spectral entropy may have a superior sensitivity in describing movement smoothness whereas normalised jerk, duration and number of peaks are more robust for subtle changes. It is therefore suggested to compare the sample entropy and spectral entropy results with the sEMG signal to validate the influence of muscle fatigue.

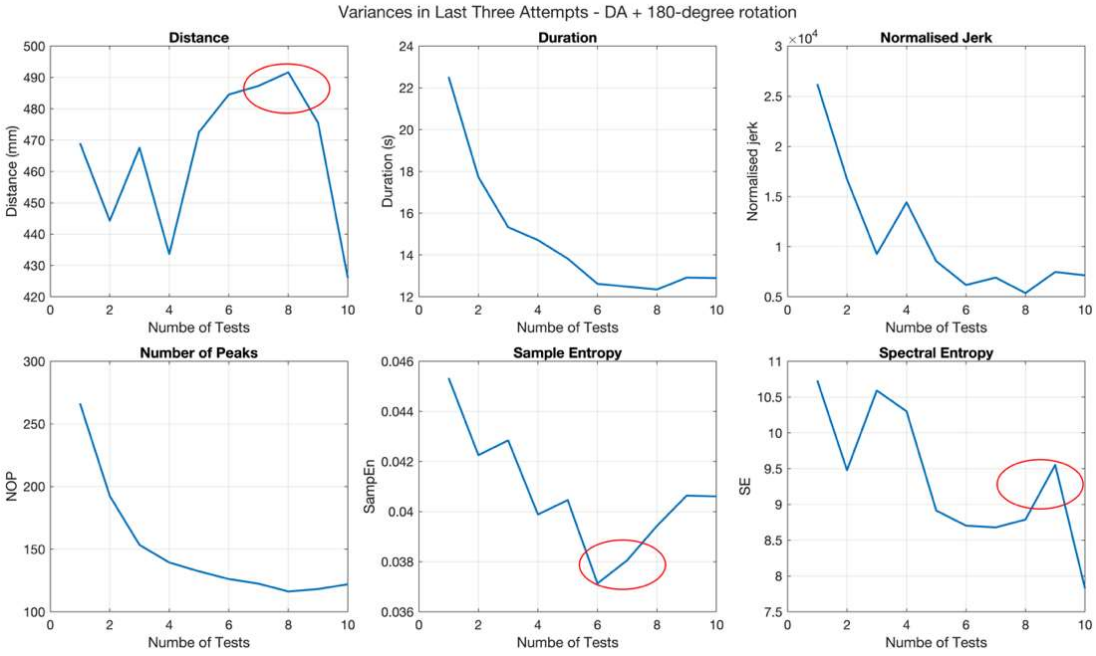

Figure 4.18 Variance in some kinematic features in the last three attempts (DA+180-degree rotation).

Inter-feature correlations changed significantly from DA to NDA group. In the DA group, distance is not correlated with any other kinematic features. However, other kinematic features had moderate to good correlations with each other. This shows insufficient sensitivity of distance in reflecting motor learning progress. However, In the NDA group, an inconsistency in the correlation was observed. For example, spectral entropy correlated negatively with duration, normalised jerk, and number of peaks in NDA with 0-degree rotation. Whereas this negative correlation changed to positive in NDA with 180-degree rotation. An explanation could be the inter-participant variability. During the consultation after experiment, 2 out of 14 participants reported capability in dominating both arms during activities of daily living. One participant specialises in PC gaming that requires frequent and fast response and aiming. Both circumstances could help participants in learning the triangle patterns much faster than others, which could cause the celling effect.

Specifically, movement duration, normalised jerk and number of acceleration peaks showed excellent correlations with each other in all movement patterns. Since normalised jerk has been verified with clinical assessment scores in existing literature, it is possible to examine the effectiveness of movement duration and number of acceleration peaks in upper limb movement assessments in the future study. Movement duration and number of acceleration peaks have the advantage over normalised jerk in terms of data collections and data processing. A single inertial measurement unit (IMU) could directly output time and acceleration data whereas normalised jerk requires additional filtering and differentiation process.

4.5.4 Movement Smoothness Assessment

The performance of movement quality classification deteriorated from the most difficult pattern (i.e., NDA with 180-degree rotation) to the least difficult pattern (i.e., DA with 0-degree rotation). Dominant arms have overall a faster learning speed than non-dominant arms since they are more frequently practiced in activities of daily living. This results to a more similar movement quality for more drawing attempts because of the ceiling effect [87] when no more obvious progress could be achieved. The ceiling effect was also supported by the fact that all ML models tented to mis-classify beginning and intermediate level. This was verified by relatively smaller F_1 scores. Therefore, it was challenging for all ML models presented in this research to classify movements conducted by dominant arms into more quality levels. This was verified by a significantly lower F_1 score (19.9% lower) and κ (29.7% lower) compared to nondominant arms (NDA) group.

Kinematic features have been successfully extracted from both Optotrak measurement system and the low-cost mouse sensor. No significant difference was observed between two sets of features except kurtosis of the velocity profile and the spectral entropy of the acceleration profile. The extracted features could reflect the motor learning progress over 10 drawing attempts on the same pattern during an experiment with 14 participants. Therefore, the research objective (c) was considered to be met.

The movement smoothness classification was achieved by categorising the continuous 10 drawing attempts into 3 different groups including beginning, intermediate and smooth based on the selected kinematic features. The research objective (d) was therefore considered to be met. However, the classification into more classes is not ideally achieved in this research. The best classification outcome was prevented by the selection of current kinematic features and the number of total attempts made during the

experiment. The results from this thesis could help establish the baseline measurements for future upper limb assessment based on machine learning and kinematic features. Table 4.9 summarises the main findings of this part of the work.

Table 4.9 Main findings on the kinematic assessment of upper limb movements.

Position Tracking	• Both mouse sensors and computer vision algorithms could potentially be used as a low-cost alternative for position tracking in a home environment with high accuracy. • Kinematic features extracted from the mouse sensor data does not show significant difference with those extracted from the Optotrak data. • A mouse sensor could be integrated into a haptic hand-held device for position tracking. • Computer vision algorithms are more suitable for the control of serious games and the detection of a safe working space of a rehabilitation robot.
Movement Type Classification	• Different movement types could be classified by a machine learning model with a similar trajectory (the triangle pattern) or different trajectories (reaching out, drawing circles, turning a key and drinking water). • Acceleration-based features are the most suitable for movement type classifications. • A standard movement repository could be established for comparative analysis on model performance and the progress monitoring.
Movement Smoothness Assessment	• Movement smoothness could be classified into three categories based on the selected kinematic features within a short period of time. • The inter-feature reliability between each kinematic feature is good in terms of describing the progression of upper limb movement smoothness. • Support Vector Machine has superior performance than the other machine learning models present in the thesis in terms of the balance between computational time and

	accuracy. It could be used as a baseline measurement for future study. • Velocity-based features are the most suitable for movement smoothness assessment. • Movement duration and peak acceleration present strong correlation with the clinically verified normalised jerk. Clinical assessment scores may be successfully predicted by those two features, which is beneficial for the telerehabilitation in a home environment without the presence of clinicians.

Recall the research question proposed in Chapter 2: *Can the application of kinematic features and machine learning models provide more sensitive and continuous quality assessment for upper limb movements in a home environment compared to a traditional clinical assessment?*

All these findings help to answer this research question. Kinematic features extracted from a low-cost mouse sensor could be used to assess upper limb movement with the help of supervised machine learning models. This method has great sensitivity in differentiating different movement patterns but is limited for differentiating movement smoothness into more than three categories from movements within a short period of time. More subtle classifications are expected to be achieved by data in a continuous longitudinal experiment. Since this method applies mouse sensor for data collection, it could be continuously conducted without professional support in a home environment. Overall, the results and findings presented in this chapter have answered the research question and met the expectations of the research.

Chapter 5 Experiment Designs and Hardware Development – Haptic Cue

In the previous chapter, kinematic assessments have been conducted using kinematic data collected from position sensors, specifically the Optotrak measurement system and a mouse sensor. The feasibility and efficacy of applying a mouse sensor for the assessment of repetitive upper limb movement smoothness have been proved. The data collection process was based on a triangle pattern displayed on a computer screen, which depends on the users to be able to receive the corresponding visual cues. However, as specified in the literature review, there are a large group of post-stroke patients and healthy people who suffer from visual impairments that may influence their ability in receiving visual cues. Therefore, finding an alternative way to deliver directional information to the visually impaired is of the research interest. In this chapter, three haptic motor designs were studied to provide directional cues, and the effectiveness of haptic delivery was verified through two independent experiments. An eccentric rotating mass (ERM) motor was firstly designed. However, this haptic solution was abandoned because of its poor performance in providing directional guidance and insufficient effectiveness and verifications. To mathematically understand the haptic output in order to deliver a strong directional guidance, a preliminary test platform was then introduced to study the dynamic behaviour of a solenoid-based haptic device. A one-degree-of-freedom (1DOF) mass-spring-damper model was established to describe the dynamic behaviour of the solenoid system. The model was verified by acceleration measurements and simulations. Additionally, the effect of different input signal waveform was also discussed. Finally, to improve the haptic delivery and reduce the size and weight of the hand-held device, a voice coil actuator (VCA) - based hand-held haptic device was finally designed and prototyped. Displacement measurements was conducted to investigate the effect of each input signal parameter on the output features, namely the vibration frequency, simplified speed, position stroke, negative stroke and stroke ratio. This relationship was then used to guide the verification process in the human-involved experiment presented in the next chapter. The remainder of this chapter is organised as follows. Section 5.1 introduces the design of ERM haptic solution and the reasons for choosing alternative haptic actuators. Section 5.2 introduces a solenoid test platform

that was described by a mathematical model and verified by acceleration measurements. Section 5.3 introduces the design and verification of a VCA hand-held haptic device. Section 5.4 presents the results of the aforementioned experiments.

5.1 Eccentric Rotating Mass

Eccentric rotating mass actuators (ERMs) are widely used from smartphones to gaming consoles to deliver haptic feedback. When power is applied, the off-centre mass will rotate and produce vibrations. Therefore, an initial attempt on the design of haptic delivery was made using two ERMs.

The ERMs used in this design are the vibrating mini motor disc (the PiHut, 102867). ERMs were powered and controlled by a commercial motor drive (DRV2605L, Adafruit). Two ERMs were attached to a frame and were controlled by an Arduino Nano 33 BLE as shown in Figure 5.1.

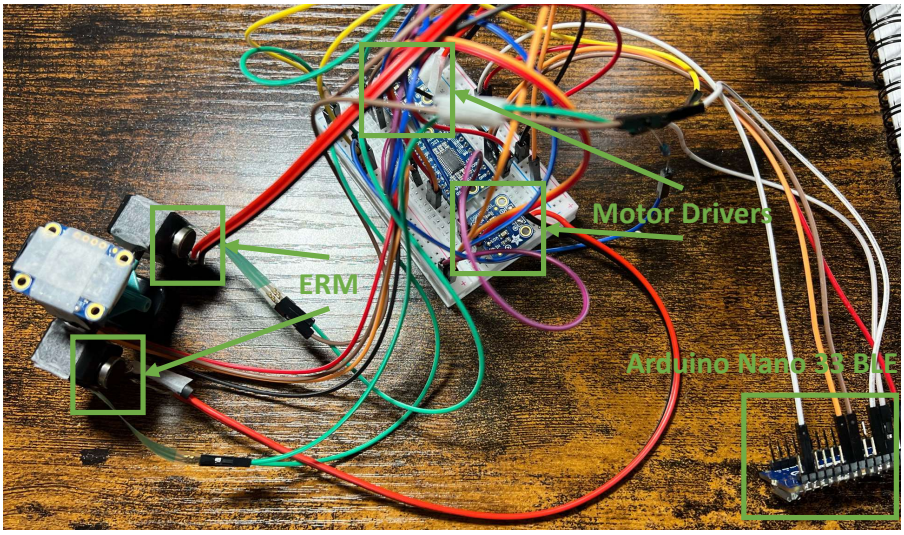

Figure 5.1 Two ERMs attached to a frame and controlled by a motor driver.

The left and right ERM could generate programmable haptic sequence and could be controlled independently. However, it was considered to be inappropriate for delivering haptic directional cues due to the nature of ERMs and the following reasons.

- ERMs are mostly suitable for vibrations with a low frequency due to the off-centre rotation movement.
- The ERM used in this design has a maximum input voltage of 5 V. The strength of the generated vibrations is strictly limited by the maximum voltage. Therefore, the haptic delivery is not clear.
- Multiple ERMs are necessary if multi-directional haptic cues are needed. The precision of directions depends highly on the number of

ERMs in the design. For example, a minimum of 9 ERMs are required if eight directional regions ($\frac{360}{8} = 45^o$ in between) are separated as shown in Figure 5.2.

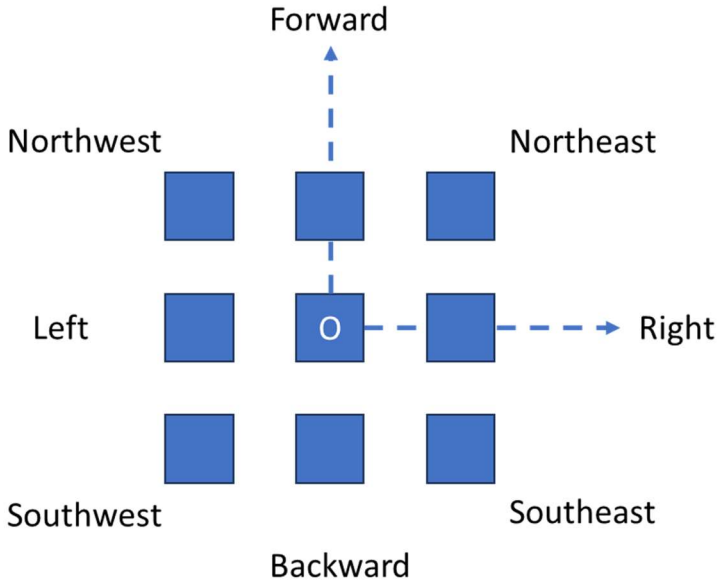

Figure 5.2 A total of 9 ERMs are needed for directional guidance along 8 directions.

- The dynamic behaviour of the motor is extremely difficult to describe mathematically without knowing the mechanical specification of the motor, such as the rotating inertia and spring constants.

Although the motor driver provides a rich selection and configurability on vibration sequence, the small ERMs presented in this work were considered unsuitable for the delivery of haptic directional cues. This initial exploration of ERMs helped to establish the key requirements for the haptic device design. Firstly, the design should deliver haptic cues with a higher vibration frequency. Otherwise, continuous feedback could not be satisfied. Secondly, the strength of the haptic output should be quantifiable and strong enough to be perceived by users. Thirdly, the direction of haptic output should be configurable to serve a 2D plane. The formal design specification of the hand-held device would be presented later in the thesis. Because ERM motors used in this thesis are nor suitable for providing directional guidance, another two types of motors would be discussed below for the generation of asymmetric vibrations.

5.2 Solenoid Test Platform

Force sensation is important for humans to receive information during activities of daily living. Haptic device could deliver haptic feedback during an activity to provide force stimuli. Previous explorations on ERMs have revealed key requirements for the design of haptic devices. To achieve this purpose, ungrounded haptic devices using linear resonant actuators (LRA) based on asymmetric vibrations have been widely studied [56, 88, 89]. The term 'ungrounded' in this context means that there is no connection between the haptic device and the ground.

Linear resonant actuators (LRA) consist of a moving mass, a spring, and an electromagnet. When current is applied, the moving mass will be accelerated by the electromagnet and spring alternately, producing vibrations. Unlike ERMs, LRA could generate high-frequency vibrations with stronger vibration amplitudes. However, normal vibrations could still not provide directional haptic feedback using either LRAs or ERMs. To solve this challenge, a novel vibration pattern is introduced.

Traditional haptic feedback such as mobile phone vibrations are symmetric, which could only serve the purpose as an alarm or a simple sense of touch. However, asymmetric vibrations could also provide directional information due to the nonlinear sensing characteristics on haptic cues of human skin [90]. When strong and weak haptic stimuli are applied to the skin sequentially, people may only feel the stronger stimuli but tend to ignore the weaker ones.

To test the asymmetric vibrations, a solenoid haptic test platform was built using a linear pushing solenoid. A pushing solenoid with a spring could be considered as a large-scale LRA. A dynamic model was first established to mathematically describe the movement of the solenoid. This model was then verified on the haptic test platform by accelerations measured using an accelerometer. The effect of various input signal shapes was finally discussed to suggest future improvements.

5.2.1 Dynamic Model of Asymmetric Vibrations

A solenoid-based haptic platform was designed and built to verify the asymmetry of the output stimuli. The proposed test platform consisted of a pushing linear solenoid (SAIA-BURGESS, 195225-230), two compression springs ($k = 110$ N/m, $c = 0.8$ Ns/s), a fixed mass ($m_{fix} = 50$ g) and an accelerometer (BNO055, Adafruit). The accelerometer was attached to the end of the solenoid moving metal core ($m_{core} = 40$ g) to measure its

acceleration output during movements. The solenoid was rigidly fixed to an aluminium base as shown in Figure 5.3.

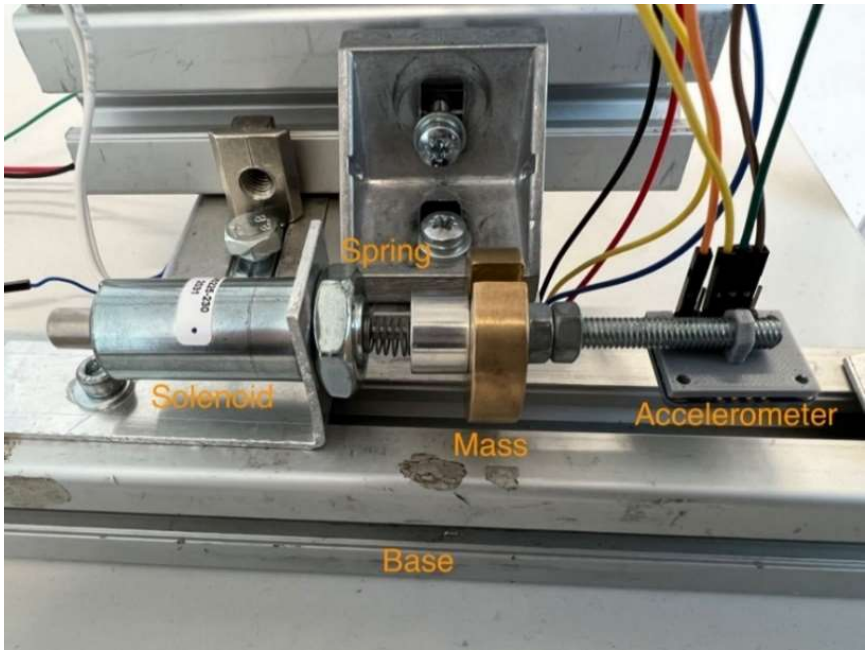

Figure 5.3 Solenoid haptic test platform.

The solenoid consists of a moving metal core and an electromagnetic coil. Because this solenoid is a pushing type, it is necessary to add a spring to retrieve the metal core back to the original position. An extra spring with the same specification is also inserted inside the solenoid between the metal core and the outside coil as illustrated in Figure 5.4.

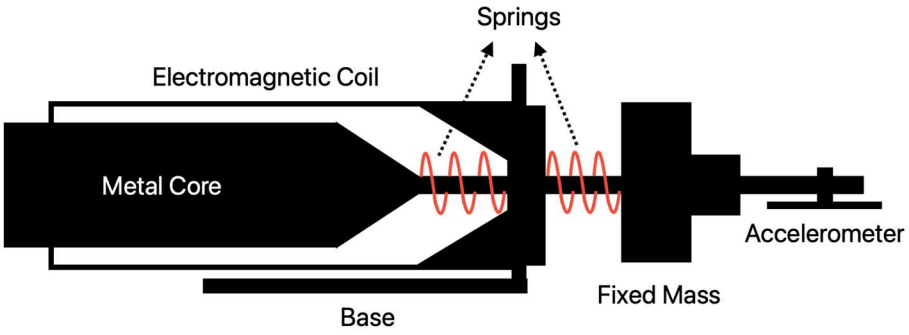

Figure 5.4 Sectional view of the solenoid haptic test platform.

The motion of the moving metal core is controlled by the input signal. For the dynamic modelling and simulation verifications, Pulse Width Modulation (PWM) signals with varying duty ratios (r) were used as the input control signal to generate asymmetric vibrations. When the current is supplied to the electromagnetic coil, the metal core will be accelerated in the positive direction (i.e., accelerometer side) while the metal core will be pushed back to the natural position by two springs when no current is supplied.

Duty ratio (r) is the measurement of the amount of working time for a PWM signal in a given period of time. Figure 5.5 presents PWM signals with three different baseline duty ratios and frequencies used in this haptic test platform with a unit scale. Higher duty ratios were used with higher frequencies. Otherwise, an insufficient amount of current could not drive the solenoid moving metal core.

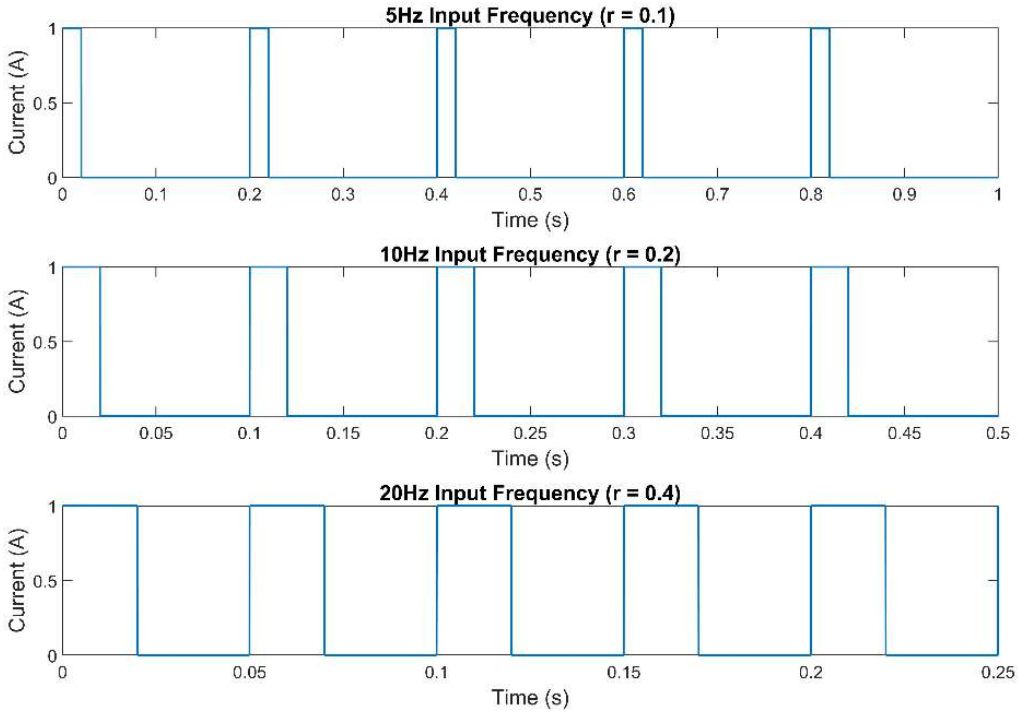

Figure 5.5 Input current (unit) signals with different frequencies and duty ratios.

Previous research has explored the potential to create asymmetric vibrations using PWM signals [59, 91]. In this research, the hypothesis is that asymmetric vibrations could be achieved and measured by accelerations when the moving metal core is accelerated asymmetrically by the PWM signal. The asymmetry depends on two variables: duty ratio (r) and spring response time (T_{re}). The spring response time is defined as the amount of time needed for the inner spring to accelerate the metal core.

When the duty ratio is small enough (e.g., $r = 0.1$ at 5 Hz) to just accelerate the metal core to compress the inner spring, the returning stroke of the metal core is dominated by the spring force F_s, resulting to a high acceleration in one direction. On the contrary, when the duty ratio is large (e.g., $r = 0.8$ at 5 Hz), there is insufficient amount of time for the springs to push the metal core to reach a large acceleration. Therefore, the spring response time (T_{re}) could not be satisfied. Consequently, the metal core could not be fully accelerated by the inner spring but dominated by the electromagnetic force F_c, resulting to a high acceleration towards the opposite direction.

In order to quantify and simulate the acceleration of the metal core created by PWM signals with varying duty ratios, a 1DOF mass-spring-damper model was created in Figure 5.6.

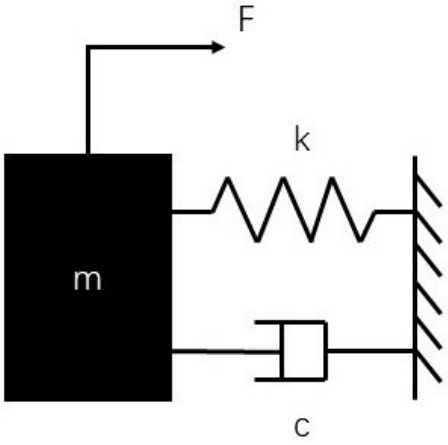

Figure 5.6 Dynamic model of the solenoid haptic test platform. Inner and outer springs are considered as parallel connection.

The equation of motion for the moving metal core is described in Eq. 5.1.

$$m\ddot{x} = F - kx - c\dot{x} \tag{5.1}$$

where: m is the total moving mass, k and c are the spring stiffness and damping constant of the parallel connected springs and F is the electromagnetic force calculated by Eq. 5.2.

$$F = B_m l_c I \tag{5.2}$$

where: B_m is the magnetic flux density, l_c is the length of the wire in the coil and I is the current.

To solve Eq. 5.1, its state space equation form is taken in Eq. 5.3.

$$\begin{cases} \dot{x} = Ax + BF \\ y = Cx + DF \end{cases} \tag{5.3}$$

where: $A = \begin{bmatrix} 0 & 1 \\ \frac{-k}{m} & \frac{c}{m} \end{bmatrix}$, $B = \begin{bmatrix} 0 \\ \frac{1}{m} \end{bmatrix}$, $C = \begin{bmatrix} 1 & 0 \\ 0 & 1 \\ \frac{-k}{m} & \frac{-c}{m} \end{bmatrix}$ and $D = \begin{bmatrix} 0 \\ 0 \\ \frac{1}{m} \end{bmatrix}$. The state variables are taken as $x = \begin{bmatrix} x_1 \\ x_2 \end{bmatrix} = \begin{bmatrix} x \\ \dot{x} \end{bmatrix}$. The outputs are $y = \begin{bmatrix} y_1 \\ y_2 \\ y_3 \end{bmatrix} = \begin{bmatrix} x \\ \dot{x} \\ \ddot{x} \end{bmatrix}$.

The weight of the accelerometer is very light ($m_{acc} = 3$ g) and the inertia introduced by the cable connection to the accelerometer was neglected. Therefore, the total moving mass $m = m_{core} + m_{fix} = 90\ g = 0.09\ kg$.

Since it is difficult to measure the magnetic flux and the length of the wire in the coil, the solenoid drive constant is defined as $d = B_m l_c$ that was

determined experimentally. Four known weights (36 g, 86 g, 136 g, and 186 g) were attached to the end of the metal core. Current was regulated by a power supply unit. The current value was recorded if the attached weight was just lifted against gravity. A linear regression between current (A) and weights (N) was made and the slope of the linear fit was considered to be the best estimate of the solenoid drive constant. The result would be presented in the next chapter.

5.2.2 Dynamic Model Verification

The dynamic model established in the previous section was verified by a comparison between the simulated acceleration and experimental acceleration of the moving metal core. To do this, a Simulink (v10.6, MathWorks) model was built as shown in Figure 5.7.

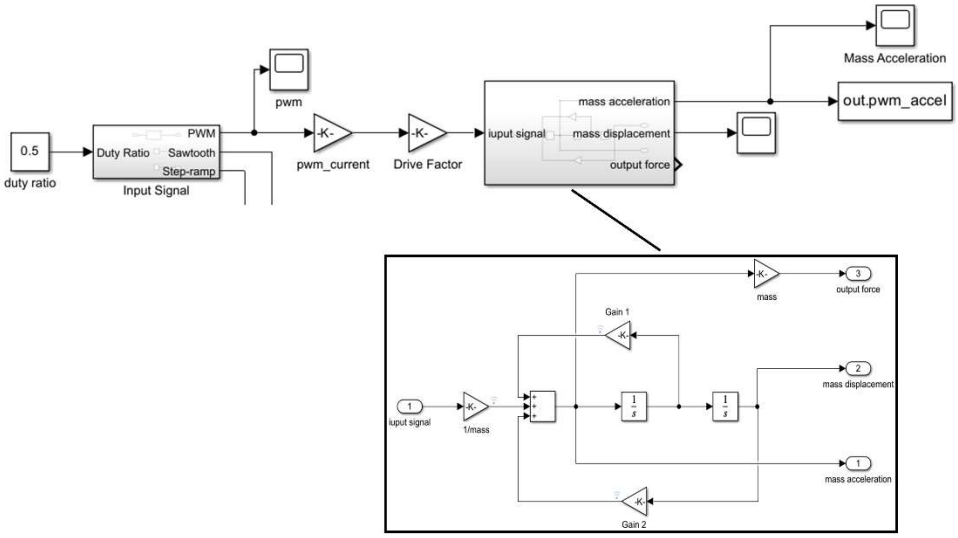

Figure 5.7 Simulink model of the solenoid dynamic model with PWM as the input signal.

The subsystem took the input signal with varying duty ratios and frequencies, and output the acceleration, displacement, and force of the moving metal core. The outputs were simulated at three frequencies (5 Hz, 10 Hz and 20 Hz) as shown in Figure 5.5. The upper limit of 20 Hz was chosen because movements with higher frequencies would overheat the solenoid electromagnetic coil, which could affect the performance of the solenoid test platform. Besides, past research has shown that asymmetric vibrations tend to become symmetric vibrations with higher frequencies [60, 91].

Outputs from the simulation were exported to a self-written MATLAB (R2021b, MathWorks) script, where the measured accelerations by the accelerometer were processed and compared. The sampling frequency of the accelerometer was set to 100 Hz. A bandpass filter with cut-off

frequencies of $f_{cl} = 5$ Hz and $f_{ch} = 20$ Hz was used to process the raw acceleration data.

Because the simulated accelerations had a much faster sampling frequency than the experimental accelerations, the resulted length of acceleration profiles were significantly different. Therefore, normal error quantification methods using data pairs like root mean square errors (RMSE) could not be used. Instead, Dynamic Time Warping (DTW) distance was applied to quantify the difference between two acceleration profiles.

DTW is a popular algorithm in the field of signal analysis for time series to measure the similarity between two signals with different lengths. It has been widely applied in speech and writing recognition [92, 93]. To compute the DTW distance for two one-dimensional time series $X = \{X_i, i = 1,2, \dots, m\}$ and $Y = \{Y_j, j = 1,2, \dots, n\}$, a distance matrix D of size $(m \times n)$ was calculated with $D_{i,j}$ representing the Euclidean distance between X_i and Y_j as described in Eq. 5.4.

$$D_{i,j} = \left\| \left(X_i - Y_j \right) \right\| \tag{5.4}$$

The object of DTW can then be described by Eq. 5.5.

$$\begin{aligned} Minimise\ d &= \sum D_{i,j} \\ Subject\ to: i_{next}, j_{next} &= \begin{cases} i, j+1 & vertical \\ i+1, j & horizontal \\ i+1, j+1 & diagonal \end{cases} \end{aligned} \tag{5.5}$$

A smaller DTW distance d indicates more similarities between the simulated and experimental acceleration signals, indicative of higher model precisions.

5.2.3 Effect of Input Signal Shape and Spring Stiffness

Apart from PWM signals, other analogue input waveforms also have the ability to create asymmetric vibrations. For this haptic test platform, sawtooth and step-ramp input waveforms were also tested in the simulation after the model verification. These two waveforms have been previously proved by other literature to be efficient in delivering asymmetric vibrations. Instead of duty ratio, the actuation time T_{ON} was used to time the signal. The actuation time is defined as the amount of time before current reaches saturation. A unit of sawtooth and step-ramp signal is illustrated in Figure 5.8.

In order to quantitively compare the haptic output from different input signal shapes, the average difference of acceleration peaks D_{ptp} was calculated as described by Eq. 5.6.

$$D_{ptp} = \frac{\sum_{i=1}^{N_{max}} A_{max}(i)}{N_{max}} - \frac{\sum_{j=1}^{N_{min}} A_{min}(j)}{N_{min}} \quad (5.6)$$

where: N_{max} and N_{min} is the number of maximum peaks and minimum peaks, respectively. A_{max} and A_{min} is the maximum and minimum acceleration peaks, respectively.

A larger difference in acceleration peaks represents more asymmetry of the haptic output. Additionally, the momentum of haptic output of three input signal shapes was also simulated and discussed.

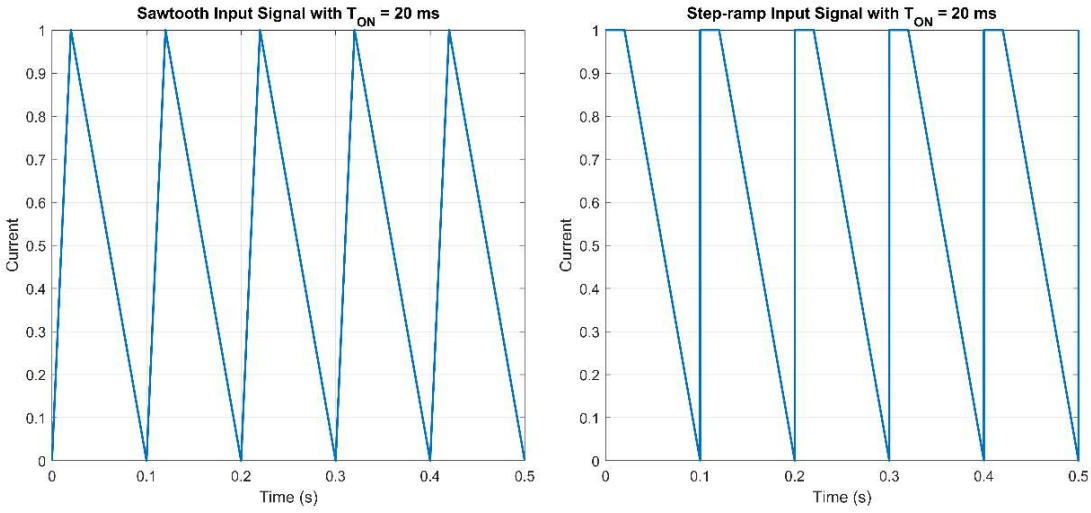

Figure 5.8 Sawtooth and step-ramp input signal with an actuation time of 20 ms.

Three different actuation time $T_{ON} = 20, 50, 80$ ms were tested for both waveforms at a frequency of 10 Hz.

Another important variable for the generation of asymmetric vibrations is the stiffness of the springs because it determines the system's response time T_{re} as discussed before. Extra stiffnesses were tested with PWM signals at a frequency of 10 Hz. The output acceleration peaks were recorded, and the peak difference was calculated to evaluate the asymmetry of the vibrations. The results of this part of the work would be presented in the next chapter.

5.3 Hand-held Haptic Device

Asymmetric vibrations could be generated by various types of motors, among which the voice coil actuator (VCA) is the most popular because of its portable size, affordable cost, and ease of control. In terms of the device design, hand-held devices have several advantages over wearable devices. Firstly, hand-held devices require less time for users to learn on how to use the device. Users could master the use of the device in a shorter amount of time, which could be beneficial for home-based rehabilitation on a daily basis.

Secondly, they could be independently used whereas most of the wearable devices often require more adequate assistance from other people during the operation, such as wearing a belt, a backpack or a pair of gloves.

To implement the VCA for haptic information delivery, a hand-held device was designed and verified in this section. The device prototype was firstly designed and manufactured. The control circuit was built for two versions: a printed circuit board (PCB) version and a breadboard version. The device was finally tested with 30 participants in order to verify the design of the device and the hypotheses regarding to the optimisation of haptic information delivery. Additionally, a VCA haptic test platform was also built in order to quantify the asymmetry of the haptic output, which would contribute to the parameterisation of the input control signal for optimised haptic delivery.

5.3.1 Device Design and Manufacturing

A product design specification is important for good quality delivery, and it helps ensure the product meets the expectations throughout the process. Therefore, a design specification was made for the hand-held haptic device as listed in Table 5.1. A brief introduction and scope were provided to guide the overall design process. Functional requirements including the construction of the device, user's experience and operation safety were also considered.

Table 5.1 Haptic device design specifications.

Introduction: A cylindrical hand-held local navigation device that produce haptic feedback by a voice coil actuator for visually impaired people.	
Basic Operation: The voice coil actuator outputs asymmetric vibrations to deliver haptic directional cues. Multidirectional guidance is achieved by a stepper motor. Users hold the device by hand and feel the directions locally.	
Scope: Assistive equipment, as a low-cost local navigation prototype for visually impaired people.	
Construction	
Materials and Process	3D printing with Polylactic Acid (PLA)
Dimensions	For the cylinder body: • Height: $90 - 110\ mm$ • Thickness: $2\ mm$ • Outer diameter: $65 - 75\ mm$

	For the motor box: • Length: $52.8\ mm$ • Width: $34.0\ mm$ • Height: $38.5\ mm$ • Thickness: $2.0\ mm$ For the cap: • Outer diameter: dependent on the outer diameter of the cylinder body. • Thickness: $1\ mm$ • Height: $30\ mm$ For the assembly: • Weight: $< 600\ g$
Quantity	Cylinder body: 1 Cap: 1 Motor box: 2 Control circuit: 2 (PCB version and breadboard version)
Reliability	The product is expected to function correctly for a minimum of 3 years.
Maintenance	The voice coil actuator (VCA) needs to be inspected regularly. Inspection of the VCA requires disassembly of the cap from the cylinder body.
User Experience	
Aesthetics	White, symmetrical, with identification of default direction.
Ergonomics	Six adhesive finger pads addressing finger positions for right hand only.
Safety	
Safety Considerations	• Scratch by sharp edges of the device or circuit board. • Electric shock ($< 5\ V$) if inappropriate use of power supply.

Safety Standards	• File or smooth the edge of the device. • Turn off power supply after use.

The material used for 3D printing is PLA that is one of the most popular materials in additive manufacturing since it is strong in strength and stiffness and can be printed with a relatively low temperature, which means it is suitable for the development of a low-cost device. Furthermore, it is a biodegradable material that is friendly to the environment.

The specific size of the cylinder body was not determined since it was dependent on the size of rotary encoders and accelerometer embedded into the cylinder body. However, the maximum size should not be exceeded, which would lead to uncomfortable user experience during operation. This maximum size was determined based on the maximum grip exertions on cylinders [94] that had a maximum value of 83 mm. The maximum weight was determined according to the weight of a bottle of water since post-stroke patients may have decreased ability in grip forces according to the results reported in [95].

The voice coil actuator (VCA) itself does not need regular inspection. However, the VCA used in this device is powered by cables that may be twisted together when changing directions. Therefore, a regular inspection on the VCA could help eliminate the effect of twisted cables, which may lead to ambiguous haptic feedback during operation.

5.3.2 Source of Vibrations

Haptic directional cues are delivered via a hand-held device as shown in Figure 5.9. The device assembly was achieved in JigSpace2 (v3.18) and each component was modelled using Shapr3D (v5.4). Figure 5.10 presents the model of every component in the hand-held device in JigSpace.

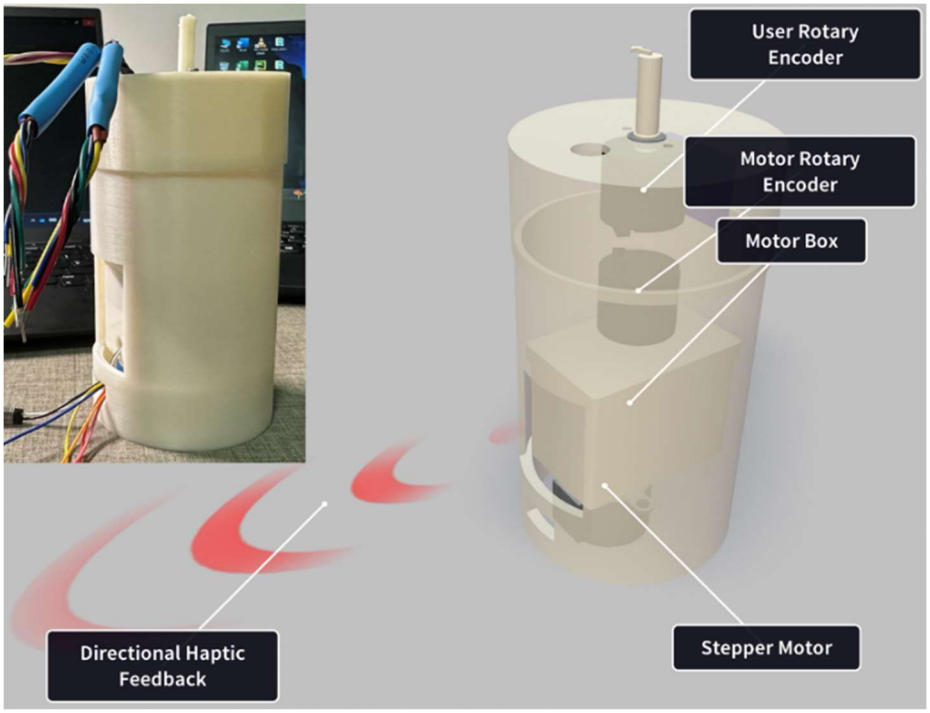

Figure 5.9 The assembly of the hand-held haptic device.

A voice coil actuator (VCA) (H2W NCM02-10-008-2JBA) was placed inside the motor box with the motor shaft fixed at both ends. This is the main vibration source to generate asymmetric vibrations. Two absolute rotary encoders (Broadcom, AEAT-6012-A06) were used to measure the rotation angle of the user shaft and the stepper motor, respectively. The user shaft encoder was placed under the top cap with the bottom of the shaft inserted into the encoder. The motor box encoder was placed on top of the motor box with the shaft inserted into the encoder. The user shaft was only used during the verification experiment to measure the perceived angle from participants. Because a single VCA can only produce unidirectional haptic cues, a stepper motor (28BYJ-48) was placed at the bottom of the cylinder body to provide flexiable direction adjustments. The IMU sensor was placed inside the cylinder top cap as a tool to integrate the assessment of movement quality from the acceleration profiles in the future version of the device.

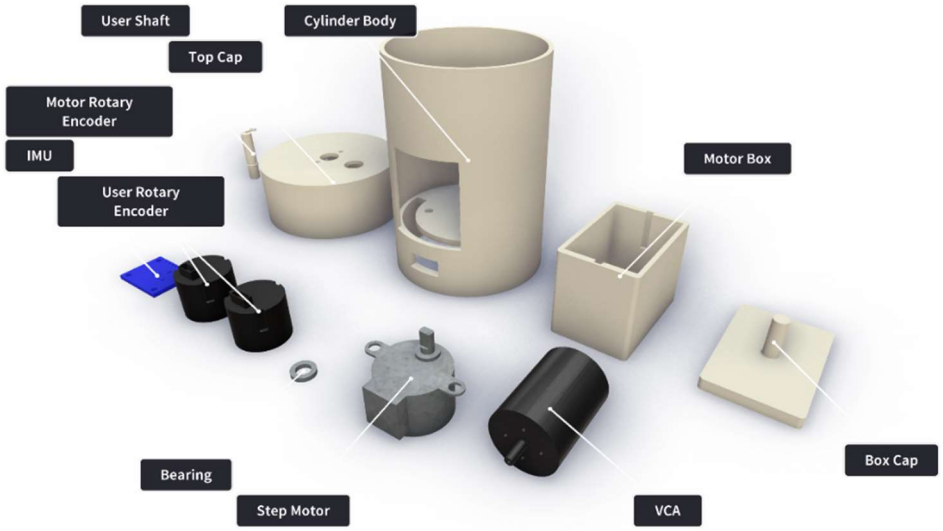

Figure 5.10 Modelling of components inside the hand-held haptic device.

A system block diagram is illustrated in Figure 5.11 to present the workflow of the system.

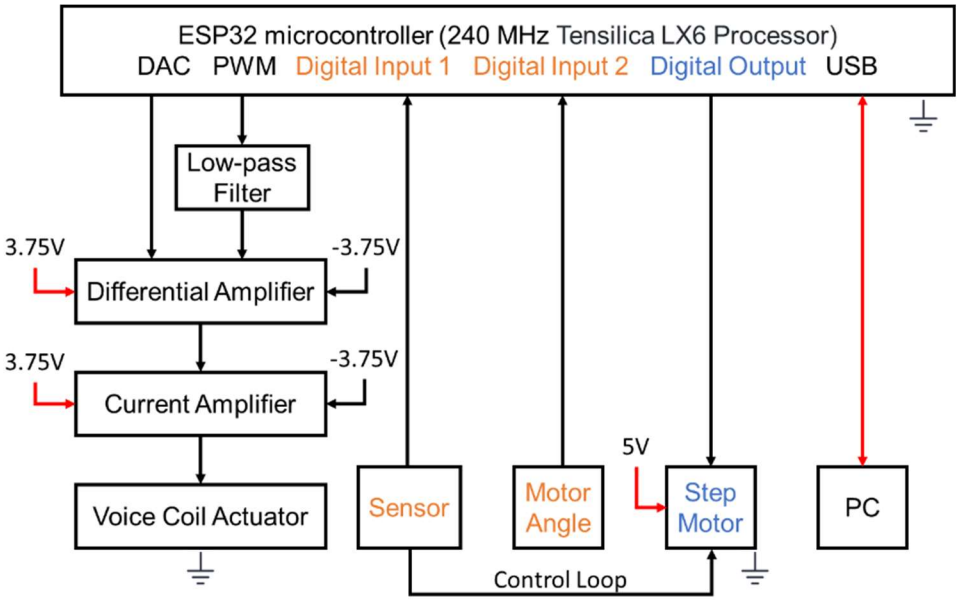

Figure 5.11 Block diagram of the haptic device.

The asymmetric vibrations were generated by a VCA using a repeating step-ramp signal as an input. The signal consists of three components as illustrated in Figure 5.12. The step-ramp signal starts with a step input to a certain voltage V_a. This will accelerate the moving metal of the VCA towards one direction, producing a positive stroke. The voltage is then held for an adjustable amount of delay time t_d. Because there is no mechanism designed to return the moving metal automatically (e.g., a compression spring), the moving metal will stay idle during the delay time. Finally, a ramp down input is achieved by repeatedly decreasing a certain amount of voltage to a cut-off voltage V_c with a ramp-down step length of S_r for several

iterations. This will slowly and gently retrieve the moving metal back to the initial position for next movement period, producing a negative stroke.

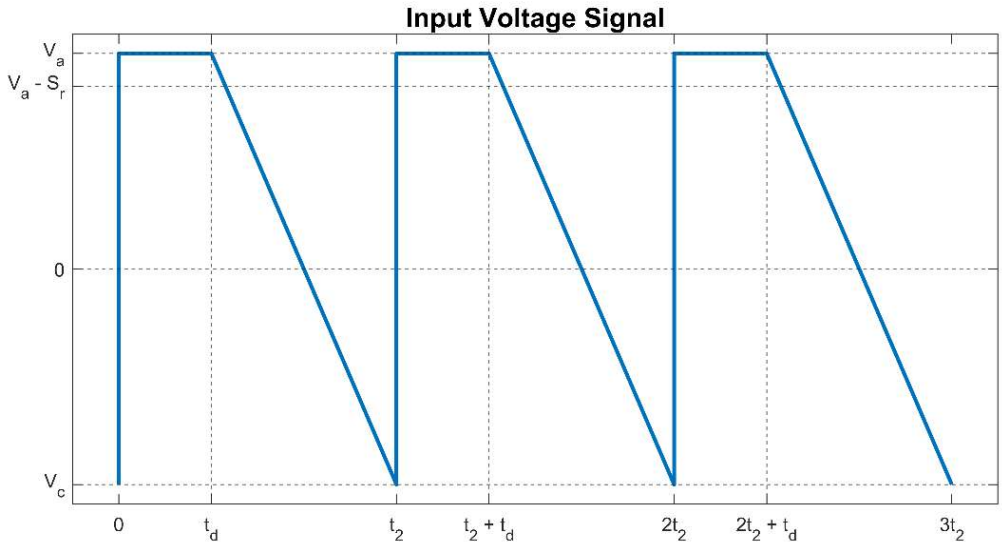

Figure 5.12 Step-ramp input signal that generates asymmetric vibrations.

The perception of haptic directional cues is highly dependent on the vibration frequency and the asymmetry of the output strokes. Therefore, in order to quantify and parameterise the input signal, three parameters of the step-ramp signal were established and studied. Delay time (t_d) is the amount of time between step input and ramp-down input. By default, this value was set to $t_d = 20$ ms based on the results shown in [60]. A larger delay time results to a lower vibration frequency. It is essential to introduce delay time as it was also reported in [60] that the lack of the delay time leads to insufficient skin displacement that causes ambiguous perception of the haptic directional cues. Ramp down step length (S_r) is the amount of voltage being decreased in each iteration. By default, this value was set to $S_r = 256$. The default value was chosen based on the vibration frequency reported in [60]. A larger ramp down step length results to a higher vibration frequency since a shorter time is used to decrease the voltage. In addition, the ramp down input was achieved using a 12-bit digital-analogue converter (DAC) (MCP4725, Microchip). Therefore, there exists a conversion from analogue values (0 - 4095) to output voltages (0 V – 3.3 V) as described in Eq. 5.7.

$$V_{output} = 0.0008 \cdot V_{analogue} \tag{5.7}$$

Cut-off voltage (V_c) is the positive voltage level where ramp down iterations stop. By default, this value was set to $V_c = 0$ V where no cut-off voltage is applied as the baseline measurement. The hypothesis regarding to the cut-off voltage is that the asymmetry between output positive and negative strokes could be increased by introducing an optimised cut-off voltage. This

hypothesis would be verified by a psychophysical experiment with 30 participants as discussed later.

In order to control the three parameters established above, a custom control circuit was designed and built with two versions: a PCB version and a breadboard version. The PCB version is a permanent solution for the control circuit, which is suitable for the final product and an experimental environment. The breadboard version is a temporary solution for the control circuit, which is suitable for circuit optimisation, module add-ons and a test environment. The circuit schematic is shown in Figure 5.13.

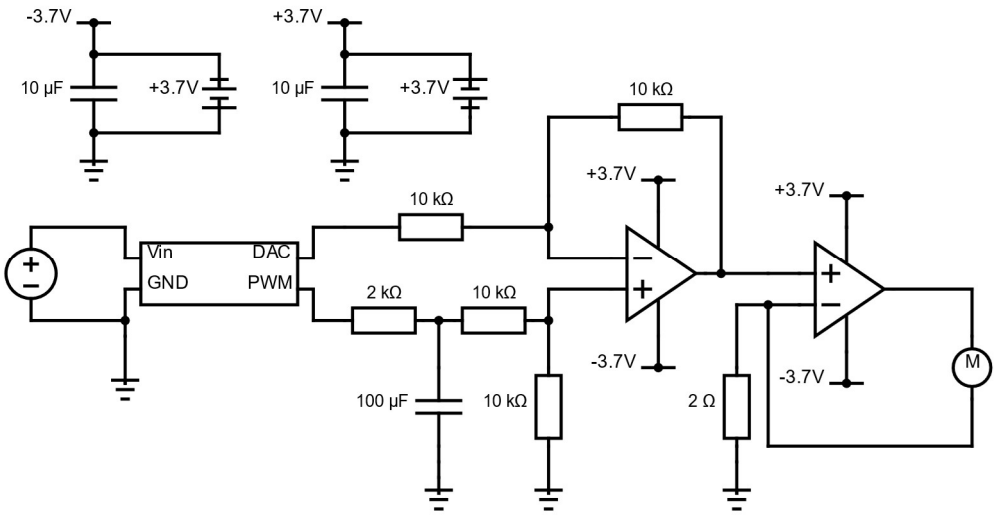

Figure 5.13 Schematic diagram of the custom control circuit for the VCA.

Two operational amplifiers were used as a differential amplifier (LM358, Texas Instrument) on the left and a current amplifier (PA75CD, Apex Microtechnology) on the right. The differential amplifier was used to regulate the input voltage (to obtain negative voltage level) and the current amplifier was used to power the voice coil actuator (VCA). The digital-analogue converter (DAC) was used to generate the desired input signal shape. A pulse width modulation (PWM) signal with a frequency of $f_{PWM} = 732$ Hz and a duty ratio of $r = 50\%$ was applied in the resistor-capacitor circuit (RC circuit). The RC circuit is commonly used as a lowpass filter in the circuit design. It is important to determine the resistor and capacitor values in a RC circuit to achieve ideal filter performance. The transfer function between the output voltage from a RC circuit V_{cap} and the input voltage V_{in} is described by Eq. 5.8.

$$G(s) = \frac{V_{cap}}{V_{in}} = \frac{\frac{1}{sC}}{R + \frac{1}{sC}} = \frac{\frac{1}{RC}}{s + \frac{1}{RC}} \tag{5.8}$$

where: R is the resistance of the resistor and C is the capacitance of the capacitor.

Because a negative voltage level is required to generate asymmetric vibrations for this design, the ideal output voltage from the lowpass filter should be the half of the DAC maximum voltage ($\frac{\max(V_{output})}{2} = \frac{3.3}{2} = 1.65\ V$). A Simulink model was built to simulate the performance of the lowpass filter. As a result, a resistance of $R = 2000\ \Omega$ and a capacitance of $C = 100\ \mu F$ was chosen to build the filter. The simulated response is shown in Figure 5.14.

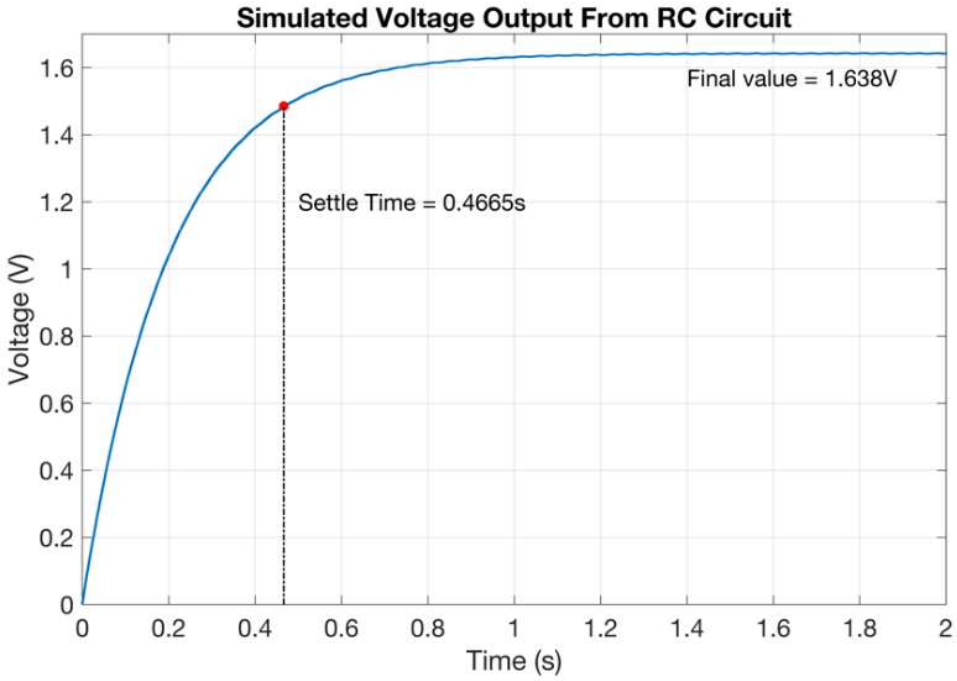

Figure 5.14 Simulated RC circuit response with $R = 2000\ \Omega$ and $C = 100\ \mu F$.

5.3.3 VCA Haptic Test Platform

In order to quantify the asymmetry of the haptic output from a VCA, a VCA haptic test platform was built using a low-friction single axis slider as shown in Figure 5.15. Existing literatures have applied measurements over accelerations for the quantification of haptic output. However, the sensory resolution of the vibrotactile amplitude was normally quantified in micrometre as shown in [96]. Therefore, displacement measurement was adopted in order to parameterise the haptic output and quantify the asymmetry of the haptic output. It is also important to verify the hypotheses based on the results of displacement measurements by the psychophysical experiment.

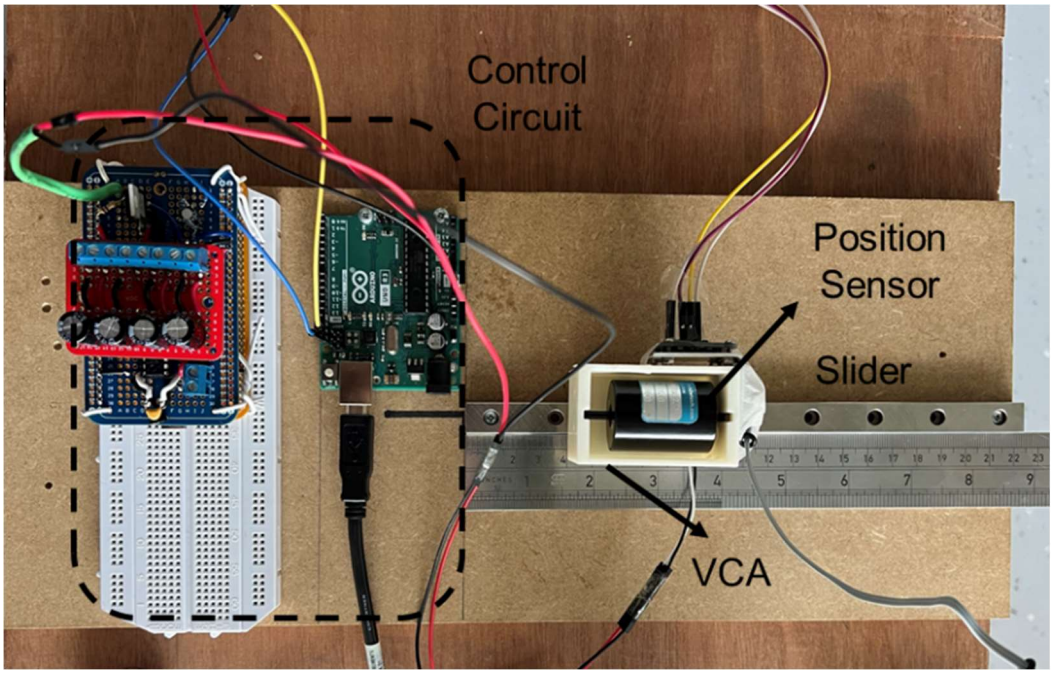

Figure 5.15 VCA haptic test platform on a slider.

Displacement measurements were made using the Optotrak Certus motion capture system with one position marker attached at the end of the motor box. Position data was captured by the NDI software and stored in CSV files for data processing. The sampling frequency of the position sensor was set to 100 Hz. The reported accuracy of the sensor is $\pm$ 0.1 mm.

Before each measurement, the motor box was placed at the original position (i.e., at 0 cm). Step-ramp input signals were then sent to the VCA. The motor box would start moving from the left to the right side of the slider due to asymmetric vibrations. Position data was recorded throughout the process. Each step-ramp input signal has a unique configuration that combines the three parameters established in the previous section. Different parameter groups were adopted in order to determine the upper and lower boundaries of the vibration frequencies because extreme frequencies (i.e., either too high or too low) could result to a failure in haptic perception.

All displacement measurements were normalised using a z-score method to enable direct comparison and haptic output parameterisation. Five parameters were established to describe a typical displacement profile from asymmetric vibrations as illustrated in Figure 5.16.

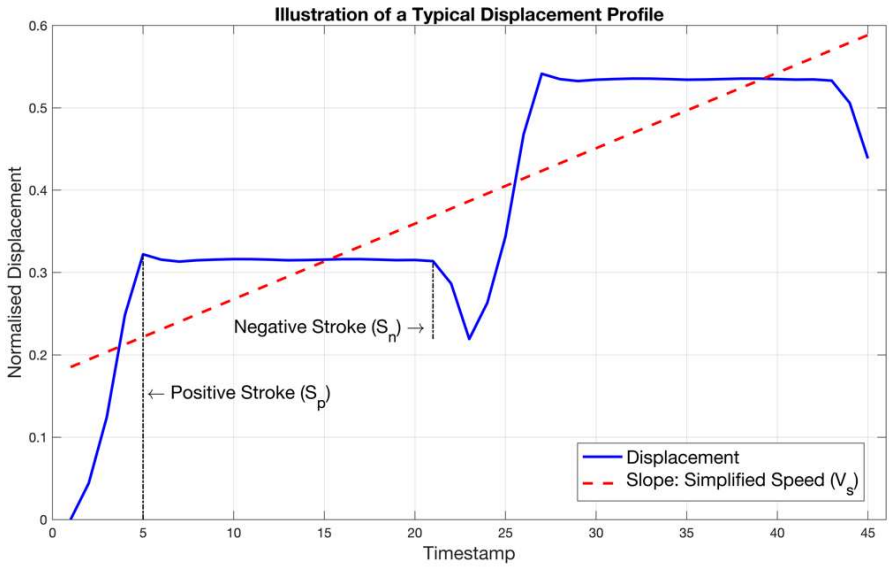

Figure 5.16 Illustration of a typical normalised displacement measurement from asymmetric vibrations.

The five parameters are defined below.

- Frequency (f_{asy} in Hz) is defined as the movement time divided by the total number of vibration cycles during the experiment.
- Simplified speed (V_s, unitless) is defined as the slope of the linear fit of the normalised displacement profile.
- Negative stroke (S_n, unitless) is defined as the normalised distance between the displacement platform (resulted from the delay time) and the negative spike (resulted from the ramp down input) in one cycle.
- Positive stroke (S_p, unitless) is defined as the normalised distance between the displacement platform and the positive spike (resulted from the step input) in one cycle.
- Stroke ratio (r_s, unitless) is defined as the negative stroke average divided by the positive stroke average as described in Eq. 5.9.

$$r_s = \frac{\sum_{i=1}^{N} S_n(i)}{\sum_{i=1}^{N} S_p(i)} \tag{5.9}$$

where: N is the number of cycles in one displacement measurement.

For both positive stroke and negative stroke, the average value over all cycles were calculated and adopted as the final parameter value for each configuration. Stroke ratio was used to quantify the asymmetry of the haptic output. A smaller stroke ratio indicates a more asymmetric haptic output.

5.4 Results

5.4.1 Solenoid Test Platform Results

5.4.1.1 Determination of the Solenoid Drive Constant

In order to verify the dynamic model of the solenoid haptic test platform, it is important to determine the solenoid drive constant d. However, because the independent measurement of magnetic flux density and the equivalent length of coil are difficult to made, a simple test was conducted to determine their product (i.e., the solenoid drive constant) experimentally. Four known weights ($36\ g$, $86\ g$, $136\ g$ and $186\ g$) were lifted by the solenoid against gravity with adjustable amount of current. The supplied current and the weights are plotted in Figure 5.17.

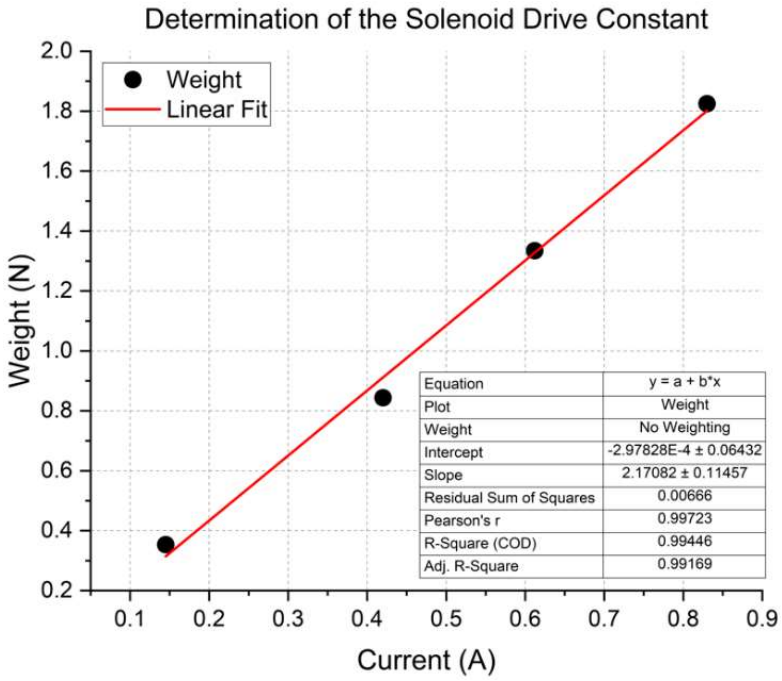

Figure 5.17 Determination of the solenoid drive constant using a linear regression method.

Based on Eq. 5.2, the slope of the line was considered to be the best estimate of the solenoid drive constant with $d = 2.17\ N/A$ and $R^2 = 0.99$.

For the remaining of the simulation, this solenoid drive constant was adopted.

5.4.1.2 Verification of the Dynamic Model

The dynamic model established by Eq. 6.3 was simulated in Simulink (v10.6, MathWorks). The parameters of the input PWM signals used in the simulations are listed in Table 5.2.

Table 5.2 Parameters of the PWM signals used in the simulation.

Frequency (f_{PWM} in Hz)	Duty Ratio (r)		
	r_{min}	r_m	r_{max}
5	0.1	0.5	0.8
10	0.2	0.5	0.8
20	0.4	0.5	0.8

Three duty ratios were adopted in the simulation. The minimum duty ratio for each PWM frequency was different because there exists a minimum working time in order for PWM signals to have sufficient power to drive the solenoid. The middle and the maximum duty ratios were kept the same for all PWM frequencies.

The simulated and measured acceleration profiles are shown in Figure 5.18.

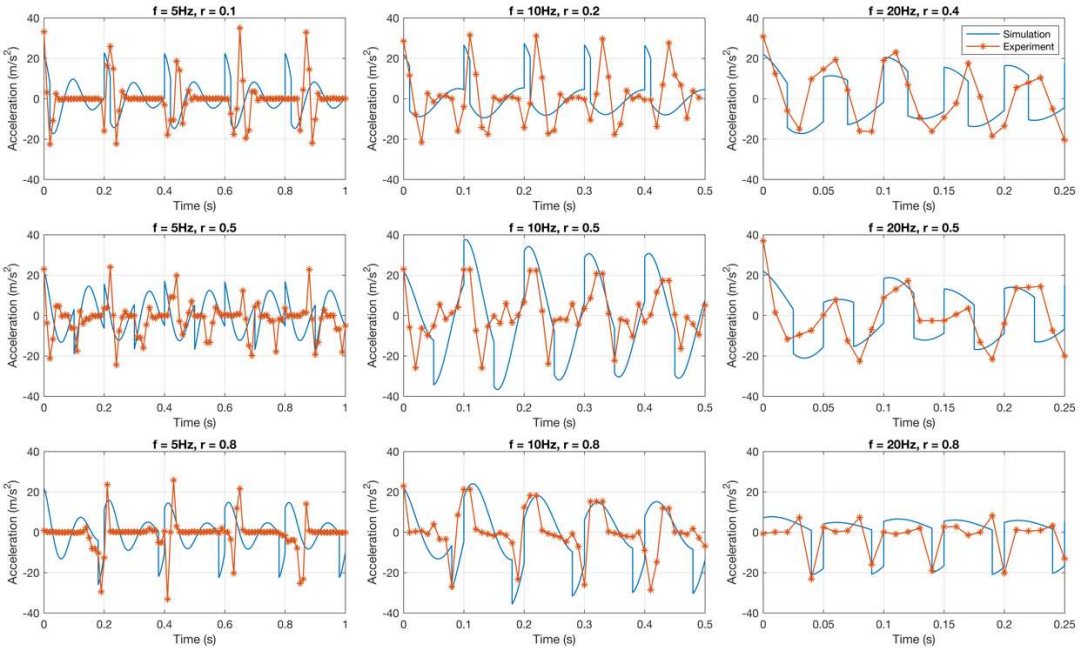

Figure 5.18 Comparison of simulated and measured accelerations for different PWM frequencies and duty ratios.

Most of the simulated and measured accelerations matched in terms of output direction and amplitude. However, a loss of damping features in the measured accelerations were observed at $f_{PWM} = 5$ Hz, especially at the minimum and maximum duty ratio.

The perception of haptic directional cues depends highly on the asymmetry of the haptic output. Even though the net acceleration in each cycle is zero, it is the amplitude difference between positive and negative peaks that results to the bidirectional force sensation. Specifically, the average value of

positive and negative peaks of the measured accelerations are listed in Table 5.3 to observe the amplitude directions.

Table 5.3 Average values of positive and negative acceleration peaks.

Frequency	Duty Ratio		
	$r = r_{min}$	$r = r_m$	$r = r_{max}$
$f_{PWM} = 5\ Hz$	29.15	14.99	17.20
	−19.16	−16.27	−22.56
$f_{PWM} = 10\ Hz$	29.70	18.68	18.27
	−16.91	−19.24	−26.20
$f_{PWM} = 20\ Hz$	22.74	16.02	7.65
	−16.95	−15.74	−20.79
Perceived Direction	Positive	Symmetric	Negative

It was observed that the absolute values of positive peaks were greater than negative peaks with minimum duty ratios regardless of PWM input frequency. The absolute difference between positive and negative peaks gradually decreased to approximately zero with medium duty ratios, and finally negative values with larger duty ratios. This change in peak value difference is shown in Figure 5.19.

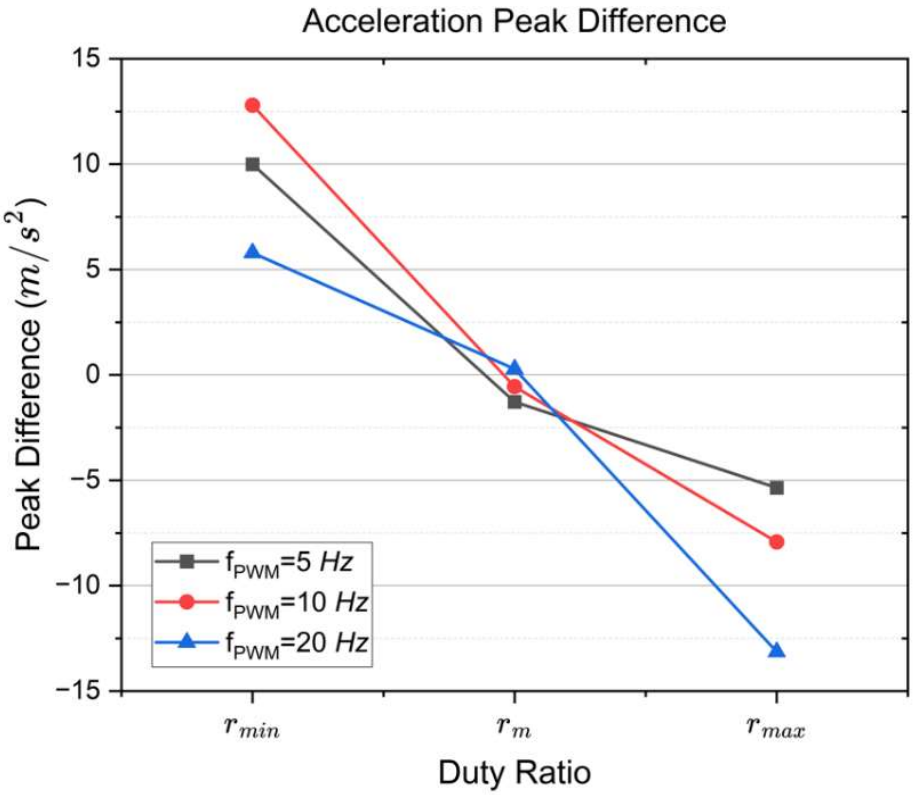

Figure 5.19 The change in acceleration peak value difference with respect to duty ratio.

In order to quantify the amplitude difference between the measured and simulated acceleration, dynamic time warping distance was calculated for all acceleration pairs and are listed in Table 5.4. The Euclidean distance definition was used for the distance calculation.

Table 5.4 Dynamic time warping distance between each acceleration pair.

Frequency	Duty Ratio			Average
	$r = r_{min}$	$r = r_m$	$r = r_{max}$	
	DTW ($\times 10^4$)			
$f_{PWM} = 5\ Hz$	6.1828	7.3611	9.1594	7.5677
$f_{PWM} = 10\ Hz$	3.4953	5.9542	4.1432	4.5309
$f_{PWM} = 20\ Hz$	1.6293	2.2945	1.3865	1.7701
Average	3.7691	5.2033	4.8964	

It was observed that the DTW distance decreased with larger PWM frequencies regardless of duty ratio. However, the effect of different duty ratios on the DTW distance was not significant. A Tukey test was used to quantify the significance level for duty ratio and PWM frequency. The results are shown in Figure 5.20.

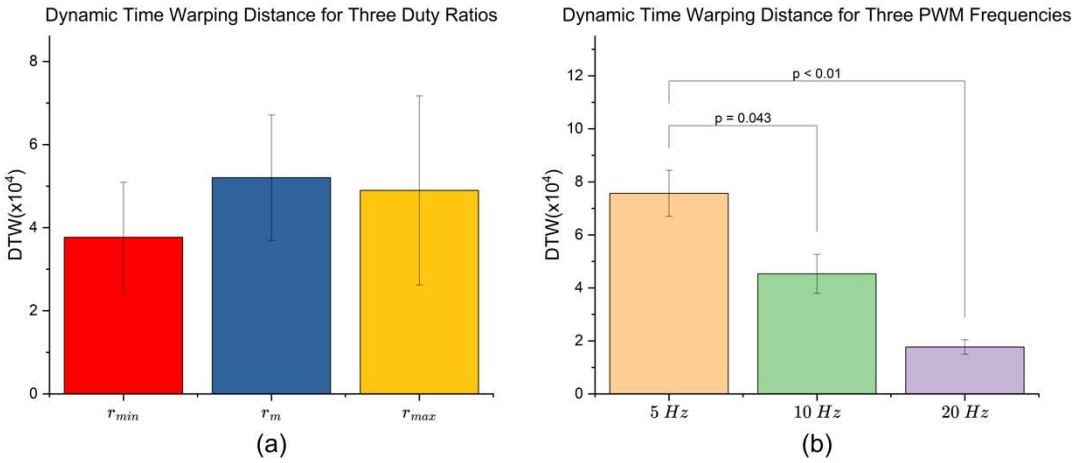

Figure 5.20 Tukey test results on (a) the effect of duty ratio and (b) the effect of PWM frequency.

It was observed that the DTW distance was significantly less than that with lower PWM frequencies at a PWM frequency of $f_{PWM} = 20$ Hz ($p = 0.043$ and $p < 0.01$). However, the effect of duty ratio was insignificant. This was consistent with the previous observation on Figure 5.18 that the measured acceleration profiles did not match well with the simulations at a PWM frequency of $f_{PWM} = 5$ Hz.

The DTW distances with the corresponding statistical analysis show improved dynamic model precision with a high PWM input frequency. Therefore, the established 1-DOF mass-spring-damper model could better represent the dynamic behaviour of the solenoid haptic test platform with a higher PWM input frequency. The established model and its verification underpin the future design of haptic device using solenoid as a vibration source to provide directional cues.

5.4.1.3 Effect of the Input Signal Shape

PWM signals have been proved to be effective in generating asymmetric vibrations by both acceleration measurements and simulations in the previous section. Apart from PWM signals, other analogue input signal shapes have also been widely applied in haptic input. To study the effect of different signal shapes on the haptic output, two analogue input signal shapes (i.e., sawtooth and step-ramp) were simulated at $10\,Hz$ using the dynamic model established before. The simulated acceleration output and the input signals are shown in Figure 5.21.

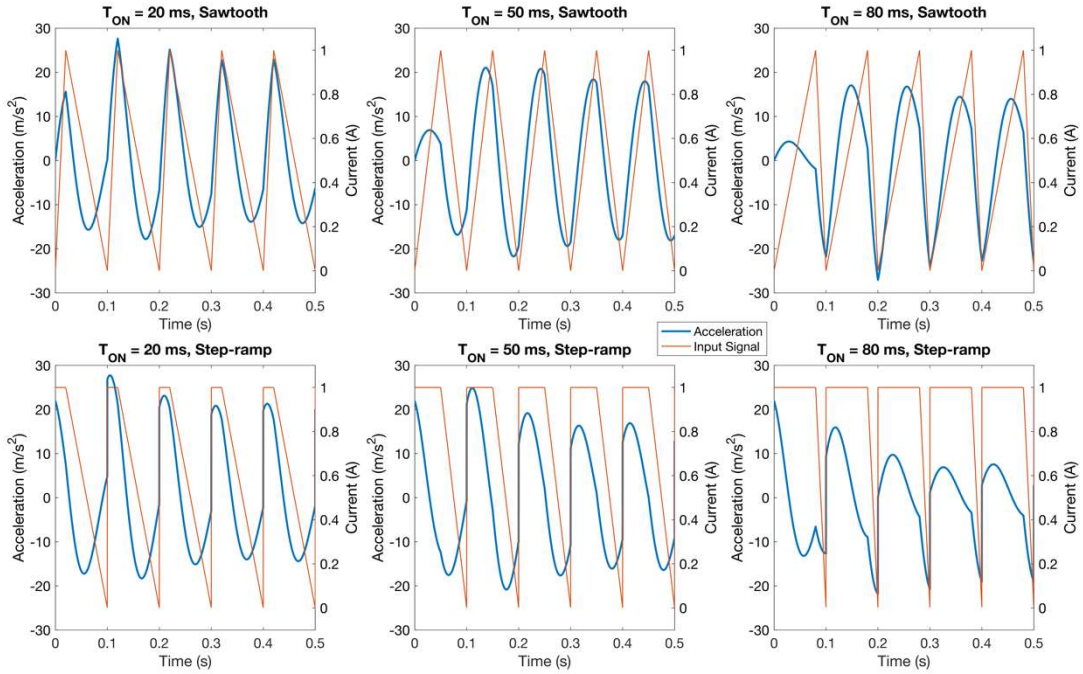

Figure 5.21 Input signals with corresponding simulated acceleration.

Similar directional change from positive to negative was observed in both sawtooth signal and step-ramp signal. When the actuation time $T_{ON} = 50$ ms, symmetric vibrations were observed. This is the same as the haptic output from a PWM signal at the same frequency. To quantitively compare the asymmetry of the haptic output from different input signal shapes, a comparison was made on the average acceleration peak values. The results are listed in Table 5.5.

Table 5.5 Average value of positive and negative acceleration peaks in different input signals.

Input Signal Shape	Actuation Time			Peak Difference
	$T_{ON} = 20\ ms$	$T_{ON} = 50\ ms$	$T_{ON} = 80\ ms$	
Sawtooth	22.83	17.01	13.31	7.49
	−15.34	−18.82	−23.92	−10.69
Step-ramp	23.00	19.85	12.42	7.19
	−15.81	17.70	−17.49	−5.07
PWM at $10\ Hz$	29.70	18.68	18.27	12.79
	−16.91	−19.24	−26.20	−7.93
Perceived Direction	Positive	Symmetric	Negative	

The peak difference was calculated by the difference between the absolute positive peak and the absolute negative peak and is shown in Figure 5.22.

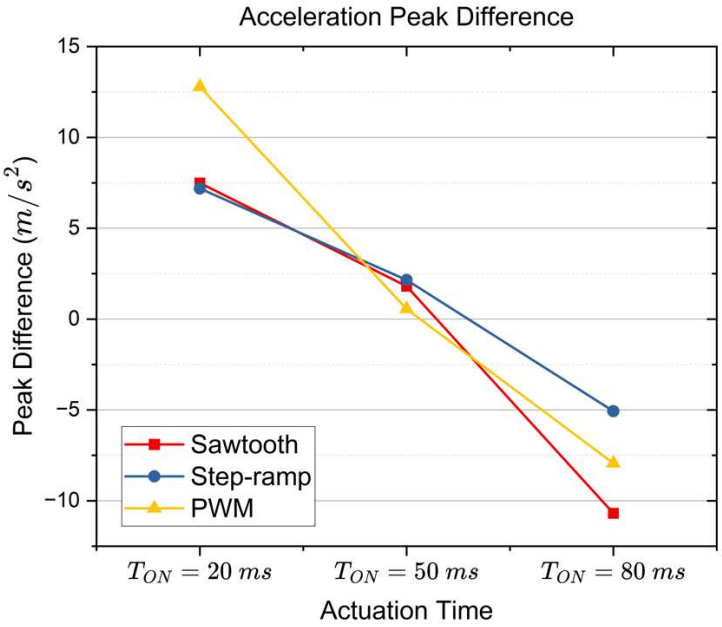

Figure 5.22 Acceleration peak difference for difference input shapes and actuation time.

With the same input frequency, PWM signals had larger peak difference compared to sawtooth signals and step-ramp signals. Although sawtooth signals and step-ramp signals had similar asymmetry in terms of acceleration peak difference, their haptic output waveforms had unique characteristics. The haptic output from both step-ramp signals and PWM signals have an abrupt change in acceleration before the peak value as a result of the step input. On the contrary, a gradual change in acceleration before the peak value was observed with sawtooth signals as a result of the ramp input. Intuitively, an abrupt change in accelerations (i.e., a larger change of momentum) is much easier perceived by people than a gradual change. The momentum of simulated haptic output for three signal shapes is shown in Figure 5.23.

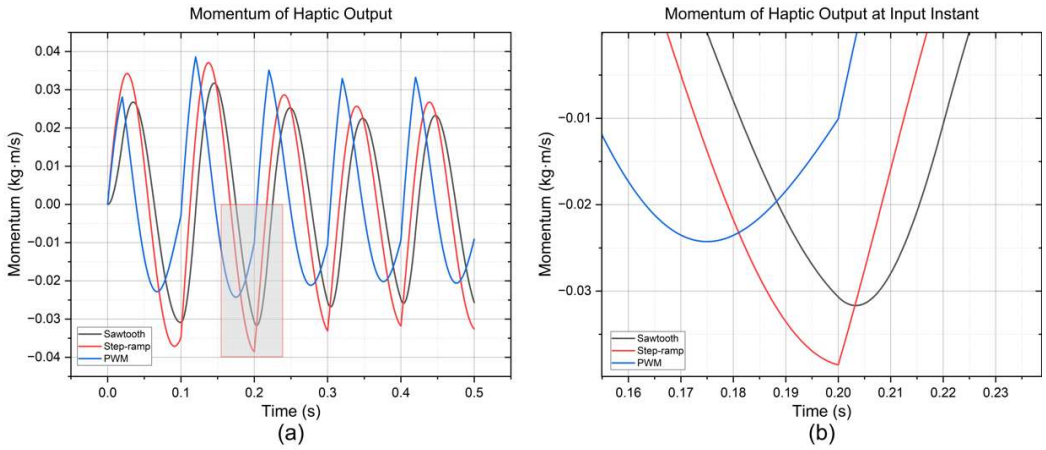

Figure 5.23 Change of momentum of haptic output for three input signal shapes (a) throughout the movement and (b) at the input instant.

It was observed that PWM signals have the largest change of momentum throughout the movement among all input signal shapes. This is consistent with the largest peak difference reflected in Figure 5.22. Sawtooth and step-ramp signals have similar momentum change with step-ramp signals being slightly larger than sawtooth signals. However, the change of momentum (i.e., the slope) at the signal input instant (e.g., at 0.2 s) for step-ramp signals and PWM signals are much larger than a sawtooth signal as shown in Figure 5.23 (b), which could theoretically provide a much clearer haptic delivery. Therefore, step-ramp and PWM signals are more suitable for providing directional cues. However, the effect of larger momentum change on the perception of haptic directional cues needs to be further studied.

For the haptic output after the peak value, abrupt changes in accelerations were also noticed with PWM signals. On the other hand, a gradual change was observed with step-ramp signals as a result of the ramp down input. The effect of this phenomenon on the perception of haptic cues was not studied in this research.

5.4.1.4 Effect of Spring Stiffness

Different spring stiffness have influence on the system's response time T_{re}. A larger stiffness could accelerate the moving metal core faster to a high acceleration, resulting in a smaller system's response time. In order to understand the effect of spring stiffness on the dynamic behaviour of the haptic test platform, four spring stiffness (i.e., $k = 70, 90, 130, 150$ N/m) were simulated with small $(r = 0.2)$ and large $(r = 0.8)$ duty ratios using the dynamic model established before at 10 Hz. Figure 5.24 presents the simulated acceleration output with different spring stiffness. Additionally, the

averages of positive and negative peak values and the peak-to-peak difference are shown in Figure 5.25.

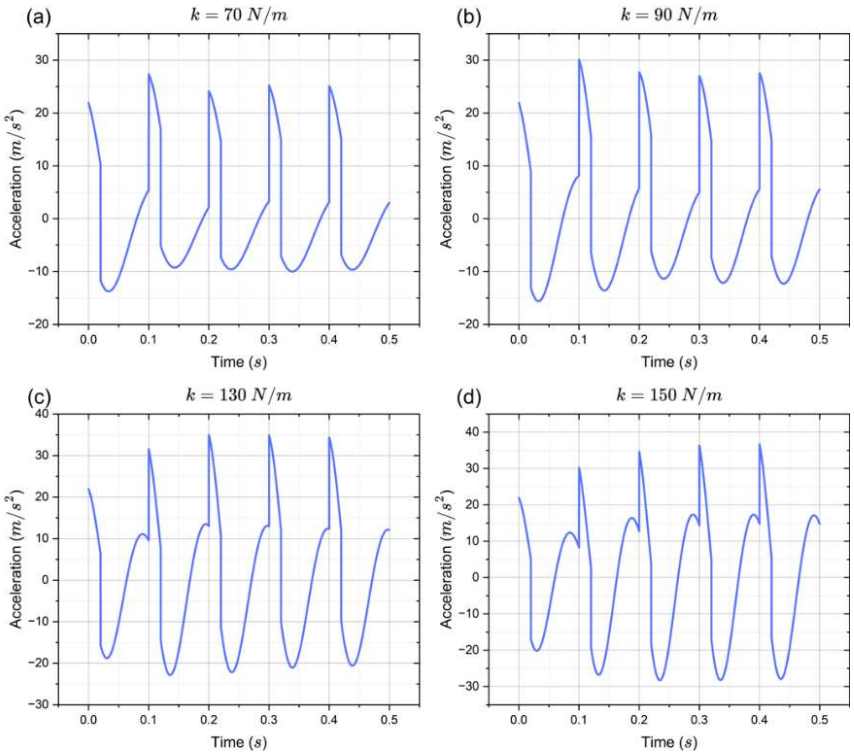

Figure 5.24 Simulated acceleration output with a spring stiffness of (a) $k = 70\ N/m$, (b) $k = 90\ N/m$, (c) $k = 130\ N/m$ and (d) $k = 150\ N/m$ with a small duty ratio.

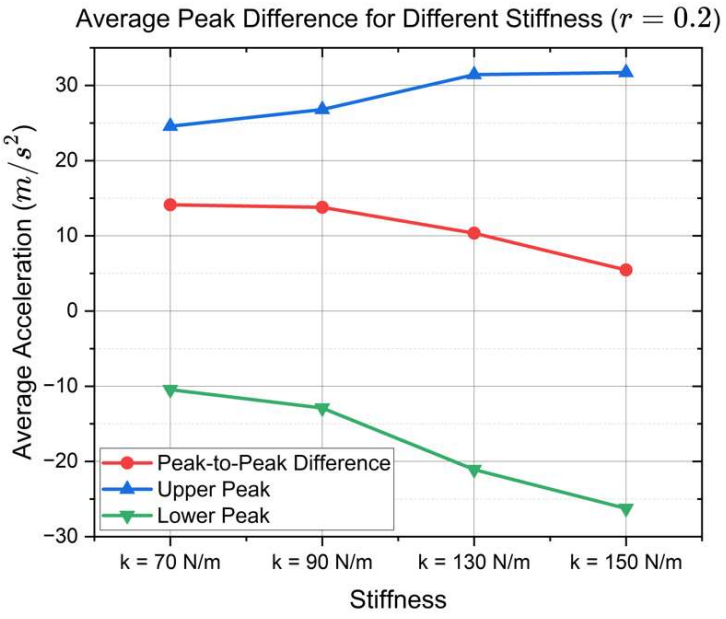

Figure 5.25 Average of upper and lower peaks and the peak difference for different stiffness with a small duty ratio.

Larger stiffness could produce a higher peak acceleration in both directions since more potential energy could be stored and released during the movement giving the same working distance. It was observed that the same direction in peak difference (i.e., positive) was obtained with a small duty

ratio $r = 0.2$ for all stiffness, which means that the change of the stiffness would not influence the direction of haptic cues. However, the peak difference decreased with larger stiffness, which would make the desired asymmetric vibrations into unwanted symmetric vibrations.

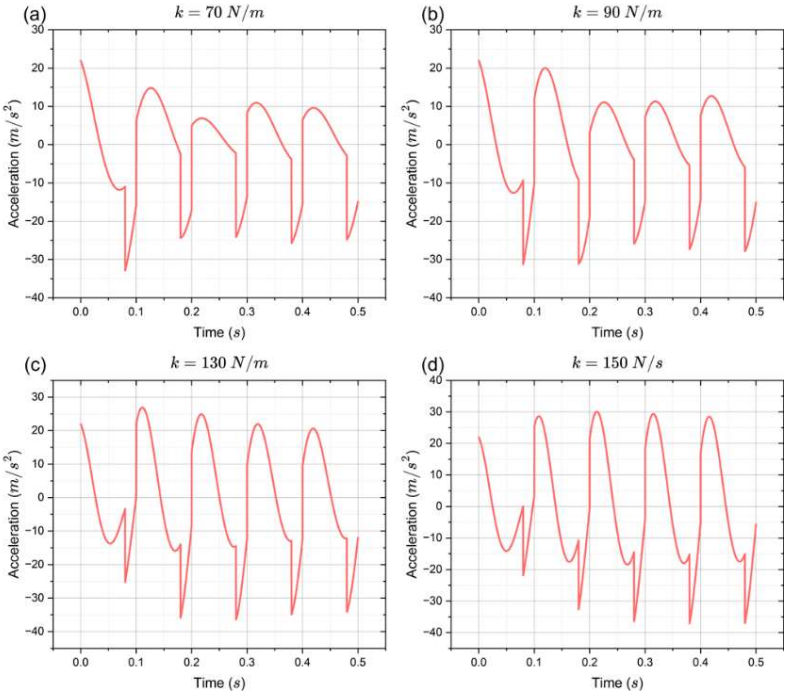

Figure 5.26 Simulated acceleration output with a spring stiffness of (a) $k = 70\ N/m$, (b) $k = 90\ N/m$, (c) $k = 130\ N/m$ and (d) $k = 150\ N/m$ with a large duty ratio.

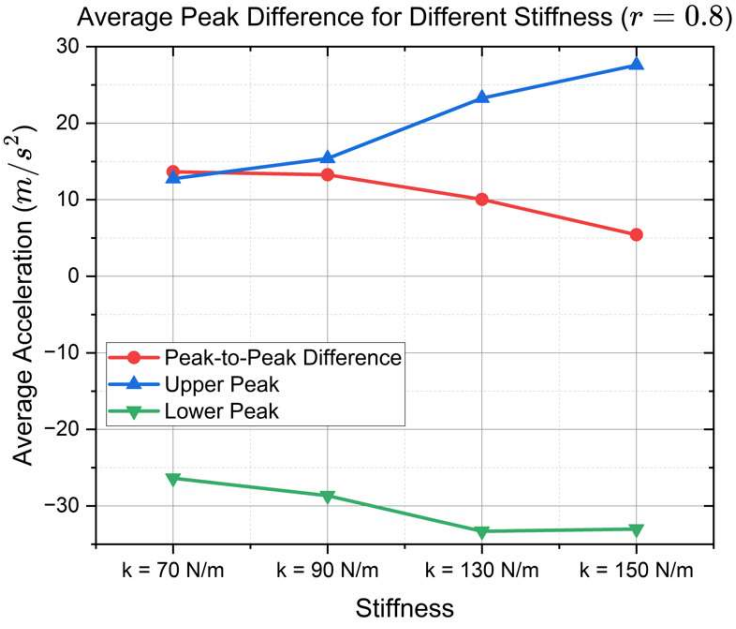

Figure 5.27 Average of upper and lower peaks and the peak difference for different stiffness with a large duty ratio.

The same procedure was conducted with a large duty ratio $r = 0.8$. The simulated acceleration outputs and average peak difference are shown in Figure 5.26 and Figure 5.27, respectively.

Similarly, it was observed that the same direction in peak difference (i.e., negative) was maintained with a large duty ratio $r = 0.8$ for all stiffness. Both positive and negative peaks were increased with a larger spring stiffness. However, the peak difference was also decreased with larger stiffness as it was observed with a small duty ratio.

The observation on the change of peak difference with respect to spring stiffness with both duty ratios also led to a common finding that the peak difference would become optimised when spring stiffness was below a certain threshold. Determining this stiffness threshold value would be extremely beneficial for haptic device design in terms of obtaining the largest asymmetry of haptic output. Similarly, an upper stiffness threshold should also be determined. Therefore, extra stiffnesses were simulated using the same dynamic model with a duty ratio of $r = 0.2$. The output acceleration with a large duty ratio $r = 0.8$ should be opposite to that with a small duty ratio. Figure 5.28 presents the average peak difference for all stiffnesses.

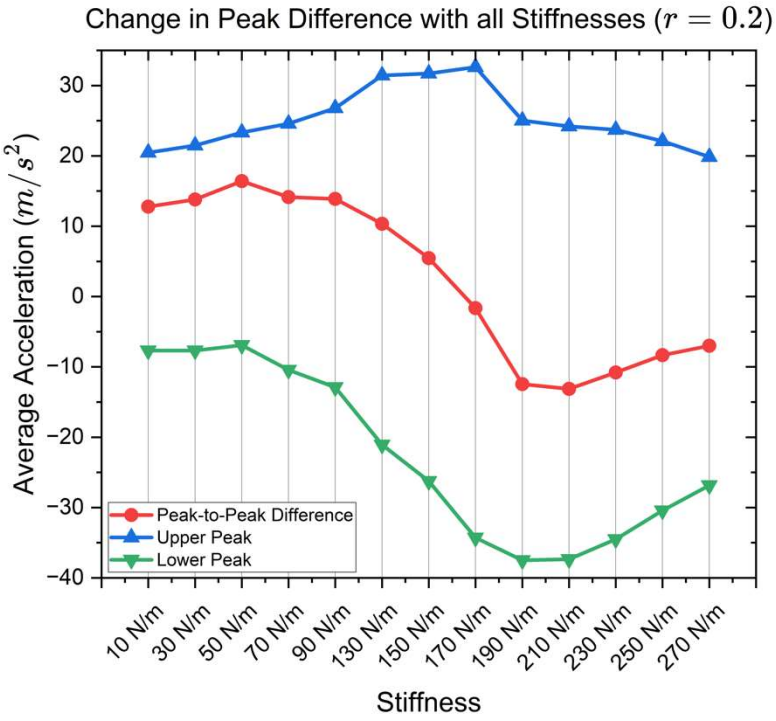

Figure 5.28 Change in peak difference with a variation in stiffness.

It was observed that when the stiffness was below 90 N/m, the peak difference for the solenoid haptic test platform would not change significantly. When the stiffness was above 150 N/m, the direction of peak difference would change from positive to symmetric and negative even with a small duty ratio. Therefore, there exists a maximum and minimum spring stiffness for each haptic system in order to generate asymmetric vibrations for the delivery of haptic directional cues along the desired direction.

5.4.2 Voice Coil Actuator Test Results

A voice coil actuator (VCA) was used to build a hand-held haptic device. A step-ramp signal was adopted as the input control signal. This input signal would be parameterised based on a VCA haptic test platform that measured the displacements resulted from asymmetric vibrations. A psychophysical experiment was finally conducted to verify the four hypotheses regarding to the delivery and the perception of haptic directional cues.

5.4.2.1 Displacement from VCA Test Platform

Three input signal parameters were established and studied, namely delay time (t_d), ramp down step length (S_r) and cut-off voltage (V_c). Five output parameters were used to quantify the haptic output, namely vibration frequency (f_{asy}), simplified speed (V_s), negative stroke (S_n), positive stroke (S_p) and stroke ratio (r_s). The aim of this test platform was two folds.

1) To determine the upper and lower limit of each input parameter so that the haptic output could be continuous and perceived by people. Therefore, a vibration frequency between 2 Hz and 10 Hz should be satisfied for this haptic device based on the results from a small-scale pre-test.
2) To optimise each input parameter so that the asymmetry of haptic output could be enhanced without significantly effecting vibration frequency. Therefore, a minimisation on the stroke ratio should be satisfied without influencing output frequency.

Displacement measurements were normalized using a z-score method since the absolute position of the motor box was not of interest in this research. On the contrary, data normalization provides direct comparison over the output features.

5.4.2.2 Delay Time

Delay time is defined as the time between the step input and the ramp-down input. In the displacement test as introduced in section 5.3.3, it was set incrementally with an increase of 10 ms. The minimum delay time was set to 0 ms and the maximum delay time was set to 50 ms. This maximum value was chosen since any delay time higher than the upper limit would result to a low output vibration frequency ($f_{asy} < 3$ Hz). The ramp down step length and the cut-off voltage were set to their default value ($S_r = 256$ and $V_c = 0$ V). Displacement measurements for different delay time are shown in Figure 5.29.

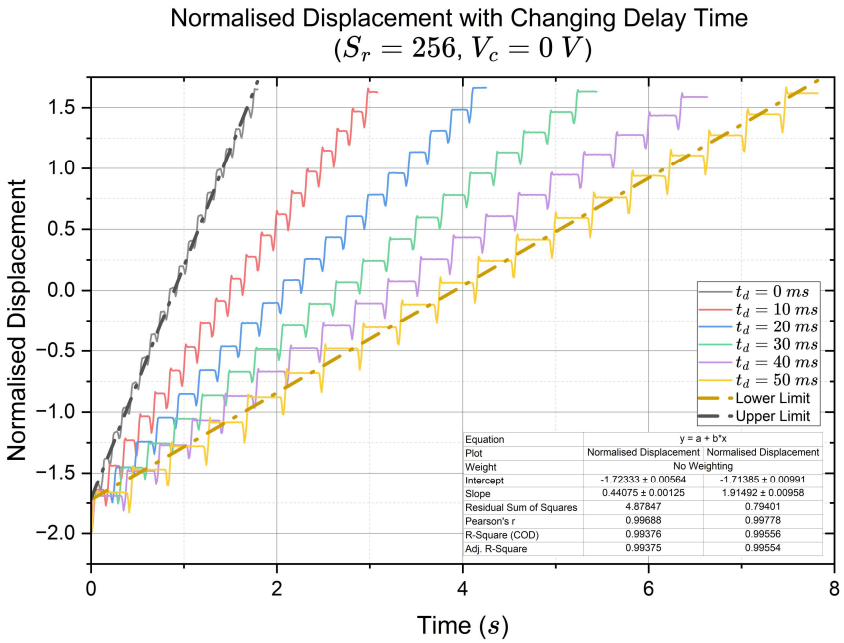

Figure 5.29 Displacement measurements for different delay time settings.

It was observed that a longer delay time would result to a lower vibration frequency f_{asy} and a slower simplified speed V_s. There existed an upper and lower limit for delay time because low-frequency vibrations could not be considered as continuous haptic feedback. The five output parameters were extracted (Appendix A1) and the change in vibration frequency, simplified speed and stroke ratio is shown in Figure 5.30. The delay time was set as categorical values.

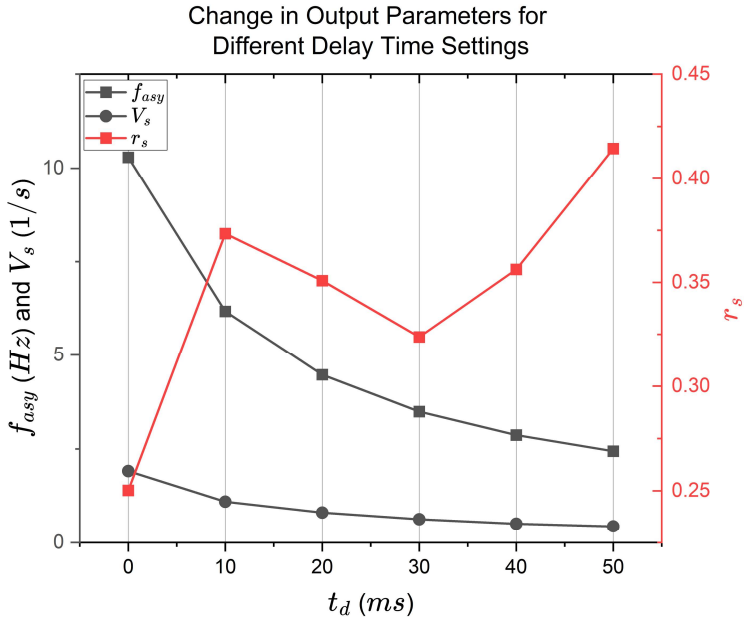

Figure 5.30 Change in vibration frequency, simplified speed, and stroke ratio for different delay time settings.

A monotonic decrease was found in both vibration frequency and simplified speed. The lowest vibration frequency (f_{asy} = 2.44 Hz) was achieved with

$t_d = 50$ ms and the highest vibration frequency ($f_{asy} = 10.29$ Hz) was achieved with $t_d = 0$ ms. However, no monotonic correlation was observed between delay time and stroke ratio although longer delay time tended to produce larger stroke ratio. As a result, there existed a trade-off between input delay time and output stroke ratio. The stroke ratio was minimised when no delay time was introduced. Therefore, it was not clear that the asymmetry of haptic output could be enhanced by only changing delay time.

5.4.2.3 Ramp Down Step Length

Ramp down step length is defined as the amount of voltage being decreased in each iteration when generating the ramp signal. A larger ramp down step length would require less time to decrease the voltage from saturation to the desired minimum voltage, producing a higher vibration frequency. Because the voltage was regulated using a 12-bit digital-analogue converter, the ramp down step length was set exponentially from $S_r = 32$ to $S_r = 2048$. Using Eq. 5.7, the corresponding voltage boundaries were $V_{sr} = 0.0256$ V and $V_{sr} = 1.6384$ V. The delay time and the cut-off voltage were set to their corresponding default value ($t_d = 20$ ms and $V_c = 0$ V). The displacement measurements for each ramp down step length were shown in Figure 5.31 (a).

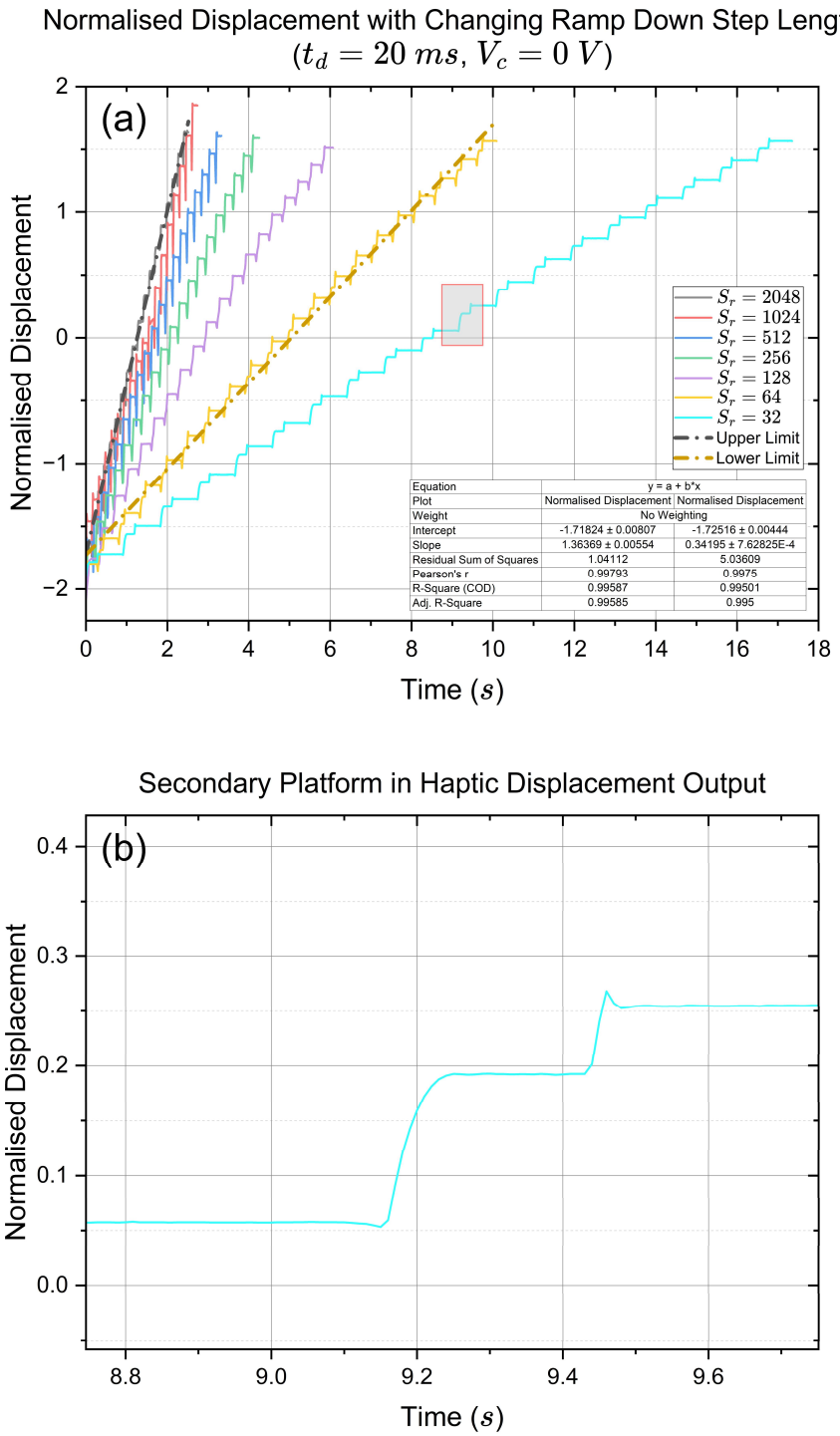

Figure 5.31 (a) Displacement measurements for different ramp down step length settings and (b) a secondary platform in the haptic output.

The upper and lower boundaries were also restricted by the vibration frequency. When ramp down step length was greater than 2048, the perception of haptic feedback could be worsened due to the high-frequency vibrations. When ramp down step length was less than or equal to 64, there was a change in displacement measurements where secondary platforms were found during positive strokes as shown in Figure 5.31 (b). The reason behind this was not quantitatively studied. However, the effect of the

secondary platforms on the perception of haptic cues were studied in the later human experiment.

The same five output parameters were extracted (Appendix A2). Ramp down step length was set as categorical values. The change in vibration frequency, simplified speed, and stroke ratio is shown in Figure 5.32.

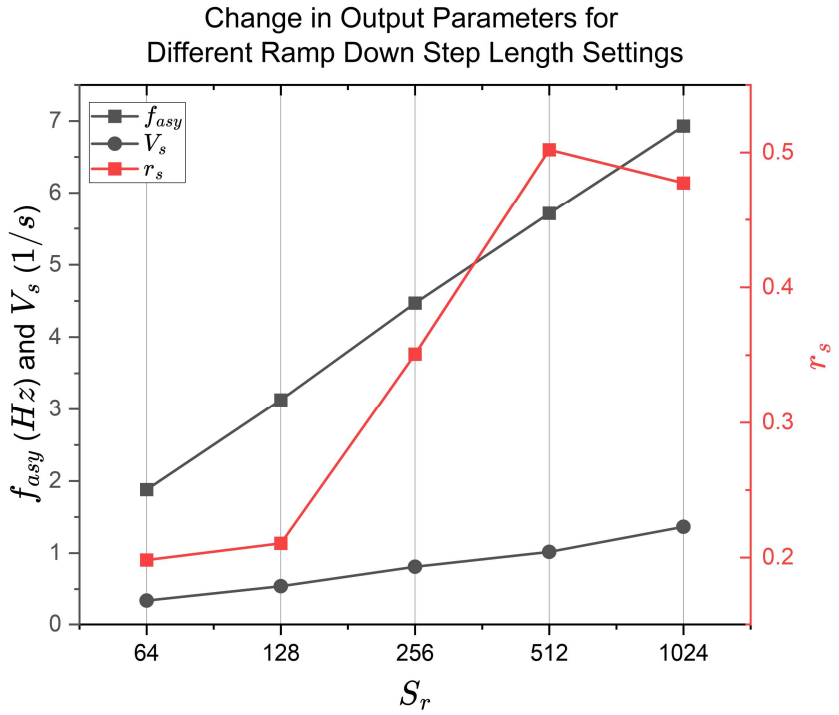

Figure 5.32 Change in vibration frequency, simplified speed, and stroke ratio for different ramp down step length settings.

Overall, a monotonic increase was found for vibration frequency, simplified speed, and stroke ratio ($R^2 = 0.99$, 0.99, 0.94). The lowest vibration frequency ($f_{asy} = 1.88$ Hz) was achieved with $S_r = 64$ and the highest vibration frequency ($f_{asy} = 6.93$ Hz) was achieved with $S_r = 1024$. The stroke ratio was ideally minimised with a minimum ramp down step length. However, as illustrated in Figure 5.32, the change of ramp down step length could also significantly change the vibration frequency. This does not comply with the second aim of the test platform. Therefore, it would be beneficial to minimise the stroke ratio while remaining vibration frequency by changing another input parameter.

5.4.2.4 Cut-off Voltage

Cut-off voltage is defined as the voltage level at which the ramp down input stops. The value of cut-off voltage is recorded before the differential amplifier. Therefore, all cut-off voltages in this work are presented with positive values. A larger cut-off voltage would reduce the work length of the returning stroke of a moving metal core, generating weaker haptic stimuli while preserving

the stronger ones. The minimum cut-off voltage was set to 0 V and the maximum value was set to 1.37 V. Delay time and ramp down step length were set to their corresponding default value. Figure 5.33 (a) presents the displacement measurement results on the haptic test platform.

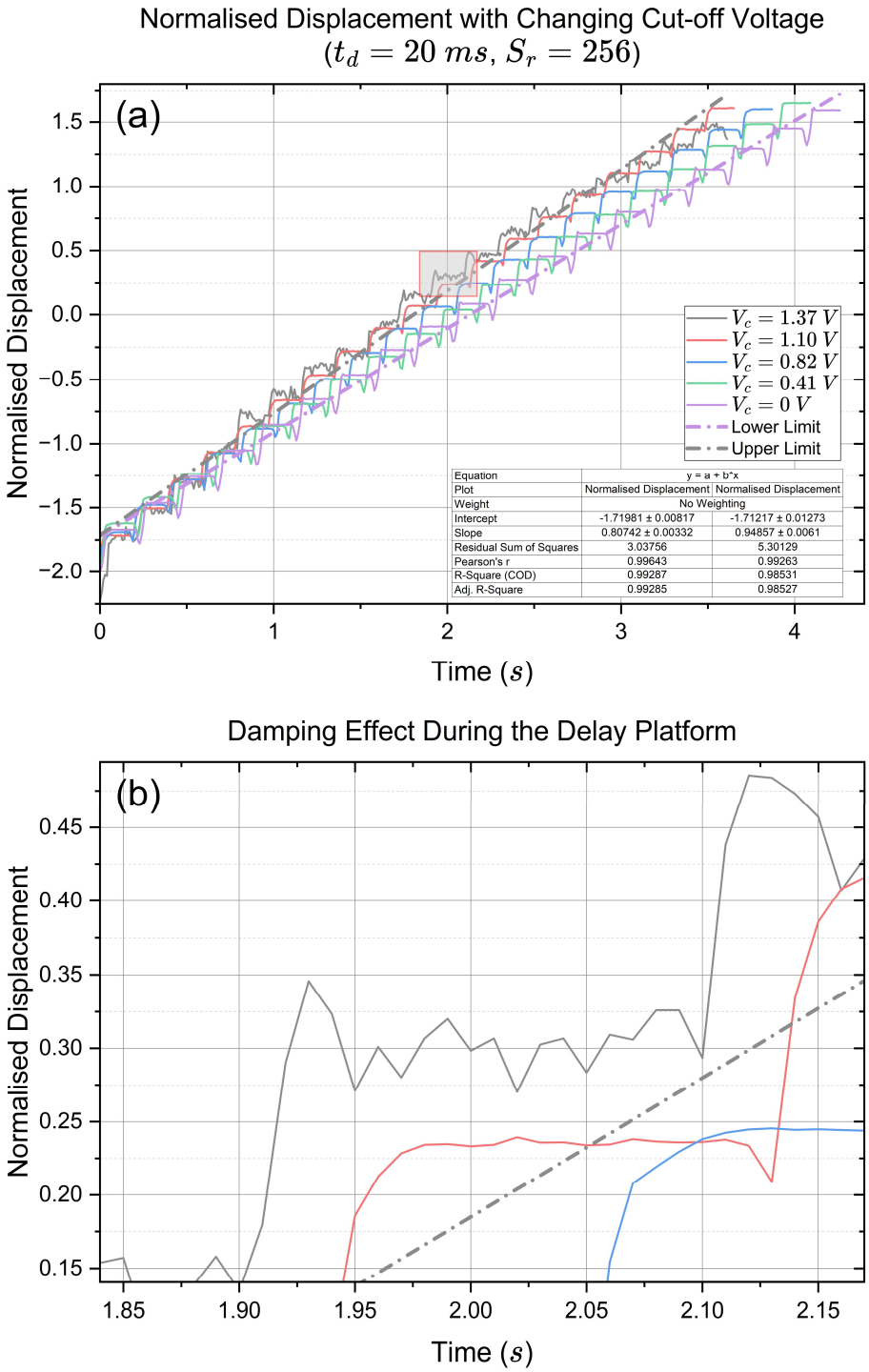

Figure 5.33 (a) Displacement measurements for different cut-off voltage settings and (b) damping effect during the delay platform.

The upper limit of the cut-off voltage was restricted by the damping effect during the delay platform as shown in Figure 5.33 (b). When cut-off voltage

was above 1.1 V, the original smooth and straight platform resulted from the delay time would become less smooth and fluctuate over time. This would have two negative impacts:

1) It was difficult to quantify positive strokes, negative strokes, and stroke ratio. The inter-measurement variability would be worsened.
2) Although the overall displacement measurement could be considered because of asymmetric vibrations, the absence of a smooth platform introduced by the delay time could result to symmetric vibration of human skin [60], which could not provide directional guidance but normal vibrations.

The same five output parameters were extracted (Appendix A3) except with a cut-off voltage of 1.37 V. Cut-off voltages were set as categorical values. The change in frequency, simplified speed and stroke ratio is shown in Figure 5.34.

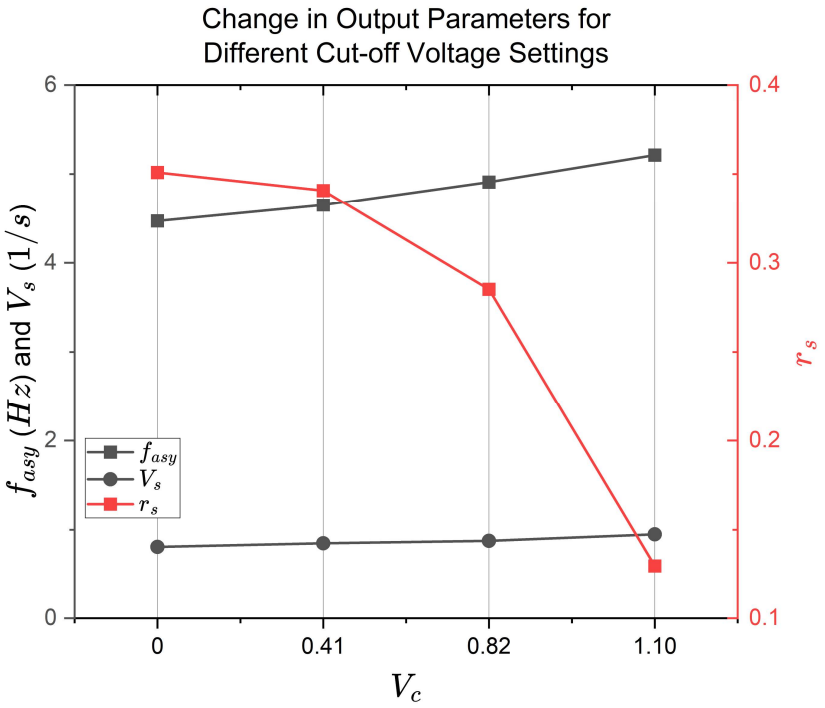

Figure 5.34 Change in vibration frequency, simplified speed, and stroke ratio for different cut-off voltage settings.

It was observed that vibration frequency and simplified speed had a linear relationship with cut-off voltage ($R^2 = 0.98$ and $R^2 = 0.99$). A larger cut-off voltage could result in a higher vibration frequency and faster simplified speed. On the other hand, a single term exponential function (monotonic decrease) was used to fit the stroke ratio ($R^2 = 0.99$). A larger cut-off voltage could significantly minimise stroke ratio. This is consistent with the optimisation aim that the change of stroke ratio would not cause significant

influence on vibration frequency and simplified speed. Therefore, optimising cut-off voltage could be an effective approach to increase the asymmetry of haptic output. The effectiveness of this approach on the perception of haptic cues would be examined in the human-based experiment.

5.4.3 Output Parameter Comparison

Since stroke ratio is defined as a fraction of negative stroke and positive stroke, it is important to make sure that this ratio is not a constant across different configurations before further analysis. Figure 5.35 presents a scatter plot between average positive stroke and negative stroke obtained from all configurations in displacement measurements.

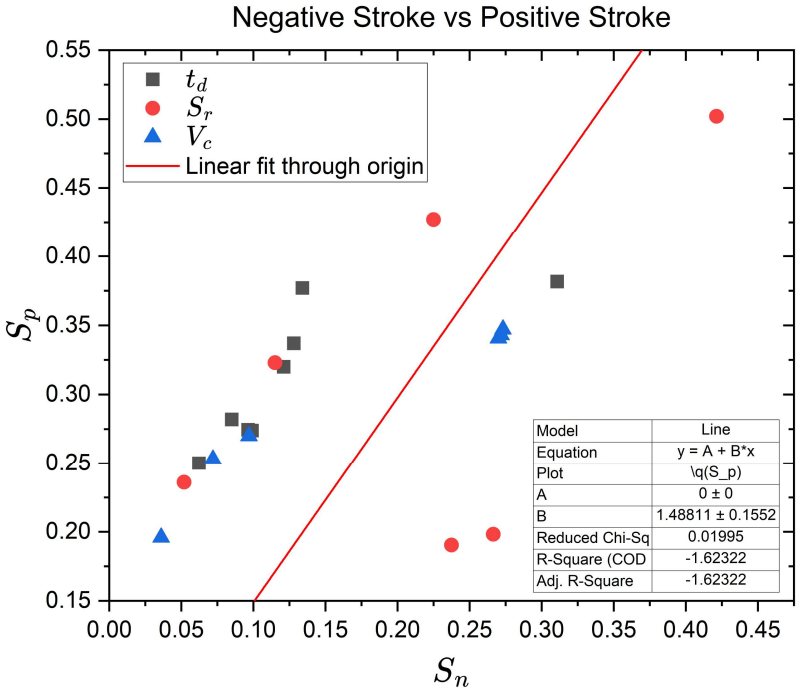

Figure 5.35 Negative stroke and positive stroke do not show strong linear correlation.

It was observed that a negative R^2 value was obtained when forcing the linear fit to cross the origin. This result shows that there is no constant stroke ratio calculated from positive stroke and negative stroke.

To quantitatively compare the effect of three output parameters, Table 5.6 presents the slope of the linear fit or the power of the exponential function of the fit on stroke ratio, vibration frequency and simplified speed.

Table 5.6 Effect of output parameters on stroke ratio, vibration frequency and simplified speed.

Parameter	f_{asy}	V_s	r_s
Delay Time	-1.432	-0.267	N.M.
Ramp Down Step Length	1.268	0.252	0.085
Cut-off Voltage	0.248	0.045	$0.36 - 0.0024e^{1.14}$

N.M.: Not monotonic

Delay time has a linear negative relationship with vibration frequency and simplified speed. Although it does not have a monotonic relationship with stroke ratio, effective haptic delivery requires the delay platform in the haptic output.

Ramp down step length has a positive linear relationship with vibration frequency, simplified speed, and stroke ratio. Although the stroke ratio could be minimised with a small ramp down step length, its relatively low vibration frequency makes haptic output discrete, which does not comply with the optimisation goal.

Cut-off voltage has a positive linear relationship with vibration frequency and simplified speed but with a significantly lower slope compared to ramp down step length. On the contrary, it has a negative exponential relationship with stroke ratio. The rate of change of stroke ratio becomes extremely fast after $V_c = 0.41$ V. This means that cut-off voltage could ideally minimise the stroke ratio without significantly influencing vibration frequency and simplified speed, which is consistent with the optimisation goal.

Therefore, it is important to conduct a human-based experiment to examine the effectiveness of the optimisation results on the perception of haptic cues.

5.5 Summary

5.5.1 Overall

In this chapter, three haptic implementations were proposed, and experiments were designed to verify the effectiveness of the implementations correspondingly.

An ERM-based haptic design was first attempted. Although the application of ERMs for haptic delivery was not ideal because of the limitations on vibration

frequency and amplitude etc., the initial exploration helped to establish the key requirements for precise haptic delivery.

A solenoid-based haptic test platform was then introduced. This platform used a single push-type solenoid controlled by PWM signals to generate asymmetric vibrations. A 1-DOF mass-spring-damper model was established in Simulink to describe the system's dynamic behaviour. An experiment was then designed to verify the validity of the dynamic model by comparing the output acceleration profiles. In the experiment, PWM signals with different frequencies and duty ratios were tested. Dynamic time warping distance was used to quantify the model precision because of the significantly different sampling frequency of two measurements. Additionally, the effect of spring stiffness and waveform were also discussed using the dynamic model.

Another haptic implementation was proposed using a voice coil actuator (VCA) controlled by step-ramp signals. Since the VCA is small in size and light in weight, it is convenient to build a hand-held haptic device using the VCA as the source of asymmetric vibrations. Therefore, a design specification for the hand-held haptic device was proposed to guide the manufacturing process.

In order to optimise the delivery of clearer haptic directional cues by the device, an experiment was designed to quantitively study the haptic input and output. The step-ramp input signal was parameterised with three adjustable variables, namely delay time, ramp down step length and cut-off voltage. The haptic output was measured by the VCA haptic test platform, where the displacements resulted from asymmetric vibrations were studied. The output was parameterised with five dependent variables, namely frequency, simplified speed, positive stroke, negative stroke, and stroke ratio. Table 5.7 summarises the input and output parameters of both haptic implementations.

Table 5.7 Summary of the inputs and outputs of two haptic systems.

Solenoid-based Haptic			
Input	PWM Duty ratio PWM Frequency Spring Stiffness Waveform	Output	Accelerations

VCA-based Haptic			
Input	Delay Time Ramp Down Step Length Cut-off Voltage	Output	Frequency Simplified Speed Positive Stroke Negative Stroke Stroke Ratio

It was assumed that the people's perception of haptic directional cues would change with respect to different output characteristics described by the five output parameters. Therefore, a psychophysical single group experiment was designed to explore the effect of output characteristics on the perception of haptic directional cues. The experiment was designed to have four stages in order to verify four hypotheses.

Compared to solenoid-based haptic implementation, the VCA-based implementation allows more control over the input signal although it requires additional circuit design to achieve the configurability. Table 5.8 summaries two haptic implementations in terms of their design, characteristics, and recommended application environment.

Table 5.8 Summary of two haptic implementations.

	Solenoid-based Haptic	VCA-based Haptic
Size	Large	Small
Weight	Heavy	Light
Cost	Low	Medium
Control Signal	PWM, Step-ramp, Sawtooth	Step-ramp
Configurable Input Parameters	2	3
Recommended Application	Fixed device Grounded(1) device	Portable device Ungrounded device

(1) The term "grounded" or "ungrounded" in the field of haptic implementation indicates if the device is physically connected to the ground or not.

5.5.2 Selection of Haptic Motors

Three haptic actuation methods were examined in this chapter. The eccentric rotating mass (ERM) motors were determined unsuitable for the delivery of haptic directional cues due to the lack of ability to provide accurate and strong multi-directional haptic feedback. However, they are easy to be programmed and compatible in size and weight. Therefore, haptic feedback based on ERM motors is especially beneficial in low-power designs and simple haptic sequence feedback. The other two haptic actuation methods applied a linear solenoid and a voice coil actuator (VCA). Both could satisfy the aim of generating strong and measurable directional cues but were controlled by different input signals. A solenoid motor was controlled by a PWM signal whereas a VCA was controlled by a step-ramp signal. Since a step-ramp signal is more configurable than a PWM signal, it is possible to optimise the former one in a psychophysical experiment for an improved haptic experience.

5.5.3 Solenoid Dynamic Model

The solenoid test platform consisted of a linear pushing solenoid with two compression springs. In order to quantitatively study the movement of the solenoid, a 1-DOF mass-spring-damper model was established. An important variable to be determined was the solenoid drive constant. It is the product of the magnetic flux and the length of the wire of the solenoid. The force generated by the solenoid is controlled by the drive constant and the current. Since different motors have different drive constants and the force is essential in the establishment of dynamic model, it is rather important to experimentally determine the drive constant for each motor before further analysis. It is also worthwhile to point out that the magnetic flux may change with respect to the operation temperature. The temperature could be influenced by various factors including the room temperature, operation voltage, current frequency etc. Consequently, there exists a trade-off between operation voltage and the strength of haptic output. Higher voltage generates larger forces but more heat during the vibration process. The magnetic flux density decreases with higher temperature, resulting in a decrease in haptic forces. Therefore, it is recommended to design a specific haptic motor that satisfy the following conditions.

- High drive constant. A haptic motor with a high drive constant does not require a high voltage (current) to generate large output force. Therefore, the temperature of the motor during operation will not be significantly influenced by voltage.

- High frequency tolerant. High frequency input signal generates more heat during the operation. A haptic motor with high frequency tolerance (between 10 Hz and 60 Hz) could satisfy frequency requirement on human perception without damage the motor.

The established dynamic model was verified by an experimental measurement on the output accelerations. The observation of the loss of damping in the measured acceleration at 5 Hz could be a result of measurement error in the spring stiffness and damping coefficient since they were determined experimentally using a mass-spring model. Additionally, the two springs in this research were inserted into the solenoid as an additional module but not original component, the dynamic behaviour of the motor-springs system may be influenced by the friction between the springs and the shaft or the solenoid body. Therefore, it is also beneficial in the future motor design to include the springs as internal components to match the motor's characteristics for a better delivery of haptic cues.

The solenoid was controlled by PWM signals with different duty ratios to generate asymmetric vibrations. The asymmetry of the haptic output changed from a positive direction to a negative direction with larger duty ratios. This was illustrated by the average of positive and negative acceleration peaks. Dynamic time warping distance was used to quantitatively compare the simulation results and experimental results. A Tukey test showed that a significant difference was found between different PWM frequencies whereas no significant difference was found between different duty ratios. This means that the 1-DOF model established in this research is particularly suitable for high-frequency (> 5 Hz) simulations and have a good applicability over a range of duty ratios.

5.5.4 Effect of Signal Shape and Spring Stiffness

The same directional change was observed from a short actuation time to a long actuation time. However, analogue signals such as step-ramp signals could generate different haptic outputs. An abrupt change in the momentum profile was observed as a result of step input in both PWM signals and step-ramp signals. This abrupt change was assumed to be much more easily perceived by human than a gradual change created by sawtooth signals. It is worth verifying this assumption in any future study. This observation also provides a new idea on the construction of haptic input signal. If a step input and a delay time are essential, the ramp-down process of voltage with respect to time could be changed from a linear relationship to a nonlinear relationship as shown in Figure 5.36.

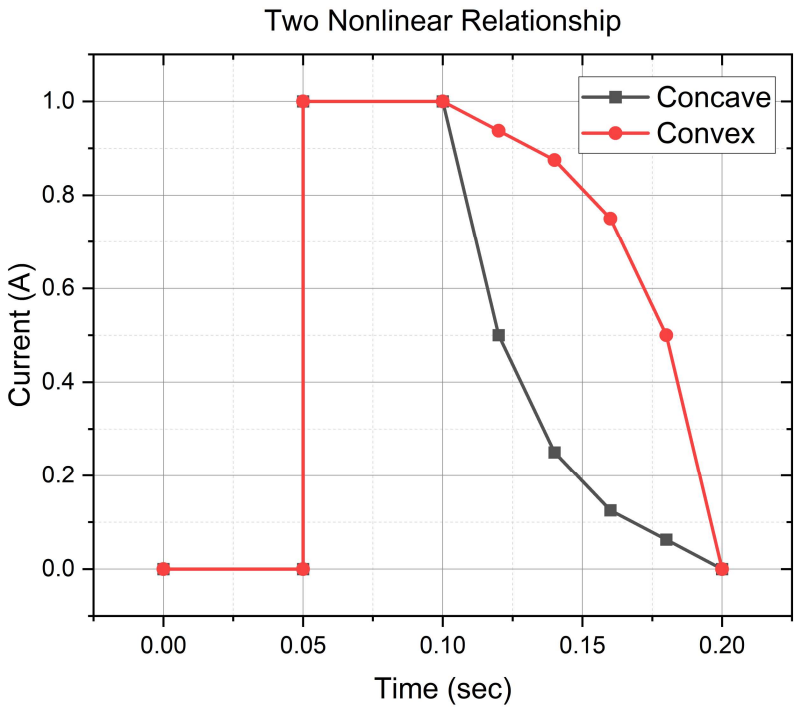

Figure 5.36 Two nonlinear ramp-down curves.

The difference between a concave curve and a convex curve is perceived by humans at the end of each vibration cycle. Convex curve is similar to a linear ramp-down but an increase in momentum towards the end of the movement. On the contrary, concave curve gradually slows down towards the end of the movement. Because humans are more sensitive to abrupt changes in momentum, concave curve has the advantage of minimising negative stroke (the stroke that returns the mass to the original position) while maintaining the positive stroke (the stroke that generates directional cues).

Apart from signal shape, spring stiffness also effectively changes the dynamic behaviour of the haptic system. A large stiffness results in large acceleration peak values but a small peak-to-peak difference. It was also found in this research that the value of peak-to-peak difference is neither linear nor monotonic with respect to spring stiffness. Therefore, for a specific haptic device, there exists an upper and lower stiffness threshold in order to obtain a maximum peak-to-peak difference. It is important to determine these thresholds using the dynamic model established in this research for optimised haptic performance.

5.5.5 Displacement Measurements

A displacement measurement was conducted in this research on 9 haptic configurations to extract 5 displacement output features, namely simplified speed, vibration frequency, positive stroke, negative stroke, and stroke ratio. Three variables were used to parameterise the input step-ramp signal,

including delay time, ramp down step length and cut-off voltage. They all have significant influence on the vibration frequency and asymmetry of haptic output. Delay time and ramp down step length would effectively change the vibration frequency and simplified speed although the monotonicity in the change of stroke ratio was only observed with various ramp down step lengths. Since stroke ratio and delay time is positively correlated, the minimisation of stroke ratio would require zero delay time. However, delay time is proved to be essential by [60] in the step-ramp signal in order for the haptic cues to be successfully perceived by humans. Therefore, other approaches need to be explored to minimise the stroke ratio. Ramp down step length also shows a positive correlation with stroke ratio. While retaining the delay time, the decrease in ramp down step length for the minimisation of stroke ratio would significantly decrease vibration frequency as well, which will influence the continuous perception of haptic cues.

Cut-off voltage is a novel approach proposed in this research to optimise stroke ratio without significantly affecting vibration frequency. It presents a negative correlation with stroke ratio but positive correlation with vibration frequency and simplified speed. However, a maximum cut-off voltage should be determined for different haptic devices since the range of voltage during operation should be sufficient to generate powerful positive stroke.

A displacement measurement has the advantage of presenting and quantifying the asymmetry of haptic output without complicated preprocess on the measurement data. However, compared to acceleration or force/torque measurement, the interaction between the haptic device and human skin could not be quantified using displacement measurements. It was also argued in [97] that the dynamic behaviour of the motor would change when the motor is connected to human body but not a rigid structure. Therefore, it is worthwhile to compare displacement measurements against acceleration or force measurements in the future study to verify the efficacy of the proposed position-based method.

Chapter 6 Human Experiment Design and Results

A single group psychophysical experiment with 30 participants was finally conducted to test the haptic device prototype in order to determine the ideal characteristics of the input control signal that provides the clearest directional cues. A psychophysical experiment was also designed to test the hypotheses regarding to the perception of haptic cues delivered by the VCA device. Section 6.1 presents the experimental design, concluding remarks.

6.1 Human Experiment Design

A psychophysical single group experiment was designed to evaluate the perception of haptic cues induced by the hand-held device. The aim of the experiment was to evaluate the effect of the five output parameters (f_{asy}, V_s, S_n, S_p and r_s) on the perception of haptic directional cues in terms of accuracy and user confidence. Additionally, the effect of haptic reference and the type of force that delivers the haptic directional cues will also be discussed. Therefore, four hypotheses were raised to be verified in the experiment.

1) By introducing cut-off voltages, the asymmetry of the haptic output can be increased (smaller r_s), which can benefit clearer delivery of the haptic directional cues.
2) When asymmetric vibrations could be perceived, there exists a stroke ratio that can produce clearer delivery of the haptic directional cues.
3) The existence of a haptic reference can help improve the sensing accuracy and user confidence.
4) Haptic directional cues delivered by shear forces give improved sensing accuracy than those delivered by normal forces.

In order to verify these hypotheses, a four-stage experiment was designed involving 9 different haptic configurations. Each configuration has unique combinations of the three input parameters (t_d, S_r and V_c) established in the previous section. Consequently, each configuration would also have different output parameters (f_{asy}, V_s, S_n, S_p and r_s). The experiment was conducted in the Rehabilitation Robotics Laboratory, University of Leeds, Leeds, UK. The study was approved by the Engineering and Physical Science Research Ethics Committee (MEEC 22-006). All participants gave written informed consent. The corresponding ethical review materials are presented in the

Appendix. The experiment procedures are described below and summarised in Figure 6.1. Figure 6.2 illustrates a participant holding the hand-held device during the experiment.

1) Initial Display. Participants were asked to experience haptic directional cues at a default direction (i.e., pointing forwards) delivered by all 9 configurations in the same order. A three-second rest time was provided in between each configuration. After the display of all 9 configurations, a one-minute rest time was provided before continuing to the second stage.
2) Left or Right. Participants were asked to specify a direction (either left or right) based on the current haptic configuration. The same 9 configurations were used at this stage. Different participants were presented with haptic configurations in unique orders. Apart from specifying the perceived direction, participant's confidence on his/her answers would also be recorded as the confidence level. The confidence level used categorical values with 0 being not sure, 1 being very sure and 2 being no directional cues were felt. The preferred configuration for each participant was finally determined by the correctness of direction and the confidence level. If multiple configurations were chosen by the same participant, the most selected one by other participants would be used for the rest of the experiment.
3) Static Test. Participants were asked to specify a random direction in a larger range ($0^o - 180^o$ semicircle range in front of the participants) based on the selected configuration in the previous stage. The haptic directional cues were presented at a random angle within the semicircle range. After a five-second display, participants were asked to use the knob to specify that random direction. Participant's specified angle and the actual haptic angle would be recorded. This process was repeated for 5 times with no rest time provided in between.
4) Dynamic Test. Participants were asked to specify a random direction in the same range with the help of a haptic reference. A haptic reference is haptic directional cues pointing forwards as a default direction. During the test, haptic cues would change from the default direction to a random angle in the same range. Participants were expected to perceive the directional changes and were asked to specify the final direction. This process was repeated for 5 times with no rest time provided in between.

5) After the entire test, participants would be asked for two questions:
   - Which test do you find it easier to tell a direction, static test, or dynamic test?
   - Did you feel more haptic feedback on your thumb side or on your more-fingers side?

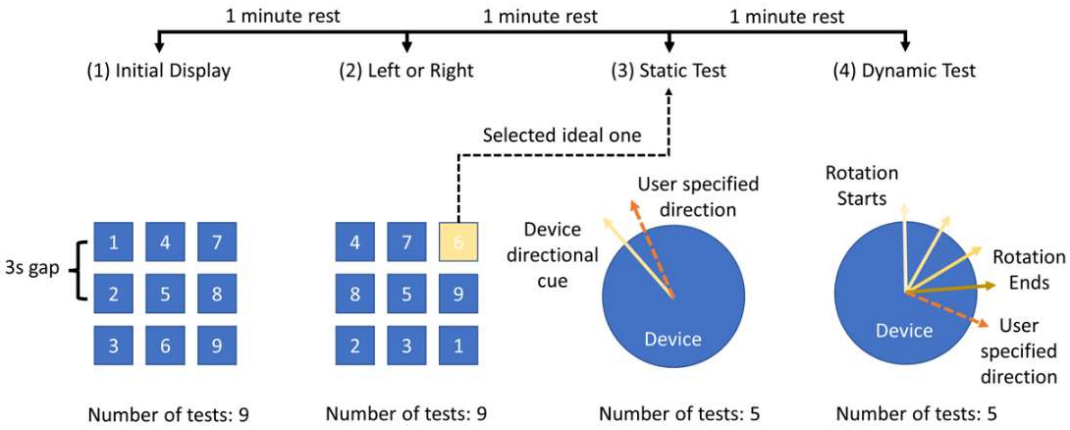

Figure 6.1 Summary of the four stages of the human perception experiment.

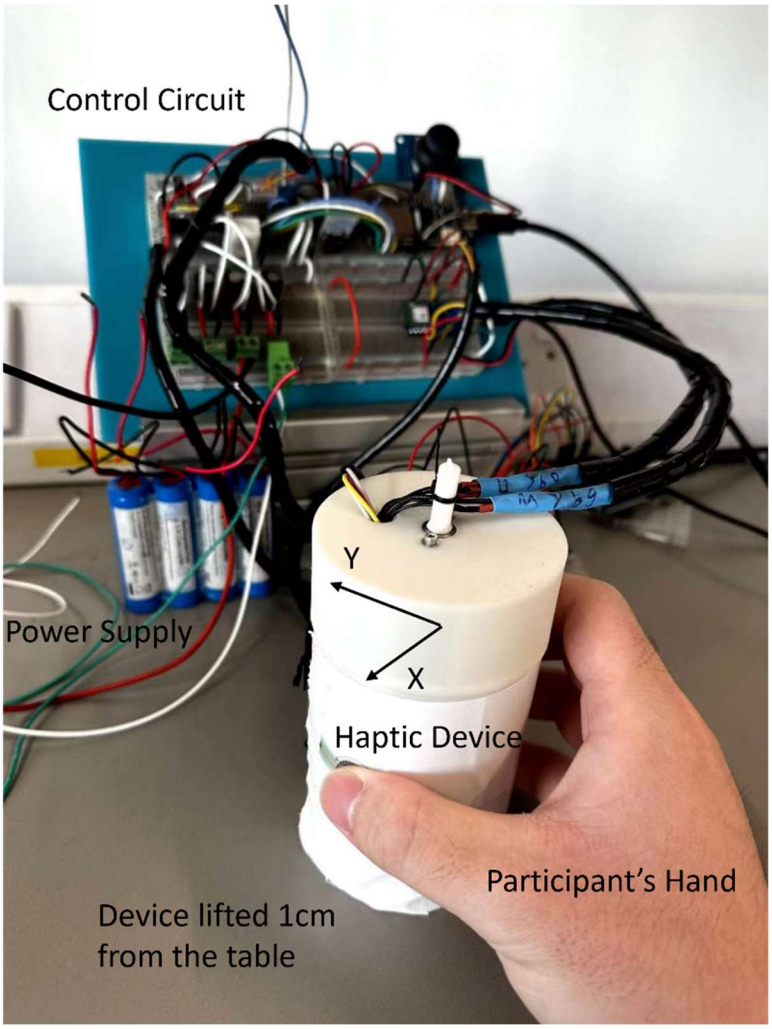

Figure 6.2 A participants was holding the hand-held haptic device during the experiment.

6.2 Human Experiment Results

The aim of the experiment was to verify the four hypotheses regarding to the perception of haptic directional cues listed in the above section and reviewed here.

1) By introducing cut-off voltages, the asymmetry of the haptic output can be increased (smaller r_s), which can benefit clearer delivery of the haptic directional cues.
2) When asymmetric vibrations could be perceived, there exists a stroke ratio r_s that can produce clearer delivery of the haptic directional cues.
3) The existence of a haptic reference can help improve the sensing accuracy and user confidence.
4) Haptic directional cues delivered by shear forces give improved sensing accuracy than those delivered by normal forces.

A total number of 30 participants were recruited in the experiment. All participants have right dominant arm. Although participants were trained on how to grip the device prior to the experiment and markers were provided for participants to locate their fingers, difference in hardness of skin, the sensitivity to skin vibration and the grip position and angle between fingers and the device could have effects on the perception results. Therefore, this experiment does not focus on the individual difference, but each haptic configuration formulated by input and output parameters. A total of 9 configurations were selected from three preliminary tests with 4 participants within the research group including the author. Due to the limitations on experiment time per participant, only upper and lower boundaries, and a value in between were selected to form these 9 configurations. The input parameters of all configurations are listed in Table 6.1.

Table 6.1 Input parameters of all haptic configurations.

Related Variable	Configuration	Input Parameters		
		$t_d\ (ms)$	$S_r\ (1/s)$	$V_c\ (V)$
Delay Time	1	20	256	0.00
	2	0	256	0.00
	3	40	256	0.00
Ramp Down Step Length	4	20	128	0.00
	5	20	64	0.00
	6	20	512	0.00
Cut-off Voltage	7	20	256	0.21
	8	20	256	0.10
	9	20	256	0.41

6.2.1 Left or Right

Number of matches (NOM) and number of unidentified answers (NOU) were used to quantitatively assess the accuracy of the haptic perception. NOM was counted when participant's specified direction was the same as the random left/right. NOU was counted when a participant could not specify a direction. Additionally, participant's confidence on the specified direction was assessed using the ordinal scale 0 or 1. Sum of confidence (SOC) was accumulated based on participant's confidence level. The results of the first stage experiment are shown in Figure 6.3 (a). The numbers on the outside circumference correspond to each configuration number listed in Table 6.1.

Ideally, a good haptic configuration should have a large NOM for higher accuracy, a small NOU for better applicability and a large SOC for better user experience. The maximum NOM and NOU for each configuration was the same as the number of participants recruited (i.e., 30). The minimum NOU was zero.

It was observed in Figure 6.3 (b) and (c) that configurations with a cut-off voltage (i.e., config. 7, 8 and 9) had a larger NOM and a smaller NOU than those without a cut-off voltage. Particularly, configurations with a cut-off voltage showed a significant increase using a Tukey test in terms of the accuracy of haptic delivery ($p = 0.023$). No significant difference was found in configurations related to delay time and ramp down step length.

The average SOC for configurations with a cut-off voltage was also higher than that without a cut-off voltage. No significant difference was found. Specifically, configurations 2 and 4 had a high NOU among all configurations, indicative of a potential poorer performance in terms of the applicability.

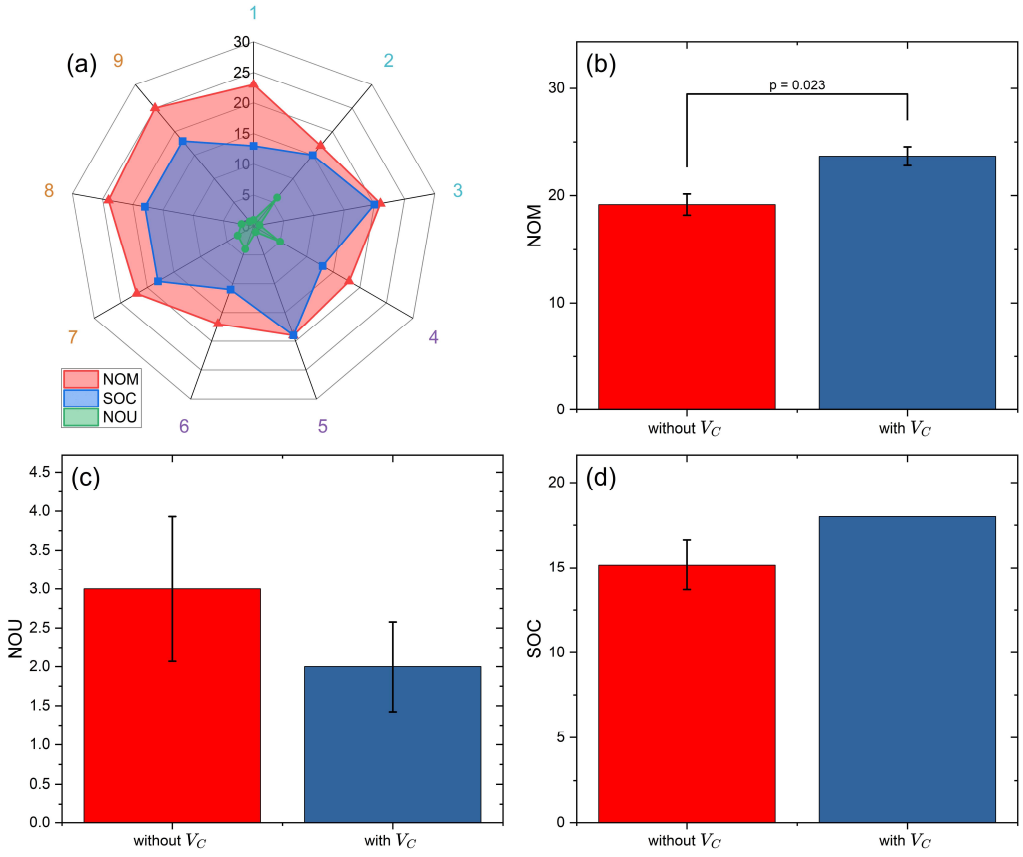

Figure 6.3 (a) Experiment results for 9 configurations and comparisons related to cut-off voltage in terms of (b) NOM, (c) NOU and (d) SOC.

To examine each configuration in terms of NUM and SOC in detail, a scatter plot is shown in Figure 6.4 and the output parameters are listed in Table 6.2.

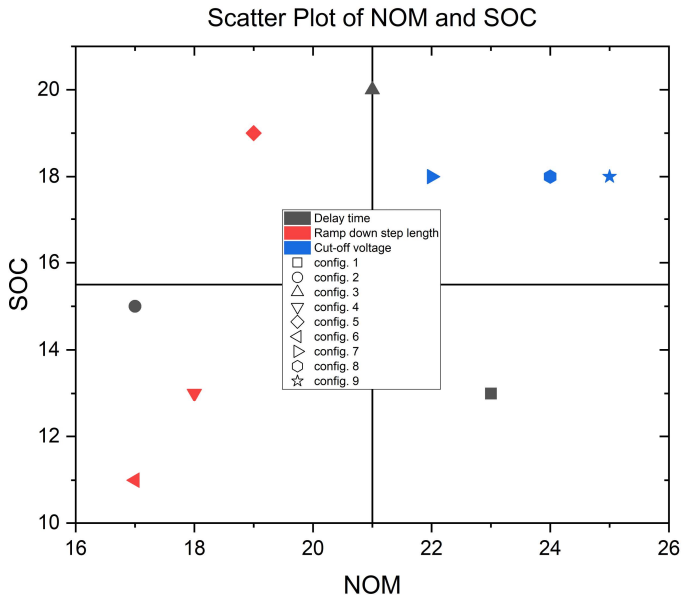

Figure 6.4 Scatter plot of each haptic configuration.

Configuration 9 had the largest NOM and configuration 3 had the largest SOC. The top right corner of the plot was the region of interest because configurations within that area had better performance in SOC and NOM. All configurations with a cut-off voltage belonged to this area. Configurations with a low vibration frequency (i.e., configurations 3 and 5) tended to provide better user's confidence on directional judgement. The bottom or left region of the plot was the poor performance region, especially the bottom left corner where both NOM and SOC were low.

Table 6.2 Output parameters for all configurations used in the experiment.

Configuration	f_{asy} (Hz)	V_s $(1/s)$	S_n	S_p	r_s
1	4.47	0.8101	0.0963	0.2745	0.3508
2	10.29	1.9150	0.0622	0.2486	0.2502
3	2.87	0.5141	0.1186	0.3107	0.3817
4	3.13	0.5404	0.0452	0.2374	0.1904
5	1.88	0.3413	0.0528	0.2664	0.1982
6	5.71	1.0280	0.2115	0.4213	0.5020
7	4.60	0.8395	0.0933	0.2719	0.3430
8	4.53	0.8234	0.0948	0.2732	0.3471
9	4.65	0.8483	0.0920	0.2700	0.3407

Blue: minimum value of the feature. Red: maximum value of the feature.

To control the experiment variability, two sets of comparisons were made based on the results shown above. Intra-parameter comparison is the comparison within each input parameter group (e.g., configuration 1, 2 and 3) and inter-parameter comparison is the comparison between each input parameter group (i.e., configuration 1, 4 and configuration 1, 9).

The first intra-parameter comparison was made for delay time group. All three configurations had a vibration frequency that could be perceived by people. However, configuration 2 ($t_d = 0\ ms$) had the lowest NOM and a low SOC among all configurations. This is consistent with the previous analysis that the platform introduced by the delay time is essential in the perception of asymmetric vibrations. Configuration 1 had a smaller stroke ratio (more asymmetry) and a larger NOM compared to configuration 3. However, this observation alone could not verify hypothesis (2) due to the lack of observations with a bigger range of stroke ratio. This would be addressed in the later analysis.

The second intra-parameter comparison was made for ramp down step length group. Configuration 5 had the smallest vibration frequency that was out of the frequency range determined through preliminary tests, which makes its NOM in the poor performance region. However, it is obvious that configuration 5 had a much larger SOC compared to configuration 4 and 6. In the previous displacement analysis, a secondary platform during the positive stroke was found when $S_r < 128$. Therefore, the effect of the secondary platform may be beneficial for improving user's confidence on directional judgement while not affecting the accuracy of haptic cues.

The final intra-parameter comparison was made for cut-off voltage group. All three configurations had excellent NOM and SOC while a small NOU. All their output parameters were very similar to each other as well.

For the inter-parameter analysis, only two comparisons were made between configurations 1 and 9, and configurations 1 and 4. Configuration 9 had a larger NOM and SOC compared to configuration 1. While their output parameters were similar, the only difference in the input parameter was the existence of a cut-off voltage in configuration 9. This observation could verify hypothesis (1) that the application of cut-off voltage could help a better delivery of haptic directional cues.

Configurations 1 and 4 had the same SOC in the poor performance region. However, configuration 1 had a larger NOM. This is because the stroke ratio of configuration 4 was significantly lower than configuration 1. This

observation contributes to hypothesis (2) that there exists an optimised stroke ratio that could help a better delivery of haptic cues. To find this optimal value, the relationship between stroke ratio and NOM is plotted in Figure 6.5 to verify hypothesis (2).

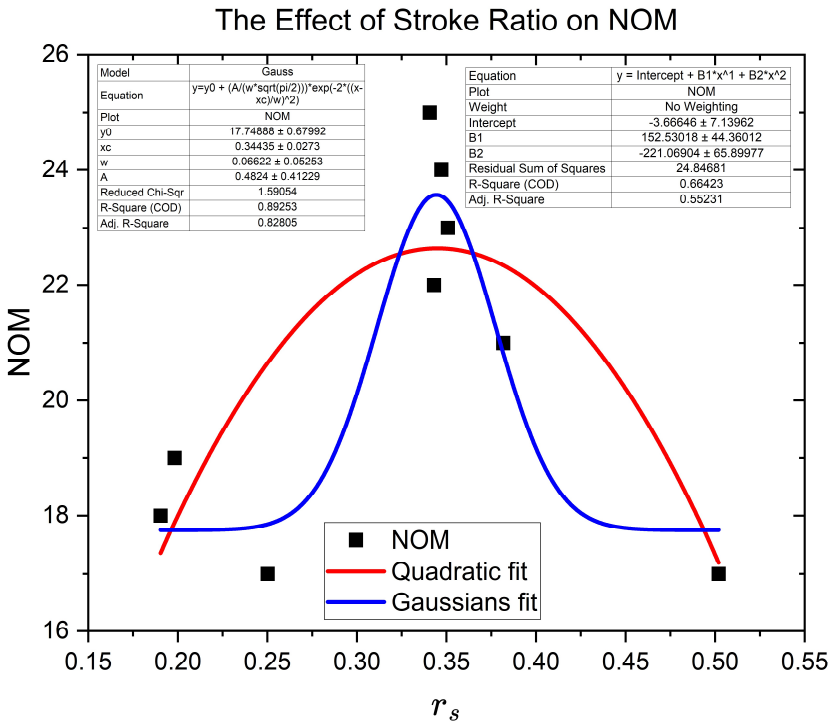

Figure 6.5 Gaussian and quadratic relationship between stroke ratio and NOM.

A quadratic function and a Gaussian probability density function was used to describe the relationship between stroke ratio and NOM with $R^2 = 0.664$ and 0.893, respectively. The Gaussian probability density function has a better goodness of fit compared to a quadratic curve. A stroke ratio of $r_s = 0.344$ predicted by the Gaussian function could achieve a maximum NOM. On the other hand, the quadratic model was not excellent in terms of goodness of fit. A stroke ratio of $r_s = 0.345$ was predicted by the quadratic function.

Apart from the stroke ratio, the relationship between NOM and the other features were also explored by a Gaussian probability density function as shown in Figure 6.6.

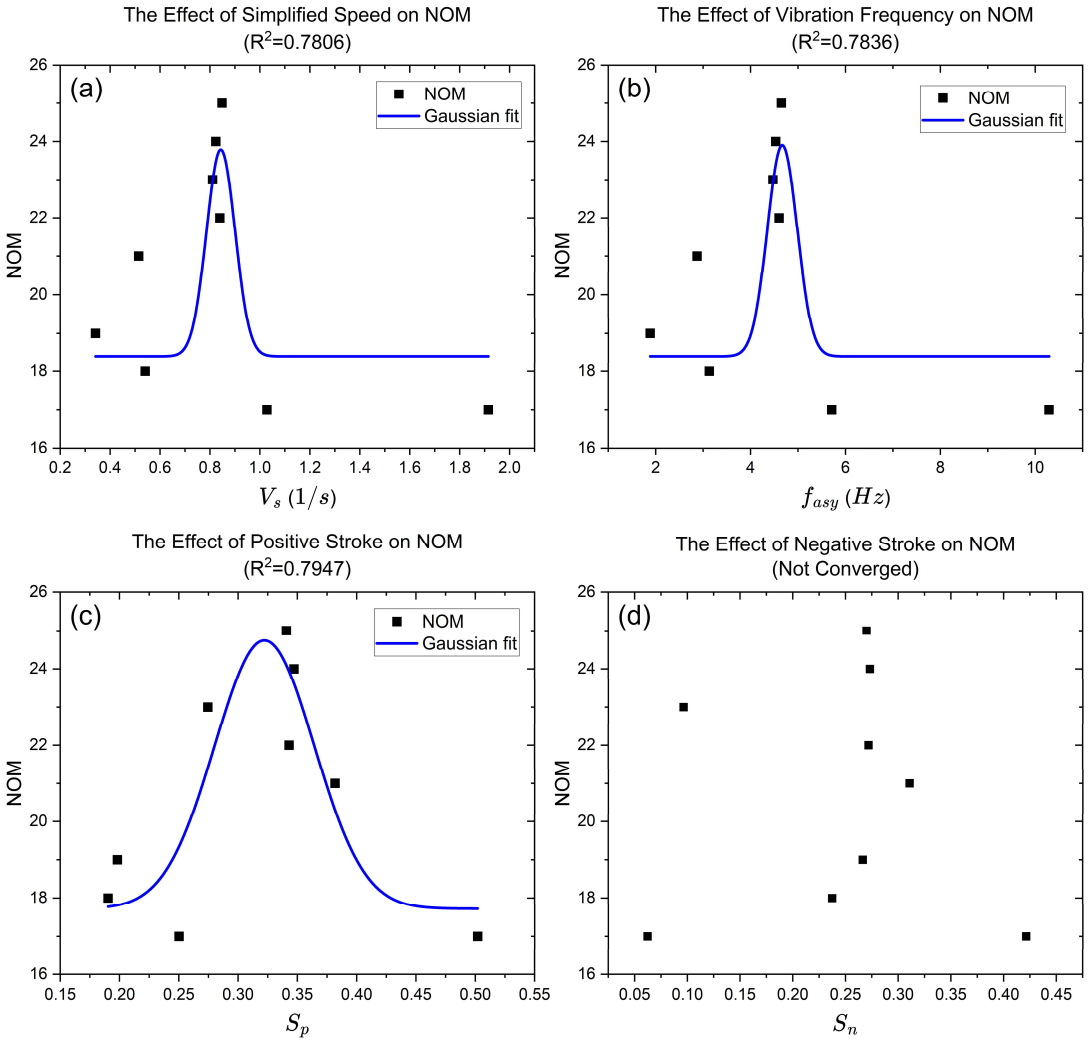

Figure 6.6 The relationship between NOM and (a) simplified speed, (b) vibration frequency, (c) positive stroke and (d) negative stroke.

Simplified speed, vibration frequency and positive stroke had a strong Gaussian correlation with NOM. This suggested that there existed an optimal value for each of the feature in order for a maximum perception rate for the haptic directional cues. However, there was no correlation found between the negative stroke and NOM.

Additionally, instead of exploring the non-linear relationship, a Pearson's correlation test was conducted on both half of the quadratic curve with $r_s = 0.345$ as the separation line to examine two sets of relationships as listed below. This value was calculated by the line of symmetry of the quadratic fit function. Figure 6.7 presents the test results for both intervals.

- The relationship between NOM, SOC and all output features.
- The relationship between each output feature.

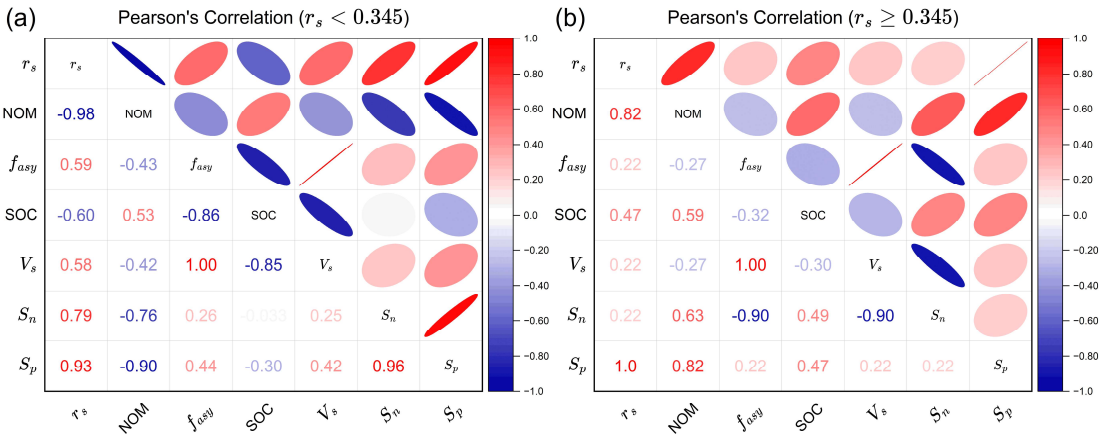

Figure 6.7 Pearson's correlation coefficients for both quadratic intervals separated by $r_s = 0.345$.

Between NOM, SOC and output features:

It was observed that NOM had a strong negative correlation with stroke ratio ($r = -0.98$) when $r_s < 0.345$, and a strong positive correlation with stroke ratio ($r = 0.82$) when $r_s \geq 0.345$. Together with the analysis of the first intra-parameter comparison, the second inter-parameter analysis and the quadratic fit, this strong negative-positive correlation between stroke ratio and NOM could verify the hypothesis (2) that there exists a stroke ratio that could benefit clearer delivery of haptic directional cues. Specifically, the optimised stroke ratio value for this hand-held device was $r_s = 0.345$.

Apart from NOM, SOC had a moderate negative correlation with stroke ratio ($r = -0.60$) when $r_s < 0.345$, and a moderate positive correlation with stroke ratio ($r = 0.47$) when $r_s \geq 0.345$. The decrease in both correlation coefficients were expected because SOC was calculated based on subjective self-assessments by participants. No consistent and moderate correlations were found between NOM/SOC and other output parameters.

Between each output feature:

It was found that simplified speed and vibration frequency had a strong linear correlation ($r = 1$) on both intervals. A weak to moderate correlation ($r = 0.22 - 0.42$) was found between positive stroke and simplified speed. Positive stroke also presented a strong correlation with stroke ratio ($r = 0.93 - 1$).

6.2.2 Static Test and Dynamic Test

Based on the experiment results from the previous stage, configuration 9 was chosen by all the participants for the static and dynamic test. Two absolute rotary encoders were used to measure the angles between participant's input from the shaft and motor's output. The absolute encoder

readings were converted to the range of $0^o - 180^o$ using a self-written MATLAB script. Root mean square error (RMSE) was computed to quantify the difference between the two angles. Because the static test and dynamic test were measured independently with the same device, method and the group of participants, a two-sample t-test was adopted to verify the significant difference between the two tests. The angle difference is shown in Figure 6.8.

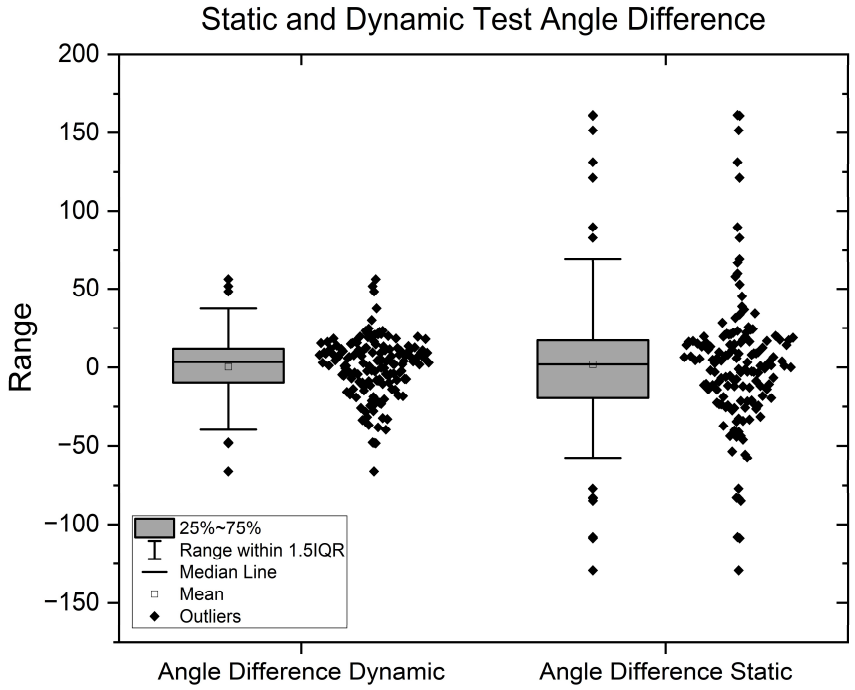

Figure 6.8 Angle difference in static test and dynamic test.

The statistics of both tests are also shown in Table 6.3.

Table 6.3 Statistics of angle difference in static test and dynamic test.

Test Type	Number of Observations	Mean	Standard Deviation	Minimum	Median	Maximum
Dynamic	150	0.32	19.21	−66.30	3.34	55.99
Static	150	1.79	42.46	−129.42	1.94	161.17

It was shown that the mean value and standard deviation of angle difference between participant's input and haptic cues decreases significantly from static test to dynamic test. This observation favoured hypothesis (3) that the existence of a haptic reference would benefit a clearer delivery of haptic directional cues. This was also supported by the result from a question asked after all tests. The question asked the participants which test was easier to tell a direction. A total of 27 over 30 participants found it easier to tell a direction in the dynamic test with the help of a haptic reference.

Another positive outcome from the dynamic test was the decrease in the number of angle phase shifts. The maximum and minimum value in the static test were very close to $\pm 180^o$. This caused a cognitive error for participants during the static test to misjudge a left/right haptic cue as the opposite. However, the extreme values in the dynamic test were strictly restricted below $\pm 70^o$. Although the extreme value in dynamic test would also result to a cognitive error within a smaller range, the possibility of correcting the error could be promising after practicing for a longer time with the specific device.

The RMSE and the result of a two-sample t-test between participant's input and haptic cues are shown in Figure 6.9.

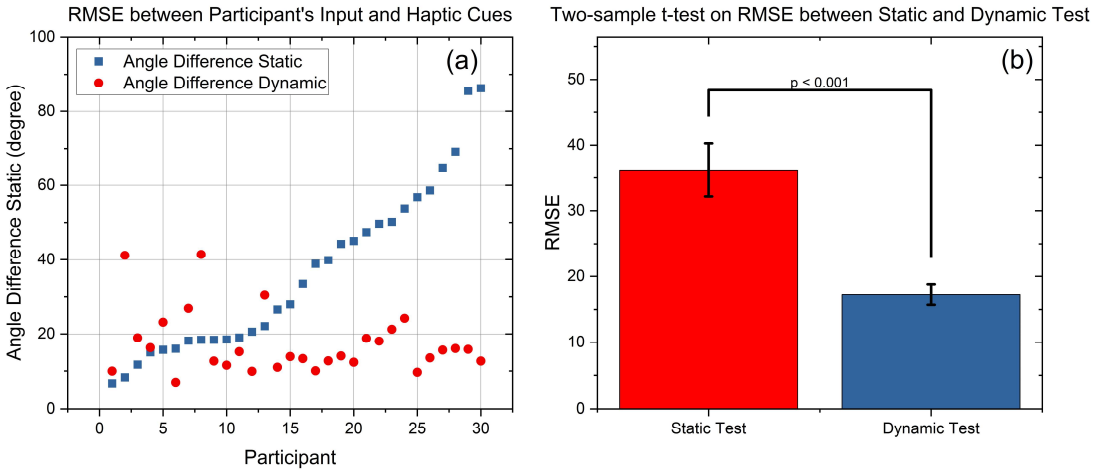

Figure 6.9 (a) RMSE for dynamic test and static test and (b) the two-sample t-test result on RMSE between two tests.

The RMSE was plotted in an ascending order for static test result and each participant's corresponding dynamic test result was also plotted. It was found that no correlation exists between two test results. A two-sample t-test was used to quantify the significance level at 5%. The resulted p value of the test was $p = 5.48e^{-5}$, in favour of the alternative hypothesis that the RMSE in the dynamic test was significantly lower than that in the static test. Therefore, based on the statistics listed in Table 7.8 and the p value of the two-sample t-test, hypothesis (3) could be verified.

6.2.3 Normal Force and Shear Force

Shear force is defined as the haptic force component along the y-axis and normal force is defined as the haptic force component along the x-axis as illustrated in Figure 6.10. The default forwards direction used during the experiment was along the positive y-axis.

Angles of 45^o and 135^o were used as the angle thresholds to determine zone 1 and zone 2. In zone 1, shear force component is greater than normal force. Therefore, the haptic feedback was dominated by shear forces. On the contrary, the haptic feedback was dominated by normal forces in zone 2. The hypothesis is that shear forces could deliver better haptic directional cues than normal forces in terms of angle accuracy.

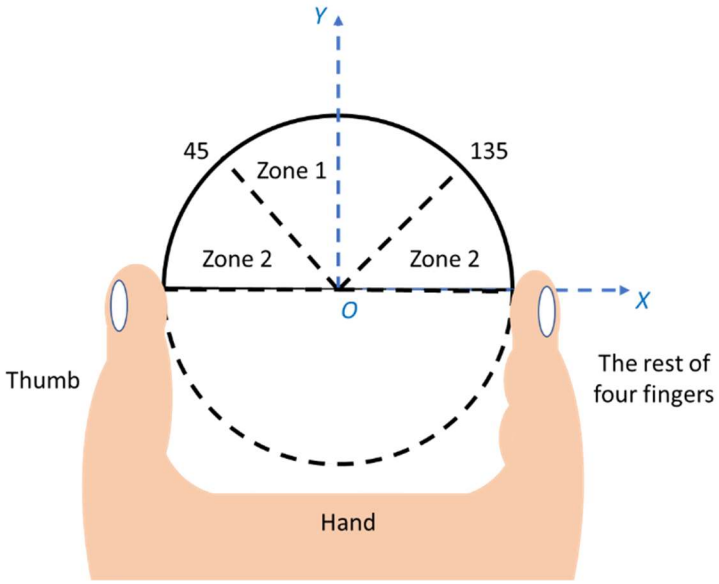

Figure 6.10 Different zones determined by dominant force with local coordinate in the haptic experiment.

The statistics between participant's input and haptic cues were calculated and are shown in Table 6.4 and the angle difference is plotted in Figure 6.11.

Table 6.4 Statistics of angle difference in different zones and tests.

Test and Zone	Number of Observations	Mean	Standard Deviation	Minimum	Median	Maximum
Static Zone 1	72	-5.71	32.84	-108.94	-0.18	89.89
Static Zone 2	78	8.70	48.92	-129.42	3.60	161.17
Dynamic Zone 1	77	1.01	21.06	-66.30	4.42	55.99
Dynamic Zone 2	73	-0.42	17.15	-47.82	2.91	37.51
Zone 1	149	-2.23	27.51	-108.94	2.08	89.89
Zone 2	151	4.29	37.29	-129.42	3.15	161.17

Overall, directional cues delivered by shear forces (zone 1) had better delivery of haptic cues in terms of direction accuracy and performance stability. The mean value, standard deviation and extreme values of shear forces were all lower than those of normal forces. Additionally, a significant difference was addressed by a two-sample t-test at 95% significance level in static test ($p = 0.037$) as shown in Figure 6.11(a). This observation together with the above statistics contributed to hypothesis (4). On the other hand, no significant difference was found in dynamic test between two zones, indictive of the effectiveness of the haptic reference. Therefore, this result also contributed to hypothesis (3).

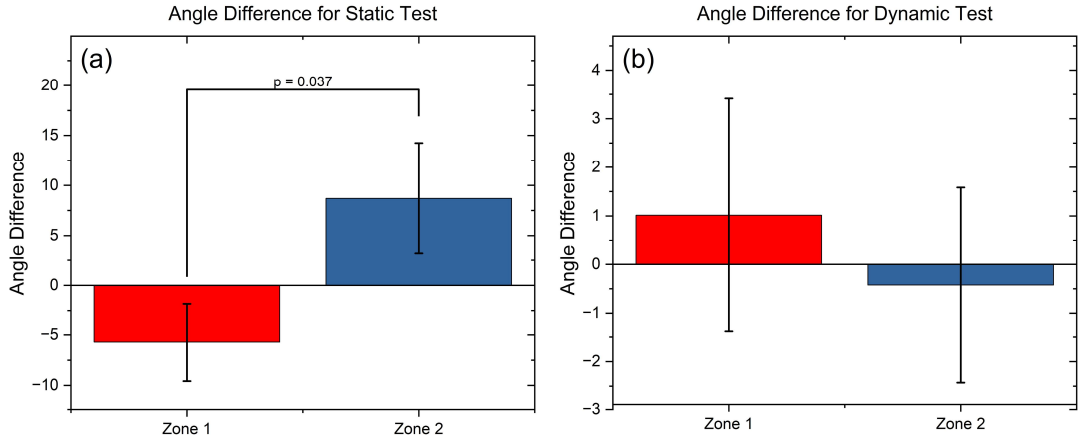

Figure 6.11 Two-sample t-test on zone difference in (a) static test and (b) dynamic test.

6.2.4 Special Concerns

Apart from force type and haptic reference, three additional factors found during the experiment may also influence the perception of haptic cues, namely the contact area, haptic exposure time and visual cues. Participants were not informed by these questions until they finish all experiment stages.

Contact area refers to the area of the device that is covered by participant's fingers. Because all participants recruited in this experiment had right dominant hand, their contact area on the right-hand side was larger than that on the left-hand side. The result is shown in Figure 6.12.

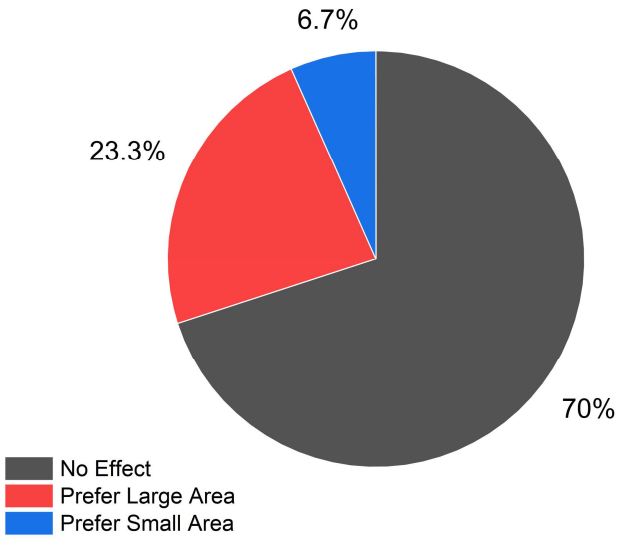

Figure 6.12 Preference on the contact area by participants.

Based on the answers from a questionnaire after the experiment, 70% of the participants found the contact area not significant in the perception of haptic directional cues. 23.3% of the participants preferred a large contact area whereas 6.7% of the participants preferred a small contact area.

Haptic exposure time is the amount of time till a participant could not specify a direction through haptic cues. Only 1 participant reported a temporary loss in the ability of the directional haptic perception after experiment. Two participants reported a decrease in the ability of the haptic perception after 12 minutes and 15 minutes, respectively. The rest of the participants did not feel a significant change in haptic perception throughout the experiment.

Participants were not asked to close their eyes in order to stop receiving visual cues during the experiment. However, only 1 participant was observed with an increase in both directional accuracy and user's confidence when visual cues were stopped in an extra static and dynamic test.

6.3 Discussion and Summary

A four-stage psychophysical experiment was designed in this research to verify the design and optimisation of the hand-held haptic device. Based on the results from the previous displacement measurements and three preliminary tests, 9 configurations were chosen during the experiment. Three evaluation metrics were used to assess the performance of each haptic configuration. Number of matches (NOM), sum of confidence (SOC) and number of unidentified (NOU) were used to describe the accuracy, user experience and applicability of each configuration.

The four hypotheses raised before the experiment was conducted are summarised below.

1) The asymmetry of haptic output would be increased by changing the cut-off voltage, which would benefit clearer delivery of haptic directional cues.
2) There exists an optimised stroke ratio that could achieve clearer delivery of haptic directional cues.
3) Participants would benefit from a haptic reference when perceiving directional guidance.
4) Haptic directional cues delivered by shear forces are clearer than those delivered by normal forces.

The asymmetry of the haptic output was quantified using stroke ratio that was calculated from the displacement measurement. It was shown in Figure 5.34 that stroke ratio exponentially decreased with larger cut-off voltage. Stroke ratio is calculated as a fraction of negative stroke over positive stroke. A small stroke ratio indicates a large pulse along the desired direction and a small pulse along the opposite direction. Since human haptic sensation is nonlinear [90], when strong and weak stimulus are applied to human skin sequentially, people perceive the stronger stimulus clearer than the weaker ones. A small stroke ratio therefore represents a stronger perception of directional cues. This is verified by a Tukey test in the left or right experiment as shown in Figure 6.3. Configurations with a cut-off voltage have significantly higher NOM and considerably lower NOU and higher SOC compared to those without a cut-off voltage, presenting superior performance in accuracy, user confidence and applicability. However, during the optimisation process on cut-off voltage, it was also found that there existed an upper threshold for cut-off voltage as shown in Figure 5.33. For the specific device developed in this research, this upper threshold value is 1.37 V. When a cut-off voltage above this threshold was adopted, though the stroke ratio was minimised, the absence of input delay would result in a failure of the perception of haptic cues. This was also reported in [60] where skin displacement would become symmetric if the input delay was removed, resulting in people feeling only normal vibrations but no directional cues.

Stroke ratio was also optimised in this study for the specific hand-held device. This was achieved by fitting a quadratic curve and a Gaussian curve between stroke ratio and NOM as shown in Figure 6.5. The commonly used psychometric curve in perception analysis was not used in this study since the change of NOM was not monotonic with respect to stroke ratio based on

the experimental results. When stroke ratio is large, the increased amount of negative stroke or decreased amount of positive stroke would reduce the difference between the sequential strong-weak stimulus, resulting in a failure of the perception of directional cues. Pearson's correlation test was also conducted on either side of the quadratic curve as shown in Figure 6.7, resulting in strong correlations between stroke ratio and NOM on both sides of the curve.

Other features such as vibration frequency, simplified speed and positive stroke also presented a strong correlation with NOM. This suggested that there existed an optimal value for these features in order for a maximum perception rate of haptic directional cues. However, the quantitative relationship between each feature was not established in this study. It was uncertain whether all the optimal values could be satisfied simultaneously. Future work should address on this issue to explore the effect of each output feature on other features.

In the dynamic test, a haptic directional reference pointing forward was presented to all participants before a directional change. It was shown in Figure 6.9 (b) that the RMSE between the actual direction and the perceived direction in dynamic test was significantly lower than that in the static test. This finding could be used to help the design of haptic directional devices when guiding the movement from different points. Instead of providing haptic cues along a constant direction, it is more beneficial to subtly change the direction of cues by a small amount of angle to the left and right sequentially (zig-zag shape) as illustrated in Figure 6.13.

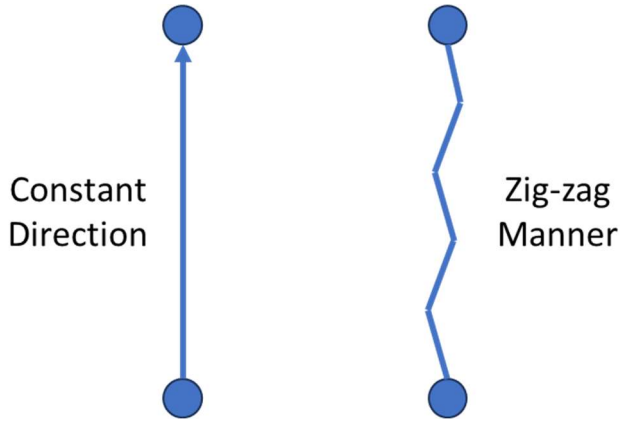

Figure 6.13 Constant direction guidance and zig-zag direction guidance.

The efficacy of the proposed zig-zag manner needs to be further studied and verified using a psychophysical experiment such as the One-interval, Two-alternatives, Forced-choice (1I, 2AFC) experiment. One interval means that only one of the two guidance manners will be presented to participants in

one trial, either the constant direction manner or the zig-zag manner. Two alternatives means that the chance of each participant receiving each manner is equal. Forced-choice means that participants have to indicate which manner was presented and it is not allowed to respond 'I don't know.' Additionally, it is also important to choose the shift angle in the zig-zag manner since there exists a minimum threshold that could be sensed in angle discrimination. In [98], this angle was reported to be 15 degrees. Analysis could be conducted on the decision model specifically for the 1I, 2AFC paradigm as described in [97].

In both static and dynamic test, it was found that haptic directional cues delivered by shear forces could be better perceived by participants in terms of accuracy and confidence than those delivered by normal forces. The theoretical explanation behind this finding was established by the Weber fraction [99]. It was determined by E.H. Weber that for many sensory modalities including haptic sensation, the change in stimulus density (difference threshold, DL) that could be discriminated by human is a constant fraction of baseline stimulus that is above the absolute threshold (RL) as described by Eq. 6.1.

$$\Delta I = kI \tag{6.1}$$

where: k is the Weber fraction, I is the baseline stimulus and ΔI is the DL that produces Just Noticeable Difference (JND) of the stimulus. For the magnitude of force, the Weber fraction lies between 0.07 and 0.1 [100] and the RL is reported to be 19 mN [101].

When the haptic device and participants are stationary, the force along the shear force direction (along the y axis in Figure 6.10) is zero. Therefore, if the force produced by haptic directional cues is greater than the RL, participants could feel a strong pulling sensation along the shear direction. However, when haptic cues are presented along the normal force direction, the DL will change with respect to the baseline stimulus that is the grip force necessary to hold the device. Thus, participants who grip the device harder find it more difficult to perceive the haptic directional cues along the normal force direction. Future study could be conducted using a force sensor to measure the grip force and force change during the presentation of haptic directional cues.

Chapter 7 Conclusions and Future Work

This thesis has presented the design and development of a hand-held haptic device for post-stroke patients with visual impairment. The device has a novelty of combining upper limb movement assessment and haptic directional guidance. The device has been validated in two independent studies: the movement assessment experiment with 14 participants and the haptic psychophysical experiment with 30 participants. All participants are healthy subjects.

Several conclusions could be drawn from both experiments. These findings form the basis for future research in the development and verification of haptic assistive devices, especially the experimental design and application in home environments.

This chapter specifies novel contributions of the research both cited and presented in this thesis and draws conclusions from the work presented in the previous chapters. The aim and objectives of the research is restated and the extent to which they were met is discussed. Future work based on the conclusions is also presented.

7.1 Conclusions

7.1.1 Overall Research Findings

The research presented in this thesis accomplished two tasks. Firstly, an upper limb movement assessment was achieved using machine learning algorithms and kinematic data. Specifically, different movement types could be successfully predicted and the progression of movement smoothness could be recognised. Secondly, haptic cues were generated and optimised for directional guidance. Specifically, the commonly-used step-ramp signal was parameterised and the effect of each parameter on the perception of haptic cues was investigated. The above results provide the guidance for developing haptic devices and conducting upper limb movement assessment based on kinematic features. This has the potential to be applied to the rehabilitation for upper limb, such as stroke. Rehabilitation after stroke using robotic devices has been studied for the last 30 years. However, most of the rehabilitation robots rely heavily on the visual information provided by a software environment such as a virtual reality and serious games. This device would target at post-stroke patients with visual

impairment who possess a certain ability to move the impaired limb independently and perceive haptic cues if the device is adopted alone. As an alternative, it could be used as an add-on module for existing upper limb rehabilitation robots like hCAAR to provide additional haptic cues for movement guidance instead of visual cues.

Movement smoothness assessment for the upper limb was traditionally made by physiotherapists during clinical exercises. These subjective and non-continuous assessments could not sensitively reflect the motor recovery process. Therefore, more personalised rehabilitation interventions could not be conducted. The use of kinematic features could address these limitations with the help of kinematic sensors. Kinematic features were objectively extracted from continuous movement data with an autonomous process. These features could sensitively reflect the change of motor function learning progress, specifically the movement smoothness, which could provide a more comprehensive understanding of the rehabilitation process. Some kinematic features like normalised jerk have also been validated with clinical assessment scores in various research setups. Additionally, these features could be used to train a machine learning model for the prediction of clinical scores and classification on movement smoothness. The research presented in this thesis focused on the latter classification tasks and have shown the feasibility of applying machine learning models for movement smoothness assessment through a single group observational experiment.

Assistive devices providing directional guidance come in various forms from wearable belts or gloves to exoskeletons. However, few of them were designed specifically for post-stroke patients with visual impairment. They not only need another form of directional guidance but also the assessment on their rehabilitation process. The research presented in this thesis focused on designing a haptic device providing directional guidance. The haptic implementation was based on asymmetric vibrations through a voice coil actuator in order to minimise the weight of the device. A psychophysical experiment reported in this thesis has demonstrated the efficacy of the proposed device and provided insight into the optimisation of haptic implementation in general.

7.1.2 Movement Smoothness Assessment Findings

7.1.2.1 Position Tracking

Assistive devices have been developed for rehabilitation purposes. Efforts have been made to deploy assistive devices not only in research or clinical

environments but also in home environments. However, traditional movement quality assessments for upper limbs require frequent visits of physiotherapists. Though recent developments on sensors have allowed a more objective quantification of the movement quality, their applications were limited by the cost of sensors and the ability to be independently used. The first part of the thesis focused on the use of a low-cost IMU sensor for movement type classification and discussed the efficacy of several position tracking methods. Machine learning models were developed to achieve classifications on both movement type and quality.

Position tracking is the basis of kinematic feature extraction and data analysis. In order to determine an ideal position tracking method in a home environment, two novel approaches were tested in this thesis. Both approaches were compared with a gold standard position sensor Optotrak. Position tracking based on mouse sensors demonstrated excellent test-retest reliability and accuracy. The measurement results were compared with those measured by Optotrak and no significant difference was observed. However, this method is limited by the range of measurement. It can only measure translational movements in a 2-dimensional plane. This measurement range, on the other hand, is sufficient for most of the post-stroke patients since there existed a few rehabilitation robots specifically designed for 2D movements without rotational ones. Another position tracking based on computer vision algorithms is the most convenient since it does not require additional hardware setups. However, its reliability and accuracy changes with respect to the working distance. Additionally, it requires specific camera setup so that no depth information is measured. The aim of position tracking is to extract kinematic features based on kinematic profiles. From this point of view, the same set of kinematic features used in the later experiment were extracted from the mouse sensor data. Except spectral entropy of the acceleration profiles and skewness of the velocity profiles, no significant difference was observed among other features. The results have demonstrated the feasibility of applying a mouse sensor for upper limb 2D movement analysis in home environments. Therefore, mouse sensors are recommended for position tracking in the hand-held device proposed in this research.

7.1.2.2 Kinematic Features and Machine Learning

Several acceleration-based features were extracted from the acceleration profiles during a movement for movement type classification. Four movements were adopted during the experiment, including reaching out,

drawing a circle, turning a key and drinking water. Maximum acceleration along each axis is the most important feature for the classification among the four movements. Random Forest, Support Vector Machine, K-nearest Neighbours and Deep Neural Networks were adopted for the classification task. Except Random Forest, all other models could achieve 100% training and test accuracy. The results suggest that acceleration-based features and distance-based machine learning models are especially suitable for movement type classification. Additionally, feature selection process such ANOVA could reduce the training time of the model while retaining current model performance, which proves the feasibility of applying online (real-time) machine learning models in the future design of rehabilitation robots.

Another classification was made based on a wider range of kinematic features extracted from position, velocity, acceleration and jerk profiles. Participants were invited to draw a multi-segment point-to-point figure in four different patterns using a mouse. The four movement patterns have a decreasing difficulty. A total of 6 out of 12 kinematic features could reflect the motor learning progress in terms of movement smoothness independently in each difficulty level. Specifically, selected kinematic features presented a moderate correlation with normalised jerk that has been validated with clinical scores in many studies to describe movement smoothness. The degree to which each kinematic feature correlates with normalised jerk decreased from the most difficult pattern to the easiest pattern. Moreover, a strong inter-feature reliability was observed within selected features including normalised jerk at each difficulty level. Both results demonstrated the efficacy of applying kinematic features to monitor the motor function learning progress in terms of movement smoothness. However, all kinematic features were extracted in a laboratory environment with pre-determined movement types. In real-world unsupervised applications, it is important to segment the movement onset and offset based on kinematic measurements automatically and accurately. It is also uncertain whether different kinematic features are the most suitable for a particular movement type.

The same four machine learning models were used for the movement smoothness classification based on kinematic features. Support Vector Machine showed superior performance than the others, which is consistent with findings from other literatures. Velocity-based features also contributed the most during the classification task. Overall, the performance of each model decreased from the most difficult pattern to the easiest pattern. It is

therefore recommended to apply Support Vector Mahine and velocity-based features for more subtle movement quality classifications.

7.1.3 Haptic Directional Guidance Findings

Assistive devices applying haptic cues have been proposed in other literature. Various types of haptic implementations have been studied including motor sequence and asymmetric vibrations. The motor sequence type requires multiple vibrators to work in a pre-defined sequence and order so that users can interpret the haptic feedback to directional cues. This inherently increases the cost of learning and always requires users to wear the haptic device, which is not friendly for post-stroke patients, especially to be used independently. On the other hand, haptic directional cues provided by asymmetric vibrations only requires two motors to serve a 2-dimensional plane. It has been designed to take the form of hand-held device, white cane, gloves that could normally be used independently without additional learning. Most importantly, users do not need to interpret the directional cues from the motor coordination to the real-world coordination if appropriately designed. Therefore, asymmetric vibrations were discussed in this thesis in terms of hardware selection and the evaluation of the input signal.

Three haptic motors were discussed in this thesis. Eccentric Rotating Mass (ERM) motors were determined to be not suitable for the generation of asymmetric vibrations for the hand-held device due to their weaker vibration effect and the large number of motors required to generate directional cues.

Solenoid motors were also tested with PWM signals as the input control. A test platform was built using the solenoid haptic implementation, and the vibration accelerations were measured by an IMU sensor. The measured accelerations were compared with the simulated accelerations from a 1-DOF mass-spring-damper model. It was found that the direction of the haptic cues changed with respect to the duty ratio of the PWM signals. It was also noticed that the spring stiffness of the haptic implementation and the waveform of the input signal had significant influence on the asymmetry of haptic output. Specifically, the change of output acceleration was nonlinear with respect to increasing stiffness. However, further optimisation of haptic output was limited by the number of parameters that can be tuned in a PWM signal. Therefore, a commonly adopted analogue step-ramp signal was finally discussed in this thesis.

The third motor presented in this thesis was a voice coil actuator (VCA). The VCA could be controlled by the step-ramp signal to generate asymmetric

vibrations. The main contribution of this part of the work is to parameterise the step-ramp signal so that a more standardised optimisation process could be followed regardless of motor type. The signal was parameterised with three variables, namely delay time, ramp down step length and cut-off voltage. To further quantify the asymmetry of haptic output, displacement profiles of the VCA was measured on a self-built test slider. Five output features were extracted from each measurement. Specifically, stroke ratio was used to describe the asymmetry of haptic output as a fraction of positive stroke and negative stroke. Finally, a psychophysical experiment was designed with 30 participants to verify the effect of optimisation. It was found that the perception of haptic cues changed nonlinearly with respect to stroke ratio. Unlike a typical psychometric curve, the relationship between the human perception and stroke ratio was not monotonic. Instead, it followed a Gaussian probability density function. This suggested that for the specific hand-held device developed in this research, there existed an optimal stroke ratio that could maximise the perception of directional cues. From the results of the dynamic test, it was found that the accuracy of the perceived directions as well as the participants' confidence on the perception increased when a haptic reference was provided before a cue. This could be used to guide the design of a haptic navigation device to improve users' experience. Furthermore, the results also showed that haptic cues delivered by shear forces were better perceived than those delivered by normal forces, which is related to the perception threshold of vibrotactile cues on human skins. Although current research has proved the feasibility of a hand-held device presenting haptic cues, limitations exist in terms of comparative analysis and performance difference in different dynamic system.

Parameterisation of haptic input has been explored in other literature, in which the input was regulated by the simulated acceleration output. Compared to the method proposed in this research, this approach has a better applicability since the input is not restricted by waveform but desired output acceleration profiles. However, the proposed method has a better translatability since the parameterisation of the input signal does not rely on other mechanical properties of the system such as spring stiffness, damping coefficient and motor's drive constant etc. A comparative analysis between two approaches verified by psychophysical experiment could provide more insight into the optimisation of haptic implementation.

Another limitation of the current work is the displacement measurement setup. Current measurement only reflected displacement profiles for the

VCA-slider system. However, the dynamic performance of the VCA-finger system may differ from the VCA-slider system. Although the purpose the current research was not to represent the VCA-finger system by VCA-slider system, it is still worthwhile to measure the displacement, force or acceleration interactions for the VCA-finger system to get a more comprehensive understanding of the haptic perception.

7.1.4 Evaluation of Research Aim and Objectives

The aim of the research was:

"The aim of this research is to design, implement and evaluate the performance of a low-cost hand-held haptic device integrating directional guidance and movement smoothness assessment using machine learning models, potentially for post-stroke patients and people with visual impairment."

The conclusions made in this chapter are based on the results of literature reviews and several experiments conducted in this thesis. The literature review showed limited work in the integration of movement smoothness assessment and directional guidance, specifically with patients after stroke as the target group. However, the work presented in this thesis has demonstrated both feasibility and efficacy of the integration through several experiments. The experiments primarily focused on the kinematic assessment of upper limb movements and the perception of haptic directional cues, which contributed to the evaluation of the developed device. Therefore, the aim of the research was met.

The objectives of the research were defined in the first chapter to reach the research aim and construct the basic structure of the thesis. Literature reviews showed that kinematic features and machine learning have been applied to assess movement quality (objective a), and various haptic implementations have been designed to provide directional cues (objective b). Limitations have been identified through the two objectives that there lacks an integration of kinematic assessment and haptic feedback. Moreover, little work has been done in terms of the parameterisation of haptic input control signal.

In order to assess movement quality, particularly movement smoothness, and to save battery life in a home environment, it is essential to recognise different movement types. Kinematic features were extracted from the acceleration profiles for the classification on movement types. The acceleration data were measured by a low-cost commercial IMU sensor

(objective c). This process was extended to position, velocity, acceleration and jerk profiles in a single group observational study with 14 participants. Three position tracking methods were discussed including a low-cost mouse sensor, a low-cost laptop camera and the gold standard Optotrak. A total of 12 kinematic features were extracted from kinematic measurements (objective c). Statistical analysis showed no significant difference between kinematic features extracted from mouse-measured data and Optotrak-measured data. All features had a good to excellent reliability.

Four machine learning models (DNN, KNN, RF and SVM) have been trained to solve two classification problems, namely the classification on movement type and on movement smoothness (objective d). Four movement types (reaching out, drawing a circle, turning a key and drinking water) were successfully classified by all models with 100% training and test accuracy when the inputs were acceleration-based features. Another four movement patterns (NDA with rotation, NDA without rotation, DA with rotation and DA without rotation) were also classified by all models with 100% training and test accuracy. The movement smoothness could be predicted either numerically into a number or categorically into beginner, intermediate and master levels with kinematic features as the inputs. The performance of the prediction decreased from the most difficult pattern (100%) to the easiest pattern (75%). Both movement pattern classification and movement smoothness classification were verified through a single group observational experiment with 14 participants (objective g). Support Vector Machine had superior performance than the others and velocity-based features were the most important predictors.

A hand-held device was designed and manufactured. The process was guided by design specifications (objective e). Three types of motor including ERM, solenoid and VCA were tested and simulated in order to determine the most ideal one for generating asymmetric vibrations. ERMs were determined to be not suitable for a set of reasons. Solenoids could generate asymmetric vibrations with PWM signals as an input, which was verified by simulated and experimental accelerations. However, the application of solenoids was limited by the heavy weight and large size. VCAs were determined to be the ideal source of asymmetric vibrations due to their sizes, weights and potentials in haptic optimisation.

The VCA was controlled by a step-ramp signal. Previous studies have demonstrated the feasibility of applying this signal for asymmetric vibrations. However, only input frequency and delay time of the signal were studied. In

order to optimise the haptic output, a step-ramp signal was parameterised by three variables including delay time, ramp down step length and cut-off voltage in this thesis (objective f). Five signal features were extracted from the position measurement of the VCA-slider system. A psychophysical experiment with 30 participants was designed to verify the optimisation process in terms of perception accuracy and confidence (objective g). Results from the experiment have shown a nonlinear quantitative relationship between the perception of haptic cues and four signal features.

This chapter draws conclusions for the current work and suggests future work (objective h).

7.1.5 Research Summary

The key findings of the research were summarised in Table 7.1.

Table 7.1 Key findings of the research.

Key points:
• Existing literatures show limited study on assistive device for post-stroke patients with visual impairments since most robot-aided rehabilitation therapies rely heavily on visual cues. • Kinematic features and the application of machine learning models can recognise different movement types and quantify movement smoothness into continuous numbers or categories. • Features extracted from specific kinematic measurements are important in movement smoothness assessment with a certain machine learning model. • Kinematic data extracted from a low-cost mouse sensor can be used for kinematic feature extraction with no significant difference compared to those extracted from more expensive and accurate sensors. • Haptic perception of humans can be improved in terms of accuracy and confidence by optimising the input parameters of a step-ramp signal. • It is necessary to conduct a comparative analysis between the parameterisation method proposed in this thesis and in other literatures.
Kinematic features and machine learning:
• Kinematic features can contribute to the movement type and movement smoothness classification. Specifically, acceleration-based

features are important for movement type classification and velocity-based features are important for movement smoothness classification. • Support Vector Machine has superior performance in movement smoothness classification task. However, there are many varieties of SVMs and other more advanced machine learning models such as Transformer. Attempts using those models may improve the overall performance on movement assessment.
Haptic feedback:
• The optimisation of step-ramp signals based on the parameterisation proposed in the thesis enhances the perception of haptic directional cues, especially with cut-off voltages and stroke ratios. • The perception of haptic cues changes nonlinearly with stroke ratios. Specifically, it follows a Gaussian probability density function curve.
Experimental design:
• The movement selected for the experiment is complex enough for the differentiation between various difficulty levels. However, it would be more beneficial and comparable if movements in a clinical exercise are adopted. • The psychophysical experiment for the haptic feedback is designed within the research group. Its process did not follow a typical psychophysical haptic paradigm. A comparative analysis is recommended between the proposed method and a classic paradigm.

Some of the work presented in this thesis have been published in peer-reviewed conferences and journals. The work related to movement assessment based on kinematic features have been invited for a presentation during the 2023 International Conference on Rehabilitation Robotics. The presentation and the poster were selected as the finalist achievement after the judging session.

7.2 Future Work

Since the integrated hand-held device has two main functions, future work should focus on each function and the application of the device on real patients in home environments.

7.2.1 Extraction of Kinematic Features and Their Applications

This thesis has demonstrated the feasibility of applying kinematic features in upper limb movement assessment, specifically movement type and movement smoothness classifications. It was found that a specific feature was essential for a particular task. For example, velocity-based features contributed the most to the movement smoothness assessment but were less effective in movement type classification. This indicates that a kinematic feature is either movement type-dependent or not suitable for movement type classification. Based on the current findings, it is hypothesised that acceleration-based features are suitable for movement type classification while velocity-based features are suitable for movement smoothness classification. Therefore, future work should focus on the experimental design to verify this hypothesis. The contribution of verifying the hypothesis is to guide the selection of the most beneficial kinematic features in upper limb movement analysis.

Firstly, it is important to choose the appropriate movements for analysis, which has been reported in [102] for post-stroke at-home recovery. It is also recommended to establish a public movement data repository for movement analysis. The public repository has accelerated the development of different algorithms and methods in computer vision field such as ImageNet [103] and in deep learning field such as MNIST [104]. Such a public dataset saves repetitive data collection time and establishes a common standard for every researcher to test and optimise their methods.

Secondly, kinematic features need to be extracted from all kinematic measurements, including position, velocity, acceleration and jerk. Depending on the place for the experiment, the measurement equipment may vary from an advanced position sensor to a low-cost mouse sensor or IMU sensors. Since a large variety of kinematic features have been published in the literature, it is crucial to select those that have been validated with a common standard such as normalised jerk for the analysis.

In terms of experimental subjects, it is more representative if post-stroke patients are recruited. However, the recruitment of real patients needs to be carefully studied for the inclusion and exclusion criteria, which are dependent on the selection of movements as well. It is also important to follow ethical requirements from both the research institute and the public health service like NHS, especially the privacy on personal data.

Finally, proper statistical analysis needs to be conducted. In order to verify the hypothesis proposed before, the same machine learning model and model optimisations are required. Analysis should focus on statistical differences between two model performances based on different sets of features for the same task. Additionally, the study on the correlation between two features may also help understand the applicability of each kinematic feature. If real patients are recruited, the correlations between the kinematic assessment scores and their clinical scores are also important for the digitalisation of healthcare and telerehabilitation.

7.2.2 Haptic Perception Experiment

The haptic implementation and the device proposed in this thesis have demonstrated the ability to provide haptic directional cues. The effect of different force types and haptic reference on the perception of haptic directional cues were also discussed. Future work should focus on two aspects: a comparative analysis between different haptic optimisation processes and the application of the proposed device in a real-world situation.

Two further comparative analyses need to be undertaken. The first one should focus on the difference between optimisation based on acceleration output and based on analogue input. A dynamic model of the proposed device in a motor-finger system could be established by extending the proposed 1DOF model in this thesis to a 2DOF model considering skin displacement as well. The idea of quantifying the asymmetry of haptic output by a stroke ratio could then be extended to skin displacement profiles rather than the VCA displacement profile. This could provide a more comprehensive understanding on the perception of haptic cues. Another experiment that could be designed is to adopt a classic haptic perception experiment to determine if the discrimination threshold of the angle changes with a haptic reference. This could be achieved by plotting two psychometric curves with one axis representing angle difference and the other axis representing the ratio of the right answers from participants. The Just Noticeable Difference (JND) could then be determined as the midpoint of the curve.

The second aspect of the future work should focus on the application of the proposed device. It could be used as an add-on module for the existing rehabilitation robots such as a hCAAR robot [105]. It is a 2D planar robot designed for post stroke rehabilitation in a home environment. The proposed device could be added as the top handle of the hCAAR robot to provide

haptic stimulations to post-stroke patients. The challenge of this application is to integrate the haptic device with the hCAAR low-level controller. An alternative is to apply the device as a general assistive device. Although it was designed for post-stroke patients with visual impairment, it could also be used as an assistive device for the visually impaired people.

However, the most important work to be done in terms of real-world application is to verify its efficacy with post-stroke patients. It is uncertain from the current work that whether the same perception optimisation process could be followed for post-stroke patients. Patients after stroke always show various symptoms depending on the area of the stroke, the rehabilitation interventions received after stroke etc. Therefore, it would be more beneficial if haptic perception experiment could be conducted among stroke subjects.

List of References

1. Nijland, R.H., van Wegen, E.E., Harmeling-van der Wel, B.C., Kwakkel, G. and Investigators, E. Presence of finger extension and shoulder abduction within 72 hours after stroke predicts functional recovery: early prediction of functional outcome after stroke: the EPOS cohort study. *Stroke*. 2010, **41**(4), pp.745-750.
2. Van der Lee, J.H., De Groot, V., Beckerman, H., Wagenaar, R.C., Lankhorst, G.J. and Bouter, L.M. The intra- and interrater reliability of the action research arm test: a practical test of upper extremity function in patients with stroke. *Arch Phys Med Rehabil*. 2001, **82**(1), pp.14-19.
3. Woodbury, M.L., Velozo, C.A., Richards, L.G., Duncan, P.W., Studenski, S. and Lai, S.M. Longitudinal stability of the Fugl-Meyer Assessment of the upper extremity. *Arch Phys Med Rehabil*. 2008, **89**(8), pp.1563-1569.
4. Chen, H.M., Chen, C.C., Hsueh, I.P., Huang, S.L. and Hsieh, C.L. Test-retest reproducibility and smallest real difference of 5 hand function tests in patients with stroke. *Neurorehabil Neural Repair*. 2009, **23**(5), pp.435-440.
5. de Sousa, D.G., Harvey, L.A., Dorsch, S. and Glinsky, J.V. Interventions involving repetitive practice improve strength after stroke: a systematic review. *Journal of physiotherapy*. 2018, **64**(4), pp.210-221.
6. Corbetta, D., Sirtori, V., Castellini, G., Moja, L. and Gatti, R. Constraint‐induced movement therapy for upper extremities in people with stroke. *Cochrane Database of Systematic Reviews*. 2015, (10).
7. Veerbeek, J.M., van Wegen, E., van Peppen, R., van der Wees, P.J., Hendriks, E., Rietberg, M. and Kwakkel, G. What Is the Evidence for Physical Therapy Poststroke? A Systematic Review and Meta-Analysis. *PLoS One*. 2014, **9**(2), p.e87987.
8. French, B., Thomas, L.H., Coupe, J., McMahon, N.E., Connell, L., Harrison, J., Sutton, C.J., Tishkovskaya, S. and Watkins, C.L. Repetitive task training for improving functional ability after stroke. *Cochrane Database of Systematic Reviews*. 2016, (11).
9. Ebben, W.P., Kindler, A.G., Chirdon, K.A., Jenkins, N.C., Polichnowski, A.J. and Ng, A.V. The Effect of High-Load vs. High-Repetition Training on Endurance Performance. *The Journal of Strength & Conditioning Research*. 2004, **18**(3).
10. Lawton, T., Cronin, J., Drinkwater, E., Lindsell, R. and Pyne, D. The effect of continuous repetition training and intra-set rest training on bench press strength and power. *J Sports Med Phys Fitness*. 2004, **44**(4), pp.361-367.
11. Prvu Bettger, J. and Resnik, L.J. Telerehabilitation in the Age of COVID-19: An Opportunity for Learning Health System Research. *Phys Ther*. 2020, **100**(11), pp.1913-1916.

12. Rowe, F.J., Hepworth, L.R., Howard, C., Hanna, K.L., Cheyne, C.P. and Currie, J. High incidence and prevalence of visual problems after acute stroke: An epidemiology study with implications for service delivery. *PLoS One*. 2019, **14**(3), p.e0213035.
13. Qassim, H.M. and Wan Hasan, W. A review on upper limb rehabilitation robots. *Applied Sciences*. 2020, **10**(19), p.6976.
14. Okamura, A.M. Haptic feedback in robot-assisted minimally invasive surgery. *Current opinion in urology*. 2009, **19**(1), p.102.
15. Kamuro, S., Minamizawa, K., Kawakami, N. and Tachi, S. Ungrounded kinesthetic pen for haptic interaction with virtual environments. In: *RO-MAN 2009-The 18th IEEE International Symposium on Robot and Human Interactive Communication*: IEEE, 2009, pp.436-441.
16. Johnson, K.O. The roles and functions of cutaneous mechanoreceptors. *Current opinion in neurobiology*. 2001, **11**(4), pp.455-461.
17. Iwata, H. History of haptic interface. *Human haptic perception: Basics and applications*. 2008, pp.355-361.
18. Elmannai, W. and Elleithy, K. Sensor-based assistive devices for visually-impaired people: Current status, challenges, and future directions. *Sensors*. 2017, **17**(3), p.565.
19. Barroga, E. and Matanguihan, G.J. A Practical Guide to Writing Quantitative and Qualitative Research Questions and Hypotheses in Scholarly Articles. *J Korean Med Sci*. 2022, **37**(16), p.e121.
20. Carpinella, I., Cattaneo, D. and Ferrarin, M. Quantitative assessment of upper limb motor function in Multiple Sclerosis using an instrumented Action Research Arm Test. *J Neuroeng Rehabil*. 2014, **11**, p.67.
21. Lang, C.E., Bland, M.D., Bailey, R.R., Schaefer, S.Y. and Birkenmeier, R.L. Assessment of upper extremity impairment, function, and activity after stroke: foundations for clinical decision making. *J Hand Ther*. 2013, **26**(2), pp.104-114;quiz 115.
22. Zhang, Z., Fang, Q. and Gu, X. Objective assessment of upper-limb mobility for poststroke rehabilitation. *IEEE Transactions on Biomedical Engineering*. 2015, **63**(4), pp.859-868.
23. Yu, L., Xiong, D., Guo, L. and Wang, J. A remote quantitative Fugl-Meyer assessment framework for stroke patients based on wearable sensor networks. *Computer methods and programs in biomedicine*. 2016, **128**, pp.100-110.
24. Sivan, M., Gallagher, J., Makower, S., Keeling, D., Bhakta, B., O'Connor, R.J. and Levesley, M. Home-based Computer Assisted Arm Rehabilitation (hCAAR) robotic device for upper limb exercise after stroke: results of a feasibility study in home setting. *Journal of neuroengineering and rehabilitation*. 2014, **11**, pp.1-17.
25. Kim, H., Miller, L.M., Fedulow, I., Simkins, M., Abrams, G.M., Byl, N. and Rosen, J. Kinematic data analysis for post-stroke patients following bilateral versus unilateral rehabilitation with an upper limb wearable robotic system. *IEEE transactions on neural systems and rehabilitation engineering*. 2012, **21**(2), pp.153-164.
26. Nordin, N., Xie, S.Q. and Wünsche, B. Assessment of movement quality in robot-assisted upper limb rehabilitation after stroke: a

review. *Journal of neuroengineering and rehabilitation*. 2014, **11**(1), pp.1-23.

27. Fitle, K.D., Pehlivan, A.U. and O'malley, M.K. A robotic exoskeleton for rehabilitation and assessment of the upper limb following incomplete spinal cord injury. In: *2015 IEEE international conference on robotics and automation (ICRA)*: IEEE, 2015, pp.4960-4966.
28. Samuel, G.S., Choo, M., Chan, W.Y., Kok, S. and Ng, Y.S. The use of virtual reality-based therapy to augment poststroke upper limb recovery. *Singapore medical journal*. 2015, **56**(7), p.e127.
29. van Dokkum, L., Hauret, I., Mottet, D., Froger, J., Métrot, J. and Laffont, I. The contribution of kinematics in the assessment of upper limb motor recovery early after stroke. *Neurorehabilitation and neural repair*. 2014, **28**(1), pp.4-12.
30. Kiper, P., Agostini, M., Luque-Moreno, C., Tonin, P. and Turolla, A. Reinforced feedback in virtual environment for rehabilitation of upper extremity dysfunction after stroke: preliminary data from a randomized controlled trial. *BioMed research international*. 2014, **2014**.
31. cheol Jeong, I. and Finkelstein, J. Computer-assisted upper extremity training using interactive biking exercise (iBikE) platform. In: *2012 Annual International Conference of the IEEE Engineering in Medicine and Biology Society*: IEEE, 2012, pp.6095-6099.
32. Urbin, M., Bailey, R.R. and Lang, C.E. Validity of body-worn sensor acceleration metrics to index upper extremity function in hemiparetic stroke. *Journal of neurologic physical therapy: JNPT*. 2015, **39**(2), p.111.
33. Colombo, R., Pisano, F., Micera, S., Mazzone, A., Delconte, C., Carrozza, M., Dario, P. and Minuco, G. Assessing mechanisms of recovery during robot-aided neurorehabilitation of the upper limb. *Neurorehabilitation and neural repair*. 2008, **22**(1), pp.50-63.
34. Celik, O., O'Malley, M.K., Boake, C., Levin, H.S., Yozbatiran, N. and Reistetter, T.A. Normalized movement quality measures for therapeutic robots strongly correlate with clinical motor impairment measures. *IEEE transactions on neural systems and rehabilitation engineering*. 2010, **18**(4), pp.433-444.
35. Hamaguchi, T., Saito, T., Suzuki, M., Ishioka, T., Tomisawa, Y., Nakaya, N. and Abo, M. Support Vector Machine-Based Classifier for the Assessment of Finger Movement of Stroke Patients Undergoing Rehabilitation. *Journal of Medical and Biological Engineering*. 2020, **40**(1), pp.91-100.
36. Mohamed, A.A., Awad, M.I., Maged, S.A. and Gaber, M.M. Automated Upper Limb Motor Functions Assessment System Using One-Class Support Vector Machine. In: *2021 16th International Conference on Computer Engineering and Systems (ICCES)*, *15-16 Dec. 2021*, 2021, pp.1-6.
37. Aguiar, L.F. and A. P. L, B. Hand gestures recognition using electromyography for bilateral upper limb rehabilitation. In: *2017 IEEE Life Sciences Conference (LSC)*, *13-15 Dec. 2017*, 2017, pp.63-66.
38. Hua, A., Chaudhari, P., Johnson, N., Quinton, J., Schatz, B., Buchner, D. and Hernandez, M.E. Evaluation of Machine Learning Models for Classifying Upper Extremity Exercises Using Inertial Measurement

Unit-Based Kinematic Data. *IEEE J Biomed Health Inform*. 2020, **24**(9), pp.2452-2460.
39. Ma, Y., Liu, D. and Cai, L. Deep Learning-Based Upper Limb Functional Assessment Using a Single Kinect v2 Sensor. *Sensors (Basel)*. 2020, **20**(7).
40. Lu, L., Tan, Y., Klaic, M., Galea, M.P., Khan, F., Oliver, A., Mareels, I., Oetomo, D. and Zhao, E. Evaluating Rehabilitation Progress Using Motion Features Identified by Machine Learning. *IEEE Trans Biomed Eng*. 2021, **68**(4), pp.1417-1428.
41. Aizawa, J., Masuda, T., Koyama, T., Nakamaru, K., Isozaki, K., Okawa, A. and Morita, S. Three-dimensional motion of the upper extremity joints during various activities of daily living. *Journal of Biomechanics*. 2010, **43**(15), pp.2915-2922.
42. Murgia, A., Kyberd, P. and Barnhill, T. The use of kinematic and parametric information to highlight lack of movement and compensation in the upper extremities during activities of daily living. *Gait & Posture*. 2010, **31**(3), pp.300-306.
43. Namdari, S., Yagnik, G., Ebaugh, D.D., Nagda, S., Ramsey, M.L., Williams, G.R. and Mehta, S. Defining functional shoulder range of motion for activities of daily living. *Journal of Shoulder and Elbow Surgery*. 2012, **21**(9), pp.1177-1183.
44. Butler, E.E., Ladd, A.L., LaMont, L.E. and Rose, J. Temporal–spatial parameters of the upper limb during a Reach & Grasp Cycle for children. *Gait & Posture*. 2010, **32**(3), pp.301-306.
45. Klotz, M.C.M., Kost, L., Braatz, F., Ewerbeck, V., Heitzmann, D., Gantz, S., Dreher, T. and Wolf, S.I. Motion capture of the upper extremity during activities of daily living in patients with spastic hemiplegic cerebral palsy. *Gait & Posture*. 2013, **38**(1), pp.148-152.
46. de los Reyes-Guzmán, A., Gil-Agudo, A., Peñasco-Martín, B., Solís-Mozos, M., del Ama-Espinosa, A. and Pérez-Rizo, E. Kinematic analysis of the daily activity of drinking from a glass in a population with cervical spinal cord injury. *Journal of neuroengineering and rehabilitation*. 2010, **7**(1), p.41.
47. Alt Murphy, M., Willén, C. and Sunnerhagen, K.S. Responsiveness of Upper Extremity Kinematic Measures and Clinical Improvement During the First Three Months After Stroke. *Neurorehabilitation and neural repair*. 2013, **27**(9), pp.844-853.
48. Qin, J., Lin, J.-H., Faber, G.S., Buchholz, B. and Xu, X. Upper extremity kinematic and kinetic adaptations during a fatiguing repetitive task. *Journal of Electromyography and Kinesiology*. 2014, **24**(3), pp.404-411.
49. Bouffard, J., Yang, C., Begon, M. and Côté, J. Sex differences in kinematic adaptations to muscle fatigue induced by repetitive upper limb movements. *Biology of Sex Differences*. 2018, **9**(1), p.17.
50. Whiting, W.C., Gregor, R.J. and Finerman, G.A. Kinematic analysis of human upper extremity movements in boxing. *The American Journal of Sports Medicine*. 1988, **16**(2), pp.130-136.
51. Busuttil, N.A., Reid, M., Connolly, M., Dascombe, B.J. and Middleton, K.J. A kinematic analysis of the upper limb during the topspin double-handed backhand stroke in tennis. *Sports Biomechanics*. 2022, **21**(9), pp.1046-1064.

52. Lloyd, D.G., Alderson, J. and Elliott, B.C. An upper limb kinematic model for the examination of cricket bowling: A case study of Mutiah Muralitharan. *Journal of Sports Sciences*. 2000, **18**(12), pp.975-982.
53. Dharma, A.A.G., Ariwa, E. and Tomimatsu, K. Green technology and wearable haptic feedback display with 5×12 arrays of vibrotactile actuators. In: *2013 IEEE Third International Conference on Consumer Electronics ¿ Berlin (ICCE-Berlin)*, *9-11 Sept. 2013*, 2013, pp.272-274.
54. Dharma, A.A.G., Oami, T., Obata, Y., Yan, L. and Tomimatsu, K. Design of a Wearable Haptic Vest as a Supportive Tool for Navigation. In: *Human-Computer Interaction. Interaction Modalities and Techniques*, *2013//*, *Berlin, Heidelberg*. Springer Berlin Heidelberg, 2013, pp.568-577.
55. Amemiya, T., Ando, H. and Maeda, T. Phantom-DRAWN: direction guidance using rapid and asymmetric acceleration weighted by nonlinearity of perception. In: *Proceedings of the 2005 international conference on Augmented tele-existence*, 2005, pp.201-208.
56. Amemiya, T., Ando, H. and Maeda, T. Virtual force display: direction guidance using asymmetric acceleration via periodic translational motion. In: *First Joint Eurohaptics Conference and Symposium on Haptic Interfaces for Virtual Environment and Teleoperator Systems. World Haptics Conference*, *18-20 March 2005*, 2005, pp.619-622.
57. Shima, T. and Takemura, K. An Ungrounded Pulling Force Feedback Device Using Periodical Vibration-Impact. In: *Haptics: Perception, Devices, Mobility, and Communication*, *2012//*, *Berlin, Heidelberg*. Springer Berlin Heidelberg, 2012, pp.481-492.
58. Rekimoto, J. Traxion: a tactile interaction device with virtual force sensation. In: *ACM SIGGRAPH 2014 Emerging Technologies*. 2014, pp.1-1.
59. Amemiya, T. and Gomi, H. Distinct Pseudo-Attraction Force Sensation by a Thumb-Sized Vibrator that Oscillates Asymmetrically. In: *Haptics: Neuroscience, Devices, Modeling, and Applications*, *2014*, *Berlin, Heidelberg*. Springer Berlin Heidelberg, 2014, pp.88-95.
60. Culbertson, H., Walker, J.M. and Okamura, A.M. Modeling and design of asymmetric vibrations to induce ungrounded pulling sensation through asymmetric skin displacement. In: *2016 IEEE Haptics Symposium (HAPTICS)*, *8-11 April 2016*, 2016, pp.27-33.
61. Dong, S., Gallagher, J., Jackson, A. and Levesley, M. Modelling and Design of Asymmetric Vibrations to Induce Bidirectional Force Sensation for Portable Rehabilitation Devices. In: *2022 International Conference on Rehabilitation Robotics (ICORR)*, *25-29 July 2022*, 2022, pp.1-6.
62. Ekin, S. *Prompt Engineering For ChatGPT: A Quick Guide To Techniques, Tips, And Best Practices.* 2023.
63. Pryzant, R., Iter, D., Li, J., Lee, Y.T., Zhu, C. and Zeng, M. *Automatic Prompt Optimization with "Gradient Descent" and Beam Search.* 2023.
64. Tanabe, T., Yano, H., Endo, H., Ino, S. and Iwata, H. Pulling Illusion Based on the Phase Difference of the Frequency Components of Asymmetric Vibrations. *IEEE/ASME Transactions on Mechatronics*. 2021, **26**(1), pp.203-213.

65. nDigital. *Optotrak Certus.* [Online]. 2015. [Accessed 25 October 2023]. Available from: www.ndigital.com/optotrak
66. Metcalf, A.G., Gallagher, J.F., Jackson, A.E. and Levesley, M.C. Multi-Domain Dynamic Modelling of a Low-Cost Upper Limb Rehabilitation Robot. *Robotics.* [Online]. 2021. **10**(4).
67. Cha, K., Wang, J., Li, Y., Shen, L., Chen, Z. and Long, J. A novel upper-limb tracking system in a virtual environment for stroke rehabilitation. *Journal of neuroengineering and rehabilitation*. 2021, **18**(1), p.166.
68. Chang, Y.-J., Han, W.-Y. and Tsai, Y.-C. A Kinect-based upper limb rehabilitation system to assist people with cerebral palsy. *Research in developmental disabilities*. 2013, **34**(11), pp.3654-3659.
69. Soleimanitaleb, Z., Keyvanrad, M.A. and Jafari, A. Object Tracking Methods:A Review. In: *2019 9th International Conference on Computer and Knowledge Engineering (ICCKE)*, *24-25 Oct. 2019*, 2019, pp.282-288.
70. Debnath, B., O'Brien, M., Yamaguchi, M. and Behera, A. A review of computer vision-based approaches for physical rehabilitation and assessment. *Multimedia Systems*. 2022, **28**(1), pp.209-239.
71. Singer, B. and Garcia-Vega, J. The Fugl-Meyer upper extremity scale. *Journal of physiotherapy*. 2017, **63**(1), p.53.
72. Yozbatiran, N., Der-Yeghiaian, L. and Cramer, S.C. A standardized approach to performing the action research arm test. *Neurorehabilitation and neural repair*. 2008, **22**(1), pp.78-90.
73. Wang, D.X., Yao, J., Zirek, Y., Reijnierse, E.M. and Maier, A.B. Muscle mass, strength, and physical performance predicting activities of daily living: a meta‐analysis. *Journal of cachexia, sarcopenia and muscle*. 2020, **11**(1), pp.3-25.
74. Schwarz, A., Kanzler, C.M., Lambercy, O., Luft, A.R. and Veerbeek, J.M. Systematic Review on Kinematic Assessments of Upper Limb Movements After Stroke. *Stroke*. 2019, **50**(3), pp.718-727.
75. Ding, C. and Peng, H. Minimum redundancy feature selection from microarray gene expression data. *J Bioinform Comput Biol*. 2005, **3**(2), pp.185-205.
76. Rabadi, M.H. and Rabadi, F.M. Comparison of the action research arm test and the Fugl-Meyer assessment as measures of upper-extremity motor weakness after stroke. *Archives of physical medicine and rehabilitation*. 2006, **87**(7), pp.962-966.
77. Ponsiglione, A.M., Ricciardi, C., Amato, F., Cesarelli, M., Cesarelli, G. and D'addio, G. Statistical Analysis and Kinematic Assessment of Upper Limb Reaching Task in Parkinson's Disease. *Sensors*. 2022, **22**(5), p.1708.
78. Richman, J.S. and Moorman, J.R. Physiological time-series analysis using approximate entropy and sample entropy. *American Journal of Physiology-Heart and Circulatory Physiology*. 2000, **278**(6), pp.H2039-H2049.
79. Kahl, L. and Hofmann, U.G. Comparison of algorithms to quantify muscle fatigue in upper limb muscles based on sEMG signals. *Medical Engineering & Physics*. 2016, **38**(11), pp.1260-1269.

80. Alberts, J.L., Saling, M., Adler, C.H. and Stelmach, G.E. Disruptions in the reach-to-grasp actions of Parkinson's patients. *Exp Brain Res*. 2000, **134**(3), pp.353-362.
81. Spolaôr, N., Cherman, E.A., Monard, M.C. and Lee, H.D. ReliefF for Multi-label Feature Selection. In: *2013 Brazilian Conference on Intelligent Systems*, *19-24 Oct. 2013*, 2013, pp.6-11.
82. Koo, T.K. and Li, M.Y. A Guideline of Selecting and Reporting Intraclass Correlation Coefficients for Reliability Research. *Journal of Chiropractic Medicine*. 2016, **15**(2), pp.155-163.
83. Pandis, N. The chi-square test. *Am J Orthod Dentofacial Orthop*. 2016, **150**(5), pp.898-899.
84. Fan, C. and Zhang, D. A note on power and sample size calculations for the Kruskal-Wallis test for ordered categorical data. *J Biopharm Stat*. 2012, **22**(6), pp.1162-1173.
85. Robnik-Šikonja, M. and Kononenko, I. Theoretical and Empirical Analysis of ReliefF and RReliefF. *Machine Learning*. 2003, **53**(1), pp.23-69.
86. Ferri, C., Hernández-Orallo, J. and Modroiu, R. An experimental comparison of performance measures for classification. *Pattern Recognition Letters*. 2009, **30**(1), pp.27-38.
87. Buitrago, M.M., Schulz, J.B., Dichgans, J. and Luft, A.R. Short and long-term motor skill learning in an accelerated rotarod training paradigm. *Neurobiology of Learning and Memory*. 2004, **81**(3), pp.211-216.
88. Amemiya, T., Ando, H. and Maeda, T. Phantom-DRAWN: direction guidance using rapid and asymmetric acceleration weighted by nonlinearity of perception. In: *Proceedings of the 2005 international conference on Augmented tele-existence*, *Christchurch, New Zealand*. Association for Computing Machinery, 2005, pp.201–208.
89. Tappeiner, H.W., Klatzky, R.L., Unger, B. and Hollis, R. Good vibrations: Asymmetric vibrations for directional haptic cues. In: *World Haptics 2009 - Third Joint EuroHaptics conference and Symposium on Haptic Interfaces for Virtual Environment and Teleoperator Systems*, *18-20 March 2009*, 2009, pp.285-289.
90. Amemiya, T., Ando, H. and Maeda, T. Lead-Me Interface for a Pulling Sensation from Hand-held Devices. *ACM Transactions on Applied Perception*. 2008, **5**, p.15.
91. Rekimoto, J. Traxion: a tactile interaction device with virtual force sensation. In: *Proceedings of the 26th annual ACM symposium on User interface software and technology*, *St. Andrews, Scotland, United Kingdom*. Association for Computing Machinery, 2013, pp.427–432.
92. Xihao, S. and Miyanaga, Y. Dynamic time warping for speech recognition with training part to reduce the computation. In: *International Symposium on Signals, Circuits and Systems ISSCS2013*, *11-12 July 2013*, 2013, pp.1-4.
93. Munich, M.E. and Perona, P. Continuous dynamic time warping for translation-invariant curve alignment with applications to signature verification. In: *Proceedings of the Seventh IEEE International Conference on Computer Vision*, *20-27 Sept. 1999*, 1999, pp.108-115 vol.101.

94. Seo, N.J. and Armstrong, T.J. Investigation of grip force, normal force, contact area, hand size, and handle size for cylindrical handles. *Hum Factors*. 2008, **50**(5), pp.734-744.
95. Stock, R., Askim, T., Thrane, G., Anke, A. and Mork, P.J. Grip strength after stroke: Rate of force development and sustained maximal grip strength. *Annals of Physical and Rehabilitation Medicine*. 2018, **61**, pp.e352-e353.
96. Brisben, A.J., Hsiao, S.S. and Johnson, K.O. Detection of vibration transmitted through an object grasped in the hand. *J Neurophysiol*. 1999, **81**(4), pp.1548-1558.
97. Jones, L.A. and Tan, H.Z. Application of Psychophysical Techniques to Haptic Research. *IEEE Transactions on Haptics*. 2013, **6**(3), pp.268-284.
98. Elhajj, I., Weerasinghe, H., Dika, A. and Hansen, R. Human Perception of Haptic Force Direction. In: *2006 IEEE/RSJ International Conference on Intelligent Robots and Systems*, *9-15 Oct. 2006*, 2006, pp.989-993.
99. Tiest, W.M.B. and Kappers, A.M.L. Cues for Haptic Perception of Compliance. *IEEE Transactions on Haptics*. 2009, **2**(4), pp.189-199.
100. Pang, X.D., Tan, H.Z. and Durlach, N.I. Manual discrimination of force using active finger motion. *Perception & Psychophysics*. 1991, **49**(6), pp.531-540.
101. Brodie, E.E.a.R., H.E. Degrees of Freedom of Movement in Weight Discrimination: Effect of Stimulus Intensity. *International Society for Psychophysics Fechner Day 86*. 1986, pp.681-687.
102. Billinger, S.A., Arena, R., Bernhardt, J., Eng, J.J., Franklin, B.A., Johnson, C.M., MacKay-Lyons, M., Macko, R.F., Mead, G.E., Roth, E.J., Shaughnessy, M. and Tang, A. Physical Activity and Exercise Recommendations for Stroke Survivors. *Stroke*. 2014, **45**(8), pp.2532-2553.
103. Deng, J., Dong, W., Socher, R., Li, L.J., Kai, L. and Li, F.-F. ImageNet: A large-scale hierarchical image database. In: *2009 IEEE Conference on Computer Vision and Pattern Recognition*, *20-25 June 2009*, 2009, pp.248-255.
104. Deng, L. The MNIST Database of Handwritten Digit Images for Machine Learning Research [Best of the Web]. *IEEE Signal Processing Magazine*. 2012, **29**(6), pp.141-142.
105. Sivan, M., Gallagher, J., Makower, S., Keeling, D., Bhakta, B., O'Connor, R.J. and Levesley, M. Home-based Computer Assisted Arm Rehabilitation (hCAAR) robotic device for upper limb exercise after stroke: results of a feasibility study in home setting. *Journal of neuroengineering and rehabilitation*. 2014, **11**(1), p.163.

List of Abbreviations

ADL	Activities of daily living
ANOVA	Analysis of Variance
ARAT	Action Research Arm Test
AUC	Area under the receiver operating characteristics
BGR	Blue-Green-Red
DA	Dominant arm
DAC	Digital-analogue converter
DNN	Deep Neural Network
DOF	Degree of freedom
DPI	Dots per inch
DTW	Dynamic Time Warping
ERM	Eccentric rotating mass
FMA	Fugl-Meyer Assessment
FMA-UE	Fugl-Meyer Assessment Upper Extremity
hCAAR	Home-based computer assisted arm rehabilitation
HSV	Hue-Saturation-Value
ICC	Intra-class coefficient
IDRO	Institute of Design, Robotics and Optimisation
IMU	Inertial measurement unit
LRA	Linear resonant actuators
ML	Machine learning
MRMR	Minimum Redundancy Maximum Relevance
NDA	Nondominant arm
NJ	Normalised jerk
NOM	Number of matches
NOP	Number of peaks
NOU	Number of unidentified answers

PCB	Printed circuit board
PWM	Pulse Width Modulation
RC	Resistor-capacitor
RF	Random Forest
RMSE	Root Mean Square Error
ROI	Region of interest
SOC	Sum of confidence
SVM	Support Vector Machine
VCA	Voice coil actuator

Appendix A

A.1 Output Features for Delay Time

The five output features were extracted from the displacement profiles with different delay time settings. Features are listed below.

t_d (ms)	f_{asy} (Hz)	V_s (1/s)	S_n	S_p	r_s
0	10.29	1.9151	0.0622	0.2486	0.2502
10	6.17	1.0993	0.1221	0.3270	0.3731
20	4.47	0.8101	0.0963	0.2745	0.3508
30	3.49	0.6314	0.0923	0.2851	0.3237
40	2.87	0.5112	0.1151	0.3231	0.3562
50	2.44	0.4413	0.1569	0.3786	0.4144

A.2 Output Features for Ramp Down Step Length

The five output features were extracted from the displacement profiles with different ramp down step length settings. Features are listed below.

S_r	f_{asy} (Hz)	V_s (1/s)	S_n	S_p	r_s
64	1.88	0.3413	0.0528	0.2664	0.1982
128	3.13	0.5404	0.0563	0.2674	0.2104
256	4.47	0.8101	0.0963	0.2745	0.3508
512	5.71	1.0163	0.2115	0.4213	0.5020
1024	6.93	1.3293	0.2315	0.4850	0.4773

A.3 Output Features for Cut-off Voltage

The five output features were extracted from the displacement profiles with different cut-off voltage settings. Features are listed below.

V_c (V)	f_{asy} (Hz)	V_s (1/s)	S_n	S_p	r_s
0	4.47	0.8101	0.0963	0.2745	0.3508
0.41	4.65	0.8483	0.0920	0.2700	0.3407

0.82	4.91	0.8757	0.0710	0.2490	0.2851
1.10	5.21	0.9338	0.0255	0.1996	0.1297

Appendix B

B.1 MEEC 21-003 Experiment Guidance for Participants

Experiment Guidance for Participants

This is the experiment guidance for participants in the research project stated below.

A Machine Learning Based Performance Classification for Post-Stroke Rehabilitation Using Kinematic Features

You are being invited to take part in a research project. Before you decide it is important for you to understand what will be the procedure of the experiment. Please take time to read the following information carefully and discuss it with others if you wish. Ask us if there is anything that is not clear or if you would like more information. Take time to decide whether or not you wish to take part.

Preparation for Recording Sessions

Before the recording sessions for each participant in this experiment, all the equipment used during the recording sessions will be fully sanitised in order to avoid potential exposure to COVID-19 virus.

During the Recording Sessions

(1) Touching Shoulder Exercise
Prior to performing the exercise, an IMU sensor will be attached to your wrist as illustrated in Figure 1.

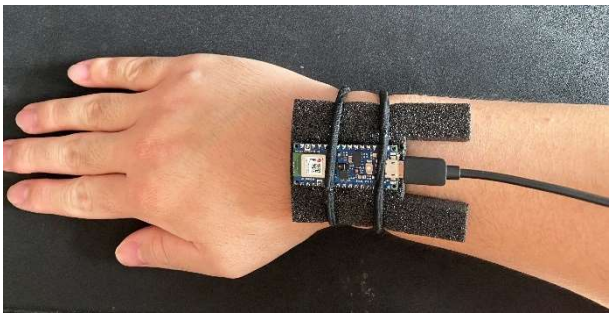

Figure 1: IMU sensor attached by two elastic bands on wrist

A soft sponge will be applied to cover the edge and the sharp pinouts on the IMU sensor to avoid direct contact with your wrist so as to minimise the potential risk of being scratched.

During one recording session, you will be asked to rest at the initial position where your impaired arm (for experiment group) or dominant arm (for control group) is aligned with your thigh with palm facing up.

After a countdown on a computer screen, you will be asked to

1. raise your impaired arm/dominant arm to touch the upper part of your opposite shoulder with your palm.
2. After touching the shoulder, you will move your arm back to the initial position.

With the above two movements being one cycle, you will be asked to perform 3 cycles with a 1-2 second rest between each cycle.

Totally 3 recording sessions will be conducted in this study, with a 1-minute rest between each recording session.

(2) Moving Mouse Exercise
The IMU sensor will be attached in the same way as in Touching Shoulder Exercise. During the recording session, you will be asked to move the mouse cursor firstly with the normal mouse setting. You will be asked to draw a pattern shown on a computer screen with your both arms, with each arm drawing the pattern for 20 times.

You will then be asked to draw the same pattern with the irregular mouse setting, where the mouse is rotated 180 degrees so that the moving direction of your hand is opposite to the mouse cursor. You will be asked to draw the pattern with this irregular setting with both arms, with each arm performing 20 times.

After the Recording Session

The IMU sensor will be removed from your wrist by the lead researcher and fully sanitised for the next participant. You are welcomed to give any feedback after your recording session.

Contact for further information

Should you have any further questions related to this study, please contact the lead researcher of this study.

Mr. Shuhao Dong

Email: mn16d2s@leeds.ac.uk

Thank you for taking the time to read through this information sheet.

Project title	*Document type*	*Version*	*Date*
A Machine Learning Based Performance Classification for Post-Stroke Rehabilitation Using Kinematic Features	Experiment Guidance for Participants	2	16/08/21

B.2 MEEC 21-003 Participant Consent Form

Consent to take part in A Machine Learning Based Performance Classification for Post-Stroke Rehabilitation Using Kinematic Features	Add your initials next to the statement if you agree
I confirm that I have read and understand the information sheet dated [16/08/2021] explaining the above research project and I have had the opportunity to ask questions about the project.	
I understand that my participation is voluntary and that I am free to withdraw at any time without giving any reason and without there being any negative consequences. In addition, should I not wish to answer any particular question or questions, I am free to decline. Contact number: 07887406049 Email: mn16d2s@leeds.ac.uk	
I understand that members of the research team may have access to my anonymised responses. I understand that my name will not be linked with the research materials, and I will not be identified or identifiable in the report or reports that result from the research. I understand that my responses will be kept strictly confidential.	
I understand that the data collected from me may be stored and used in relevant future research in an anonymised form.	
I understand that relevant sections of the data collected during the study, may be looked at by individuals from the University of Leeds or from regulatory authorities where it is relevant to my taking part in this research.	
I agree to take part in the above research project and will inform the lead researcher should my contact details change.	

Name of participant	
Participant's signature	
Date	
Name of lead researcher	Shuhao Dong
Signature	
Date*	

*To be signed and dated in the presence of the participant.
Once this has been signed by all parties the participant should receive a copy of the signed and dated participant consent form, the letter/ pre-written script/ information sheet and any other written information provided to the participants. A copy of the signed and dated consent form should be kept with the project's main documents which must be kept in a secure location.

Project title	*Document type*	*Version*	*Date*
A Machine Learning Based Performance Classification for Post-Stroke Rehabilitation Using Kinematic Features	Participant Consent Form	2	16/08/21

B.3 MEEC 21-003 Participant Information Sheet

Participant Information Sheet

Please refer to the Research Privacy Notice provided with this information sheet.

A Machine Learning Based Performance Classification for Post-Stroke Rehabilitation Using Kinematic Features

You are being invited to take part in a research project. Before you decide it is important for you to understand why the research is being done and what it will involve. Please take time to read the following information carefully and discuss it with others if you wish. Ask us if there is anything that is not clear or if you would like more information. Take time to decide whether or not you wish to take part.

Purpose of the Project

This research project is part of the upper limb rehabilitation using robotic device. This particular research aims to use kinematic features to classify post-stroke patients into different groups for individual optimised rehabilitation intervention with the aid of machine learning. The measured data will also be useful for simulating post-stroke movement acceleration profile in order to achieve more accurate classification and any further studies related to kinematic features.

Background: Stroke is the leading cause of human disability and death in the UK (Public Health England, 2018). It was estimated that the number of people affected by stroke will be increased by 27% in the EU by 2047 (Wafa et al. 2020). It is extremely difficult for post-stroke patients to perform activities of daily living without any rehabilitation intervention. Currently, apart from traditional physiotherapy, robotic systems have been widely applied to support the recovery process. However, since the recovery is changing throughout the rehabilitation process, the most appropriate intervention strategy may vary from stages to stages. Thus, it is necessary to classify post-stroke patients into different groups so that optimised training sessions may be designed for each individual.

The classification requires performance assessment. Clinical scores (e.g. Fugl-Meyer assessment et al.) are wide applied due to their effectiveness with respect to the whole recovery process. However, since these scores are categorical, they are not continuous throughout the whole rehabilitation process to reflect subtle improvement. Besides, these scores are normally made by clinicians, which means they can be subjective. Thus, it is necessary to introduce objective assessments based on kinematic features to achieve accurate classification.

Therefore, this particular research aims to gather kinematic features from each post-stroke individual to perform the assessment and further classification.

Why have I been chosen?

For participants in the control group, you are chosen because you have no existing disability in upper limb and would like to take part in this research by your own decision after reading all the provided materials. Your data will be protected and used as the base line measurement for our ongoing research project.

The minimum participant for the control group is 10.

Do I have to take part?

Taking part in this research is entirely voluntary and you as the participant may withdraw from the study at any time with all your personal information deleted without penalty and do not have to give a reason for doing so. If you decide to take part you will be given this information sheet to keep, a copy of the experimental procedure to look over and will be asked to sign a consent form.

What do I have to do? / What will happen to me if I take part?

The recording sessions will last for 10 minutes for each participant. All participants will only have to participate once unless further notice is given.

During each single recording session, the participant will be asked to sit on a chair with a comfortable position, being able to perform activities freely with their upper limb.

1. The participant will be asked to put the impaired arm / dominant arm at the initial position where the arm is fully relaxed and aligned with his/her thigh with palm facing up.
2. The participant will then be asked to raise the arm and use the palm to touch the upper part of the opposite shoulder, and finally move back to the initial position independently for three times. A 1-2 second rest is required between each attempt in order for the participant to fully relax the arm. Totally 3 attempts are required.

For each participant, totally 3 recording sessions are required. A 1-minute rest is necessary between each recording session should any participant would like to have one.

It is the participant's responsibility to obey the instructions listed above and in the experiment procedure document. It is also required for all the participants to protect any equipment used in the experiment.

No lifestyle restrictions are needed as a result of or prior to the participation.

What are the possible disadvantages and risks of taking part?

1. Under the current influence of COVID-19, there is a risk of being exposed to COVID-19 virus. This will be minimised by following the restriction rules from the government and the university. The IMU sensor (for data recording) and the elastic bands (for attaching IMU sensor on the wrist) will be fully sanitised after recording sessions for each participant.
2. Scratch by the sharp edge or component on the IMU sensor. The edge and the pinouts on the IMU sensor may hurt participants. This will be minimised by covering a soft sponge on the IMU sensor to avoid direct contact with participants.

What are the possible benefits of taking part?

Whilst there are no immediate benefits for those people participating in the project, it is hoped that this work will:

1) Help develop a novel assessment tool for upper limb performance, which can then be used as the preparation for optimised rehabilitation intervention for each individual for better rehabilitation results.
2) Help simulate post-stroke movement kinematic profiles so that more accurate models could be developed to serve the classification process.
3) Contribute to finding the relationship between clinical scores and kinematic features so that better recovery monitoring and predictions could be made to serve clinicians and patients.

Use, dissemination, and storage of research data

The collected data will be encrypted and stored on the University of Leeds OneDrive. There is the potential for data collected from this research being published in journal or conference articles. No identifiable information will be public. During publication, anonymised data will be made available to third parties.

What will happen to my personal information?

All data for publication will be anonymised with no trace of personal information published. If you wish to quite this research study, all your personal data will be deleted however the collected kinematic data will be retained.

What will happen to the results of the research project?

All the contact information that we collect about you during the course of the research will be kept strictly confidential and will stored separately from the research data. We will take steps wherever possible to anonymise the research data so that you will not be identified in any reports or publications.

The results from this study will be published within a PhD thesis by October 2023 (latest to October 2024). Data collected from this study may also be used in journal or conference papers where anonymisation will be strictly followed.

What type of information will be sought from me and why is the collection of this information relevant for achieving the research project's objectives?

For participants in the control group, your personal data including age, gender, presence of other disabilities will be recorded along with the kinematic data during the recording sessions. Your data will be used as the base line measurement for our developed classification models.
For participants in the experiment group, your personal data including age, gender, time after stroke, presence of other disabilities and the clinical scores for upper limb assessment will be recorded along with the kinematic data during the recording sessions. Your data will be used to

1) Validate the proposed kinematic-based assessment tool.
2) Simulate the post-stroke acceleration profile for training the classification models.

Who is organising/ funding the research?
The research has been organised by the University of Leeds. The lead researcher of this study is funded by China Scholarship Council.

Contact for further information

Should you have any further questions related to this study, please contact the lead researcher of this study.

Mr. Shuhao Dong

Email: mn16d2s@leeds.ac.uk

Thank you for taking the time to read through this information sheet.

Project title	*Document type*	*Version*	*Date*
A Machine Learning Based Performance Classification for Post-Stroke Rehabilitation Using Kinematic Features	Participant Information Sheet	2	16/08/21

B.4 MEEC 21-003 Risk Assessment for Participants

Risk Assessment for Participants

This is the risk assessment for participants in the research project stated below.

A Machine Learning Based Performance Classification for Post-Stroke Rehabilitation Using Kinematic Features

You are being invited to take part in a research project. Before you decide it is important for you to understand the potential risk of participating this experiment. Please take time to read the following information carefully and discuss it with others if you wish. Ask us if there is anything that is not clear or if you would like more information. Take time to decide whether or not you wish to take part.

Hazards and Risk Ratings

Hazard Type	How might the hazard cause harm	Who may be harmed	Control measures	Action by
COVID-19 transmission through social contact	Infection with COVID-19 (6)	Staff Participant	Social distancing guidelines observed (3)	Shuhao Dong
COVID-19 transmission through contaminated IMU sensor	Infection with COVID-19 (6)	Staff Participant	The IMU sensor will be disinfected with disinfectant wipes between trials. Hand sanitiser will be used before and after touching the IMU sensor (3)	Shuhao Dong
Scratch by the edge or sharp component on the IMU sensor	Scratch the skin (6)	Staff Participant	The IMU sensor will be covered by a soft sponge (2)	Shuhao Dong

Severity / Likelihood	Insignificant (1)	Minor (2)	Moderate (3)	Serious (4)	Critical (5)
Almost Certain (5)	Moderate (5)	Substantial (10)	Substantial (15)	Intolerable (20)	Intolerable (25)
Likely (4)	Tolerable (4)	Moderate (8)	Substantial (12)	Intolerable (16)	Intolerable (20)
Possible (3)	Tolerable (3)	Moderate (6)	Moderate (9)	Substantial (12)	Substantial (15)
Unlikely (2)	Tolerable (2)	Tolerable (4)	Moderate (6)	Moderate (8)	Substantial (10)
Rare (1)	Tolerable (1)	Tolerable (2)	Tolerable (3)	Tolerable (4)	Moderate (5)

Figure 1: Risk assessment reference.

Contact for further information

Should you have any further questions related to this study, please contact the lead researcher of this study.

Mr. Shuhao Dong

Email: mn16d2s@leeds.ac.uk

Lead researcher signature: _____ Head of School signature: _____

Thank you for taking the time to read through this risk assessment.

Project title	*Document type*	*Version*	*Date*
A Machine Learning Based Performance Classification for Post-Stroke Rehabilitation Using Kinematic Features	Risk assessment	3	08/10/21

Appendix C

C.1 MEEC 22-006 Experiment Guidance for Participants

Experiment Guidance for Participants

This is the experiment guidance for participants in the research project stated below.

The ideal characteristics of the input signal for providing the strongest haptic directional cue in a hand-held device for a rehabilitation purpose

You are being invited to take part in a research project. Before you decide it is important for you to understand what will be the procedure of the experiment. Please take time to read the following information carefully and discuss it with others if you wish. Ask us if there is anything that is not clear or if you would like more information. Take time to decide whether or not you wish to take part.

Before for the Experiment

Before the experiment, participants will need to read every document (i.e., Experiment guidance, information sheet and risk assessment) provided and sign the consent form in order to take part in the experiment.

During the Experiment

This experiment consists of two stages. In stage 1 of the experiment, participants will be asked to hold the device and feel different haptic guidance in order to choose the strongest one. In stage 2 of the experiment, participants will experience more dynamic using environment that matches some activities of daily living.

(3) Stage 1 – Rank different setups
You will be asked to hold a device of similar size as a coffee cup (R: 66mm x H: 110mm) as shown in Figure 1 on a table comfortably. You will then be displayed with 9 different haptic configurations (3 within each group and a total of 3 groups) all at once with a 3s gap in between. Each configuration will last approximately 10s. The purpose of this initial display is to let you get familiar with directional cues in terms of haptic feedback. You will then be asked if you are willing to take part in the following study of the experiment and a 1-minute rest will be provided.

Figure 1: Experiment device

In the second test, the same 9 configurations will be displayed to you with a different order. The test time and rest time will be the same as the initial display. After the test for each group, you will be asked which direction you think the device is guiding you to (either left or right) and how confident you are about the answer (not sure, sort of, very sure). This experiment procedure is also shown in Figure 2.

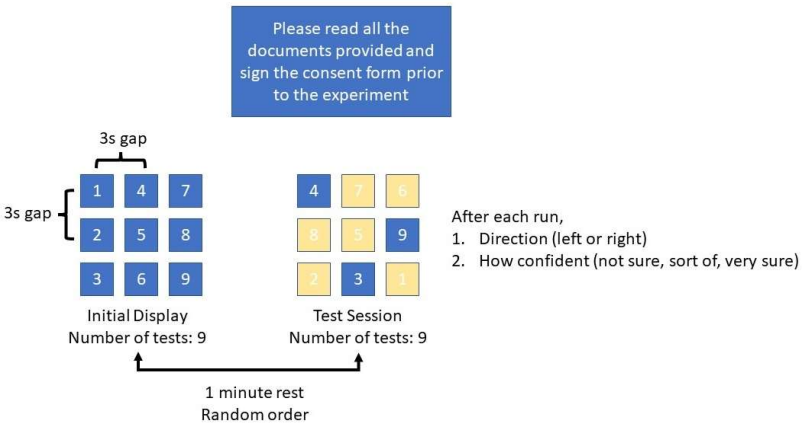

Figure 2: Experiment procedure at stage 1

(4) Stage 2 – Static and Dynamic Test

In the static test, you will be asked to hold the device as shown in Figure 1 comfortably on a table. When the test begins, you will be asked to use a rotary encoder (a device that you can rotate to indicate the direction) to specify the direction to which you believe the directional cue is guiding you. A total of 10 tests will be conducted with a 3s rest time in between. Each test will take approximately 10s. There will be 2 tests among the 10 that will not show any directional cues (i.e., normal vibrations). This is introduced to reduce your learning effect. When you think you are having one of those non-directional haptic cues, you can tell this to the investigator during the test.

In the dynamic test, you will need to hold the device while the device is operating. The direction of the haptic cues will be constantly changed while you are holding the device. You will need to specify the final directional cue when the operation of the device stops. This procedure will be repeated for 10 times and each one will last approximately 10s. After this test, you will be asked for two question regarding to your feel on the perception of haptic cues.

Finally, you will be asked to follow the directional cues and complete a certain pattern. This pattern may be a triangle, a rectangle, an “8” shape etc. The pattern you have to complete will be randomly allocated when you finish the previous tests. When you follow the cues, some position sensors will be attached onto your back of the hand in order to track you hand position during the movement. This experiment procedure is shown in Figure 3.

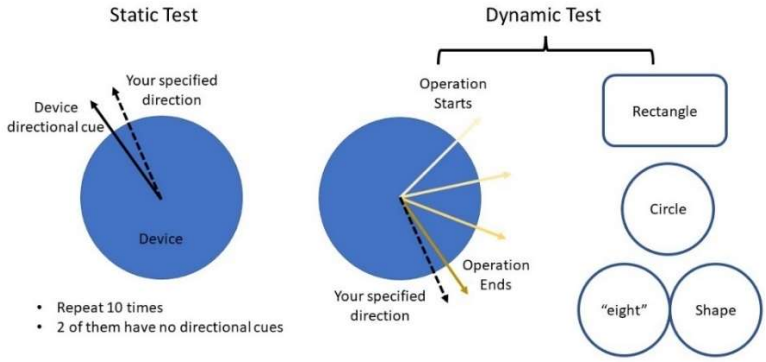

Figure 3: Experiment procedure at stage 2

After the Experiment

You may leave the experiment area after you finish all the tests if there are no further questions. All your personal data will be kept anonymously on University of Leeds OneDrive and not accessible by people out of the investigator's research group. Please leave you consent form to the investigator as this is an important material for ethical reasons.

Contact for further information

Should you have any further questions related to this study, please contact the lead researcher of this study.

Mr. Shuhao Dong

Email: mn16d2s@leeds.ac.uk

Thank you for taking the time to read through this information sheet.

Project title	*Document type*	*Version*	*Date*
The ideal characteristics of the input signal for providing the strongest haptic directional cue in a hand-held device for a rehabilitation purpose	Experiment Guidance for Participants	2	20/09/22

C.2 MEEC 22-006 Participant Consent Form

Consent to take part in The ideal characteristics of the input signal for providing the strongest haptic directional cue in a hand-held device for a rehabilitation purpose	Add your initials next to the statement if you agree
I confirm that I have read and understand the information sheet dated [13/09/2022] explaining the above research project and I have had the opportunity to ask questions about the project.	
I understand that my participation is voluntary and that I am free to withdraw at any time without giving any reason and without there being any negative consequences. In addition, should I not wish to answer any particular question or questions, I am free to decline. Contact number: 07887406049 Email: mn16d2s@leeds.ac.uk	
I understand that members of the research team may have access to my anonymised responses. I understand that my name will not be linked with the research materials, and I will not be identified or identifiable in the report or reports that result from the research. I understand that my responses will be kept strictly confidential.	
I understand that the data collected from me may be stored and used in relevant future research in an anonymised form. I understand the data collected from me will be kept for 10 years for research validation.	
I understand that relevant sections of the data collected during the study, may be looked at by individuals from the University of Leeds or from regulatory authorities where it is relevant to my taking part in this research.	
I agree to take part in the above research project and will inform the lead researcher should my contact details change.	

Name of participant	
Participant's signature	
Date	
Name of lead researcher	Shuhao Dong
Signature	
Date*	

*To be signed and dated in the presence of the participant.
Once this has been signed by all parties the participant should receive a copy of the signed and dated participant consent form, the letter/ pre-written script/ information sheet and any other written information provided to the participants. A copy of the signed and dated consent form should be kept with the project's main documents which must be kept in a secure location.

Project title	*Document type*	*Version*	*Date*
The ideal characteristics of the input signal for providing the strongest haptic	Participant Consent Form	2	06/12/22

directional cue in a hand-held device for a rehabilitation purpose			

C.3 MEEC 22-006 Participant Information Sheet

Participant Information Sheet

Please refer to the Research Privacy Notice provided with this information sheet.

The ideal characteristics of the input signal for providing the strongest haptic directional cue in a hand-held device for a rehabilitation purpose

You are being invited to take part in a research project. Before you decide it is important for you to understand why the research is being done and what it will involve. Please take time to read the following information carefully and discuss it with others if you wish. Ask us if there is anything that is not clear or if you would like more information. Take time to decide whether or not you wish to take part.

Purpose of the Project

This research project is part of the upper limb rehabilitation using robotic device. This particular research aims to find the ideal characteristics of the input signal that can provide the strongest haptic directional cues and also to study the effect of the device status in delivering the directional cues in a hand-held device.

Background: Stroke is the leading cause of human disability and death in the UK (Public Health England, 2018). It was estimated that the number of people affected by stroke will be increased by 27% in the EU by 2047 (Wafa et al. 2020). It is extremely difficult for post-stroke patients to perform activities of daily living without any rehabilitation intervention. Currently, apart from traditional physiotherapy, robotic systems have been widely applied to support the recovery process. However, most of the robots are vision-based systems, which is not ideal for stroke patients with vision loss or vision deficit. Therefore, it is beneficial to build a rehabilitation system with haptic feedback that is able to indicate directions. This physical force interactions will also help patients without vision deficit to rebuild their neuroplasticity.

Why have I been chosen?

You are chosen because you have no existing disability in upper limb and would like to take part in this research by your own decision after reading all the provided materials. Your data will be protected and used as the base line measurement for our ongoing research project.

Do I have to take part?

Taking part in this research is entirely voluntary and you as the participant may withdraw from the study at any time with all your personal information deleted without penalty and do not have to give a reason for doing so. If you decide to take part you will be given this information sheet to keep, a copy of the experimental procedure to look over and will be asked to sign a consent form.

What do I have to do? / What will happen to me if I take part?

The participants will be informed of the consent and experiment information sheet prior to any experiment. A signature to confirm the willingness of participating in the experiment is required to start the experiment. Participants may require withdraw from the experiment at any time before stage 2 of the experiment.

People will get used to the haptic pattern and effect very quickly during the experiment. This learning effect may influence the accuracy and validity of the experiment since two different hypotheses need to be verified. Thus, 2 visits are required with each experiment stage. The expected gap between two visits is maximum 7 days.

At stage 1 of the experiment, firstly participants will be asked to hold a device of similar size as a coffee cup (R: 66 mm x H: 110 mm) on a table comfortably. Then participants will experience 9 different haptic configurations. Each configuration will last approximately 10s and a 3s rest will be given between each haptic cue. After each configuration, participants will be asked to specify the direction they feel and rate how confident they are about their answers. Approximately 5 minutes will be required for each participant at stage 1.

At stage 2 of the experiment, participants will be asked to hold the same device on a table comfortably. At this stage, statistically preferred configurations will be used for the test. Participants will be randomly allocated with a configuration for this experiment. In static test, participants will be asked to rotate a rotary encoder on top of the hand-held device to indicate where they believe the directional cue is guiding. A total of 10 measurements will be taken with 2 being no directional cues to reduce the learning effect. Each measurement will take approximately 10s. In dynamic test, participants will be asked to hold the device first. The haptic directional cues will be generated while rotating around the centre of the device. The participants will be asked to specify the final direction after the rotation using the rotary encoder provided on top of the device. A total of 10 measurements will be taken. Each measurement will take approximately 10s. Finally, participants will be asked to follow the directional cues to complete a certain pattern (e.g., circle, 8 shape, rectangle etc.). The position information will be recorded either by Optotrak (An accurate movement capture system using IR camera) or a computer vision programme.

It is the participant's responsibility to obey the instructions listed above and in the experiment procedure document. It is also required for all the participants to protect any equipment used in the experiment.

No lifestyle restrictions are needed as a result of or prior to the participation.

What are the possible disadvantages and risks of taking part?

3. Being scratched by the sharp edge or component on the device. The edge of the device may hurt participants. This will be minimised by coving soft tape and rounded edge design.
4. Being instantly burned by Optotrak sensors. Optotrak works based on IR light. When the frequency of the collection is high, there is a chance of feeling an instant burning on the skin where the sensor is aiming at. This will be minimised by regulating the way how to attach those sensors on participants' skin. This action will be finished and inspected by the principal investigator of this project. An instant removal will be done when this situation happens.

What are the possible benefits of taking part?

There are no immediate benefits for people participating in the project. However we appreciate those who would like to help us improve the development of haptic robots for rehabilitation purposes.

Use, dissemination, and storage of research data

The collected data will be encrypted and stored on the University of Leeds OneDrive during the PhD study in the university. And the end of the PhD, the anonymised data will be uploaded to a data repository (figshare) for research verification. Data will be held for 10 years after the experiment to support research reproducibility. There is the potential for data collected from this research being published in journal or conference articles. No identifiable information will be public. During publication, anonymised data will be made available to third parties. According to the UK General Data Protection Regulation (GDPR), data collected in this experiment belongs to the special category data (data related to health). Based on the Article 6 (1) (a) and Article 9 (2) (a), this data collection process is lawful, fair

and transparent, and data processing is allowed after your explicit consent. If you wish not to use your data in any potential publication or thesis, please inform us when you sign the consent form.

What will happen to my personal information?

All data for publication will be anonymised with no trace of personal information published. If you wish to quite this research study, all your data will be deleted. Your personal contact information will be deleted at the end of the project.

What will happen to the results of the research project?

All the contact information that we collect about you during the course of the research will be kept strictly confidential and will stored separately from the research data during the project. At the end of this project, your contact information will be deleted. We will take steps wherever possible to anonymise the research data so that you will not be identified in any reports or publications.

The results from this study will be published within a PhD thesis by October 2023 (latest to October 2024). Data collected from this study may also be used in journal or conference papers where anonymisation will be strictly followed.

What type of information will be sought from me and why is the collection of this information relevant for achieving the research project's objectives?

In stage 1, we only ask for the direction you feel and your confidence level.

This information is collected because a statistically preferred system configuration will be selected based on all the participants' feedback. This will also help to validate our hypothesis raised during the preliminary test, which is beneficial to determine the ideal characteristics of the input signal for generating the strongest directional cues.

In stage 2, we will ask your movement position data of you hand when you follow the directional cue to complete a certain pattern. This information is collected so that we can compare your movement track with someone else's who is using the alternative system configuration. This comparison will help to determine whether the status of the device will influence the user's perception of the directional cues.

Who is organising/ funding the research?

The research has been organised by the University of Leeds. The lead researcher of this study is funded by the University of Leeds and China Scholarship Council.

Contact for further information

Should you have any further questions related to this study, please contact the lead researcher of this study.

Mr. Shuhao Dong

Email: mn16d2s@leeds.ac.uk

Thank you for taking the time to read through this information sheet.

Project title	*Document type*	*Version*	*Date*
The ideal characteristics of the input signal for providing the strongest haptic directional cue in a hand-held device for a rehabilitation purpose	Participant Information Sheet	2	06/12/22

C.4 MEEC 22-006 Risk Assessment for Participants

Risk Assessment for Participants

This is the risk assessment for participants in the research project stated below.

The ideal characteristics of the input signal for providing the strongest haptic directional cue in a hand-held device for a rehabilitation purpose

You are being invited to take part in a research project. Before you decide it is important for you to understand the potential risk of participating this experiment. Please take time to read the following information carefully and discuss it with others if you wish. Ask us if there is anything that is not clear or if you would like more information. Take time to decide whether or not you wish to take part.

Hazards and Risk Ratings

Hazard Type	How might the hazard cause harm	Who may be harmed	Control measures	Action by
Being scratched by the sharp edge of the component	Skin scratch (6)	Staff Participants	Shap edges are rounded or covered by soft tapes (3)	Shuhao Dong
Being burned by IR light sensors	An instant burning feeling when the sensor is aiming at the skin instead of the camera (6)	Participants	The sensor will only be accessible by the principal investigator and participants will have to attach this sensor under the guidance of the investigator (2)	Shuhao Dong
Personal data (including name and hand movement data) being stolen	Data stolen or accessed by unauthorised parties (6)	Participants	Data will be kept anonymously on University of Leeds OneDrive and no identifiable information will be collected throughout the experiment (2)	Shuhao Dong

Severity / Likelihood	Insignificant (1)	Minor (2)	Moderate (3)	Serious (4)	Critical (5)
Almost Certain (5)	Moderate (5)	Substantial (10)	Substantial (15)	Intolerable (20)	Intolerable (25)
Likely (4)	Tolerable (4)	Moderate (8)	Substantial (12)	Intolerable (16)	Intolerable (20)
Possible (3)	Tolerable (3)	Moderate (6)	Moderate (9)	Substantial (12)	Substantial (15)
Unlikely (2)	Tolerable (2)	Tolerable (4)	Moderate (6)	Moderate (8)	Substantial (10)
Rare (1)	Tolerable (1)	Tolerable (2)	Tolerable (3)	Tolerable (4)	Moderate (5)

Figure 1: Risk assessment reference.

Contact for further information

Should you have any further questions related to this study, please contact the lead researcher of this study.

Mr. Shuhao Dong

Email: mn16d2s@leeds.ac.uk

Thank you for taking the time to read through this risk assessment.

Project title	*Document type*	*Version*	*Date*
The ideal characteristics of the input signal for providing the strongest haptic directional cue in a hand-held device for a rehabilitation purpose	Risk assessment	1	13/09/22

C.5 MEEC 22-006 Data Management Plan

University of Leeds Data Management Plan (DMP) Template

Researcher Name	Shuhao Dong
Project Title	The ideal characteristics of the input signal for providing the strongest haptic directional cue in a hand-held device for a rehabilitation purpose
Faculty	Faculty of Engineering and Physical Sciences
KRISTAL Reference Number (if applicable)	
Supervisor(s) name (if applicable)	Prof. Martin Levesley, Dr. Justin Gallagher, Dr. Andrew Jackson
Funder	University of Leeds, China Scholarship Council
Scheme	
Research Start Date	01/10/2022
Research End Date	01/04/2023
Ethical review number	MEEC 22-006
DMP review due	

Date	Version	Author	Change notes
02/10/2022	1	Shuhao Dong	File Created
06/12/2022	2	Shuhao Dong	Special category data

Please provide a brief overview of your project including proposed research methods

Haptic guidance has been applied widely in our daily applications such as phones and cars' control panel etc. This physical excitation to human skin together with the receptors on human skin makes it possible to generate a sensible directional cue via motor asymmetrical vibrations. This directional cue has been proved by existing research to be beneficial for the recovery of stroke patients with/without vision loss. It also has the potential to be used with VR (virtual reality) and AR (augmented reality) technology to provide additional physical force cue that can be helpful to tele-rehabilitation process. The most common way to generate asymmetrical vibrations is to supply the motor with asymmetrical current input.

Thus, the aim of this research is to specify the ideal characteristics of the input current signal that can provide the strongest directional cue. Three key variables will be studied in this research, namely delay time, ramp down step length and cut-off voltage. For each key variable, 3 different configurations were chosen based on the preliminary study on the motor behaviour.

The entire experiment is divided into 2 stages. In stage 1, participants will be asked to experience all haptic configurations and finally 4 configurations (out of 9) will be chosen based on participants' feedback. In stage 2, participants will be asked to run through static (hold the device still in a single position) and dynamic (hold the device and follow the directional cue) tests, in which they will be asked to specify the direction they feel based on the haptic cue.

This research is part of a PhD project funded by the University of Leeds (201088930) and China Scholarship Council (201907000162). The potential participants will be recruited in the School of Mechanical Engineering.

1. What data will be produced? What data will be used from other sources?

1. Survey data:
   - Participants' name, age and their consent form for participating the experiment.
   - The specified direction (forward, backward, left or right) by participants, and their confidence level for the answers (1-3).
2. Software:
   - A C++ programme will be generated to control the motor used in the project.
   - MATLAB codes will be generated to analyse and visualise the error between users' specified direction and expected direction.
3. Data studied:
   - Sensor data (rotary encoder and position sensor)

4. Data from other sources: None

2. Where will data be stored? How will data be structured? Include file formats and approximate volume.

The estimated data size including files, figures, programmes will be no larger than 500MB. All the data will be stored in university's OneDrive. The collected data from participants will be recorded into a csv file (Microsoft Excel) and data will be analysed and visualised using MATLAB.
The name of the file should be in the format below: *purpose_of_the_file_version_date*. For purpose of the file, it can be raw data, position data, angle data etc. For data collected from individuals, add the participant's number between purpose and the version. Data collected from individuals will be stored in …/Haptics_Exp/date/IND_Data directory. For processed data and MATLAB programme, the directory is …/Haptics_Exp/Processing.
The version number will be recorded by the file name. A txt document will also be created to track the version change and a summary of updates.
Upon finishing the experiment, data collected in this session will be directly stored in OneDrive through a laptop that has been tested by the university.

3. Access to data during the project. Give details of collaborators and any controls.

The data will not be shared with anyone outside the research team during the project. The supervisory team my need access to the data for collaborating and assistance during the project. If the supervisory team need to access the data, the principal investigator will only share the data needed via university's OneDrive. Since data will not be shared with people outside the research team during the project, there is no need for a data sharing agreement.

4. Ethics and legal compliance: are there any 'special' requirements for your data? Any contractual or consent issues? Key policies (internal and external)

The university's information protection policy and advice on data protection have been read carefully. The data collected in this experiment belongs to the special category data, specifically personal data concerning health. In order to process the data, the conditions listed in Article 6 and Article 9 of the UK GDPR have been carefully reviewed. Participants will be asked to sign the consent form after being noticed the purposes of data collection to give consent. This satisfied the Article 6 (1) (a). Therefore, the data collection process is lawful, fair and transparent. Participants will also be noticed about the aim of the data

processing after collection. Therefore, Article 9 (2) (a) explicit consent has been satisfied to process the data. The processed and anonymised data will not be shared unless explicit consent from the participants has been given. There is no need to do a data protection impact assessment (DPIA) for this experiment (small scale, not used to determine access to a product, service, opportunity or benefit, not include genetic or biometric data). Since the data processing is based on Article 9 (2) (a) explicit consent, there is no need to satisfy DPA Schedule 1 conditions.
The data will be fully anonymised using the participant's number.
Data will be deleted upon finishing the PhD degree in the university.
Participant consents will be recorded by paper upon entering the experiment.

5. How will data be documented and described? Methodologies and protocols.

A txt file will be created to document the data when changes are applied. Appropriate labels and file names will be adopted to well classify the data.
A document will be generated to record how the data is collected. Details are included in the corresponding ethical application section C2 and C3.
It is important for this research to be reproducible. This research is to study how human react to haptic directional cues. Only when the research is reproducible can the hypothesis of the research be validated to be useful for the majority of the people. Thus, it is also beneficial to record the process of data collection and the specific equipment and sensors used during the project.
A C++ programme will be created to control the two motors used in the project. The version of the programme and the update log will be recorded in a txt file and the comment lines in the programme.
A MATLAB programme will be created to analyse the visualise the data. This programme will also be used to randomly allocate participant number to each individual during the project.
All programmes will be stored in university's OneDrive.

6. Training and support

Training for data analysis and presentation would be beneficial.
This training can be accessed in multiple ways:

- Read current literature in related field in order to learn the method of data analysis for specific data type and data visualisation.
- Coursera also provide data analysis courses.
- Careful readings on the Guide to the UK General Data Protection Regulation (UK GDPR) in order to satisfy all the necessary conditions for data collection, data processing and data sharing.

7. What are the plans for data sharing beyond project partners? Include justification if some of your data needs to be restricted. Include data and code. Include repository.

Raw data will not be shared with anyone outside the research group. However, processed data will be presented in the final thesis for PhD degree and publications to journal and conference papers.
There is a section in the participant consent form for data sharing for publication and thesis. Processed data will only be published if participants agree.
Data will only be used for PhD thesis and potential publications so there will be a delay in accessing processed data.
The data will be kept in university's OneDrive till the end of the PhD when access to

OneDrive is terminated. After PhD, the data will be stored in a trusted research data repository (figshare).
8. What Intellectual Property will be generated? How will IP be protected and exploited? No patent, no commercial applications. This study is for research only.
9. Who is responsible for managing the data? What resources will you need? The principal investigator of the ethical application is responsible for managing the data. The data involved in this project is not complex. The supervisory team may give support for data analysis. Special care on the data management is required as this is special category data.
10. Ongoing data curation / data housekeeping - you may find it useful to include a retention table All the data related to this project will be kept in university's OneDrive in order to access and analyse during the final year of the PhD study. Data will be deleted upon finishing the PhD and potential publications. This information will be shared with the supervisory team.

End of Project

At the end of a project and/or before you leave the institution, you should ensure that data and research materials are deposited with the School or a trusted data repository and documented in such a way that they can be found and understood.

Dataset name	Location	Person responsible
Haptics_directional_cues	Figshare	Shuhao Dong